Palladium Catalyzed Reductive Amination of Unactivated C-O Bonds:

Towards the use of bio-renewable resources as starting materials

Alejandra Dominguez-Huerta

Thesis submitted to McGill University in partial fulfilment
of the requirements for the degree of
Doctor of Philosophy

Department of Chemistry
McGill University
Montreal, Quebec, Canada

April 2021

Abstract

Alejandra Dominguez-Huerta Supervisor: Professor Dr. Chao-Jun Li
McGill University

This thesis describes the design and development of reductive amination methodologies of unactivated carbon-oxygen bonds using palladium on charcoal as a heterogeneous catalyst. The underlying premise is the transformation of starting materials that can be obtained from bio-renewable resources into commodity chemicals. Specifically, 2-cyclohexen-1-one and phenol were used as lignin building-block surrogates for C-N bond formation.

The first chapter places the work developed in this thesis both in a global and a scientific context. Its objective is to provide an overview of our societal needs while describing the latest scientific developments related to this thesis topic. Thus, it begins by exploring the United Nation's Sustainable Goals, followed by an overview of petroleum and lignin chemistry, and finishes with a review on amino acid *N*-modification.

In chapter two, the development of a novel methodology for the *N*-arylation of α-amino acids using 2-cyclohexen-1-one is described. Palladium on carbon was chosen as the catalyst, and several reaction conditions were explored to obtain optimal yields. This methodology's attractiveness lies in the absence of an aryl halide or protecting group on the 2-cyclohexen-1-one for the *N*-arylation to proceed. The reaction requires substoichiometric amounts of base and oxygen as the terminal oxidant. Aliphatic amino acids were ideal substrates for the reaction, and cyclohexanone provided the *N*-biarylated amino acids in good yields (up to 74%).

Chapter three describes efforts to improve the harsh conditions required for the *N*-arylation of α-amino acids, resulting in the development of a novel methodology for their *N*-cyclohexylation in water, at room temperature, using phenol as a coupling partner. The reaction successfully achieves *N*-cyclohexylation for 17 out of the 20 naturally occurring amino acids without racemization with up to quantitative yields. Furthermore, small peptides were also successful substrates for the reaction.

The fourth chapter explores the possibility of applying the latter methodology for the formation of one- and two-component peptide staples using tyrosine as a handle. The one component staple was

investigated using acetyl-lysine and acetyl-tyrosine, while the two-component staple was investigated using acetylated-tyrosine 2,2'-(ethylenedioxy)bis(ethylamine). While model substrates proved to couple successfully under previously optimized conditions, concentration and characterization proved to be challenging for working with larger peptides. Additional experiments exploring the possibility of using tyrosine amination as a pH responding hydrogel are also described in this chapter.

Finally, chapter five explores the possibility of synthesizing diphenylamines from phenol and ammonia formate as a convenient ammonia surrogate. Seventeen different diarylamines were synthesized with palladium on charcoal as the catalyst, with yields ranging from good to excellent. Notably, water and CO_2 were the only byproducts generated from this transformation. Triphenylamine was also obtained in combination with the methodology described in Chapter 1.

Résumé

Cette thèse décrit la conception et le développement de méthodologies d'amination réductives utilisant le palladium sur charbon en tant que catalyseur hétérogène. Le principe sous-jacent à cette thèse est la transformation de matière première pouvant être obtenues à partir de ressources bio-renouvelables en produits chimiques de base. Plus précisément, le 2-cyclohexen-1-one et le phénol ont été utilisés pour la formation de liaisons C-N comme molécules modèles de substitution remplaçant les unités constituant la lignine.

Le premier chapitre place les travaux développés dans cette thèse à la fois dans un contexte global et scientifique. L'objectif est de donner un aperçu de nos besoins sociétaux tout en décrivant les derniers développements scientifiques liés à ce sujet de thèse. Ainsi, les objectifs durables des Nations Unies seront d'abord exploré, depuis un aperçu de la chimie du pétrole et de la lignine sera donné, avant de terminer par un examen de la *N*-modification des acides aminés.

Dans le chapitre deux, le développement d'une nouvelle méthodologie pour la *N*-arylation d'acides α-aminés à l'aide de 2-cyclohexen-1-one est décrit. Le palladium sur charbon a été choisi comme catalyseur, et plusieurs conditions de réaction ont été explorées afin d'obtenir des rendements optimaux. L'attractivité de cette méthodologie réside dans l'absence d'halogénure d'aryle ainsi que de groupe protecteur sur le 2-cyclohexène-1-one lorsque la *N*-arylation se déroule. La réaction nécessite des quantités sous-stœchiométriques de base et d'oxygène comme oxydant terminal. Les acides aminés aliphatiques se montrent être des substrats idéaux pour la réaction, et le cyclohexanone a fourni les acides aminés *N*-biarylés avec de bons rendements (jusqu'à 74%).

Le chapitre trois décrit les efforts visant à améliorer les conditions difficiles requises pour la *N*-arylation des acides α-aminés, en aboutissant au développement d'une nouvelle méthodologie pour leur *N*-cyclohexylation dans l'eau, à température ambiante, en utilisant le phénol comme partenaire de couplage. La réaction accomplit avec succès la *N*-cyclohexylation pour 17 des 20 acides aminés naturels sans racémisation avec des rendements jusqu'à quantitatifs. En outre, les petits peptides sont également des substrats efficaces pour la réaction.

Le quatrième chapitre explore la possibilité d'appliquer cette dernière méthodologie pour la formation d'agrafes peptidiques à un ou deux composants en utilisant la tyrosine comme poignée. L'agrafe à un composant a été étudiée à l'aide d'acétyl-lysine et d'acétyl-tyrosine, tandis que l'agrafe à deux composants a été étudiée à l'aide de tyrosine acétylée 2,2 '- (éthylènedioxy) bis (éthylamine). Alors que les substrats modèles se sont avérés être couplés avec succès dans des conditions précédemment optimisées, la concentration et la caractérisation se sont avérées difficiles pour travailler avec des peptides plus longs. Des expériences supplémentaires explorant la possibilité d'utiliser l'amination de la tyrosine pour former un hydrogel sensible au pH sont également décrites dans ce chapitre.

Finalement, le chapitre cinq explore la possibilité de synthétiser des diphénylamines à partir de phénol et de formiate d'ammonium utilisé comme un substitut plus pratique à l''ammoniac pratique. Dix-sept diarylamines différentes ont été synthétisées en utilisant du palladium sur charbon de bois comme catalyseur et avec des rendements bons à excellents. L'eau et le CO_2 étaient les seuls sous-produits générés par cette transformation. La triphénylamine a également été obtenue en combinaison avec la méthodologie décrite dans le premier chapitre.

May all beings be happy and safe, may their hearts be filled with joy.

Fragment of the Metta Sutta
Sutta Nipata 1.8

Acknowledgements

First and foremost, I want to thank my supervisor C.J. Li for his support throughout my degree. Prof. Li welcomed me into his laboratory and guided me towards becoming the person that I am today. I am genuinely grateful for his unconditional support and for showing me nothing but kindness throughout the years. I truly appreciate all his mentorship and will forever remember his genius and humanity.

Secondly, I want to thank my professors and the staff of the McGill Department of Chemistry. Every professor I encountered in the department has inspired me with their knowledge and passion for science. I feel truly grateful to have received your instruction. I want to thank everyone in the HRMS and NMR facilities for helping me run experiments and for all your efforts to ensure I can make the most out of the results. I am also grateful to the administrative staff who allowed me to continually grow by helping me get approval for every program and opportunity that sparked my curiosity and for always doing so with a smile. Thank you so much for all your support.

Thirdly, I want to express my deepest gratitude to all my colleagues. While laboratory and graduate work might have been quite solitary, I never felt alone. Even during the pandemic, I always knew that I had a group of supportive friends ready to share their knowledge, their caring, and their laughter with me. I am genuinely grateful to have met all of you and to have shared this journey together.

I would also like to thank the funding sources that made it possible for me to complete this degree, in particular Consejo Nacional de Ciencia y Tecnologia (CONACYT) and Secretaria de Educacion Publica (SEP). I am delighted to say that both of these Mexican funding agencies have allowed me to surpass myself, and I am eager to contribute to my country's development in any possible way in years to come.

Lastly, I would like to thank my family, in particular my parents and siblings. Completing this degree was arduous, and without their unlimited support I would have never made it to the starting line, let alone the finish line. Thank you for continually reminding me that just being is enough, that laughter makes suffering more bearable, for always believing in me, and for loving me into being. I love you infinitely. Thank you for sharing life with me.

Every one of you, and everyone with whom I have had the fortune of crossing paths during the last couple of years, will forever be a part of me. For this reason, I am confident that all my successes are also yours, for I would not be who I am today without your advice, your guidance, and your understanding. May you also fulfill your goals, and may all your kindness, compassion, and generosity be multiplied by eons and returned to you as infinite blessings.

Contributions and publications

During my doctoral research, the following literature reviews and research publications have resulted from my dissertation, and are therefore the basis for discussion within this dissertation:

Dominguez-Huerta, A.; Perepichka, I.; Li, C.-J., Direct Synthesis of Diphenylamines from Phenols and Ammonium Formate Catalyzed by Palladium. *ChemSusChem* 2019, *12* (13), 2999.

Dominguez-Huerta, A.; Dai, X.-J.; Li, C.-J. *et al.* Exploration of new reaction tools for late-stage functionalization of complex chemicals*. Can. J. Chem.* 2018, *97*, 67.

Dominguez-Huerta, A**.**; Perepichka, I.; Li, C.-J., Catalytic *N*-modification of α-amino acids and small peptides with phenol under bio-compatible conditions. *Comms. Chem.* 2018, *1* (1)*,* 45.

Zeng, H.; Qiu, Z.*; Dominguez-Huerta, A.*; Li, C.-J. *et al*. An Adventure in Sustainable Cross-Coupling of Phenols and Derivatives via Carbon–Oxygen Bond Cleavage. *ACS Catal.* 2016, *7* (1), 510

Chapter 4 of this thesis concerns unpublished work in collaboration with the undergraduate summer student Anita Wang who helped expand the substrate scope for the one- and two-component tyrosine staple.

Table of contents

Chapter 3

Chapter 4

Chapter 5

List of Schemes

Chapter 1

Chapter 2

Chapter 3

Chapter 4

Chapter 5

List of Figures

Chapter 1

Chapter 2

Chapter 3

Chapter 4

Chapter 5

List of Tables

Chapter 1

Chapter 2

Chapter 3

Chapter 4

Chapter 5

List of Equations

List of Abbreviations

2-MeTHF	2-methyltetrahydrofuran
Ac	acetate
acac	acetylacetonate
API	American Petroleum Institute
Ar	aryl
BINAP	2,2'-bis(diphenylphosphino)1,1'-binaphthyl
BINOL	1,1'-bi-2-naphthol
Bn	benzyl
Boc	*tert*-butyloxycarbonyl protecting group
Bu	butyl
C-C	carbon-carbon
C-H	carbon-hydrogen
C-N	carbon-nitrogen
C-O	carbon-oxygen
cod	cyclooctadiene
Cp*	pentamethylcyclopentadienyl
Cy	cyclohexyl
dba	dibenzylideneacetone
DBU	1,8-diazabicyclo[5.4.0]undec-7-ene
DCM	dichloromethane
DFT	density functional theory
DIPEA	*N*,*N*-diisopropylethylamine
dmpe	1,2-bis(dimethylphosphino)ethane
DMSO	dimethyl sulfoxide
dppb	1,4-bis(diphenylphosphino)butane
dppe	1,2-bis(diphenylphosphino)ethane
dppf	1,1'-bis(diphenylphosphino)ferrocene
dpph	1,6-bis(diphenylphosphino)hexane
dppm	bis(diphenylphosphino)methane
dppp	1,3-bis(diphenylphosphino)propane
dr	diastereomeric ratio
EDX	energy-dispersive X-ray spectroscopy
ee	enantiomeric excess
E-factor	environmental factor
EQ	environmental quotient
equiv	equivalents
Et	ethyl
h	hours

[H]	reductant
HIV	human immunodeficiency virus
HRMS	high resolution mass spectrometry
IBX	2-iodoxybenzoic acid
ICP-AAS	inductively coupled plasma-atomic absorption spectroscopy
*i*Pr	isopropyl
IR	infra-red spectroscopy
J	coupling constant
[M]	metal complex
m	*meta*
Me	methyl
MeCN	acetonitrile
m.p.	melting point
N	normal
NHC	*N*-heterocyclic carbene
NMR	nuclear magnetic resonance spectroscopy
nOe	nuclear Overhauser effect
nor	norbornadiene
o	*ortho*
[O]	oxidant
OAc	acetate
OLED	organic light-emitting diode
p	*para*
Ph	phenyl
PIDA	phenyliodonium diacetate
Piv	pivalate
PivOH	pivalic acid
p*K*a	logarithmic acid dissociation constant
ppm	parts per million
Pr	propyl
p-TsOH	*para*-toluenesulfonic acid
PXRD	powder X-ray diffraction
pybox	bis(oxazolinyl)pyridine
r.t.	room temperature
SDS	sodium dodecyl sulfate
SLES	sodium lauryl sulfate
TBAB	tetrabutylammonium bromide
TBAF	tetrabutylammonium fluoride
*t*Bu	*tert*-butyl
TEM	transmission electron microscopy
TEMPO	2,2,6,6-tetramethylpiperidinyloxyl

TFA	trifluoroacetate or trifluoroacetic acid
THF	tetrahydrofuran
TIPS	triisopropylsilyl
TLC	thin layer chromatography
TMG	tetramethylguanidine
TMS	trimethylsilyl
UV-Vis	Ultraviolet-visible spectroscopy
XPS	X-ray photoelectron spectroscopy

Chapter 1. Introduction

The work developed in this thesis is placed into both a global and a scientific context by first providing an overview of our societal needs and finishing with specific scientific developments in the relevant field related to this thesis. Thus, it begins by exploring the United Nation's Sustainable Goals, followed by an overview of petroleum and lignin chemistry, and finishes with a review on amino acid *N*-modification.

1.1 A Global Perspective of Green Chemistry

In September 2015, the General Assembly of the United Nations adopted the 2030 agenda for sustainable development.[1] This agenda has been summarized into the seventeen Sustainable Development Goals (SDGs, Figure 1) and a set of 169 specific targets to measure and achieve them. Their purpose is to attain our society's overall well-being and the prosperity of our planet by 2030. Notably, resource management is closely intertwined with the fulfillment of these resolutions.

Figure 1. The United Nation's Sustainable Development Goals[2]

From a chemical point of view, goals 9 and 12 must be highlighted as they address the efficient allocation of resources. SDG 9 encourages the development of sustainable industries through the adoption of environmentally sound technologies and industrial processes;[1] while SDG 12 strives towards sustainable production patterns by efficient management of our natural resources. Within the specific targets of SDG 12, is the management of chemicals throughout their lifecycle; reducing, recycling and reusing; and removing inefficient usage of fossil fuel subsidies.[1]

The aim of these two SDGs could be summarized as aiming to elongate the lifetime of our resources by developing processes that are "benign by design." With this latter resolution being at the core of green chemistry's 12 principles (Figure 2),[3] in a general sense, green chemistry focuses on developing chemical processes that do not risk human health or threaten the environment. Upon analyzing these principles, one can conclude that chemistry plays a role at the molecular level for sustainability to be achieved.[4] It is essential to ensure that chemical processes bolster responsible practices, given that chemistry renders a service that touches practically every industry, ranging anywhere from the production of batteries to pharmaceuticals. In the words of Prof. Paul Anastas, fundamental chemistry must, therefore, be "…healthful rather than toxic, renewable rather than depleting, and restoring rather than degrading…".[5]

While several of these principles might seem obvious, the lack of a framework made it challenging for chemists to place value on the entire supply chain of a chemical reaction instead of placing value exclusively on the products of any given process. Thus, several chemical processes have been transformed since the publication of the 12 principles of green chemistry.[6] Upon the publication of the United Nations' SDGs, chemists took it upon themselves to strive for far more inclusive practices, especially within the chemical industry.[7-11] It is essential to highlight that greener alternatives not only represent an opportunity for chemical innovation and social advancement, but are also exceptional business opportunities. According to the 2019 OECD report on Chemicals Management, the chemical industry is one of the world's largest, valued at USD 5.7 trillion in 2017, and expected to reach a value of USD 22 trillion by 2060.[12] On the other hand, the fulfillment of the SDG's by 2030 has been estimated to be worth USD 12 trillion in development opportunities.[13]

Thus, it is clear that chemistry benefits from substantial economic and social drivers. Nonetheless, these opportunities are currently leveraged only by a small group, with 42% of the global chemical production in 2017 coming from OECD countries.[14] In other words, 37 out of 195 countries controlled almost half of the entire chemical industry in 2017. This power imbalance has caused an erosion of trust in the public perception of the industry.[15] Furthermore, innovation in the chemical sector has been deemed risky, expensive, challenging, and lengthy,[16] and for good reason. Currently, most companies allot 4 to 6% of their total annual sales to R&D,[14] only to have some of the most prolonged cycles for product development. The latter is depicted in Table 1, where the time cycles for new products and new processes for different industries are directly compared.[16]

The 12 Principles of Green Chemistry	
1	**Prevention:** It is better to prevent waste than to treat or clean up waste after it has been created
2	**Atom economy:** Synthetic methods should be designed to maximize the incorporation of all materials used in the process into the final product
3	**Less hazardous chemical syntheses:** Wherever practicable, synthetic methods should be designed to use and generate substances that possess little or no toxicity to human health and the environment
4	**Designing safer chemicals:** Chemical products should be designed to effect their desired function while minimizing their toxicity
5	**Safer solvents and auxiliaries:** The use of auxiliary substances (e.g., solvents, separation agents, and others) should be made unnecessary wherever possible and innocuous when used
6	**Design for energy efficiency:** Energy requirements of chemical processes should be recognized for their environmental and economic impacts and should be minimized. If possible, synthetic methods should be conducted at ambient temperature and pressure
7	**Use of renewable feedstocks:** A raw material or feedstock should be renewable rather than depleting whenever technically and economically practicable
8	**Reduce derivatives:** Unnecessary derivatization (use of blocking groups, protection/deprotection, temporary modification of physical/chemical processes) should be minimized or avoided if possible because such steps require additional reagents and can generate waste
9	**Catalysis:** Catalytic reagents (as selective as possible) are superior to stoichiometric reagents
10	**Design for degradation:** Chemical products should be designed so that at the end of their function they break down into innocuous degradation products and do not persist in the environment
11	**Real-time analysis for pollution prevention:** Analytical methodologies need to be further developed to allow for real-time, in-process monitoring and control prior to the formation of hazardous substances
12	**Inherently safer chemistry for accident prevention:** Substances and the form of a substance used in a chemical process should be chosen to minimize the potential for chemical accidents, including releases, explosions, and fires

Figure 2. Principles of green chemistry.[3]

Table 1. Time cycle for new products and processes for different industries[16]

Industry	Time cycle for new products (years)	Time cycle for new processes (years)
Personal computers	< 0.5	2-4
Semiconductors	1-2	3-10
Pharmaceuticals	7-15	5-10
Petrochemicals	10-20	20-40

Despite these drawbacks, society has pushed forward for faster implementation of these processes through consumer movements that support environmentally responsible businesses.[15] This push has prompted enterprises to evaluate their products and processes by their (1) economic, (2) environmental, and (3) social factors, also known as a product's "triple bottom line."[17] Furthermore, green chemistry initiatives have been proven to decrease the associated costs of waste removal and safety liabilities, as well as to increase regulatory compliance and manufacturing security.[16] This evidence points to green chemistry as a design strategy that can maximize efficiency while minimizing health and environmental hazards by focusing not only on applications but also on new products' implications.[17] Moreover, this approach can help establish transparency throughout the supply chain and increase public acceptance of new technologies by re-establishing trust through actions.

Green chemistry is a driver for innovation that can help redesign any stage of a chemical's life cycle. There are four main components in a chemical's life cycle: (1) The sourcing of raw materials, (2) The transformation of the raw materials through any given chemical process, (3) The use, as well as the health and environmental impact of the products obtained, and (4) The end of life for all chemicals involved throughout this process.[17] This cycle is more clearly illustrated in Figure 3.

Figure 3. The lifecycle of a chemical[18]

Traditionally, raw materials for chemicals have been sourced from petroleum feedstocks. While only 3-5% of the total petroleum consumption is designated to chemicals, petroleum sources represent over 98% of chemical feedstocks.[19] Crude oil is processed through refining, generating bulk organic materials like benzene, ethylene, propylene, xylene, toluene, etc. These basic chemicals then undergo

chemical processing to give fertilizers, industrial chemicals, plastics, etc. These products go to different industries for further processing before reaching the end consumer.[14] This flow is depicted in Figure 4.

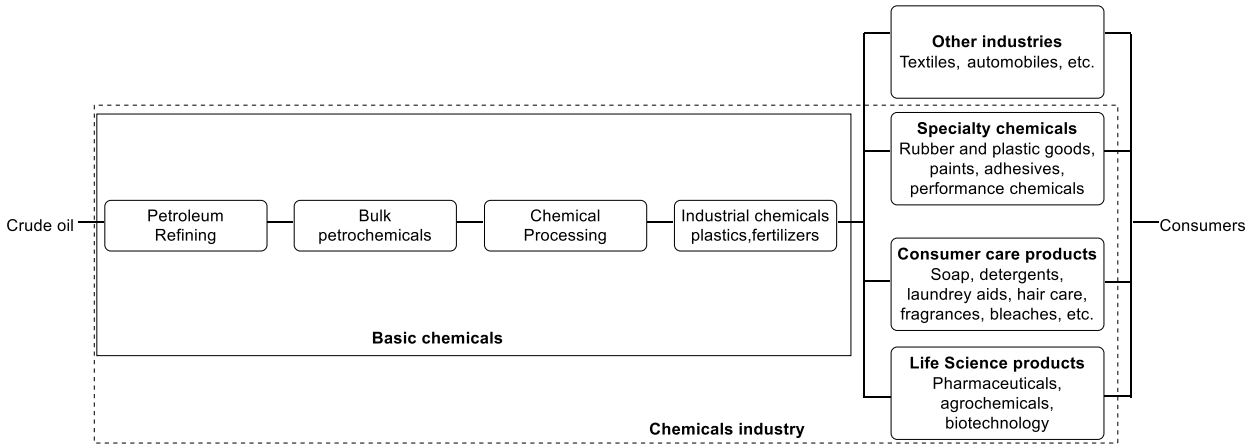

Figure 4. Overview of the basic chemicals and industries derived from crude oil[14]

The British Petroleum Company (BP) predicts that the world demand for petroleum will continue to increase despite different regulations coming into place (Figure 5). In all anticipated situations (1) oil continues to play a significant role throughout 2040, with demand ranging from 80 Mb/d to 130 Mb/d, and (2) trillions of dollars in investment are required to meet the required global oil demands.[20] Furthermore, due to the rising popularity of electric cars and efficient engine development, the usage distribution of petroleum is expected to shift. The share dedicated to transportation is predicted to decline starting in 2025, while its conversion to petrochemicals is expected to rise steadily (Figure 6).[21]

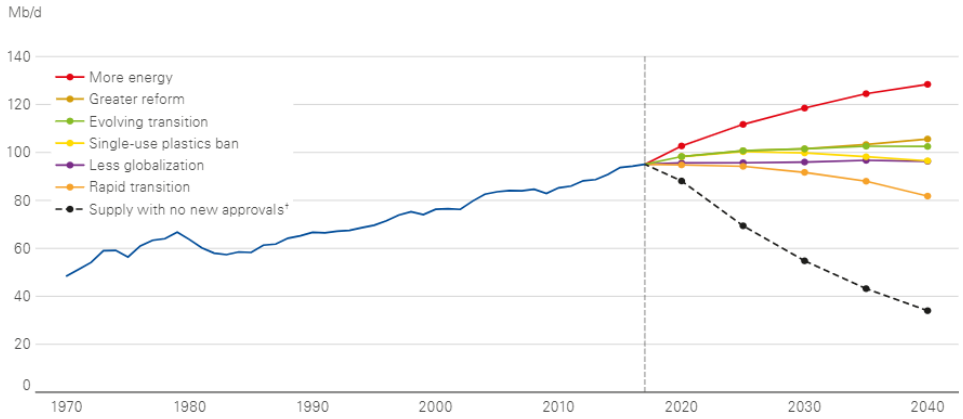

Figure 5. Demand and supply of crude oil and natural gas liquids[20]

† Based on the International Energy Agency's 2018 world energy outlook assumption that future investment is limited to developing existing fields and there is no investment in new production areas.
Mb/d = million barrels per day.

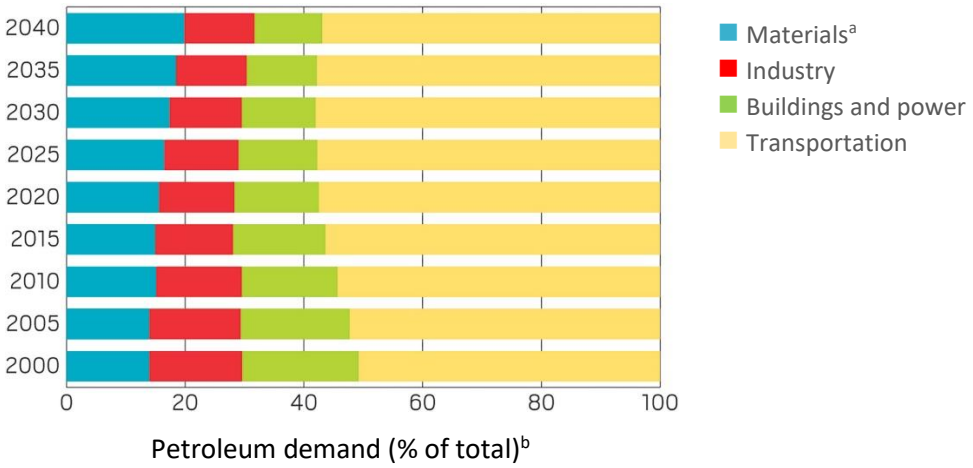

Figure 6. Projection of the share of petroleum demand[21]

a. Materials are non-combustion uses of liquids, such as petrochemicals, lubricants, and bitumen. b**.** Includes crude oil, natural gas, biofuels, coal-derived liquids, gas-derived liquids, and refinery processing gains.

While a massive investment in the oil sector is one approach to closing the oil supply gap with the predicted demand, this would immediately invalidate both the efforts towards achieving the SDGs and the 12 principles of green chemistry. Thus, one solution is investigating renewable resources that could in part replace oil as a raw material. Moving towards renewable feedstocks would bring benefits to chemists, chemical companies, and consumers alike.[17] For chemists, it would represent an opportunity for innovation. For companies, it would provide a source of starting material not dependent on fluctuation in oil prices. For society, it would represent an advancement towards safer and more environmentally responsible chemicals. In the words of Langdon Winner, green chemistry must focus on "work that locates the center of research in an area of basic scientific ignorance that lies at the heart of a social problem," [22] further highlighting the great importance of addressing this challenge.

1.2 Petroleum Chemistry

To understand why petroleum plays such a critical role as a feedstock for chemicals, it is necessary to break down this complex mixture into its different components. Broadly speaking, crude oil is a complex mixture of hydrocarbons which, depending on their chain length, are present in either the gaseous, liquid or solid state.[23] Minor amounts of other elements such as sulfur, nitrogen, oxygen, iron, copper, nickel, and vanadium have also been identified and are ubiquitously present.[24] The exact molecular composition of crude oil depends heavily on the sediment from which it is extracted. However, the proportion of chemical elements in oil is fairly consistent.[24] The ranges for these elemental proportions are depicted in Figure 7.

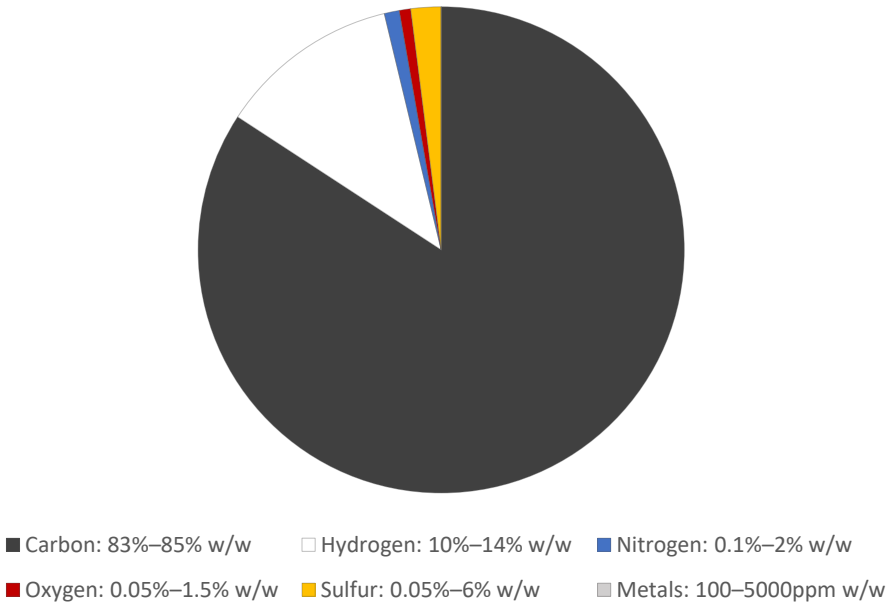

Figure 7. Elemental composition of crude oil[25]

The roughest oil classification is commonly done by analyzing its specific gravity and subsequently categorizing it as a light or heavy crude.[23] The specific gravity varies inversely with the H/C atomic ratio. As previously depicted, this varies widely depending on the source. Specific gravities for various crude oils range from 0.7 to 1.0 and are often expressed in degrees API.[23] Transforming specific gravities to degrees API results in a broader range that goes from 70 to 5, allowing for a more precise categorization (Equation 1). This classification, while vague, has vast economic impacts. According to the Canadian Energy Research Institute, light crudes have a WTI differential cost of CDN$1.00/bbl due to lower quality than the West Texas Intermediate (WTI) international standard toll, which includes gathering, tankage and transport of

CDN$4.00/bbl. On the other hand, heavy crudes have a WTI differential of CDN$8.00/bbl and a toll of CDN$6.00/bbl.[26]

$$°API = \frac{141.5}{Specific\ gravity} - 131.5$$

Equation 1. Conversion from specific gravity to degrees API[23]

API stands for American Petroleum Institute

Another way to describe crude oil is to relate it to the mass of its components obtained upon distillation.[27] An overview of the wide variety of products derived from petroleum, based on the number of carbons and their distillation ranges, is summarized in Figure 8.[23] A widely adopted profiling, provided by categorizing petroleum by the main hydrocarbon fractions obtained upon extraction, is SARA. The name of this profiling is an acronym of the four main hydrocarbon fractions obtained from petroleum: Saturates, Aromatics, Resins and Asphaltenes.[27, 28] The separation of crude oil by SARA is illustrated in Figure 9.[24, 28] The complexity of describing a specific fraction increases with the number of carbon atoms, and SARA falls short in this regard. Thus, improved profilings, such as Extended-SARA (E-SARA),[28] have been reported in an attempt to further characterize petroleum. For a comprehensive review regarding developments in novel categorization techniques of petroleum, in particular heavy fractions, please refer to the comprehensive 2020 review by S. Simon *et al.*[27]

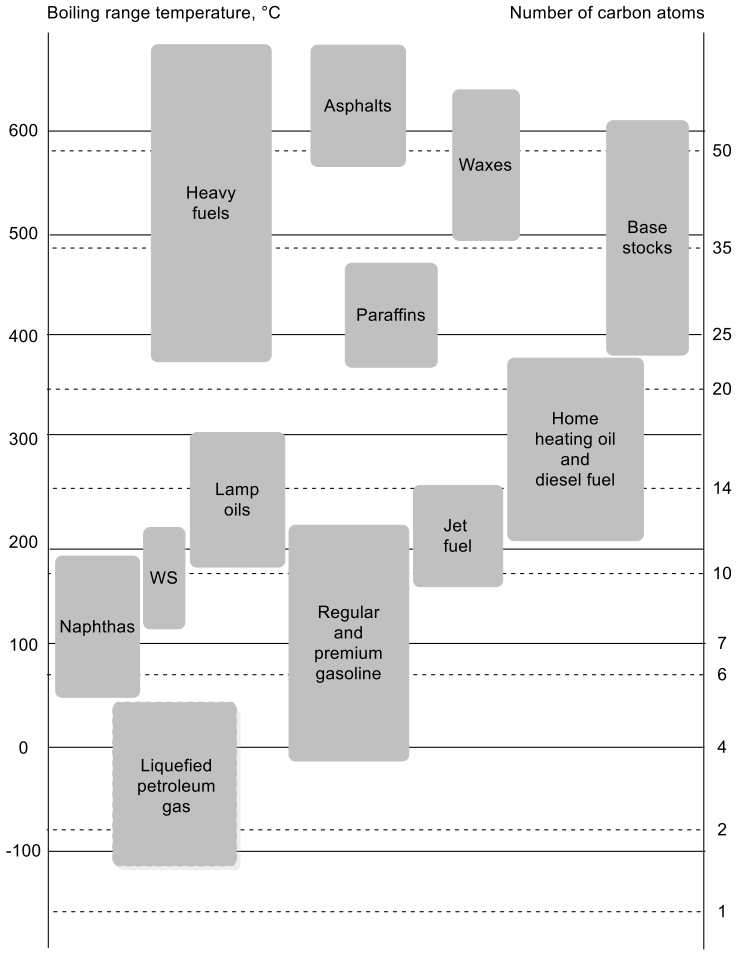

Figure 8. Principal petroleum products by boiling range temperature and number of carbon atoms[29]

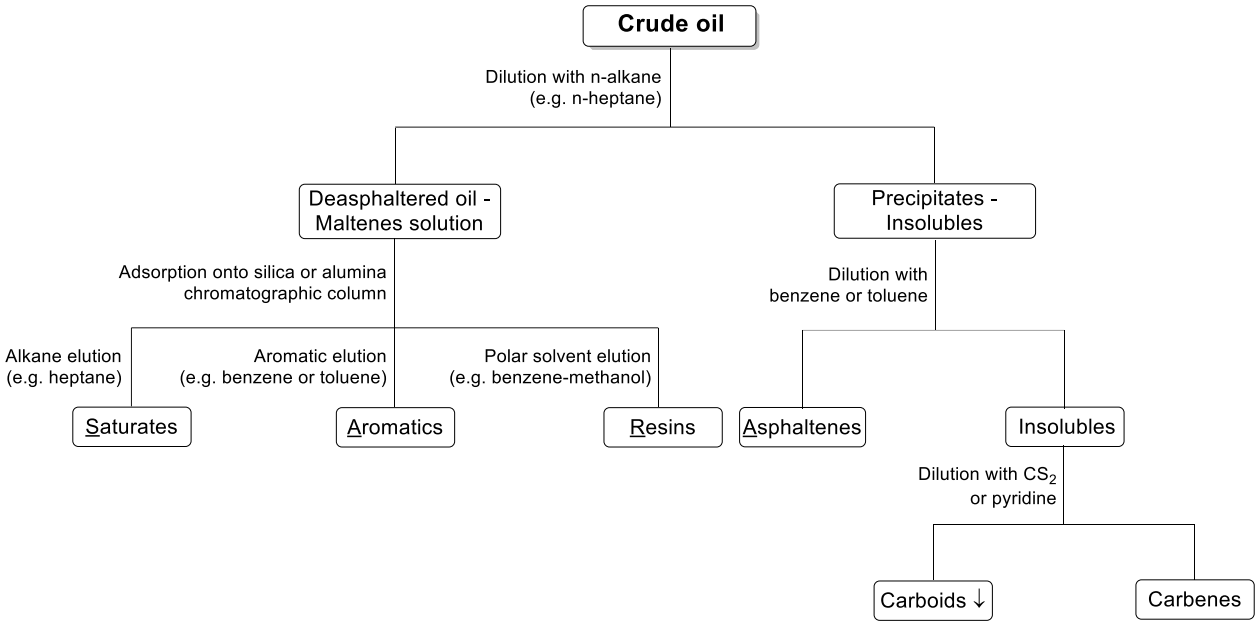

Figure 9. Fractions of crude oil by SARA[24, 28]

Although somewhat overlapping, these fractions serve to describe the main hydrocarbons found in crude oil in a practical manner.[30] Saturates refers to saturated hydrocarbons that can be further classified as paraffins or naphthenes. Paraffins or alkanes are saturated hydrocarbons with straight or branched chains but without any ring structure.[31] On the other hand, naphthenes or cycloalkanes are saturated hydrocarbons containing one or more rings which may have paraffinic side chains.[31] Aromatics refers to any hydrocarbon with an unsaturated ring structure stabilized by resonance due to the overlap of π-orbitals.[32] Belonging to the aromatics fraction are benzene, toluene, xylenes (BTX), and ethylbenzene, some of the most important precursors in the petrochemicals industry (Figure 10).[32]

Resins and asphaltenes have significantly higher boiling points.[31] The distinction between the two is that resins are miscible in n-heptane (or pentane) whereas asphaltenes are not. This is due to an increase in aromaticity resulting in robust π-stacking interactions due to the higher molecular weight of the asphaltene fraction (>1000 $gmol^{-1}$).[34a] In addition, there is a higher presence of heteroatoms, such as nitrogen and sulfur, and a higher amount of metals due to coordination to the manifold ring systems.[31] These compounds are generally considered a nuisance due to their negative impact on the environment and on our health.[23] Furthermore, they impair catalyst activity by coke deposition.[23] In petroleum chemistry, resins are molecules with condensed aromatic systems; either being catacondensed, meaning they have four adjacent aromatic hydrogens - such as in chrysene; or being pericondensed, an even more

condensed aromatic ring system - such as in pyrene (Figure 10).[31, 33] The asphaltene fragment precipitates during production, causing dreadful well and reservoir plugging.[31] Furthermore, it can stabilize emulsions, causing difficulty for oil-water separations.[27] By definition, carbenes and carboids are less soluble than the asphaltenes and are often classified within the asphaltene fraction.[34b] These fractions are the onset of coke formation.[34b] It is worth noting that the term carbene in petroleum chemistry is different to the one in organic chemistry, and does not refer to a divalent carbon intermediate, but rather to a polyaromatic fraction of oil derived from asphaltenes that is soluble in CS_2, as shown in Figure 9.

It is important to point out that alkenes, such as ethylene and propene, are also essential building blocks in the petrochemicals industry.[35] However, given that cracking is unavoidable during distillation, it cannot be concluded that olefins are native to crude oil despite them being found in distilled fractions.[31] Nevertheless, some petroleum reservoirs have been verified to contain considerable portions of olefins, causing revision to the original theory.[31] The presence of dienes or acetylenes remains unfounded.[31]

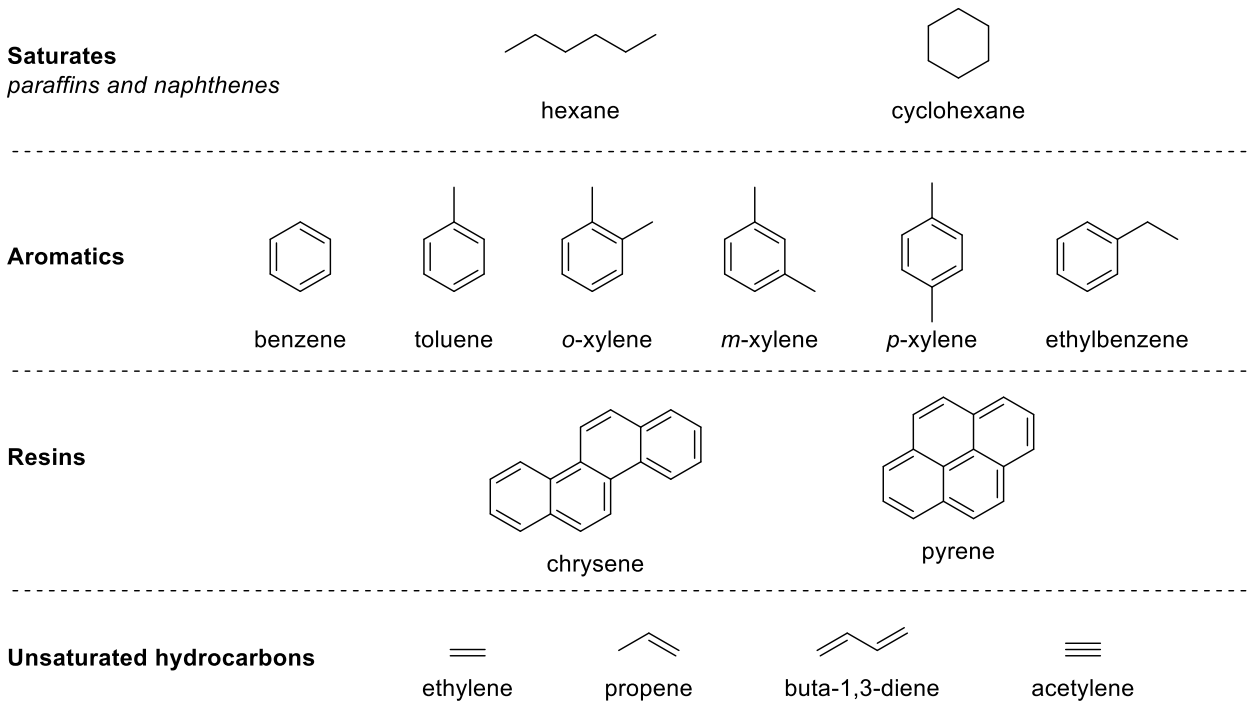

Figure 10. Selected examples of diverse hydrocarbons found in petroleum

1.2.1 Benzene

Benzene is one of the building blocks with widespread use in the petrochemical industry. It is an important precursor to many commercial products such as phenol, nylon, and styrene.[32] It was first commercialized as an explosive during World War II; until then, it was only used as a solvent or as a gasoline blender given its good gasoline octane characteristics.[35] Due to increasing demand for benzene, it started to be recovered from coke ovens at steel mills. Coke is a nearly pure form of carbon resulting from heating coal above 2000 °C in the absence of air.[35] Since there is a small percentage of complex resins in coal, these aromatic systems can crack apart, leaving behind benzene rings (conversion < 25%) and coke.[35] Other manufacturing processes, including catalytic reforming of hexane or cyclohexane to benzene, toluene hydrodealkylation, and toluene disproportionation, were also developed to keep up with the demand for benzene.[35] In the 1970's benzene was discovered as a by-product in olefin plants that used naphtha or heavy gas oil as feedstocks.[35]

Benzene is conformed of six sp^2 hybridized carbon atoms, each symmetrically positioned at 1.39 Å from each other to form a hexagon (average C=C length for non-aromatic compounds is 1.33 Å).[36] It is a very stable molecule (33 kcal/mol more stable than an acyclic molecule with three double bonds) due to the even delocalization of the six π electrons through the overlapped p orbitals, which grant benzene its aromaticity.[36] Given benzene's stability, it does not react under the same conditions as simple alkenes. Nonetheless, benzene can undergo five different types of electrophilic aromatic substitutions, namely: (1) halogenation, (2) nitration, (3) sulfonation, (4) Friedel-Crafts alkylation, and (5) Friedel-Crafts acylation (Figure 11).

Halogenation occurs in the presence of a Lewis acid catalyst with diatomic halogen molecules. This process occurs through the generation of a strong electrophile (i.e. $Cl^{\delta+}$, $Br^{\delta+}$, or $I^{\delta+}$) which is subsequently stabilized by the formation of a σ-complex, a delocalized cation, upon the electrophilic attack of the benzene.[36] The ring's aromaticity is restored upon loss of a proton.[36] Halogenated benzenes can be used for a plethora of chemical transformations, making them valuable intermediates in synthetic chemistry. Nitration of benzene is also possible by submitting benzene to a mixture of concentrated nitric and sulfuric acids.[36] Sulfuric acid protonates nitric acid to produce a nitronium ion (NO_2^+) through the displacement of a water molecule. Given that the nitronium ion is a strong cationic electrophile, benzene undergoes electrophilic substitution through the formation of a σ-complex. Nitrobenzenes are also versatile compounds due to their viable transformation to anilines by reduction of the nitro group.

Sulfonation can be achieved through a slow reaction between benzene and sulfuric acid, similar to the formation of the nitronium ion; one molecule of sulfuric acid protonates another one to ultimately yield benzenesulfonic acid.[36] The Friedel-Crafts alkylation requires an alkyl halide, an alkene, or an alkyne, which can be polarized with a Lewis acid. In the case of unsaturated compounds, the presence of a proton-releasing co-catalyst is required.[37] Upon forming a polar addition complex through the coordination of the Lewis acid to the alkylating agent, the σ-complex is formed, and aromaticity is re-established through proton loss.[37] Finally, the Friedel-Crafts acylation occurs similarly but by using an acyl halide or anhydride in the presence of a Lewis acid catalyst. However, in this case, two equivalents of the Lewis acid coordinate to the carbonyl group of the acylating agent to form an acylium ion, R-C≡O$^+$, in ionizing solvents.[37]

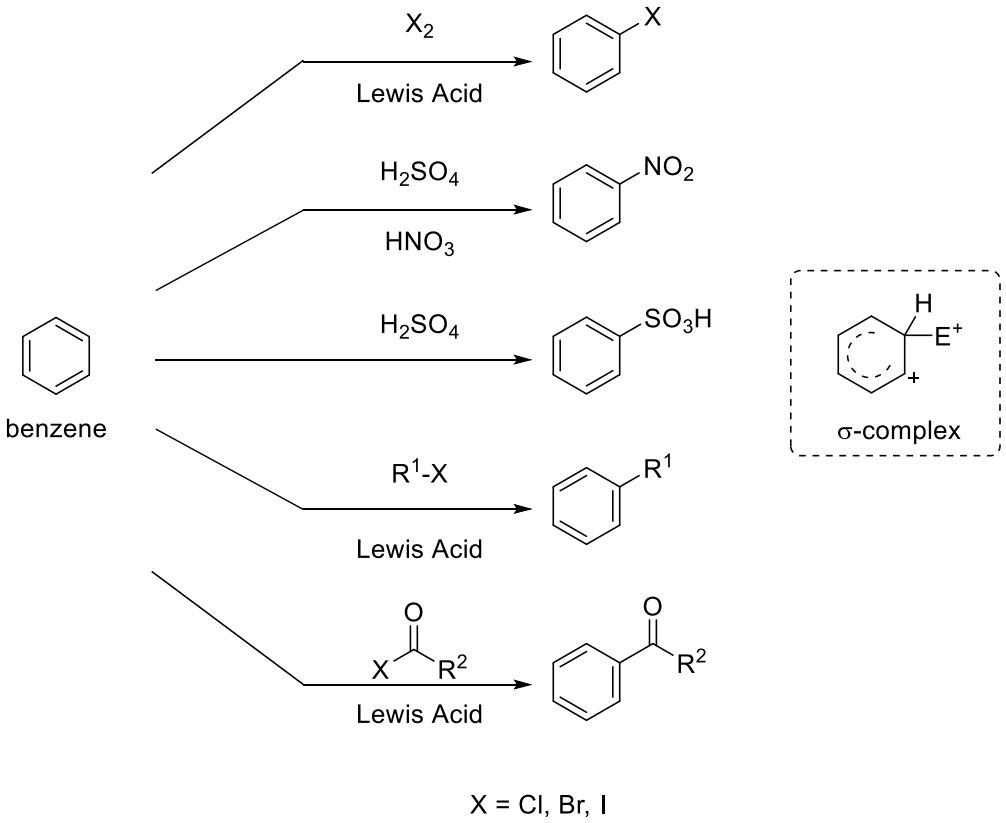

Figure 11. Electrophilic substitution of benzene

A significant number of chemical transformations rely on substitution reactions of the aforementioned benzene derivatives, especially aryl halides. Aryl halides are versatile electrophiles and substrates to a plethora of metal-catalyzed cross-coupling reactions. Given that their sourcing relies solely

on the refinement of petroleum and subsequent electrophilic substitution, it leads to highly polluting processes that also result in halogen persistence.[4] Furthermore, in the 20th century, environmental regulators responded to the conclusive evidence that benzene was a carcinogen, even when present in trace amounts in gasoline vapours.[35] Nonetheless, before petroleum deposits were exploited, the only available sources of pure organic compounds were microorganisms, plants, and animals.[38] Therefore, organic synthesis and the production of dyes and pigments were limited by the availability and transformation of these natural feedstocks.[38] Upon the discovery of petrochemicals, the quantities became sufficient to satisfy the growing demand of the chemical industries, which started to include industrial production of synthetic pharmaceuticals such as acetylsalicylic acid.[38]

Ultimately, petroleum feedstocks are biomaterials that have been under reductive conditions for millions of years, resulting in the stripping of all their functionalities to yield simple hydrocarbon molecules.[4] Chemists have learned how to add complexity to these simple molecules, despite this superfluous process' negative connotations.[4] Natural feedstocks are inherently different from petrochemicals, as they are complex molecules with high degrees of oxidation.[17] Learning how to harness molecules with high degrees of oxidation would allow us to use renewable feedstocks as starting materials for the chemical industry.[4]

1.3 Lignin Chemistry

In choosing natural feedstocks as an alternative to petrochemicals, the sustainability of the material of choice needs to be considered. An ideal renewable raw material must (1) be sustainably sourced, (2) preserve the natural biodiversity of its ecosystem, (3) ideally be valorized from useless wastes from other sustainable industries, and (4) be transformed through cost-effective and sustainable methodologies at an industrial scale.[9]

Renewable hydrocarbon sources include enzymatic fermentation products of biomass, vegetable oils, selected microalgae with high lipid content, and lignin.[39] Lignin is a polyaromatic polymer in plant cell walls, and it is considered the most abundant noncarbohydrate polymer on earth,[40] accounting for 30% of all terrestrial nonfossil carbon.[39] In addition, lignin is a major industrial side product mainly coming from the pulp and paper industry and cellulosic ethanol production.[41] In 2019, the annual amount of lignin waste was approximated to be between 150 to 200 million tons.[39] Historically, lignin has been burnt for heat and power, with less than 2% of lignin available being sold to formulate dispersants, adhesives, and surfactants.[42] The value of lignin that is burnt is estimated to be $0.18 USD/kg.[41] In comparison, lignin employed for chemical purposes is valued at $1.08 USD/kg, highlighting the importance of developing methods to utilize lignin as a platform for different chemicals.[41] Nonetheless, the aromaticity and carbon richness of lignin renders it an attractive starting biomacromolecule as renewable feedstock.[40]

Lignin is a three-dimensional polymer with a molecular weight of 1000-15000 Da, and is a highly stable crosslinked polymer consisting primarily of methoxylated phenylpropane structures.[39] In plant cell tissues, lignin performs a binding and hardening function by filling the space between cellulose and hemicellulose whilst protecting these polysaccharides against biochemical stresses.[39] The percentage of lignin found in a plant varies depending on the source. For example, grass contains 17-24% w/w lignin, softwood contains 18-25% w/w lignin, and hardwood contains 27-33% w/w lignin.[42] Lignin is biosynthetically generated through the radical polymerization of three main monomers: *p*-coumaryl, coniferyl, and sinapyl alcohols (Figure 12).[39] More than 50% of lignin is constituted by these monolignols being bound mostly through β-O-4 ether bonds, with β-1 bonds also considerably found but to a lesser extent (Figure 13).[39, 43] These linkages are considerably robust as emphasized by their high bond dissociation energies (BDE, Figure 13). Other linkages found include α-O-4 (BDE 60 ±14 kcal/mol), 4-O-5 (BDE 78-83 kcal/mol), β-β' (66-82 kcal/mol), β-5 (125-128 kcal/mol), and 5-5' linkages (BDE 115-118 kcal/mol).[44, 45]

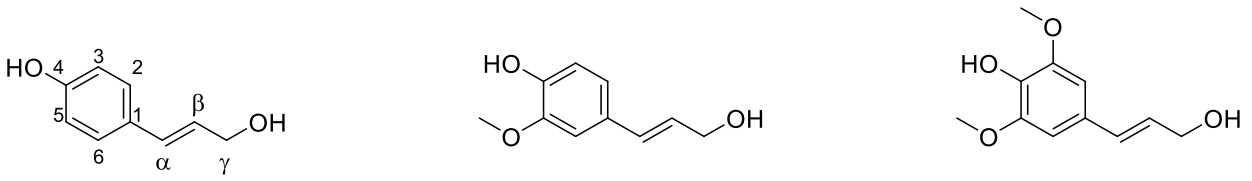

Figure 12. Monolignols

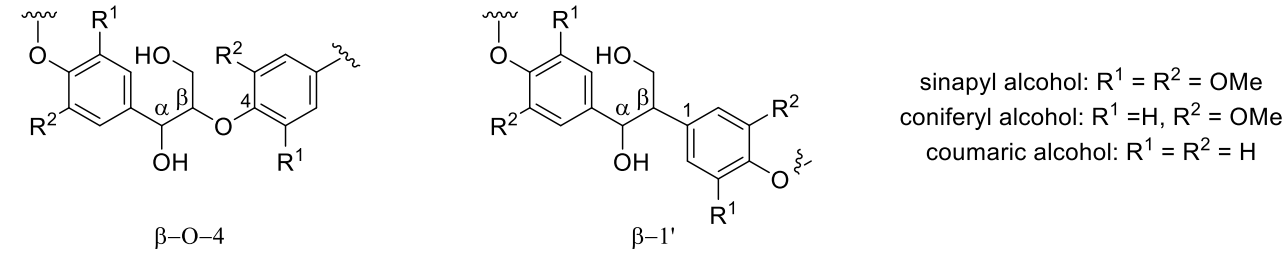

Figure 13. Most common phenolic linkages found in lignin and their bond dissociation energies[44, 45]

While the breakage of these phenolic linkages is key to yielding lignin-derived platform chemicals, the first step in lignin valorization is extracting this biopolymer from the cellulose and hemicellulose matrix in which it is found (Figure 14). Lignin must be first obtained via fractionation, and its polymeric structure will vary significantly depending on the isolation method used, thus altering its chemical properties. Natural, untreated lignin is referred to as protolignin, and its exact structure is still unknown due to this isolation caveat.[39] Several isolation methods have been reported.[39, 41] These methods can be classified into two major categories: (1) methods resulting in significant structural modifications (Table 2) and (2) methods resulting in mild structural modifications (Table 3).[39, 41] Yoo *et al*. have also described the effect of different pretreatment strategies based on their impact to preserve the polysaccharide fractions.[46]

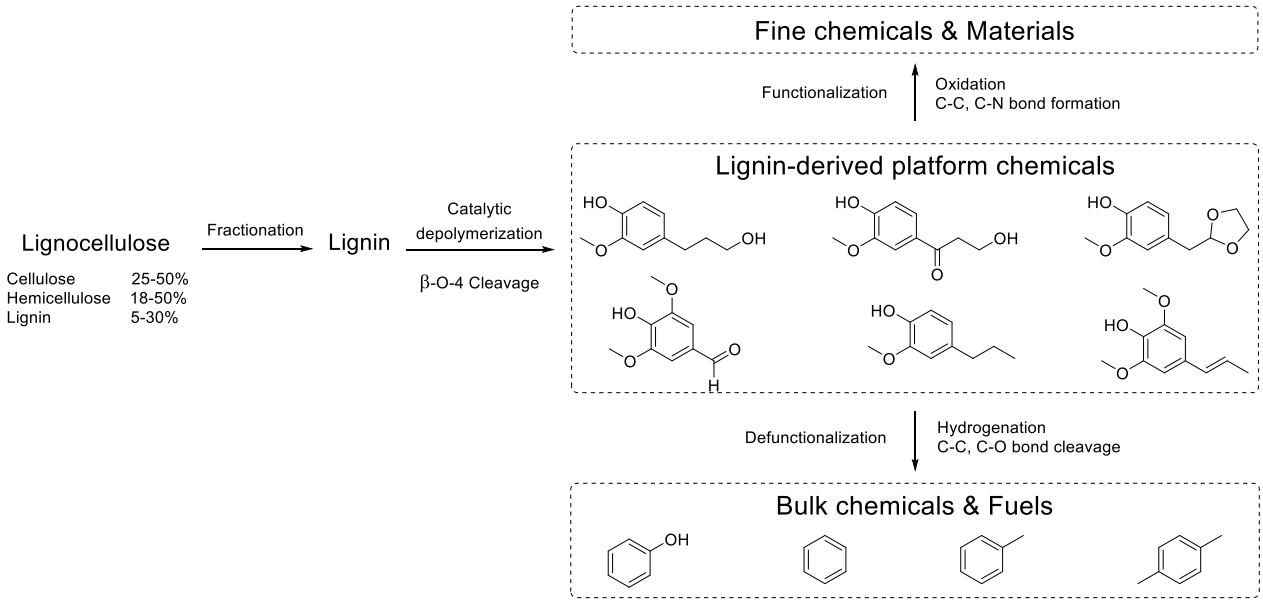

Figure 14. Overview of the transformation of lignocellulose into lignin-derived platform chemicals

Table 2. Fractionation procedures that cause significant structural modifications[39, 41]

Name	Conditions	Modifications
Kraft lignin	$Na_2S_{(aq)}$ + $NaOH_{(aq)}$, 170 °C, pH 13	1.5-3% sulfur incorporation as thiol
Klason lignin	72% H_2SO_4, 140 °C, pH 2-12	Significant damage to the native structure
Sulfite lignin	Sulfites or bisulfites	4-8% sulfur incorporation as sulfonate – water soluble
Alkali lignin	$NaOH_{(aq)}$, 150-170 °C, pH 11-13	

Table 3. Fractionation procedures that cause mild structural modifications[41]

Name	Conditions	Modifications
Organosolv lignin	Organic solvent extraction (e.g. EtOH/H_2O) 150-200 °C	Leads to partial degradation of β-O-4 linkages. Might lead to repolymerization.
Milled-wood lignin (MWL)	Extensive grinding + solvent extraction (Björkman process)	Milling can add carbonyl and hydroxyl groups. Yield 20-40%
Ionic liquid (IL) lignin	ILs treatment	Difficult to separate and recycle costly ILs
Cellulolytic enzyme lignin (CEL) and enzymatic mild acidolysis lignin (EMAL)	Cellulolytic enzymes + solvent extraction	EMAL and CEL give the highest molecular weights for isolated lignin

Once the isolation of lignin is achieved, lignin needs to be depolymerized to yield various platform chemicals. As previously mentioned, botanical origin and the fractionation method through which lignin was obtained will impact the efficacy of the depolymerization method. The addition of functionalities (especially those containing sulfur) will affect the role of the catalysts. In addition, if the molecular weight of the resulting lignin is too large, it might not allow for effective interaction with heterogeneous catalysts. Specific depolymerization methods may lead directly to the attainment of bulk chemicals (e.g. phenol, BTX), fuels (e.g. cyclohexane), and fine chemicals (e.g. vanillin, syringaldehyde, benzaldehyde).

The depolymerization methods can be classified as (1) reductive, (2) oxidative, (3) acid-catalyzed, (4) base-catalyzed, (5) thermal, and (6) enzymatic. Comprehensive reviews regarding these processes have been authored by Arapova *et al.*[39], Sun *et al*.[41], Cao *et al*.[47], and Gale et al.[48] Thus, only a brief introduction to each of these strategies is provided in Figure 15. For specific methodologies categorized by the type of their bond cleavage capacity, consult the thorough review of Shen *et al*.[45] For a review focused on reductive depolymerizations involving hydrogen in model compounds, refer to the work of Jing *et al*.[49] Electrochemical depolymerization of lignin has been reviewed by Garedew *et al*.[50] Advances in enzymatic depolymerization of lignin have been summarized by Chan *et al*.[44] and Weiss *et al*.[51]

Noble metals are most commonly used as heterogeneous catalysts for the depolymerization of lignin. Often, very active noble catalysts are alloyed to generate bimetallic catalysts to improve activity or selectivity. Supports also play a significant role based on their surface area and microporosity. Nonetheless, their acidity; basicity; particle size; pore size and shape; and hydrophobicity and hydrophilicity; will also impact the reaction's efficiency.[48] Solvent plays a significant role, and selection will depend on the catalytic system used.[48]

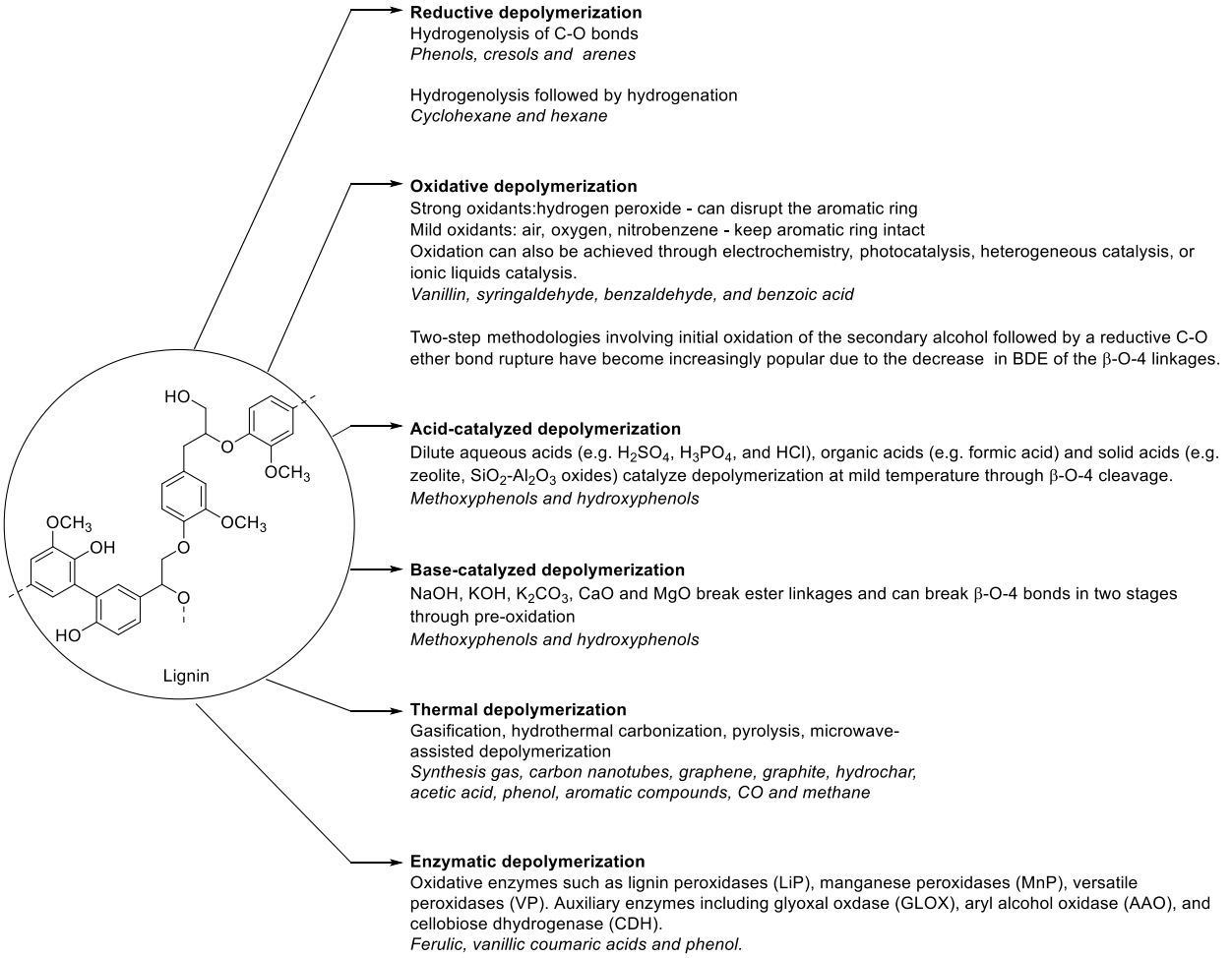

Figure 15. Depolymerization methods and main fragments obtained

Although selectivity and product distribution continue to be a challenge for the transformation of lignin, significant advances have been achieved. Among the products obtained from lignin, we can list saturates,[52] arenes, phenols, and moieties ready for incorporation into natural products,[38] or pharmaceuticals.[41] Additional value-products include jet fuel, food additives, carbon fibre, hydrogels, cleaners, and resins.[48] Although all of these chemicals add to the desirability of using lignin as a biorenewable resource, we will focus on phenol precisely due to its applicability in the production of nylon, pharmaceuticals, cosmetics, and biofuels.[45]

1.3.1 Phenol

Phenol is one of the most sought-after target products from lignin. Methoxy bonds, C_{aryl}-OMe, and carbon-carbon bonds, C_{aryl}-C_{α}, need to be effectively cleaved to generate the desired product from lignin. Selective cleaving of the methoxy C_{aryl}-OMe bonds is challenging, as the phenolic hydroxyl groups need to be maintained. Thus, catalysts that can provide modest catalytic hydrogenolysis and low hydrogenation activity are required for this process to be carried out successfully.[45] The selectivity of hydrogenolysis can be enhanced with bimetallic catalysts to finely tune the activity of the catalyst. Supported metal sulfide catalysts (e.g. $CoMoS/ZrO_2$) have also been tested. However, the loss of sulfur limits their application.[49] Metals commonly used are Ni, Ru, Pd, Fe, Co, and W.[48] Supported gold catalysts have also attracted considerable attention due to their high selectivity.[49] It is worth noting that the size of metal nanoparticles can affect the hydrogenation activity, catalytic activity, and distribution of the products.[49] Regarding cleavage of the C_{aryl}-C_{α} bonds, acid-catalyzed dealkylation has been proved to be the most effective and appropriate for industrial applications.[45] Most experiments of this nature have been performed using lignin model compounds, with the main challenge being the potential disproportionation and transalkylation of the starting material. HZSM-5 zeolite is one of the solid acid materials that has shown the best performance in this regard. Combinations of heterogeneous catalysts with the zeolite have also proven successful in this regard and provide a breakthrough towards the industrial production of phenol and olefins from lignin.[45] Advances in phenol production from lignin model compounds and lignin are summarized in Table 4.[45]

Table 4. Overview of the production of phenol from lignin model compounds and lignin[45]

Feedstock	Catalyst	Medium	Major product	Phenol yield	Ref.
propylphenol	H-ZSM-5	H_2O	phenol and propylene	98 mol%	[53, 54]
ethylphenol	H-ZSM-5	H_2O	phenol and ethylene	95 mol%	[55]
2-methoxy-4-propylphenol	Pt/C + zeolite	H_2O	phenol	60 mol%	[56]
2-methoxy-4-propylphenol	Au/TiO2 + H-ZSM-5	benzene	phenol and cresol	60 mol%	[57]
pine wood	Pt/C + MoP/SiO_2 + ZSM-5	benzene	phenol and olefin	9.6 mol%	[58]
organosolv lignin oil	Ni/SiO_2 + Hierarchical ZSM-5	H_2O	phenol and propylene	20% w/w	[59]
organosolv poplar lignin	Ru/CeO_2 + $CuCl_2$	H_2O	phenol	13% w/w	[60]

Currently, phenol is synthesized through either (1) the reaction of functionalized benzene, (2) the oxidation of alkyl-substituted benzene, (3) through the direct oxidation of benzene, or (4) through aliphatic transformation. Since no reagent can directly hydroxylate the benzene ring due to the inability

of any reagent to generate the necessary ^{+}OH electrophile, additional synthetic manipulations departing from the available substituted benzene products are required. Industrially, phenol is obtained through the cumene (Scheme 1) or the Dow process (Scheme 2). The cumene process also produces acetone, and 98% of the world's production of these products is achieved through this strategy.[61] At a small scale, phenol can be obtained by reducing the nitro group, followed by diazotization of the resulting aniline and displacement of N_2 to introduce a hydroxyl group (Scheme 3).[36] Other non-lignin sources of phenol include its extraction from coal tar using strong alkaline media, deep eutectic solvents,[62, 63] or through high-flux centrifugal extraction.[64]

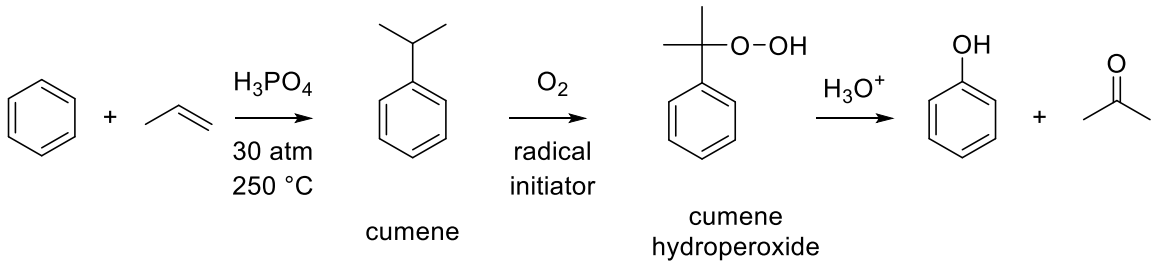

Scheme 1. Cumene process

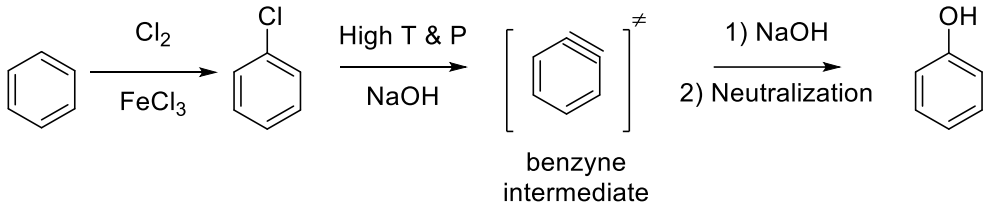

Scheme 2. Dow process

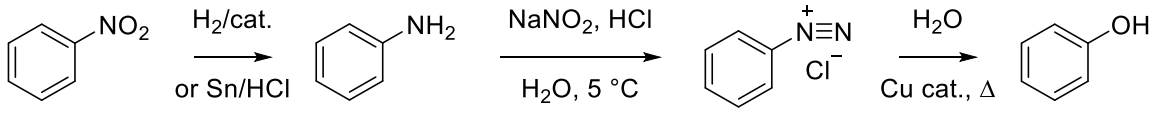

Scheme 3. Nitrobenzene to phenol

Phenol is an appealing target molecule due to its potential to replace aryl halides as substrates in cross-coupling reactions. Nonetheless, the hydroxyl group in phenols is very reactive due to its acidity; pK_a

10 compared to cyclohexanol, pK_a 16.[36] Furthermore, the C_{aryl}–O bond has a high dissociation energy. Thus, earlier studies focused on finding ways to transform phenols into phenol derivatives as a way to remove the acidic proton and reduce the BDE of the C_{aryl}–O bond (Scheme 4).[65] Several methodologies have been developed using various phenol derivatives and have been previously reviewed and summarized by our group.[65] However, it is far more desirable to directly cross-couple phenols with nucleophiles *via* C_{aryl}–O cleavage.

Phenol cross-coupling in the gas phase was first explored in 1966 and has since been optimized for amminolysis, with some gas-phase thiolation efforts.[65] Furthermore, these processes require very high temperatures (above 250 °C), carefully designed heterogeneous catalysts, and continuous flow reactors, limiting the applicability of these methodologies.[65] The first example of phenol cross-coupling in the liquid phase was reported in 1985, where phenol and cyclohexanol can be coaminated with ammonia by employing cyclohexanol as the hydrogen transfer reagent in the presence of Pd/C as the catalyst at 250 °C.[66] In 2012, our group developed a dehydrogenative aromatization process using 2-cyclohexen-1-one (and cyclohexanone) as the substrate to yield aromatic ethers or anilines (Scheme 5).[67]

In 2015, inspired by our findings and notable findings from Stahl,[68, 69] our group reported a mild and highly efficient methodology to directly couple phenol with amines (Scheme 6). [70]

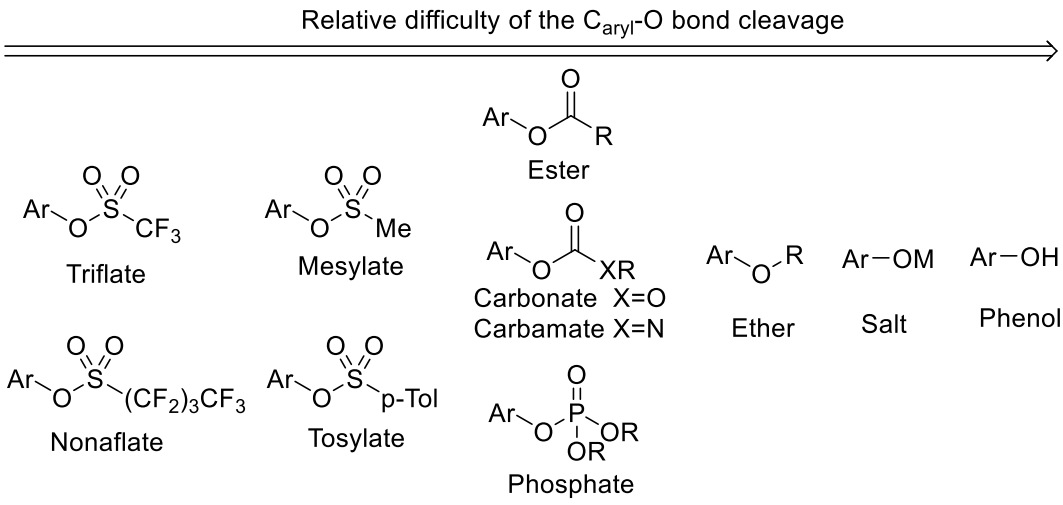

Scheme 4. Relative difficulty of cross-coupling reactions with phenol and derivatives[65]

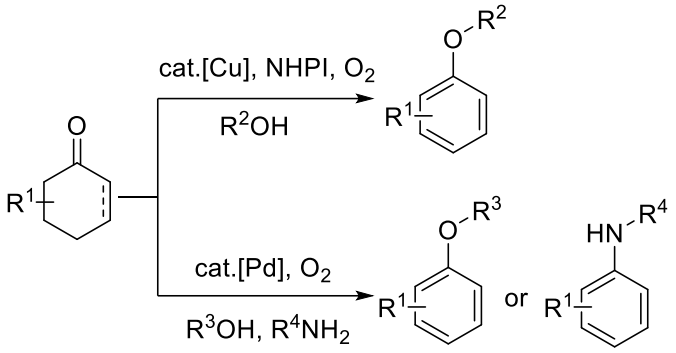

Scheme 5. Oxidative catalytic dehydrogenative aromatization[67]

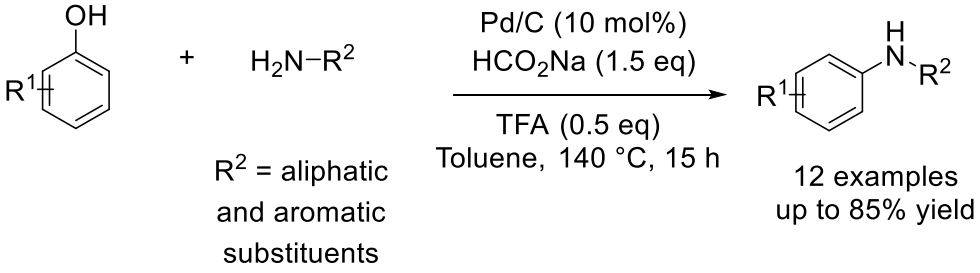

Scheme 6. Formal direct cross-coupling of phenol with amines[70]

This procedure achieves the coupling of phenol with amines by using sodium formate as the hydride source and Pd/C as the catalyst, in the presence of catalytic amounts of TFA. This transformation proceeds through a hydrogen-borrowing strategy which consists of dearomatizing the ring to generate a ketone, condensation of the amine to the ring, and rearomatization to yield the corresponding aromatic compounds (Scheme 7).[70] The reaction tolerates a broad scope of phenols, catechols and naphthols with primary, secondary, aliphatic and aromatic amines as nucleophiles. The reaction can also be performed in a flow reactor.[71]

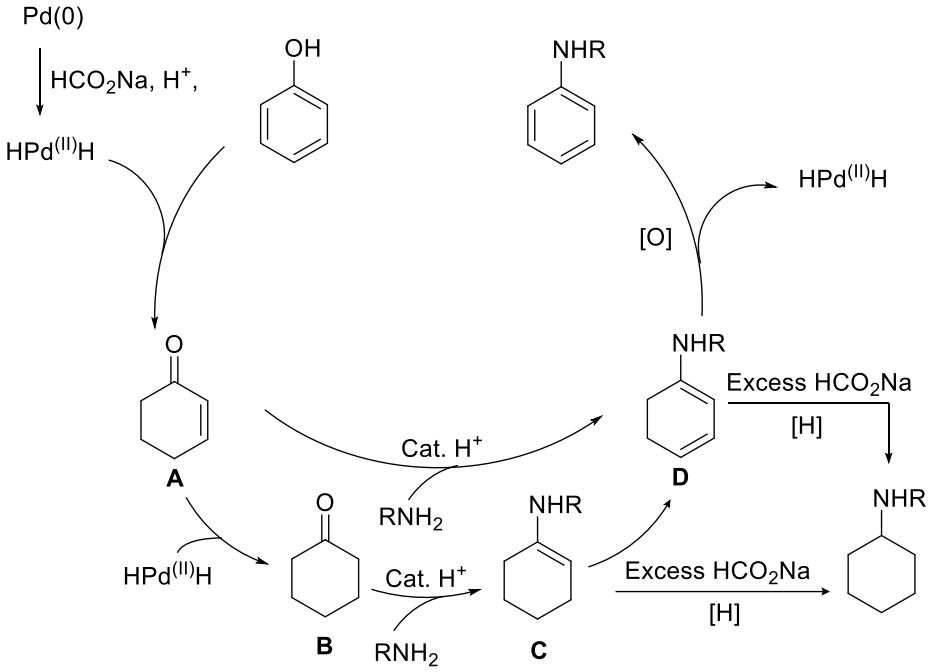

Scheme 7. Proposed mechanism for the direct cross-coupling of phenol with amines[70]

.

1.4 Amino Acids and their *N*-Modification

While lignin can serve as a biorenewable hydrocarbon supply, amino acids can serve as a source for nitrogen and chirality. Amino acids are simple organic compounds containing at least one amino and one carboxylic function. α -amino acids have a primary amino group (except for proline) and a carboxylic group substituent on the same carbon atom (Figure 16). More than 700 amino acids have been discovered in nature, and most of them are α-amino acids.[72] Bacteria, fungi and algae and other plants provide nearly all of these, which exist either in the free form or bound up into larger biomolecules.[72] Since deciphering the genetic code, 22 proteinogenic L-α-amino acids have been encoded.[73] These serve as building blocks in living cells for protein synthesis, and they are fundamental to all life forms as building blocks for peptides and proteins.[72] There are many production methods, such as extraction, chemical synthesis, fermentation, and enzymatic conversion. [74] Most amino acids are now produced by fermentation, which is suitable for large-scale production of optically active compounds, although some such as glycine or dl-methionine are still made through chemical synthesis or enzymatic production.[74]

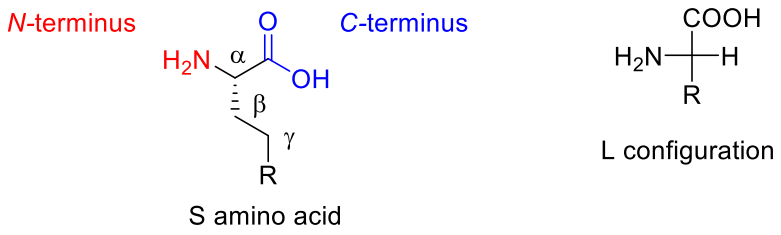

Figure 16. Amino acid structure and configuration

Peptides typically display high potency and target selectivity, making them valuable leads in developing new therapeutics, however, converting lead peptides to drugs represents a considerable challenge. [75] This is due to the lack of oral bioavailability of peptides due to their susceptibility to proteolysis in the gut, inefficient transport across the intestinal wall, proteolytic degradation in the bloodstream, and rapid clearance by the kidney.[75]

The *N*-terminus is a ubiquitous and practical handle, which can introduce diverse functional groups that can significantly alter the amino acid's physiological and pharmacological activities,[76, 77] especially when incorporated into peptides.[78] This is due to the loss of hydrogen-bonding potential at the affected site, reducing main-chain hydrogen bonds' role and potentially altering its binding properties.[75] Including

N-modified amino acids into a peptide sequence has been shown to enhance potency, change receptor subtype selectivity, and protect the peptide from proteolytic degradation.[75] In addition to their potential as structural backbones for pharmaceuticals[79, 80] and agrochemicals, [79, 81, 82] α-amino acids also play an essential role in organic synthesis and may function as organocatalysts[83-85] or ligands.[86] Furthermore, these modifications can facilitate the characterization of the *N*-terminal amino acid when adding fluorescent tags that can help identify them by light-absorbing methods[76] or in a peptide chain by mass spectrometry.[87]

Unfortunately, the sluggish nucleophilicity of amino acids, their pH sensitivity, and the broad range of functionalities at the α-position makes them challenging substrates for any coupling reaction. Despite these challenges, the *N*-arylation of amino acids has been achieved using the classical Ullmann[88, 89] or the Buchwald-Hartwig coupling reactions.[90] *N*-mono-alkylation has been often attained by reductive aminations using boron or transition metal complexes as the reducing agents,[91, 92] and most recently, through hydrogen-borrowing strategies allowing the use of aliphatic alcohols as the alkylating reagents.[93, 94] However, challenges such as the use of organic halides, low selectivity and high temperatures remain to be addressed.

1.5 Summary and Outlook

The need for sustainable chemical transformation is critical to our society's continuous development, as highlighted by the 2030 agenda for sustainable development of the United Nations. The vast majority of chemicals rely on petroleum supplies, which not only invalidates the efforts towards achieving the sustainable development goals but will also require a significant investment in heavy oil refinement due to depletion of this nonrenewable resource. Lignin is a biorenewable resource that could in part replace oil as a raw material. Lignin is a polyaromatic polymer in plant cell walls and is considered the most abundant noncarbohydrate polymer on earth. While its isolation and depolymerization pose significant challenges, significant advances have been made in both regards. Phenol is commonly a target product of lignin depolymerization. Studies have shown that it is possible to obtain this product from natural lignin using catalytic systems involving platinum, nickel, or ruthenium. Phenol is appealing due to its applicability in cross-coupling reactions. However, most strategies require the modification of the hydroxyl group to generate a more labile C_{aryl}-O bond while removing the acidic phenolic proton. More atom efficient methodologies involving the reduction and rearomatization of the phenolic ring have been developed, allowing for more direct phenol utilization in organic synthesis.

On the other hand, amino acids are a naturally abundant and biorenewable source of chirality and nitrogen. Their *N*-modification is a challenging yet essential endeavor required for increasing the stability of these compounds, especially when incorporated into pharmaceuticals or agrochemicals. *N*-arylation of amino acids has been achieved through Ullman and Buchwald-Hartwig couplings, requiring aryl halides or triflates as cross-coupling partners. *N*-mono-alkylation has been attained by reductive aminations and, most recently, through hydrogen-borrowing strategies allowing the use of aliphatic alcohols as the alkylating reagents. Given that no methodologies had been developed for the formal cross-coupling of phenol with α-amino acids, the development and optimization of the given methodology is the subject of the following chapters.

References

1. UN General Assembly, *Transforming Our World: The 2030 Agenda for Sustainable Development* [Online]; United Nations: New York, 2015. https://sustainabledevelopment.un.org/post2015/transformingourworld/publication (accessed March 9, 2020).

2. United Nations, 2015. Sustainable Development Goals. https://sdgs.un.org/goals (accessed March 9, 2020).

3. Anastas, P. T.; Warner, J. C., *Green Chemistry: Theory and Practice*. Oxford University Press: Oxford, UK, 2000.

4. Anastas, P. T.; Zimmerman, J. B., The Molecular Basis of Sustainability. *Chem* **2016,** *1* (1), 10-12.

5. Anastas, P. T.; Zimmerman, J. B., The United Nations sustainability goals: How can sustainable chemistry contribute? *Curr. Opin. Green Sustain. Chem.* **2018,** *13*, 150-153.

6. Anastas, P. T.; Eghbali, N., Green Chemistry: Principles and Practice. *Chem. Soc. Rev.* **2010,** *39* (1), 301-312.

7. Axon, S.; James, D., The UN Sustainable Development Goals: How can sustainable chemistry contribute? A view from the chemical industry. *Curr. Opin. Green Sustain. Chem.* **2018,** *13*, 140-145.

8. Burgman, M.; Tennant, M.; Voulvoulis, N.; Makuch, K.; Madani, K., Facilitating the transition to sustainable green chemistry. *Curr. Opin. Green Sustain. Chem.* **2018,** *13*, 130-136.

9. Hitce, J.; Xu, J.; Brossat, M.; Frantz, M.-C.; Dublanchet, A.-C.; Philippe, M.; Dalko-Csiba, M., UN sustainable development goals: How can sustainable/green chemistry contribute? Green chemistry as a source of sustainable innovations in the cosmetic industry. *Curr. Opin. Green Sustain. Chem.* **2018,** *13*, 164-169.

10. Lambin, A.; Corpart, J.-M., UN sustainable development goals and green chemistry, key points for sustainably innovating at Roquette, a global leader in plant-based ingredients. *Curr. Opin. Green Sustain. Chem.* **2018,** *13*, 137-139.

11. Pavez, P.; Honores, J.; Millán, D.; Isaacs, M., UN sustainable development goals: How can sustainable/green chemistry contribute? *Curr. Opin. Green Sustain. Chem.* **2018,** *13*, 154-157.

12. OECD, *Saving Costs in Chemicals Management: How the OECD Ensures Benefits to Society* [Online]; OECD Publishing: Paris, 2019. https://doi.org/10.1787/9789264311718-en (accessed June 9, 2020).

13. BCG, 2020. Moving Beyond Corporate Social Responsibility. https://www.bcg.com/en-ca/capabilities/social-impact/business-society.aspx (accessed January 31, 2020).

14. OECD. *Environmental Outlook for the Chemicals Industry* [Online]; OECD: Paris, 2001. https://www.oecd.org/env/ehs/2375538.pdf (accessed June 9, 2020).

15. Reibstein, R., A more ethical chemistry. *Curr. Opin. Green Sustain. Chem.* **2017,** *8*, 36.

16. Warner, J. C.; Cannon, A. S.; Dye, K. M., Green chemistry. *Environ. Impact Assess. Rev.* **2004,** *24* (7), 775-799.

17. Mulvihill, M. J.; Beach, E. S.; Zimmerman, J. B.; Anastas, P. T., Green Chemistry and Green Engineering: A Framework for Sustainable Technology Development. *Annu. Rev. Environ. Resour.* **2011,** *36* (1), 271-293.

18. OECD. *40 Years of Chemical Safety at the OECD: Quality and Efficiency* [Online]; OECD: Paris, 2011. www.oecd.org/env/ehs/48153344.pdf (accessed June 9, 2020).

19. Ragauskas, A. J.; Williams, C. K.; Davison, B. H.; Britovsek, G.; Cairney, J.; Eckert, C. A.; Frederick, W. J.; Hallett, J. P.; Leak, D. J.; Liotta, C. L.; Mielenz, J. R.; Murphy, R.; Templer, R.; Tschaplinski, T., The Path Forward for Biofuels and Biomaterials. *Science* **2006,** *311* (5760), 484-489.

20. *BP Energy Outlook,* 2019 ed.; British Petroleum Company; BP p.l.c.: London, UK,2019.

21. Tullo, A. H., Why the future of oil is in chemicals, not fuels. *Chem. Eng. News* **2019,** *97* (8).

22. Winner, L., The Whale and the Reactor: A Personal Memoir. *J. Am. Cult.* **1980,** *3* (3), 446-455.

23. Wauquier, J.-P. *Petroleum Refining, Volume 1 – Crude Oil, Petroleum Products, Process Flowsheets.* Technip Editions: Paris, 1995.

24. Speight, J. G., *Heavy oil recovery and upgrading*. Elsevier: Cambridge, MA, 2019.

25. Speight, J. G., *The chemistry and technology of petroleum.* 5th ed.; CRC Press, Taylor and Francis: Hoboken, 2014.

26. Millington, D., *Low crude oil prices and their impact on the Canadian economy*. Canadian Energy Research Institute: Canada, 2016.

27. Simon, S.; Ruwoldt, J.; Sjöblom, J., A critical update of experimental techniques of bulk and interfacial components for fluid characterization with relevance to well fluid processing and transport. *Adv. Colloid Interface Sci.* **2020,** *277*, 102-120.

28. Qiao, P.; Harbottle, D.; Tchoukov, P.; Masliyah, J.; Sjoblom, J.; Liu, Q.; Xu, Z., Fractionation of Asphaltenes in Understanding Their Role in Petroleum Emulsion Stability and Fouling. *Energy Fuels* **2017,** *31* (4), 3330-3337.

29. Wauquier, J.-P. Pure Components. In *Petroleum Refinining, Volume 1 – Crude Oil, Petroleum Products, Process Flowsheets.* Technip Editions: Paris, 1995; pp 2.

30. Murgich, J., Molecular Simulation and the aggregation of the heavy fractions in crude oils. *Mol. Simul.* **2003,** *29*, 451-461.

31. Speight, J. G., *The Chemistry and Technology of Petroleum,* 5th ed.; CRC Press: Boca Raton, 2014.

32. Matar, S.; Hatch, L. F., Crude Oil Processing and Production of Hydrocarbon Intermediates. In *Chemistry of Petrochemical Processes*, 2nd ed.; Matar, S.; Hatch, L. F., Eds. Gulf Professional Publishing: Woburn, 2001; pp 49-110.

33. Yen, T. F., *Chemistry for Engineers*; Imperial College Press: London, 2008.

34. Speight, J. G., Molecular Weights of Nonvolatile Fractions. In *Handbook of Petroleum Analysis*, 2nd ed.; Winefordner, J.D., Ed.; John Wiley & Sons: US, 2001; a) p. 356, b) p 367

35. Burdick, D. L.; Leffler, W. L., 3. Benzene. In *Petrochemicals in Nontechnical Language*, 4th ed.; PennWell: Tulsa, OK, 2010.

36. Clayden, J.; Warren, S. G.; Greeves, N. *Organic Chemistry*, 2nd ed.; Oxford University Press: Oxford, 2012.

37. Kürti, L.; Czakó, B. *Strategic applications of named reactions in organic synthesis: background and detailed mechanisms*, 1st ed.; Elsevier Academic Press: Amsterdam, 2005.

38. Kuhlborn, J.; Gross, J.; Opatz, T., Making natural products from renewable feedstocks: back to the roots? *Nat. Prod. Rep.* **2020,** *37* (3), 380-424.

39. Arapova, O. V.; Chistyakov, A. V.; Tsodikov, M. V.; Moiseev, I. I., Lignin as a Renewable Resource of Hydrocarbon Products and Energy Carriers (A Review). *Pet. Chem.* **2020,** *60* (3), 227-243.

40. Abdelaziz, O. Y.; Hulteberg, C. P., Lignin Depolymerization under Continuous-Flow Conditions: Highlights of Recent Developments. *ChemSusChem* **2020**, *13* (17), 4382-4384.

41. Sun, Z.; Fridrich, B.; de Santi, A.; Elangovan, S.; Barta, K., Bright Side of Lignin Depolymerization: Toward New Platform Chemicals. *Chem. Rev.* **2018,** *118* (2), 614-678.

42. Bajwa, D. S.; Pourhashem, G.; Ullah, A. H.; Bajwa, S. G., A concise review of current lignin production, applications, products and their environment impact. *Ind. Crops Prod.* **2019,** *139*, 111526.

43. Christopher, L. P.; Yao, B.; Ji, Y., Lignin Biodegradation with Laccase-Mediator Systems. *Front. Energy Res.* **2014,** *2* (12).

44. Chan, J. C.; Paice, M.; Zhang, X., Enzymatic Oxidation of Lignin: Challenges and Barriers Toward Practical Applications. *ChemCatChem* **2020,** *12* (2), 401-425.

45. Shen, X.; Xin, Y.; Liu, H.; Han, B., Product-oriented Direct Cleavage of Chemical Linkages in Lignin. *ChemSusChem* **2020**, *13*, 4367-4381.

46. Yoo, C. G.; Meng, X.; Pu, Y.; Ragauskas, A. J., The critical role of lignin in lignocellulosic biomass conversion and recent pretreatment strategies: A comprehensive review. *Bioresour. Technol.* **2020,** *301*, 122784.

47. Cao, Y.; Chen, S. S.; Zhang, S.; Ok, Y. S.; Matsagar, B. M.; Wu, K. C. W.; Tsang, D. C. W., Advances in lignin valorization towards bio-based chemicals and fuels: Lignin biorefinery. *Bioresour. Technol.* **2019,** *291*, 121878.

48. Gale, M.; Cai, C. M.; Gilliard-Abdul-Aziz, K. L., Heterogeneous Catalyst Design Principles for the Conversion of Lignin into High-Value Commodity Fuels and Chemicals. *ChemSusChem* **2020,** *13* (8), 1947-1966.

49. Jing, Y.; Dong, L.; Guo, Y.; Liu, X.; Wang, Y., Chemicals from Lignin: A Review of Catalytic Conversion Involving Hydrogen. *ChemSusChem* **2020**, *13*, 4181-4198.

50. Garedew, M.; Lin, F.; Song, B.; DeWinter, T. M.; Jackson, J. E.; Saffron, C. M.; Lam, C. H.; Anastas, P. T., Greener Routes to Biomass Waste Valorization: Lignin Transformation Through Electrocatalysis for Renewable Chemicals and Fuels Production. *ChemSusChem* **2020**, *13*, 4214-4237.

51. Weiss, R.; Guebitz, G. M.; Pellis, A.; Nyanhongo, G. S., Harnessing the Power of Enzymes for Tailoring and Valorizing Lignin. *Trends Biotechnol.* **2020**, *38* (11), 1215-1235.

52. Han, X.; Guo, Y.; Liu, X.; Xia, Q.; Wang, Y., Catalytic conversion of lignocellulosic biomass into hydrocarbons: A mini review. *Catal. Today* **2019,** *319*, 2-13.

53. Liao, Y.; d'Halluin, M.; Makshina, E.; Verboekend, D.; Sels, B. F., Shape selectivity vapor-phase conversion of lignin-derived 4-ethylphenol to phenol and ethylene over acidic aluminosilicates: Impact of acid properties and pore constraint. *Appl. Catal., B* **2018,** *234*, 117-129.

54. Liao, Y.; Zhong, R.; Makshina, E.; d'Halluin, M.; van Limbergen, Y.; Verboekend, D.; Sels, B. F., Propylphenol to Phenol and Propylene over Acidic Zeolites: Role of Shape Selectivity and Presence of Steam. *ACS Catal.* **2018,** *8* (9), 7861-7878.

55. Verboekend, D.; Liao, Y.; Schutyser, W.; Sels, B. F., Alkylphenols to phenol and olefins by zeolite catalysis: a pathway to valorize raw and fossilized lignocellulose. *Green Chem.* **2016,** *18* (1), 297-306.

56. Zhang, J.; Lombardo, L.; Gözaydın, G.; Dyson, P. J.; Yan, N., Single-step conversion of lignin monomers to phenol: Bridging the gap between lignin and high-value chemicals. *Chinese J. Catal.* **2018,** *39* (9), 1445-1452.

57. Huang, X.; Ludenhoff, J. M.; Dirks, M.; Ouyang, X.; Boot, M. D.; Hensen, E. J. M., Selective Production of Biobased Phenol from Lignocellulose-Derived Alkylmethoxyphenols. *ACS Catal.* **2018,** *8* (12), 11184-11190.

58. Ouyang, X.; Huang, X.; Boot, M. D.; Hensen, E. J. M., Efficient Conversion of Pine Wood Lignin to Phenol. *ChemSusChem* **2020,** *13* (7), 1705-1709.

59. Liao, Y.; Koelewijn, S.-F.; Van den Bossche, G.; Van Aelst, J.; Van den Bosch, S.; Renders, T.; Navare, K.; Nicolaï, T.; Van Aelst, K.; Maesen, M.; Matsushima, H.; Thevelein, J. M.; Van Acker, K.; Lagrain, B.; Verboekend, D.; Sels, B. F., A sustainable wood biorefinery for low–carbon footprint chemicals production. *Science* **2020,** *367* (6484), 1385-1390.

60. Wang, M.; Liu, M.; Li, H.; Zhao, Z.; Zhang, X.; Wang, F., Dealkylation of Lignin to Phenol via Oxidation–Hydrogenation Strategy. *ACS Catal.* **2018,** *8* (8), 6837-6843.

61. Coker, A. *Phenol, Acetone, Cumene*; Nexant: Nexant, February 2012.

62. Jiao, T.; Zhuang, X.; He, H.; Li, C.; Chen, H.; Zhang, S., Separation of Phenolic Compounds from Coal Tar via Liquid–Liquid Extraction Using Amide Compounds. *Ind. Eng. Chem. Res.* **2015,** *54* (9), 2573-2579.

63. Jiao, T.; Qin, X.; Zhang, H.; Zhang, W.; Zhang, Y.; Liang, P., Separation of phenol and pyridine from coal tar via liquid–liquid extraction using deep eutectic solvents. *Chem. Eng. Res. Des.* **2019,** *145*, 112-121.

64. Zhao, Y.; Mao, X.; Li, W.; Gu, X.; Wang, G., Study on extraction phenol from coal tar with high flux centrifugal extractor. *Int. J. Coal Sci. Technol.* **2017,** *4* (4), 333-341.

65. Zeng, H.; Qiu, Z.; Domínguez-Huerta, A.; Hearne, Z.; Chen, Z.; Li, C.-J., An Adventure in Sustainable Cross-Coupling of Phenols and Derivatives via Carbon–Oxygen Bond Cleavage. *ACS Catal.* **2017,** *7* (1), 510-519.

66. Hamada, H.; Yamamoto, M.; Kuwahara, Y.; Matsuzaki, T.; Wakabayashi, K., The Co-amination of Phenol and Cyclohexanol with Palladium-on-carbon Catalyst in the Liquid Phase. An Application of a Hydrogen-transfer Reaction. *Bull. Chem. Soc. Jpn.* **1985,** *58* (5), 1551-1555.

67. Girard, S. A.; Hu, X.; Knauber, T.; Zhou, F.; Simon, M.-O.; Deng, G.-J.; Li, C.-J., Pd-Catalyzed Synthesis of Aryl Amines via Oxidative Aromatization of Cyclic Ketones and Amines with Molecular Oxygen. *Org. Lett.* **2012,** *14* (21), 5606-5609.

68. Iosub, A. V.; Stahl, S. S., Palladium-Catalyzed Aerobic Dehydrogenation of Cyclic Hydrocarbons for the Synthesis of Substituted Aromatics and Other Unsaturated Products. *ACS Catal.* **2016,** *6* (12), 8201-8213.

69. Girard, S. A.; Huang, H.; Zhou, F.; Deng, G.-J.; Li, C.-J., Catalytic dehydrogenative aromatization: an alternative route to functionalized arenes. *Org. Chem. Front.* **2015,** *2* (3), 279-287.

70. Chen, Z.; Zeng, H.; Girard, S. A.; Wang, F.; Chen, N.; Li, C.-J., Formal Direct Cross-Coupling of Phenols with Amines. *Angew. Chem., Int. Ed.* **2015,** *54* (48), 14487-14491.

71. Jumde, V. R.; Petricci, E.; Petrucci, C.; Santillo, N.; Taddei, M.; Vaccaro, L., Domino Hydrogenation–Reductive Amination of Phenols, a Simple Process To Access Substituted Cyclohexylamines. *Org. Lett.* **2015,** *17* (16), 3990-3993.

72. Barrett, G. C.; Elmore, D. T. *Amino Acids and Peptides*. Cambridge University Press: Cambridge, UK, 1998.

73. Rejsek, K.; Formanek, P.; Vranova, V. *Soil Amino Acids: Quality, Distribution and Site Ecology*. Nova Science Publishers Inc.: New York, US, 2010.

74. Tonouchi, N.; Ito, H. Present Global Situation of Amino Acids in Industry. In *Amino Acid Fermentation*, Yokota, A.; Ikeda, M., Eds. Springer Japan: Tokyo, 2017; pp 3-14.

75. Hughes, A. B., *Amino Acids, Peptides and Proteins in Organic Chemistry, Analysis and Function of Amino Acids and Peptides*. John Wiley & Sons, Incorporated: Somerset, Germany, 2011.

76. Modification of Amino Groups. In *Current protocols in protein science*, Coligan, J.E.; Dunn, B.M.; Ploegh, H.D.; Speicher, D.W.; Wingfield, P.T., Eds.; Wiley-VCH Verlag GmbH: 1996.

77. Park, J. D.; Kim, D. H., Cysteine Derivatives as Inhibitors for Carboxypeptidase A: Synthesis and Structure−Activity Relationships. *J. Med. Chem.* **2002,** *45* (4), 911-918.

78. Liu, W. X.; Wang, R., Endomorphins: potential roles and therapeutic indications in the development of opioid peptide analgesic drugs. *Med. Res. Rev.* **2012,** *32* (3), 536-580.

79. Drauz, K.; Grayson, I.; Kleemann, A.; Krimmer, H.-P.; Leuchtenberger, W.; Weckbecker, C., Amino acids. In *Ullmann's Fine Chemicals*, Wiley-VCH Verlag GmbH: 2014; Vol. 1, pp 165-222.

80. Mendez-Samperio, P., Peptidomimetics as a new generation of antimicrobial agents: current progress. *Infect. Drug Resist.* **2014,** *7*, 229-237.

81. Zhao, J.; Qu, W.; Lin, D.; Kong, L.; Huang, Q.; Li, F.; Zhe, D., Application of α-amino acids in agrochemicals synthesis. *Nongyaoxue Xuebao* **2010,** *12* (4), 371-382.

82. Lamberth, C., Amino acid chemistry in crop protection. *Tetrahedron* **2010,** *66* (36), 7239-7256.

83. Xie, H.; Hayes, T.; Gathergood, N., Amino Acid Organocatalysis. In *Amino Acids, Peptides and Proteins in Organic Chemistry*, Wiley-VCH Verlag GmbH: 2009; pp 281-337.

84. Xu, L.-W.; Lu, Y., Non-Proline Amino Acid Catalysts. In *Comprehensive Enantioselective Organocatalysis: Catalysts, Reactions, and Applications*, Wiley-VCH Verlag GmbH: 2013; Vol. 1, pp 51-68.

85. Zhao, X.; Zhu, B.; Jiang, Z., Acyclic Amino Acid Based Bifunctional Chiral Tertiary Amines, Quaternary Ammoniums and Iminophosphoranes as Organocatalysts. *Synlett* **2015,** *26* (16), 2216-2230.

86. Zhang, F.-L.; Hong, K.; Li, T.-J.; Park, H.; Yu, J.-Q., Functionalization of C(sp3)–H bonds using a transient directing group. *Science* **2016,** *351* (6270), 252-256.

87. Takashi, N., Chemistry in Proteomics: An Interplay between Classical Methods in Chemical Modification of Proteins and Mass Spectrometry at the Cutting Edge. *Curr. Proteomics* **2006,** *3* (1), 33-54.

88. Sharma, K. K.; Sharma, S.; Kudwal, A.; Jain, R., Room temperature *N*-arylation of amino acids and peptides using copper(I) and β-diketone. *Org. Biomol. Chem.* **2015,** *13* (16), 4637-4641.

89. Sharma, K. K.; Mandloi, M.; Rai, N.; Jain, R., Copper-catalyzed *N*-(hetero)arylation of amino acids in water. *RSC Adv.* **2016,** *6* (99), 96762-96767.

90. King, S. M.; Buchwald, S. L., Development of a method for the *N*-arylation of amino acid esters with aryl triflates. *Org. Lett.* **2016,** *18* (16), 4128-4131.

91. Baxter, E. W.; Reitz, A. B., Reductive Aminations of Carbonyl Compounds with Borohydride and Borane Reducing Agents. In *Organic Reactions*, John Wiley & Sons, Inc.: 2004.

92. Song, Y.; Sercel, A. D.; Johnson, D. R.; Colbry, N. L.; Sun, K.-L.; Roth, B. D., A simple method for preparation of *N*-mono- and *N,N*-di-alkylated α-amino acids. *Tetrahedron Lett.* **2000,** *41* (43), 8225-8230.

93. Xu, C.-P.; Xiao, Z.-H.; Zhuo, B.-Q.; Wang, Y.-H.; Huang, P.-Q., Efficient and chemoselective alkylation of amines/amino acids using alcohols as alkylating reagents under mild conditions. *Chem. Commun.* **2010,** *46* (41), 7834-7836.

94. Yan, T.; Feringa, B. L.; Barta, K., Direct *N*-alkylation of unprotected amino acids with alcohols. *Sci. Adv.* **2017,** *3* (12).

Chapter 2 . *N*-Arylation of α-amino acids using cyclohexenone

2.1 Background

The *N*-arylation of amino acids has been a longtime sought by chemists. As discussed in the previous chapter, amino acid *N*-arylation can impact the amino acid's physiological interactions due to the loss of hydrogen bonding potential at the *N*-terminus.[1] In addition, the introduction of the aryl can induce other non-covalent interactions,[2] while simultaneously blocking the possibility of chain elongation through amide-bond formation.[3] These modified qualities make *N*-arylated amino acids especially attractive for drug design and development, as these moieties can be recognized by a biological target while blocking its conventional pathway. Furthermore, the aromatic π-system can form non-covalent interactions with other molecules bearing π-electrons through π stacking, with halogens through halogen-π interactions, or with cations in a cation-π interaction, allowing these moieties to interact more efficiently at a macromolecule's binding site.[2] π-Interactions range from 1.8 to 5 kcal/mol (with π-cation interactions being the strongest).[2] These interactions occur when two aromatic rings are positioned face-to-face with a slight offset. This is due to the electrostatic attraction generated from the positively charged σ-framework with the negatively charged p-cloud or the ring, and the offset arises as the positive charge is largely on the peripheral due to the exposed hydrogen atoms.[4] These Van der Waals forces are proportional to the area of contact, thus weakened depending on the necessary offset.[4]

Some examples of incorporating *N*-arylated amino acids into bio-active compounds include PKC activators,[5] VLA-4 antagonists,[6] and bradykinin antagonists.[7] Protein kinase C is composed of 11 isozymes, making the synthesis of selective activators crucial to identify individual isozymes in physiological processes.[5] While inhibitors target enzymes, antagonists target receptors. VLA-4 stands for very late antigen 4. It is a transmembrane receptor present in leukocytes that bind to endothelial cells and lead to leukocyte infiltration before causing tissue damage in inflammatory diseases such as asthma, multiple sclerosis and arthritis.[6] Lastly, bradykinin is a nonapeptide that is implicated in various physiological responses such as pain, rhinitis, inflammation and allergies, causing pain and swelling.[7]

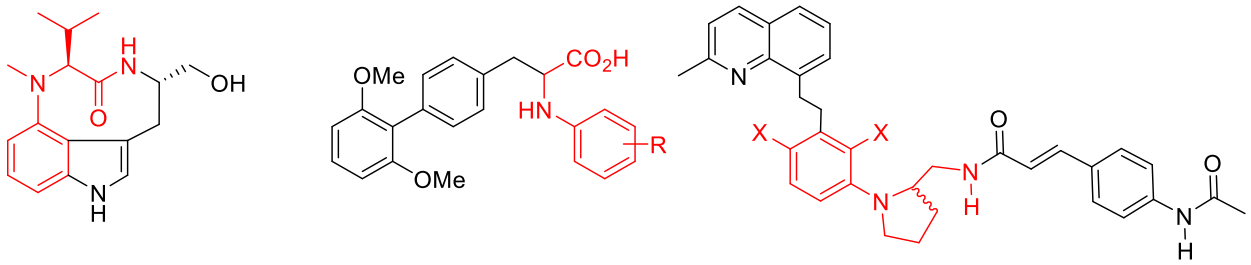

Figure 2.1 Selected examples of bioactive compounds with *N*-arylated amino acids

The synthesis of *N*-arylated amino acids has been carried out using hypervalent iodine[8] or nucleophilic aromatic substitution.[9, 10] More recently, the *N*-arylation of amino acids has been achieved through cross-coupling reactions using copper,[11, 12] palladium,[9, 13, 14] or enzymes[15] as catalysts. The aromatic coupling partners in these reactions are aryl halides, in the case of the Ullmann reaction, or aryl halides or pseudo-halides, in the case of the Buchwald-Hartwig coupling. These reactions proceed through oxidative addition to generate the corresponding aryl-copper or aryl-palladium species, followed by ligand displacement by coordination of the amino acid to the metal and completing the catalytic cycle through reductive elimination to yield the corresponding *N*-arylated product.[16]

Jain *et al.* reported in 2016 a successful microwave-induced Ullmann coupling for obtaining *N*-arylated α-amino acids.[11] Previously reported copper-catalyzed methods employed harsh conditions, including high temperatures, stoichiometric use of copper, and use of DMF or DMSO solvents, that ultimately resulted in racemization. This methodology allows for the *N*-arylation of natural and unnatural amino acids in its zwitterionic form with electronically and sterically diverse aryl and heteroaryl coupling partners without affecting the enantiopurity of the product, rendering this methodology especially attractive. Remarkably, strongly electron-withdrawing groups, including *o*-nitro, *p*-trifluoromethyl, *o,p*-difluoro, and *m,m*-difluoro, were well tolerated as substrates.

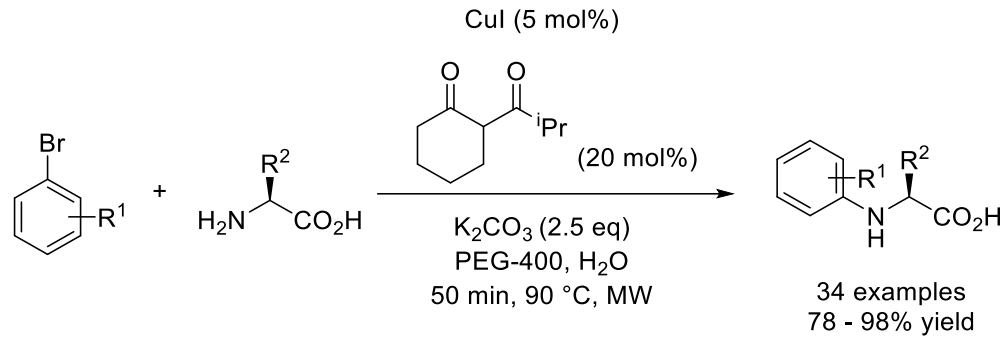

Scheme 2.1 Microwave-assisted Ullman coupling for the *N*-arylation of α-amino acids[11]

In 2016, 21 years after the first report of the Buchwald-Hartwig reaction, the group of Buchwald reported an optimized method for the palladium-catalyzed *N*-arylation of α- and β-amino esters.[13] The reaction tolerated methyl, *tert*-butyl, and benzyl esters as substrates. Reaction conditions result in minimal racemization of the amino acid ester. This reaction's success is attributed in part to the *t*-BuBrettPhos third-generation (G3) precatalysts, which enable the use of mild reaction conditions. The *N*-arylation of hydrophobic, aromatic, and polar amino acid esters was successfully achieved. The group of Proulx has more recently adopted this procedure for the *N*-arylation of resin supported peptides.[17]

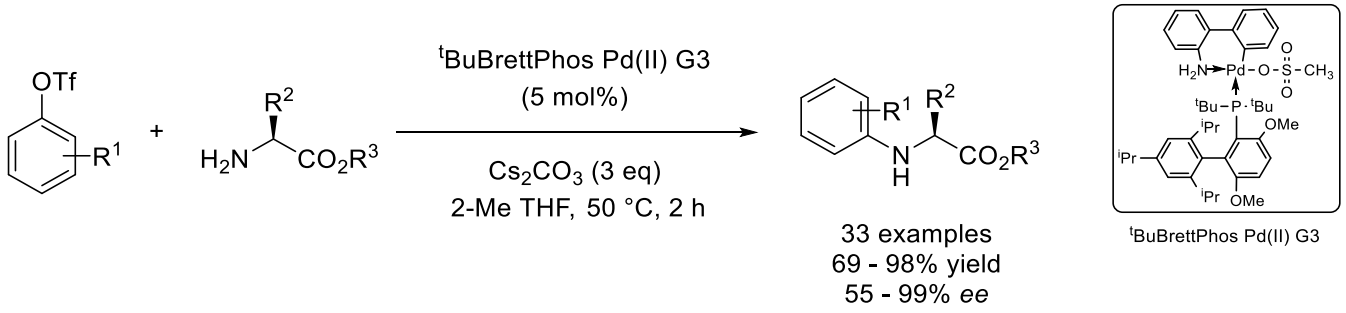

Scheme 2.2 Buchwald-Hartwig coupling for the *N*-arylation of α-amino esters[13]

In 2019, the group of Poelarends reported a biocatalytic route for the asymmetric synthesis of various *N*-arylated aspartic acids using ethylendiamine-*N,N*'-disuccinic acid lyase (EDDS lyase) as a biocatalyst.[15] This strategy uses arylamines and fumarate as substrates, yielding the corresponding products upon enzymatic transformation. The enzyme demonstrated to have a broad receptivity to different arylamines and was limited to fumarate as the electrophile. Nonetheless, the products were obtained with high enantiomeric excess. This methodology greatly differs from other chemical strategies in the sense that chirality is created from fumarate, a prochiral α,β-unsaturated acid to form the Cα

stereocenter of the target *N*-arylated amino acid in a single asymmetric step, showing both the importance of this type of building blocks, as well as the development of biocatalysts for organic synthesis.

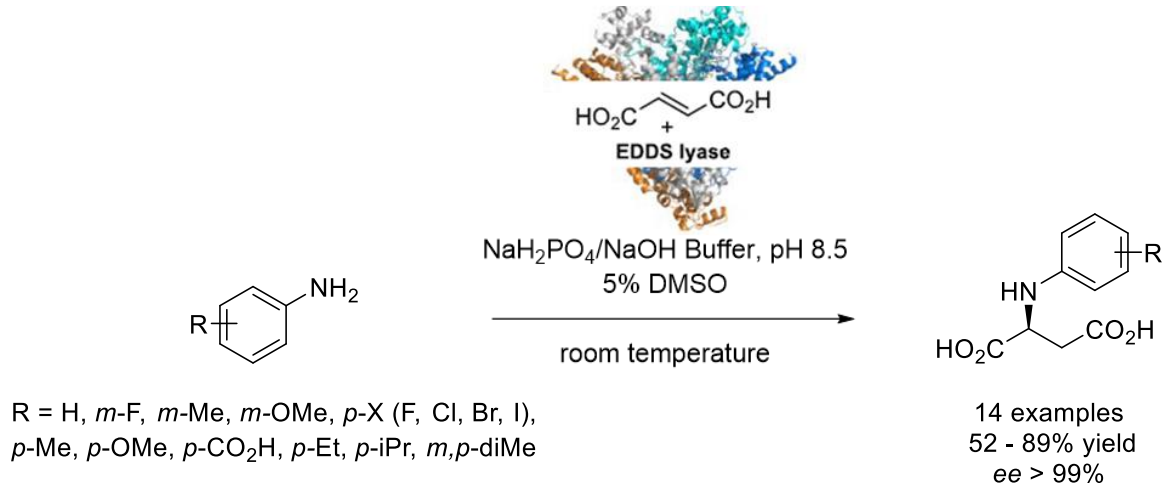

Scheme 2.3 Biocatalyzed synthesis of *N*-arylated aspartic acids[15]

2.2 Research objectives and plan

Given that most methodologies developed for the *N*-arylation of α-amino acids have mostly focused on using aryl halides or aryl triflates as the starting materials, we sought to find conditions for a more direct *N*-arylation without the need of pre-functionalized phenolic moieties. Based on previous research in our group using 2-cyclohexen-1-one and phenol to obtain *N*-alkylated[18, 19] and *N*-arylated[20-22] amines, we focused on testing α-amino acids as potential coupling partners under the reported conditions.

Amino acids are challenging substrates for coupling reactions due to their low nucleophilicity, pH sensitivity, and the broad range of reactive functionalities at the α-position. Initially, we tested phenol as the arylating reagent for L-alanine methyl ester hydrochloride under the previously reported conditions by our group (Scheme 2.4).[20] However, decarboxylation of the starting material was observed due to the high temperature required for the de- and re-aromatization of phenol. Only trace amounts of the desired product were detected by NMR despite modifying the amounts of sodium formate and triflic acid present in the reaction mixture.

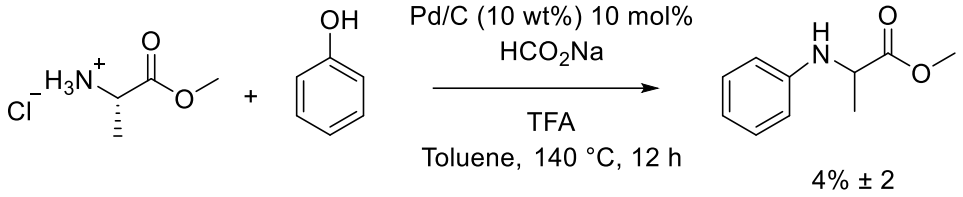

Scheme 2.4. Initial screening of the reaction between L-alanine methyl ester hydrochloride and phenol using previously reported conditions by our group[20]

In light of these results, we decided to remove complexity from our initial plan and solely focus on the *N*-coupling feasibility. Thus we decided on (1) using glycine as the model substrate to avoid difficulties due to the amino acid's side chain, (2) use the methyl ester hydrochloride salt of the amino acid to prevent the formation of 2,5-diketopiperazines (dimerization product) and avoid decarboxylation, and (3) use 2-cyclohexen-1-one instead of phenol as the coupling partner to remove the dearomatization step required for the condensation to occur, allowing us to focus solely on the condensation and aromatization steps of the reaction (Scheme 2.5).

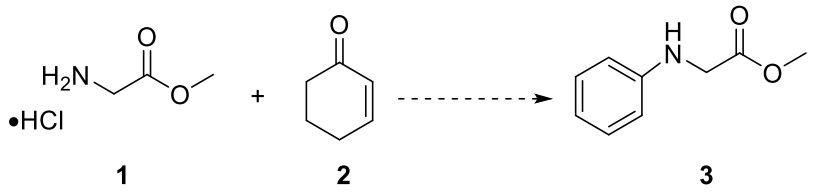

Scheme 2.5. Model reaction for the coupling of α-amino acids with 2-cyclohexen-1-one

We opted to first test different solvents due to the poor solubility of the hydrochloride salts in toluene, followed by the screening of acids and bases as additives in order to favour imine formation. While prior deprotonation of the substrate would have allowed for better solubility, the formation of 2,5-diketopiperazines remained a challenge, forcing us to work with the salts. Lastly, we would explore the substrate scope before revisiting the possibility of using phenol as a coupling partner.

2.3 Results and discussion

2.3.1 Condition Screening

The transformation was initially tested at a 0.2 M concentration using palladium on carbon with a 10 mol% Pd loading under an argon atmosphere and an excess amount of 2-cyclohexen-1-one (**2**) to facilitate nucleophilic addition. The reaction was first tested using dioxane as the solvent (Table 2.1, entry 1). The desired *N*-arylated product **3** was obtained in 26% yield, together with 107% phenol (**5**). In addition, *N*-Cyclohexylated glycine (**4**) was obtained as a byproduct in 9% yield and ketal **6** as a side product in 16% yield. We presumed that the yield might be improved if the solubility of salt **1** was enhanced. Thus, we tested different alcohols as co-solvents (Table 2.1, entries 2-4). An increase in yield for product **3** was observed. However, side product **6** was consistently observed despite different alcohols being present in the reaction mixture. Furthermore, there was high variability in the yield for reactions being run under the same conditions. We reckoned that ketal **5** had to be the result of the starting material **1** undergoing hydrolysis. Having glycine in its free carboxylic form would lead to decomposition of the starting material due to decarboxylation, as had been previously observed. In order to test this hypothesis, the reaction was run with 0.5 equiv of water (Table 2.1, entry 5), and with water as a co-solvent (Table 2.1, entry 6). Indeed, the formation of product **3** was suppressed, while the building of ketal **6** was still observed. To circumvent this obstacle a less hygroscopic solvent was tested. Toluene yielded desired product **3** in 47% yield with higher reproducibility and without the formation of side product **6** (Table 2.1, entry 7). Although results were nearly identical to those from entry 4, the hygroscopic nature of dioxane deterred us from choosing it as the solvent.

With the optimal solvent at hand and having observed the feasibility of the desired *N*-arylation, different additives were tested to favour imine formation (Table 2.2). Imine formation is favoured at a pH of 4.5, with acids catalyzing the hydrolysis while bases ensure the availability of the lone pair of electrons in the nitrogen for the nucleophilic attack to the ketone to be possible. Given that glycine was being used in its hydrochloric salt form, an addition of only 10 mol% of the acid additives was tested (Table 2.2, entries 2-5). Acid additives did not improve the reaction yield, and stronger acids decreased the formation of product **3**. Basic additives were then tested (Table 2.2, entries 6-11). Calcium carbonate gave the best results, yielding 63% of **3**, and 15% of **4** (Table 2.2, entry 10). Increasing the quantity of base resulted in the loss of activity (Table 2.2, entry 11).

Table 2.1 Solvent screening for the palladium-catalyzed *N*-arylation of glycine methyl ester hydrochloride using 2-cylohexen-1-one

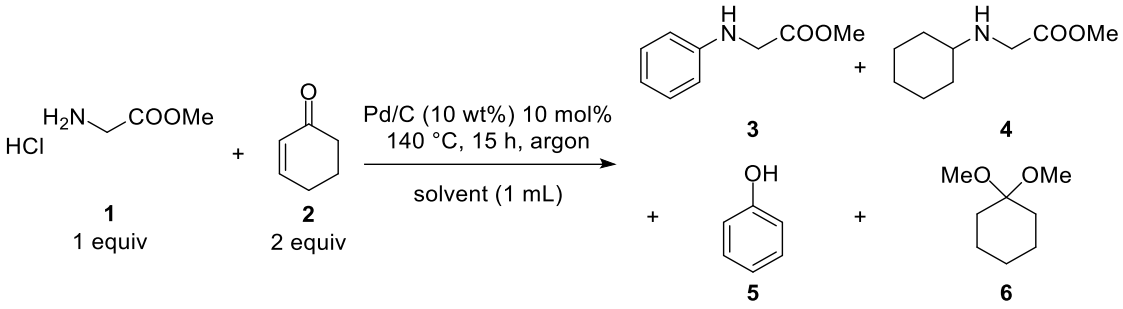

entry	solvent	yield (%)			
		3[a]	**4**[b]	**5**[b]	**6**[b]
1	dioxane	26 ± 10	9 ± 10	107	16 ± 14
2	dioxane : MeOH 8:2	31 ± 21	Traces	83	14 ± 12
3	dioxane : ^{i}PrOH 8:2	31 ± 1	Traces	112	32 ± 16
4	dioxane : ^{t}BuOH 8:2	47 ± 6	14 ± 7	97	Traces
5	dioxane + 0.5 equiv H_2O	7	ND	44	13
6	dioxane : H_2O 8:2	ND	ND	60	24
7	toluene	47 ± 6	20 ± 13	104	Traces

Reaction conditions: **1** (0.24 mmol, 1 equiv.), **2** (0.48 mmol, 2 equiv.), Pd/C (5 wt%, 0.48 mmol), additive, Ar saturated toluene (1 mL), 15 h, 140 °C, in a high pressure microwave vial. [a] Yield determined by ^{1}H NMR using 1,3,5-trimethoxybenzene as the internal standard. [b] Yield determined by GC-MS. ND: not detected.

Table 2.2. Acidic and basic additive screening for the palladium-catalyzed *N*-arylation of glycine methyl ester hydrochloride using 2-cylohexen-1-one

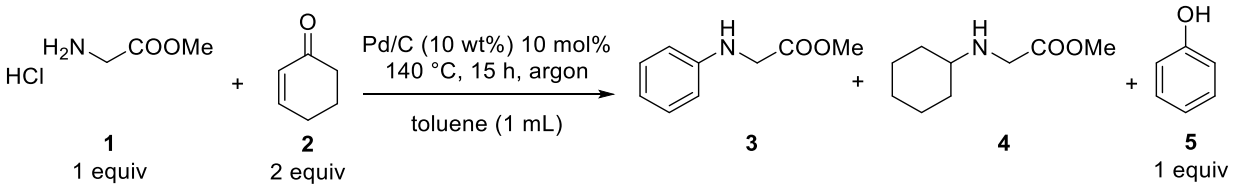

entry	additive (mol%)	yield (%)		
		3[a]	**4**[b]	**5**[b]
1	-	47	20	98
2	AcOH (10)	44	22	94
3	TFA (10)	42	14	69
4	MsOH (10)	36	17	95
5	TFSA (10)	32	16	92
6	DMAP (50)	40	ND	91
7	$NaHCO_3$ (50)	45	18	77
8	Cs_2CO_3 (50)	40	30	88
9	K_2CO_3 (50)	42	24	90
10	$CaCO_3$ (50)	63	15	95
11	$CaCO_3$ (60)	44	28	72

Reaction conditions: **1** (0.24 mmol, 1 equiv.), **2** (0.48 mmol, 2 equiv.), Pd/C (5 wt%, 0.48 mmol), additive, Ar saturated toluene (1 mL), 15 h, 140 °C, in a high pressure microwave vial. [a] Yield determined by ^{1}H NMR using 1,3,5-trimethoxybenzene as the internal standard. [b] Yield determined by GC-MS. ND: not detected.

The formation of compound **4** was investigated by kinetic studies (Figure 2.2). From these results, it appears that the excess of hydrogen obtained from the dehydrogenation of both the intermediate leading to product **3** and the dehydrogenation of **2** to give phenol (**5**), eventually creates an H_2 saturated reaction atmosphere leading to the formation of product **4.** We originally thought that product **4** might be a reaction intermediate, however, it is clear that it decomposes with time without increasing the yield of product **3.** Thus, we hypothesized that finding a way to remove H_2 from the reaction media might lead to higher yields of the desired product **3**.

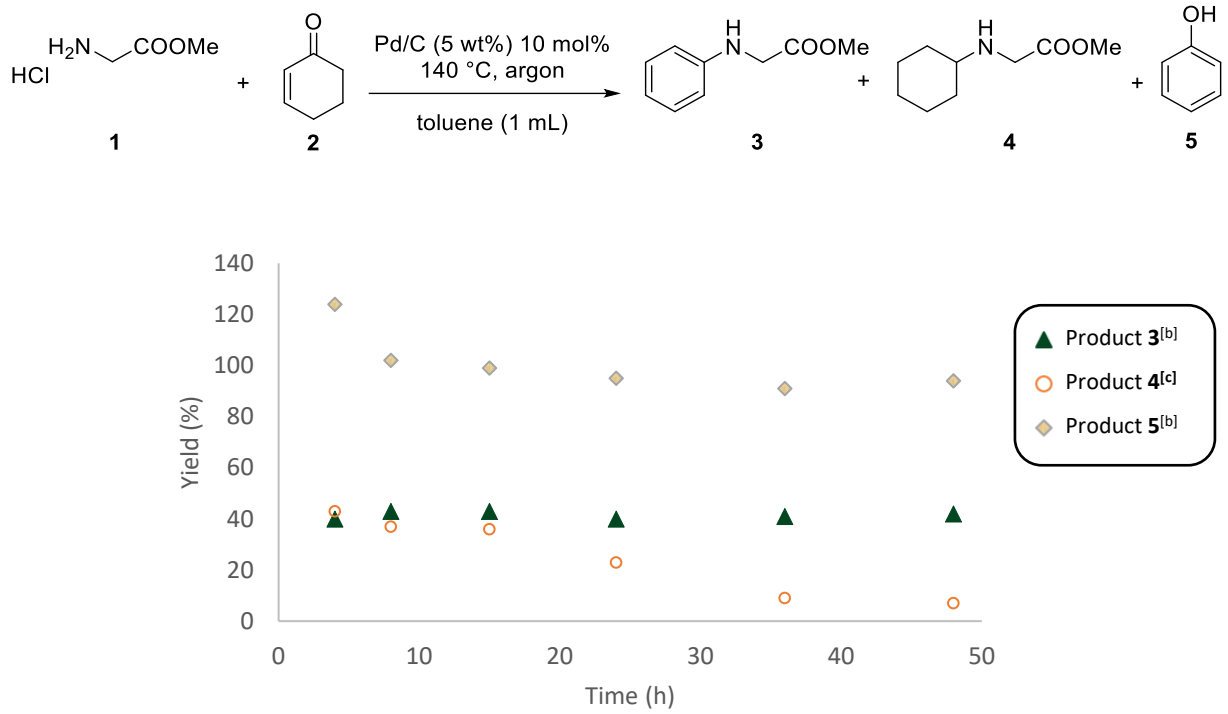

Figure 2.2. Kinetic studies under argon[a]

[a] Reaction conditions: **1** (0.24 mmol, 1 equiv), **2** (0.48 mmol, 2 equiv), Pd/C (5 wt%, 0.48 mmol), argon saturated toluene (1 mL), 140 °C, in a high pressure microwave vial.

[b] Yield determined by ^{1}H NMR using 1,3,5-trimethoxybenzene as the internal standard.

[c] Yield determined by GC.

Running the reaction under an atmosphere of oxygen was investigated to decrease the concentration of H_2 present in the reaction.[23] This led to a 64% yield of **3** and a decrease in the formation of **4** to 8%. Traces of the bis(arylated)ated product **7** were also detected. The formation of product **7** indicated an increase in the catalytic activity of the system (Table 2.3, entry 1). This result prompted us to investigate lower amounts of base in the system, with 20 mol% of $CaCO_3$ proving optimal for the formation of **3** in 69% yield (Table 2.3, entry 3).

Table 2.3. Oxidative atmosphere to quench formation of PdH_2 and increase the catalyst's turnover

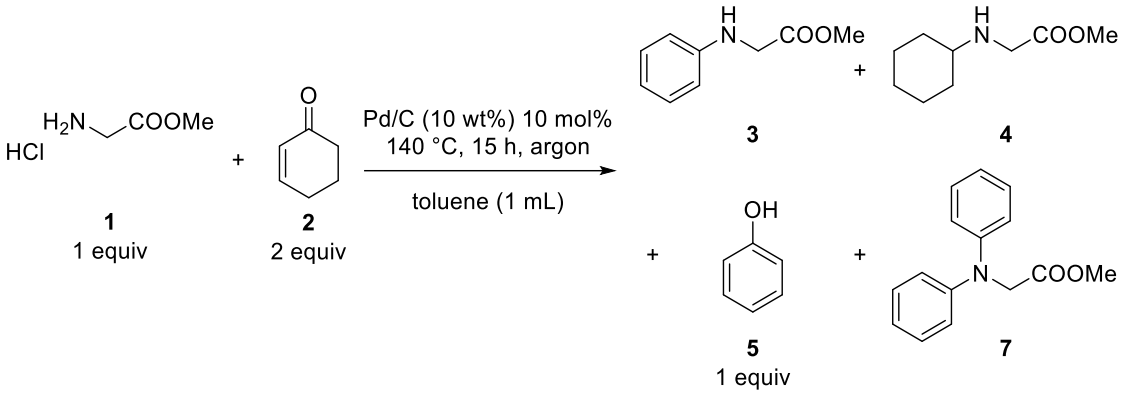

entry	atm	additive (mol%)	yield (%)			
			3[b]	**4**[b]	**5**[b]	**7**[a]
1	O_2	-	64	8	82	traces
2	O_2	$CaCO_3$ (30)	52	ND	105	8
3	O_2	$CaCO_3$ (20)	69 ± 3	7 ± 1	81 ± 8	traces

Reaction conditions: **1** (0.24 mmol, 1 equiv.), **2** (0.48 mmol, 2 equiv.), Pd/C (5 wt%, 0.48 mmol), additive, oxygen saturated toluene (1 mL), 15 h, 140 °C, in a high pressure microwave vial. [a] Yield determined by ^{1}H NMR using 1,3,5-trimethoxybenzene as the internal standard. [b] Yield determined by GC-MS. ND: not detected.

Having observed that the yield of product **3** remained constant regardless of how long the reactions were being run for, a kinetic profile for the oxidative conditions was performed (Table 2.4). This study showed that the reaction was completed within 4 hours, obtaining the desired product **3** in 74% yield (Table 2.4, entry 5).

Table 2.4 Kinetic studies using optimized parameters[a]

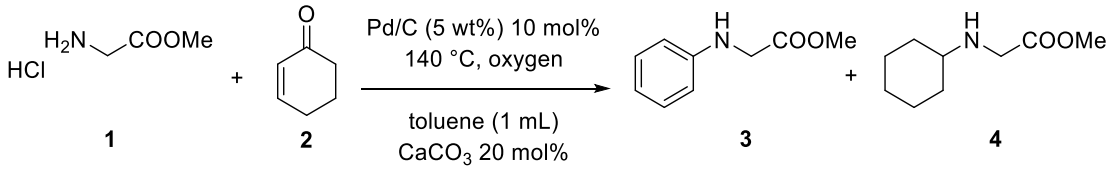

1 **2** **3** **4**

entry	time (h)	yield (%) **3**[b]	yield (%) **4**[c]
1	0.5	32	6
2	1	49	10
3	2	66	18
4	3	66	19
5	4	74	10
6	6	72	14
7	8	74	6
8	15	69	7

[a] Reaction conditions: **1** (0.24 mmol, 1 equiv), **2** (0.48 mmol, 2 equiv), Pd/C (5 wt%, 0.48 mmol), oxygen saturated toluene (1 mL), 140 °C, in a high pressure microwave vial.

[b] Yield determined by ^{1}H NMR using 1,3,5-trimethoxybenzene as the internal standard.

[c] Yield determined by GC.

ND: not detected.

2.3.2 Substrate scope

With the optimized conditions in hand, various amino acids and cyclohexenones were tested as substrates (Figure 2.3). Overall, amino acids with aliphatic R^1 chains gave the best reaction yields. Glycine *tert*-butyl ester afforded the product **3a** in 25% yield. Compared to glycine methyl ester, the lower yield might be the result of the *tert*-butyl group being cleaved under the reaction conditions, leading to de-carbonylation of the starting material. β-Alanine gave a lower product yield of **3b**, which might result from the increased nucleophilicity at the N-H group upon increasing the distance between the carboxylic group and the nitrogen, rendering it more likely to stay protonated under the reaction conditions. Amino acids can racemize following the formation of the Schiff base as the α-proton can be abstracted from the pseudo-anhydride imine intermediate.[19, 24] The enantiomeric retention of products **3c** (52% *ee*), **3d** (97% *ee*) and **3e** (100% *ee*) indicates that the substitution and steric hinderance at the α-position can impact the rate in which the acid-base equilibrates, leading to improved enantiomeric retention. *Tert*-butyl protected serine (Figure 2.3, product **3i**) gave higher yields than other heteroatom-containing amino acids (**3p-3x**). Deprotected or benzyl protected serine (**3p**, **3q**) led to decomposition of the starting material and diphenylamine formation. Amino acids with aromatic R^1 chains (phenylglycine, phenylalanine and tyrosine) gave poor yields (**3j**-**3l**), as dearomatization of the R^1 chain was also obtained as a side product. The cyclohexenone scope proved to be more limited (products **3m**-**3o**). Based on previous work by our group, we anticipated that sterics and electronics would have substantial effects,[21] a result which seemed to be enhanced when using less nucleophilic amines, since imine formation happens more reluctantly (**3y-3aac**). We theorize that racemization occurs upon deprotonation at the α-position, therefore making it harder for sterically hindered substrates to racemize.

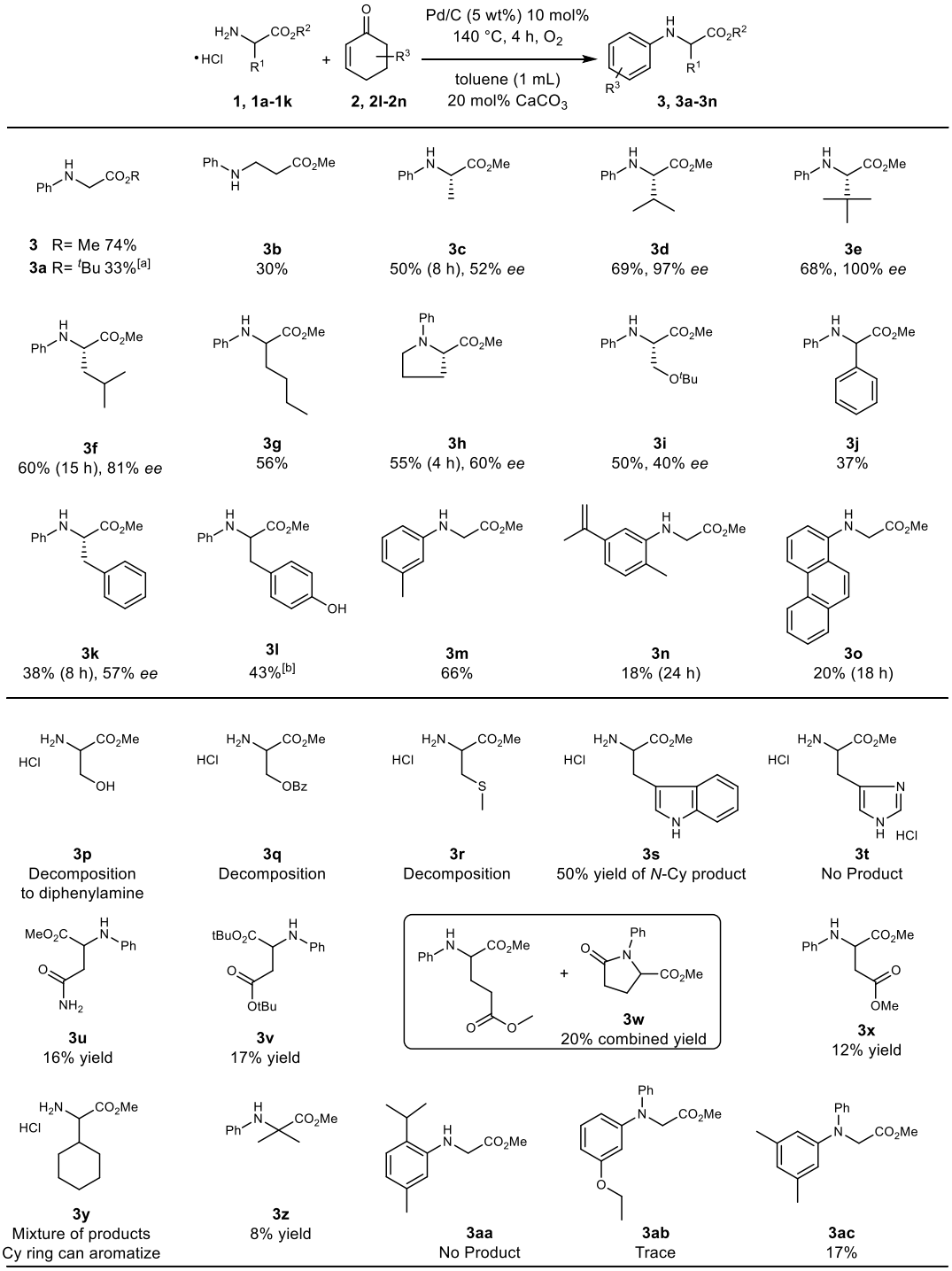

Figure 2.3 Amino acid and cyclohexenone substrate scope for the *N*-arylation reaction
Reaction conditions: **1**, **1a-1k** (0.24 mmol, 1 equiv.), **2**, **2l-2n** (0.48 mmol, 2 equiv.), Pd/C (5 wt%, 0.48 mmol), $CaCO_3$ (0.048 mmol, 0.2 equiv.), O_2 saturated toluene (1 mL), 140 °C. [a]50 mol% of $CaCO_3$ was used. Modified reaction times are shown in parenthesis. [b]O-*t*Bu tyrosine methyl ester •HCl was used as starting material.

In parallel, cylohexanone (**8**) was tested as a possible substrate, based on the fact that 2-cyclohexen-1-one has the potential to be reduced during the reaction process. Under the optimized conditions (Table 2.5, entry 1), the formation of bis(arylated)ated product **7** was obtained in higher yields than when 2-cyclohexen-1-one was used as the substrate. Upon increasing the catalyst loading to 20 mol%, the base to 5.0 equiv., and running the reaction for 24 h, bis(arylated)ated product **5** was obtained in 65% yield (Table 2.5, entry 2). We propose that the requirement for higher loading of Pd/C is because an oxide shell forms on palladium throughout the reaction, as was observed by XPS. When 2-cyclohexen-1-one (**2**) was tested under the latter conditions, 55% yield of product **7** was obtained.

Table 2.5 *N*-Arylation of glycine methyl ester hydrochloride using cyclohexanone under different conditions

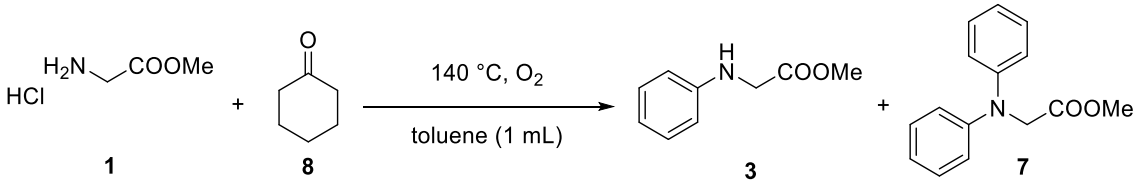

1 **8** **3** **7**

entry	conditions	yield (%)[a] **3**	**7**
1[a]	2 equiv. **8**, Pd/C (5 wt%) 10 mol%, 0.2 equiv. $CaCO_3$, 15 h	58	10
2[b]	4 equiv. **8**, Pd/C (5 wt%) 20 mol%, 5.0 equiv. $CaCO_3$, 24 h	26	65

Yields determined by ^{1}H NMR using 1,3,5-trimethoxybenzene as the internal standard. [a]Reaction conditions: **1** (0.24 mmol, 1 equiv.), **8** (0.48 mmol, 2 equiv.), Pd/C (5 wt%, 0.48 mmol), $CaCO_3$ (0.048 mmol, 0.2 equiv.), O_2 saturated toluene (1 mL), 140 °C, 15h, in a high pressure microwave vial. [b]Reaction conditions: **1** (0.24 mmol, 1 equiv.), **8** (0.96 mmol, 4 equiv.), Pd/C (5 wt%, 0.96 mmol), $CaCO_3$ (1.2 mmol, 5.0 equiv.), O_2 saturated toluene (1 mL), 140 °C, 24 h.

Finally, the optimized reaction conditions were tested with phenol as a coupling partner. Unfortunately, no reaction was observed. Nonetheless, this result was not unusual, given that there is no hydride source present in the reaction. Given this, the initial reduction of phenol to 2-cyclohexen-1-one or cyclohexanone cannot proceed, leading to the observed results.

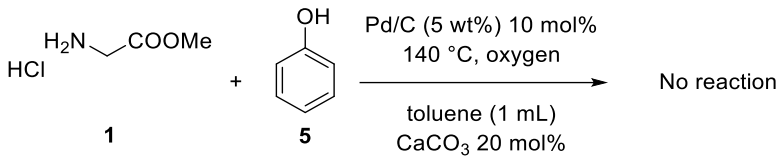

Scheme 2.6 Palladium-catalyzed *N*-arylation of glycine methyl ester hydrochloride using phenol

2.3.3 Mechanistic considerations

We propose the following mechanism for this transformation (Scheme 2.7). Initially, the addition of the amino acid to 2-cyclohexen-1-one occurs with water loss to generate imine intermediate **A. A** can subsequently undergo α-palladation, forming intermediate **C**, which can effectively undergo β-hydride elimination. This step releases species **D**, which can quickly tautomerize to give the desired product **E**, as well as the $HPd^{(II)}H$ species. The dihydride species can then regenerate the $Pd^{(0)}$ catalyst upon releasing H_2. The addition of O_2 can accelerate this process. ICP studies were performed after reaction completion, and it was determined that leaching of $Pd^{(II)}$ had occurred, further confirming the presence of this species as an intermediate. This $Pd^{(II)}$ species is most likely present in the form of $PdCl_2$ given the presence of the Cl^- species as the counterion for the amino acid salts.

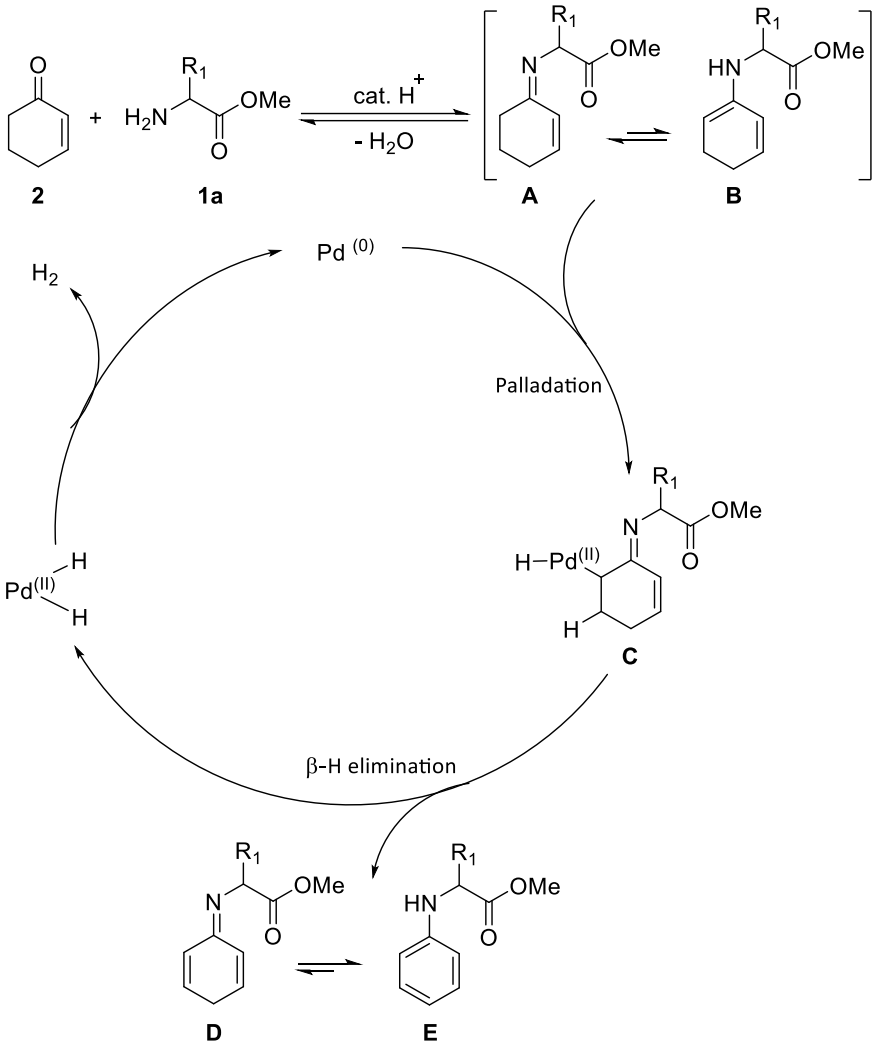

Scheme 2.7 Proposed mechanism for the palladium-catalyzed *N*-arylation of glycine methyl ester hydrochloride using 2-cylohexen-1-one

2.3.4 Additional experiments

While previous work in our group regarding the arylation of secondary amines used Pd (II) as the catalyst,[21] we have only achieved arylation of primary amines using heterogeneous Pd (0) catalysts.[20] We reasoned that this might be due to primary amines readily coordinating to the Pd (II) heterogeneous catalysts, leading to decomposition of the starting material by β-hydride elimination. The only Pd(II) that afforded the desired product **3** was $Pd(TFA)_2$ (Table 2.6, entry 3). However, it quickly formed a palladium mirror on the walls of the reaction vessel. On the other hand, $Pd^{(0)}$ species (Table 2.6, entries 7-10) afforded the desired product in moderate yields regardless of them being Lewis acidic or basic, except for

$Pd(PPh_3)_4$. These results strongly suggest that Pd(0) is the active catalytic species, in agreement with similar reported catalytic systems.[25]

Table 2.6 Different palladium catalysts for the *N*-arylation reaction using 2-cyclohexen-1-one[a]

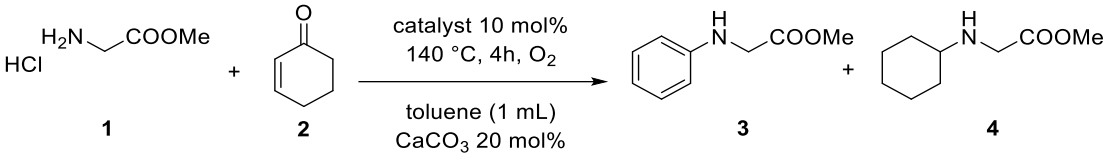

entry	catalyst	yield (%)	
		3[b]	**4**[c]
1	Pd/C (5 wt%)	74	10
2	$Pd(TFA)_2$ + 20 mol% 2-NMe_2Py	traces	N.D.
3	$Pd(TFA)_2$[d]	25	N.D.
4	$Pd(OAc)_2$	traces	N.D.
5	$PdCl_2$	traces	N.D.
6	$PdCl_2(PPh_2Me)_2$	N.D.	N.D.
7	$Pd(PPh_3)_4$	N.D.	N.D.
8	Pd/Al_2O_3 (10 wt%)	57	19
9	$Pd/CaCO_3$	42	17
10	$Pd(dba)_2$	57	N.D.

[a] Reaction conditions: **1** (0.24 mmol, 1 equiv), **2** (0.48 mmol, 2 equiv), catalyst (10 mol% palladium loading), $CaCO_3$ (0.048 mmol, 0.2 equiv) , O_2 saturated toluene (1 mL), 140 °C. [b] Yield determined by ^1H NMR using 1,3,5-trimethoxybenzene as the internal standard. [c] Yield determined by GC-MS. [d] Palladium mirror forms immediately after starting the reaction. N.D.= not detected.

XPS studies were performed using the model reaction (yielding product **3**) to analyze the possibility of an oxide-shell forming on the palladium catalyst. The surface analysis revealed the presence of the following elements: C, O, Cl, Pd, Ca and N (Figure 2.4). The nitrogen present on the Pd/C might explain why yields are lower than the conversion, which was consistently 100%. Deconvolution of the XPS spectra of the catalyst before and after the reaction are shown below (Figures 2.5, 2.6). Analysis of the fresh catalyst shows Pd^0 as the sole species, whereas the catalyst after reaction shows a mixture of Pd^0 and oxidized palladium, Pd^{II}. The shift of the new peak (336.8 eV) might indicate the presence of PdO and/or $PdCl_2$. The former might be the result of oxidation with the O_2 atmosphere. While the latter, might be the result of the Cl anions from the amino acid salts being adsorbed onto the surface of the oxidized catalyst.[23]

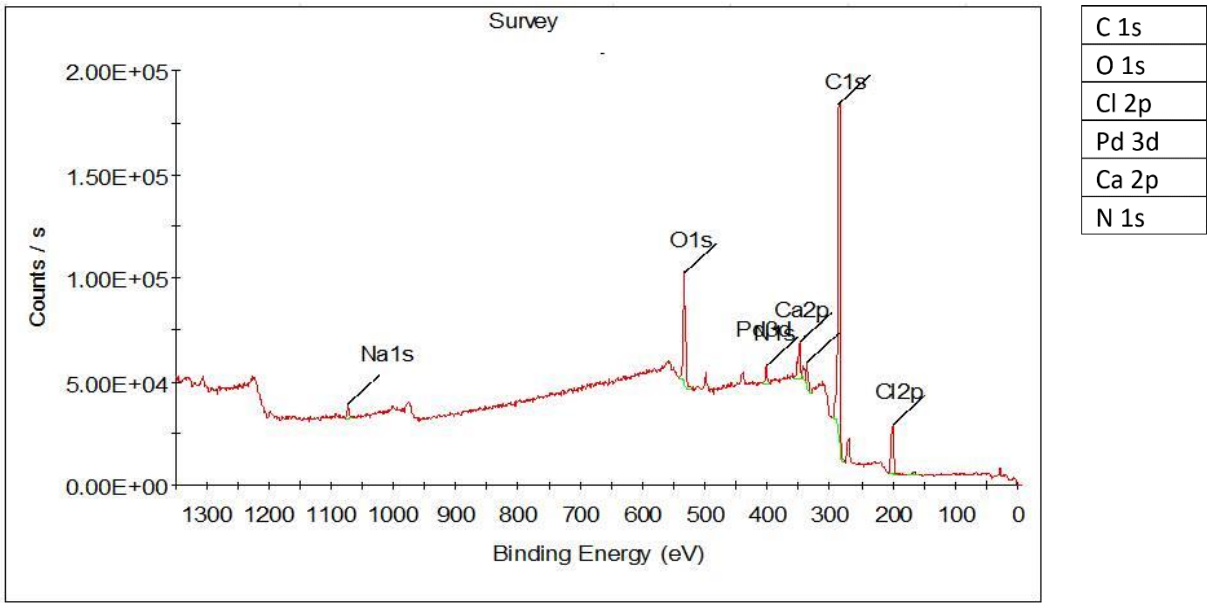

Figure 2.4 Elemental survey of the catalyst after reaction

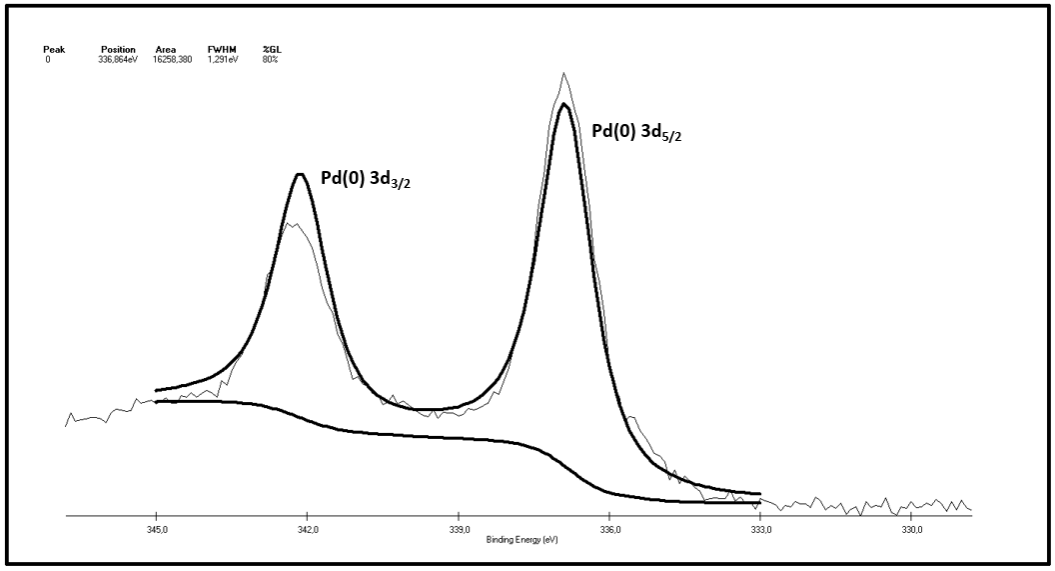

Figure 2.5 Deconvolution of the XPS survey for the fresh catalyst

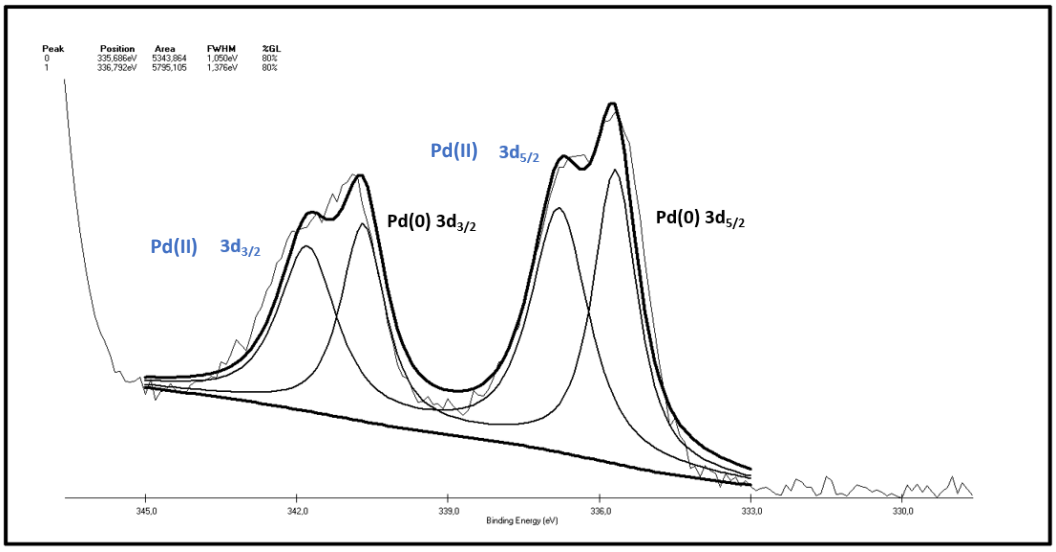

Figure 2.6 Deconvolution of the XPS survey of the catalyst after the reaction

2.4 Conclusion and outlook

In this chapter we reported efforts to develop a methodology for the *N*-arylation of amino acids without the need for aryl halides as arylating reagents. Upon screening several reaction conditions, we achieved a novel *N*-arylation of α-amino acids with 2-cyclohexen-1-one. Various amino acids can be arylated with cyclohexanone using Pd/C as the catalyst, substoichiometric amounts of base, and oxygen as the terminal oxidant. In addition, the use of cyclohexanone provides *N*-bis(arylated)ated amino acids in good yields. Aliphatic amino acids were ideal substrates for the reaction, as sterics and electronics greatly impacted the reaction yield. A mechanism for the reaction was also proposed, and additional experiments such as ICP and XPS were performed in order to support our proposal.

Lastly, while this work presents a novel methodology for amino acid *N*-arylation, several challenges remain to be addressed. First, the high temperature necessary for re-aromatization leads to undesired reaction pathways such as decarboxylation and racemization of the enantiomerically pure starting materials. Furthermore, the reaction is run in toluene, limiting its overall sustainability and applicability to biological systems. Moreover, phenol was not successfully used as a starting material, one of the initial desired outcomes. Thus, finding reaction conditions that could satisfy these requirements would increase the overall impact of the methodology.

2.5 Contributions

Prof. Chao-Jun Li realized project conceptualization. Methodology, experimentation and characterization was performed by myself with the assistance of Dr. Inna Perepichka. Dr. Alain Li ran and deconvoluted the XPS spectra. Julio Terra helped in designing and setting the ICP analysis. High resolution mass spectrometry was performed by Dr. Nadim Saadeh and Dr. Alexander Wahba at the McGill University Department of Chemistry Mass Spectrometry Laboratory. The publication manuscript, which shares some common content with this thesis chapter, was written by myself, edited and proofread by Dr. Zoë Hearne, Dr. Wenbo Liu, and Dr. Zihang Qiu and Prof. Chao-Jun Li.

2.6 Experimental section

2.6.1 General Information

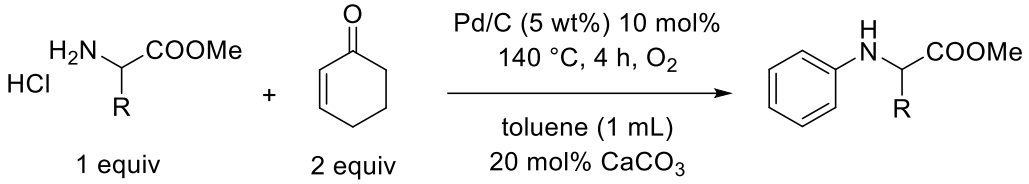

All reactions were run in 5 mL U-shaped microwave vials using aluminum seals with silicone septa. Reaction vials and stir bars were washed with aqua regia, neutralized using a saturated solution of $NHCO_3$, thoroughly rinsed with distilled water and acetone, and left overnight in a drying oven at 110 °C. Prior to use, vessels were flamed dried and allowed cooled down to ambient temperature in a desiccator.

In U- shaped microwave vial, charged with a stir bar, the amino acid (0.24 mmol, 1 equiv), $CaCO_3$ (4.8 mg, 0.048 mmol, 0.2 equiv), and the preactivated Pd/C (5% wt) (0.48 mmol, 51.1 mg) were added under air. The vial was flushed with oxygen three times and 1 mL of dry, oxygen saturated toluene was then added under an oxygen flow. 2-Cyclohexen-1-one (0.48 mmol, 47 µL) was finally added to the vial via syringe. The vial was capped with a silicon lined aluminum seal and was submerged to a preheated oil bath at 140 °C with stirring at 500 rpm for the indicated time. The reaction vessel was then lifted from the oil bath and left to cool down to room temperature without interrupting the stirring. The aluminum cap was removed, and the reaction mixture was diluted using ethyl acetate. The Pd/C was then removed by filtration by using a Pasteur pipette filled with 1 cm of celite, washing with ethyl acetate. The solvent was removed in vacuo, and the residue was analyzed by GCMS and NMR, yields were obtained by NMR upon adding 1,3,5-trimethoxybenzene as the internal standard. Isolation was done through preparatory TLC using the indicated solvent system.

Note 1: Palladium on carbon was activated in large batches (3-5 g) by heating to 140 °C under vacuum, with stirring, for at least one hour; Pd/C was kept in a desiccator for a week before repeating this procedure.

Note 2: In order to saturate toluene with oxygen, oxygen gas was bubbled through the dry solvent for 2 hours before use.

Note 3: Different results were obtained when using different sources of the Pd/C catalyst.[26, 27]

2.6.2 Analytical Data

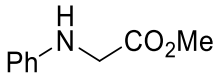

3

Product was isolated by thin layer chromatography in a system of 40% CH_2Cl_2 in hexanes, R_f=0.2

^{1}H NMR (500 MHz, $CDCl_3$) δ 7.23 – 7.17 (t, 2H), 6.76 (t, *J* = 7.3 Hz, 1H), 6.62 (d, *J* = 7.8 Hz, 2H), 4.28 (br, 1H), 3.93 (s, 2H), 3.79 (s, 3H). ^{13}C NMR (125 MHz, $CDCl_3$) δ 171.8, 147.1, 129.5, 118.4, 113.1, 52.4, 45.8.

HRESI-MS calc. for $C_9H_{12}NO_2$ $[M+H]^+$ 166.0863, found 166.0861

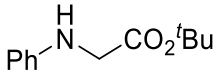

3a

Product was isolated by thin layer chromatography in a system of hexanes: ethyl acetate (3: 0.5), R_f=0.6

^{1}H NMR (500 MHz, $CDCl_3$) δ 7.19 (dd, *J* = 8.4, 7.5 Hz, 2H), 6.74 (t, *J* = 7.3 Hz, 1H), 6.61 (d, *J* = 7.7 Hz, 2H), 4.38 (br, 1H), 3.80 (s, 2H), 1.49 (s, 9H). ^{13}C NMR (125 MHz, $CDCl_3$) δ 170.4, 147.3, 129.4, 118.2, 113.2, 82.1, 46.7, 28.2.

HRMS calc. for $C_{12}H_{17}NO_2Na$ $[M+Na]^+$ 230.1151, found 230.1157

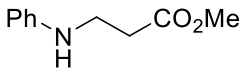

3b

Product was isolated by thin layer chromatography R_f=0.8 in a system of hexane: ethyl acetate: dichloromethane (2:1:1)

^{1}H NMR (500 MHz, $CDCl_3$) δ7.21 – 7.16 (m, 2H), 6.76 – 6.70 (m, 1H), 6.63 (dd, *J* = 8.5, 0.9 Hz, 2H), 4.06 (br, 1H), 3.70 (s, 3H), 3.46 (t, *J* = 6.4 Hz, 2H), 2.63 (t, *J* = 6.4 Hz, 2H).

^{13}C NMR (125 MHz, $CDCl_3$) δ173.0, 147.6, 129.5, 117.97, 113.24, 51.9, 39.6, 33.8.

HRMS calc. for $C_{10}H_{14}NO_2$ $[M+H]^+$ 180.1019, found 180.1016

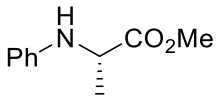

3c

Product was isolated by thin layer chromatography in a system of 30% CH_2Cl_2 in hexanes R_f=0.30

^{1}HNMR (500 MHz, $CDCl_3$) δ 7.18 (dd, *J* = 8.4, 7.5 Hz, 2H), 6.74 (t, *J* = 7.3 Hz, 1H), 6.61 (d, *J* = 7.8 Hz, 2H), 4.16 (q, *J* = 6.9 Hz, 1H), 4.16 (br, 1H), 3.73 (s, 3H) 1.48 (d, *J* = 6.9 Hz, 3H).^{13}C NMR (125 MHz, $CDCl_3$) δ 175.2, 146.7, 129.5, 118.5, 113.5, 52.4, 52.1, 19.1.

HRAPCI-MS calc. for $C_{10}H_{14}NO_2$ $[M+H]^+$ 180.1019, found 180.1018

HPLC analysis ((DAICEL chiral OJ-H, 10% IPA–hexanes, 1.0 mL/min, 254 nm) indicated 52% ee: t_R (minor) = 14.0 min, t_R (major) = 22.9 min. In agreement with literature values.[13]

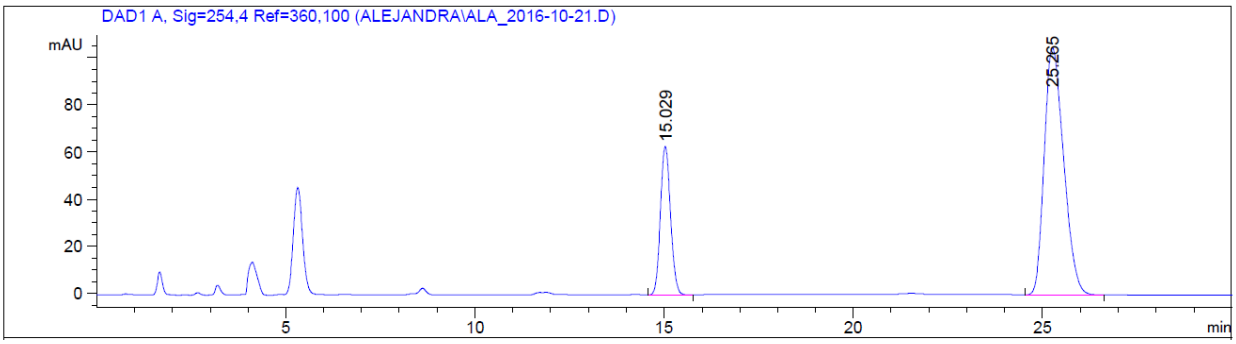

Peak #	RetTime [min]	Type	Width [min]	Area [mAU*s]	Height [mAU]	Area %
1	15.029	BB	0.2904	1168.12976	62.99067	23.8198
2	25.265	BB	0.5582	3735.90039	104.72784	76.1802

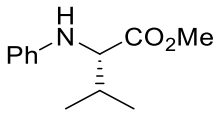

3d

Product was isolated by thin layer chromatography in a system of 5% ethyl acetate in hexanes, R_f=0.3

^{1}H NMR (500 MHz, $CDCl_3$) δ 7.19 – 7.14 (m, 2H), 6.73 (t, *J* = 7.3 Hz, 1H), 6.63 (d, *J* = 7.7 Hz, 2H), 4.11 (br, 1H), 3.87 (d, *J* = 5.9 Hz, 1H), 3.71 (s, 3H), 2.12 (dq, *J* = 13.5, 6.8 Hz, 1H), 1.05 (d, *J* = 6.9 Hz, 3H), 1.02 (d, *J* = 6.8 Hz, 3H). ^{13}C NMR (125 MHz, $CDCl_3$) δ 174.3, 147.4, 129.5, 118.4, 113.7, 62.6, 52.0, 31.7, 19.2, 18.9.

HRESI-MS calc. for $C_{12}H_{18}NO_2$ $[M+H]^+$ 208.13321, found 208.13290

HPLC analysis ((DAICEL chiral OJ-H, 5% IPA–hexanes, 1.0 mL/min, 254 nm) indicated 97% ee: t_R (minor) = 11.4 min, t_R (major) = 21.16 min.

DL-3c

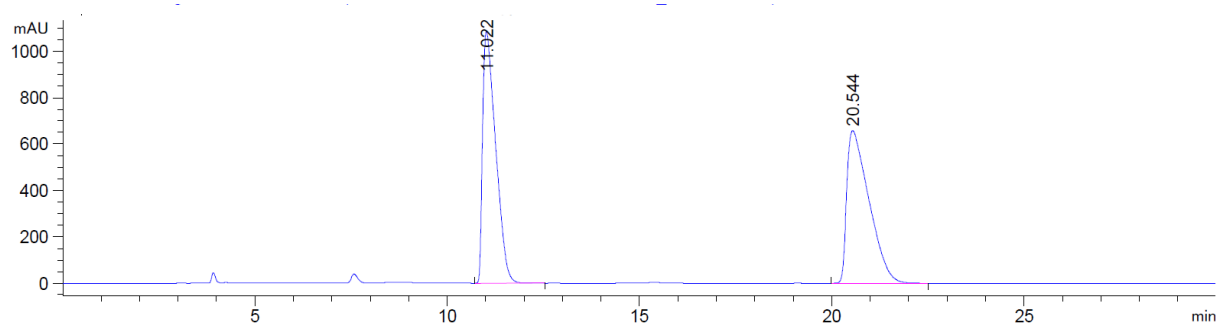

Peak #	RetTime [min]	Type	Width [min]	Area [mAU*s]	Height [mAU]	Area %
1	11.022	BB	0.3499	2.56746e4	1085.52722	49.3223
2	20.544	BB	0.6156	2.63801e4	658.11902	50.6777

L-3c

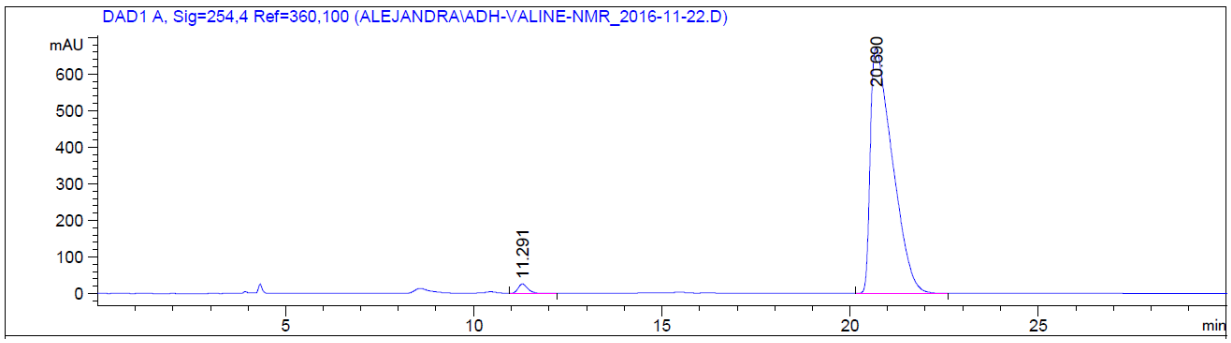

Peak #	RetTime [min]	Type	Width [min]	Area [mAU*s]	Height [mAU]	Area %
1	11.291	BB	0.2678	441.20041	25.25135	1.5914
2	20.690	BB	0.6207	2.72830e4	670.60022	98.4086

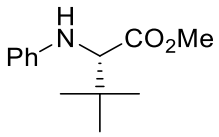

3e

Product was isolated by thin layer chromatography in a system of hexanes: ethyl acetate (3: 0.5), R_f=0.65

^{1}H NMR (500 MHz, $CDCl_3$) δ 7.17 (dd, *J* = 8.5, 7.4 Hz, 2H), 6.73 (t, *J* = 7.3 Hz, 1H), 6.65 (d, *J* = 7.8 Hz, 2H), 4.16 (br, 1H), 3.81 (s, 1H), 3.68 (s, 3H), 1.06 (s, 9H). ^{13}C NMR (125 MHz, $CDCl_3$) δ 174.1, 147.8, 129.5, 118.5, 113.9, 65.6, 51.7, 34.6, 26.9.

HRESI-MS calc. for $C_{13}H_{20}NO_2$ $[M+H]^+$ 222.1489, found 222.1486

HPLC analysis (DAICEL chiral OJ-H, 10% IPA–hexanes, 1.0 mL/min, 254 nm) indicated 100% ee: t_R (not observed)= 26.5 min, t_R (major) = 39.9 min.

DL-3d

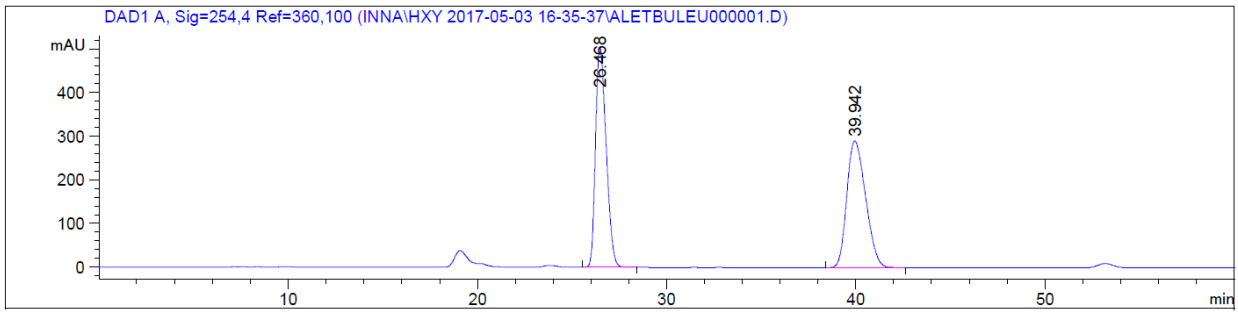

Signal 1: DAD1 A, Sig=254,4 Ref=360,100

Peak #	RetTime [min]	Type	Width [min]	Area [mAU*s]	Height [mAU]	Area %
1	26.468	BB	0.6088	1.96940e4	505.24619	49.6360
2	39.942	BB	1.0867	1.99828e4	289.72604	50.3640

L-3d

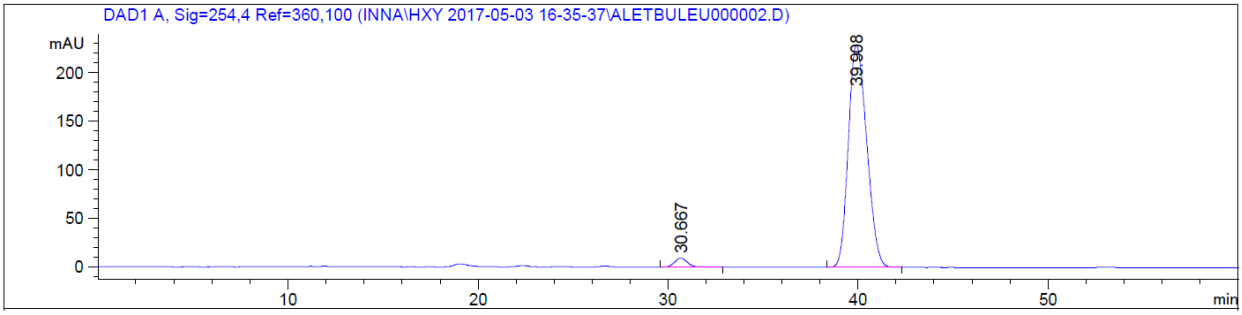

Signal 1: DAD1 A, Sig=254,4 Ref=360,100

Peak #	RetTime [min]	Type	Width [min]	Area [mAU*s]	Height [mAU]	Area %
1	30.667	BB	0.7311	442.06027	9.22376	2.7933
2	39.908	BB	1.0661	1.53834e4	228.30119	97.2067

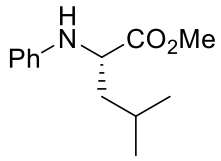

3f

Product was isolated by thin layer chromatography in a system of 5% ethyl acetate in hexanes, R_f=0.45

^{1}H NMR (500 MHz, $CDCl_3$) δ 7.18 (dd, *J* = 8.3, 7.5 Hz, 2H), 6.74 (t, *J* = 7.3 Hz, 1H), 6.63 (d, *J* = 7.8 Hz, 2H), 4.12 – 4.09 (m, 1H), 3.98 (br, 1H), 3.71 (s, 3H), 1.81 (tt, *J* = 13.4, 6.7 Hz, 1H), 1.71 – 1.61 (m, 2H), 1.00 (d, *J* = 6.6 Hz, 3H), 0.95 (d, *J* = 6.6 Hz, 3H). ^{13}C NMR (125 MHz, $CDCl_3$) δ 175.4, 147.1, 129.5, 118.5, 113.5, 55.3, 52.2, 42.5, 25.0, 22.9, 22.3.

HRESI-MS calc. for $C_{13}H_{20}NO_2$ $[M+H]^+$ 222.1489, found 222.1486

HPLC analysis ((DAICEL chiral OJ-H, 10% IPA–hexanes, 1.0 mL/min, 254 nm) indicated 84% ee: t_R (minor) = 10.2 min, t_R (major) = 17.2 min. In agreement with literature values.[13]

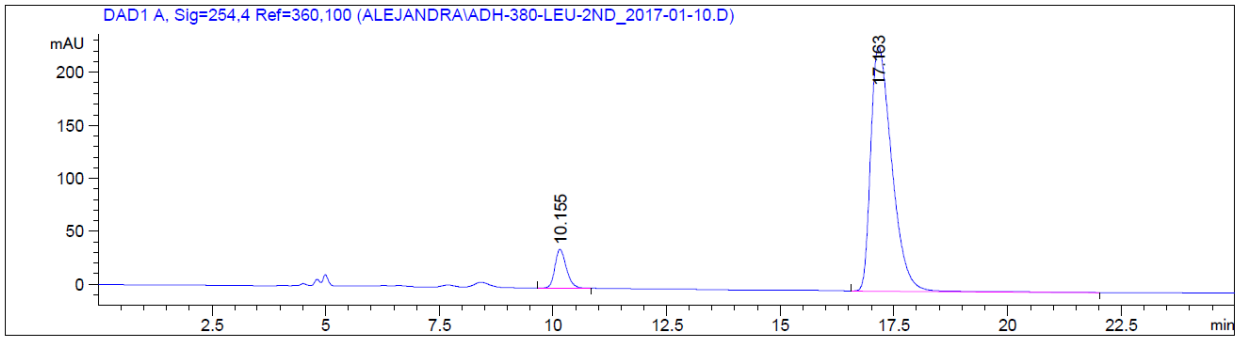

Peak #	RetTime [min]	Type	Width [min]	Area [mAU*s]	Height [mAU]	Area %
1	10.155	BB	0.2705	642.12982	36.63871	7.9706
2	17.163	BB	0.4975	7414.09424	230.38000	92.0294

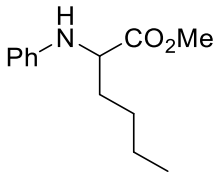

3g

Product was isolated by thin layer chromatography in a system of 30% CH_2Cl_2 in hexanes, R_f=0.15

^{1}H NMR (500 MHz, $CDCl_3$) δ 7.20 – 7.15 (m, 2H), 6.73 (t, *J* = 7.3 Hz, 1H), 6.61 (dd, *J* = 8.5, 0.9 Hz, 2H), 4.08 (br, 1H), 4.06 (t, *J* = 6.5 Hz, 1H), 3.72 (s, 3H), 1.89 – 1.80 (m, 1H), 1.75 (dd, *J* = 14.1, 7.0 Hz, 1H), 1.47 – 1.28 (m, 4H), 0.91 (t, *J* = 7.1 Hz, 3H). ^{13}C NMR (125 MHz, $CDCl_3$) δ 174.9, 147.0, 129.5, 118.4, 113.5, 56.7, 52.2, 33.0, 27.9, 22.6, 14.0.

HRAPCI-MS calc. for $C_{13}H_{20}NO_2$ $[M+H]^+$ 222.1489, found 222.1486

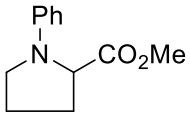

3h

Product was isolated by thin layer chromatography in a system of 5% ethyl acetate in hexanes, R_f=0.24

^{1}H NMR (500 MHz, $CDCl_3$) δ 7.23 (dd, *J* = 8.5, 7.4 Hz, 2H), 6.72 (t, *J* = 7.3 Hz, 1H), 6.56 (d, *J* = 8.0 Hz, 2H), 4.26 (dd, *J* = 8.6, 1.9 Hz, 1H), 3.72 (s, 3H), 3.59 (td, *J* = 8.5, 3.1 Hz, 1H), 3.37 (dd, *J* = 15.8, 7.9 Hz, 1H), 2.34 – 2.25 (m, 1H), 2.23 – 2.10 (m, 2H), 2.11 – 1.93 (m, 1H). ^{13}C NMR (125 MHz, $CDCl_3$) δ 175.2, 146.8, 129.4, 116.8, 112.1, 60.9, 52.3, 48.4, 31.1, 24.0.

HRESI-MS calc. for $C_{12}H_{16}NO_2$ $[M+H]^+$ 206.1176, found 206.1185

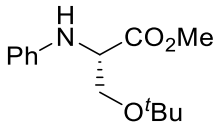

3i

Product was isolated by thin layer chromatography in a system of hexanes: ethyl acetate (3: 0.5), R_f=0.5

^{1}H NMR (500 MHz, $CDCl_3$) δ 7.17 (t, *J* = 7.9 Hz, 2H), 6.74 (t, *J* = 7.3 Hz, 1H), 6.63 (d, *J* = 7.9 Hz, 2H), 4.54 (br,

1H), 4.20 (t, *J* = 4.1 Hz, 1H), 3.78 (dd, *J* = 8.8, 4.0 Hz, 1H), 3.73 (s, 3H), 3.69 (dd, *J* = 8.8, 4.2 Hz, 1H), 1.17 (s, 9H). ^{13}C NMR (125 MHz, $CDCl_3$) δ 172.9, 146.9, 129.4, 118.5, 113.8, 73.6, 62.6, 57.4, 52.3, 27.5.

HRESI-MS calc. for $C_{14}H_{21}NO_3Na$ $[M+Na]^+$ 274.1414, found 274.1406

HPLC analysis ((DAICEL chiral OJ-H, 2% IPA–hexanes, 0.8 mL/min, 254 nm) indicated 40% ee: t_R (minor) = 18.4 min, t_R (major) = 25.4 min

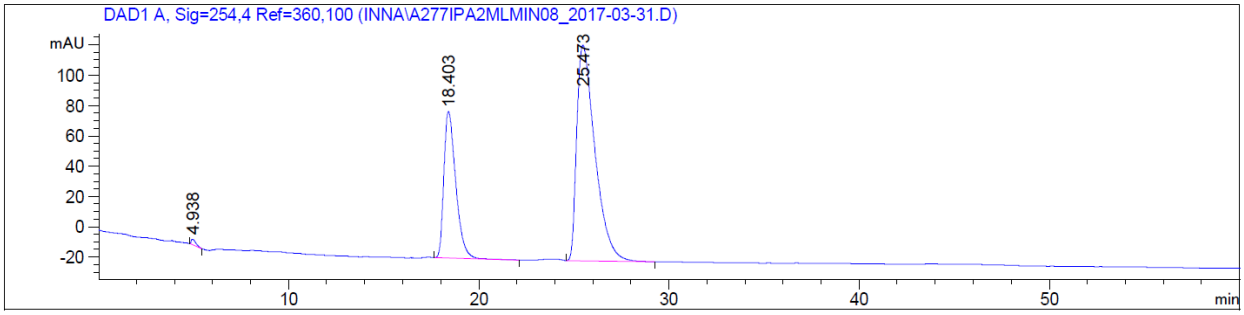

Peak #	RetTime [min]	Type	Width [min]	Area [mAU*s]	Height [mAU]	Area %
1	4.938	BB	0.2682	61.83662	3.46460	0.4502
2	18.403	BB	0.6682	4195.90674	96.70419	30.5496
3	25.473	BB	1.0126	9476.97266	142.36989	69.0001

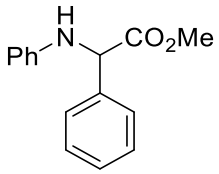

3j

Product was isolated by thin layer chromatography in a system of 25% dichloromethane in hexanes, R_f=0.25

^{1}HNMR (500 MHz, DMSO-d_6) δ 7.55 – 7.47 (m, 2H), 7.40 – 7.35 (m, 2H), 7.34 – 7.29 (m, 1H), 7.05 (dd, *J* = 8.4, 7.4 Hz, 2H), 6.67 (d, *J* = 7.7 Hz, 2H), 6.56 (t, *J* = 7.3 Hz, 1H), 6.32 (d, *J* = 8.1 Hz, 1H), 5.24 (d, *J* = 8.1 Hz, 1H), 3.63 (s, 3H). ^{13}C NMR (125 MHz, DMSO-d_6) δ 172.3, 146.9, 137.8, 128.8, 128.6, 128.0, 127.6, 116.8, 113.0, 59.6, 52.2.

HRESI-MS calc. for $C_{15}H_{15}NO_2Na$ $[M+Na]^+$ 264.0995, found 264.0989

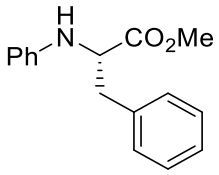

3k

Product was isolated by thin layer chromatography in a system of 30% dichloromethane in hexanes, R_f=0.11

^{1}H NMR (500 MHz, DMSO-d_6) δ 7.30 – 7.26 (m, 4H), 7.24 – 7.17 (m, 1H), 7.05 (t, *J* = 7.8 Hz, 2H), 6.59 – 6.51 (m, *J* = 8.0 Hz, 3H), 6.06 (d, *J* = 9.0 Hz, 1H), 4.22 (dd, *J* = 15.2, 8.1 Hz, 2H), 3.55 (s, 3H), 3.08 – 2.97 (m, 1H).

^{13}C NMR (125 MHz, $CDCl_3$) δ 173.0, 146.5, 136.4, 129.5, 129.4, 128.7, 127.2, 118.6, 113.7, 57.9, 52.2, 38.8.

HRESI-MS calc. for $C_{16}H_{18}NO_2$ $[M+H]^+$ 256.1332, found 256.1328

HPLC analysis ((DAICEL chiral OJ-H, 10% IPA–hexanes, 1.0 mL/min, 254 nm) indicated 57% ee: t_R (minor) = 35.5 min, t_R (major) = 46.5 min. In agreement with literature values.[13]

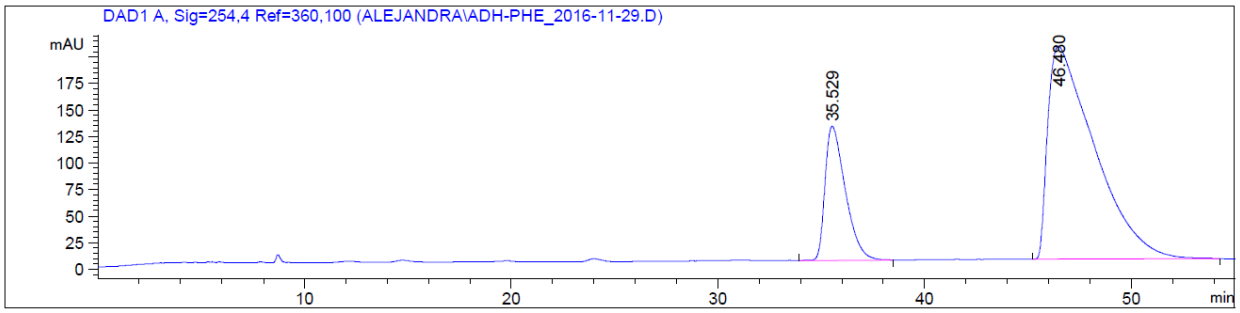

Peak #	RetTime [min]	Type	Width [min]	Area [mAU*s]	Height [mAU]	Area %
1	35.529	BB	1.0352	8615.74512	126.40659	21.4601
2	46.480	BB	2.2228	3.15320e4	200.93112	78.5399

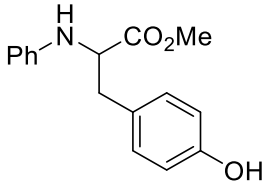

3l

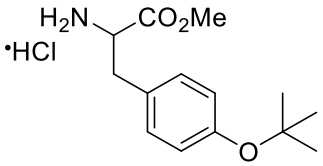

1l

Amino acid **1l** was used as starting material to obtain product **3l.** Product **3l** was isolated by thin layer chromatography in hexanes: ethyl acetate (3 : 0.5), R_f= 0.15

^{1}H NMR (500 MHz, $CDCl_3$) δ 7.17 (dd, *J* = 8.5, 7.4 Hz, 2H), 7.02 (d, *J* = 8.5 Hz, 2H), 6.77 – 6.71 (m, 3H), 6.60 (d, *J* = 7.8 Hz, 2H), 4.96 (br, 1H), 4.32 (t, *J* = 6.1 Hz, 1H), 4.06 (br, 1H), 3.67 (s, 3H), 3.07 (qd, *J* = 13.8, 6.1 Hz, 2H). ^{13}C NMR (500 MHz, $CDCl_3$) δ 173.9, 154.8, 146.4, 130.6, 129.5, 128.4, 118.7, 115.6, 113.8, 58.0, 52.3, 37.9.

HRESI-MS calc. for $C_{16}H_{18}NO_3$ $[M+H]^+$ 272.1281, found 272.1276

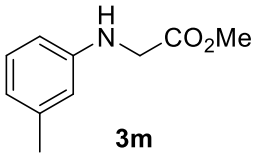

3m

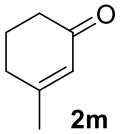

2m

Cyclohexenone **2m** was used as starting material to obtain product **3m**. Product **3m** was isolated by thin layer chromatography in hexanes: ethyl acetate (3 : 0.5), R_f= 0.35

^{1}H NMR (500 MHz, $CDCl_3$) δ 7.10 (t, *J* = 7.7 Hz, 1H), 6.61 (d, *J* = 7.4 Hz, 1H), 6.51 – 6.44 (m, 2H), 3.93 (br, 2H), 3.78 (s, 3H), 2.29 (s, 3H). ^{1}H NMR (500 MHz, $CDCl_3$) δ 171.6, 146.6, 139.4, 129.4, 119.9, 114.5, 110.8, 52.4, 46.2, 21.7.

HRAPCI-MS calc. for $C_{10}H_{14}NO_2$ $[M+H]^+$ 180.1019, found 180.1020

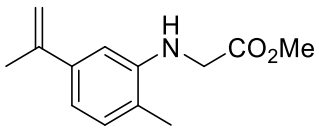

3n

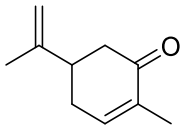

2n

Cyclohexenone **2n** was used as starting material to obtain product **3n.** Product **3n** was isolated by thin layer chromatography in hexanes: ethyl acetate (3 : 0.5), R_f= 0.4

^{1}H NMR (500 MHz, $CDCl_3$) δ7.04 (d, *J* = 7.7 Hz, 1H), 6.82 (dd, *J* = 7.7, 1.7 Hz, 1H), 6.58 (d, *J* = 1.6 Hz, 1H), 5.30 (br, *J* = 0.7 Hz, 1H), 5.03 – 5.01 (m, 1H), 4.23 (br, 1H), 2.99 (s, 2H), 3.81 (s, 3H), 2.21(s, 3H), 2.13 (d, *J* = 0.5 Hz, 3H). ^{13}C NMR (125 MHz, $CDCl_3$) δ171.7, 144.7, 143.8, 140.5, 130.1, 122.1, 115.4, 111.6, 107.3, 52.3, 45.8, 22.0, 17.1.

HRMS calc. for $C_{13}H_{18}NO_2$ $[M+H]^+$ 220.1332, found 220.1324

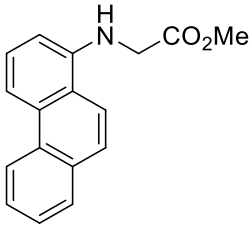

3o

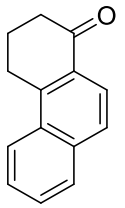

2o

Cyclohexenone **2o** was used as starting material to obtain product **3o.** Product **3o** was isolated by thin layer chromatography hexanes: ethyl acetate (3 : 0.5), R_f= 0.8

^{1}H NMR (500 MHz, $CDCl_3$) δ 8.67 (d, *J* = 8.2 Hz, 1H), 8.16 (d, *J* = 8.5 Hz, 1H), 7.92 – 7.85 (m, 2H), 7.76 (d, *J*= 9.2 Hz, 1H), 7.66 – 7.62 (m, 1H), 7.62 – 7.57 (m, 1H), 7.53 (t, *J* = 8.0 Hz, 1H), 6.68 (d, *J* = 7.7 Hz, 1H), 5.13 (br, 1H), 4.11 (s, 2H), 3.85 (s, 3H). ^{13}C NMR (125 MHz, $CDCl_3$) δ 171.8, 143.1, 132.0, 131.4, 130.7, 128.6, 127.3, 126.7, 126.7, 126.1, 123.5, 120.8, 118.9, 113.2, 106.9, 52.6, 46.22.

HRMS calc. for $C_{17}H_{15}NO_2Na$ $[M+Na]^+$ 288.0995, found 288.0993

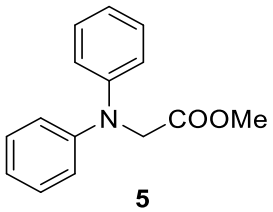

5

Product was isolated by thin layer chromatography in hexanes: ethyl acetate (3 : 0.5), R_f=0.6

^{1}H NMR (500 MHz, $CDCl_3$) δ 7.28 (t, *J* = 7.9 Hz, 4H), 7.04 – 6.97 (m, 6H), 4.47 (s, 2H), 3.75 (s, 3H). ^{13}C NMR (125 MHz, $CDCl_3$) δ 171.5, 147.5, 129.4, 122.1, 120.8, 54.1, 52.2.

HRMS calc. for $C_{15}H_{15}NO_2Na$ $[M+Na]^+$ 264.0995, found 264.0984

2.7 References

1. Hughes, A. B. *Amino Acids, Peptides and Proteins in Organic Chemistry, Analysis and Function of Amino Acids and Peptides*. John Wiley & Sons Inc.: Somerset, Germany, 2011.

2. Anighoro, A., Underappreciated Chemical Interactions in Protein–Ligand Complexes. In *Quantum Mechanics in Drug Discovery*, Heifetz, A., Ed. Springer US: New York, NY, 2020; pp 75-86.

3. Barrett, G. C.; Elmore, D. T., *Amino Acids and Peptides*. Cambridge University Press: Cambridge, United Kingdom, 1998.

4. Fleming, I., *Molecular Orbitals and Organic Chemical Reactions*. Ed. Wiley: Hoboken, N.J., 2010.

5. Neamati, N.; Hong, H.; Mazumder, A.; Wang, S.; Sunder, S.; Nicklaus, M. C.; Milne, G. W. A.; Proksa, B.; Pommier, Y., Depsides and Depsidones as Inhibitors of HIV-1 Integrase: Discovery of Novel Inhibitors through 3D Database Searching. *J. Med. Chem.* **1997,** *40* (6), 942-951.

6. Doherty, G. A.; Kamenecka, T.; McCauley, E.; Van Riper, G.; Mumford, R. A.; Tong, S.; Hagmann, W. K., *N*-Aryl 2,6-dimethoxybiphenylalanine Analogues as VLA-4 Antagonists. *Bioorg. Med. Chem. Lett.* **2002,** *12* (5), 729-731.

7. Lee, J.; Reynolds, C.; Jetter, M. C.; Youngman, M. A.; Hlasta, D. J.; Dax, S. L.; Stone, D. J.; Zhang, S.-P.; Codd, E. E., Design And Synthesis of Novel Pyrrolidine-Containing Bradykinin Antagonists. *Bioorg. Med. Chem. Lett.* **2003,** *13* (11), 1879-1882.

8. McKerrow, J. D.; Al-Rawi, J. M. A.; Brooks, P., Use of Diphenyliodonium Bromide in the Synthesis of Some *N*-Phenyl α-Amino Acids. *Synth. Commun.* **2010,** *40* (8), 1161-1179.

9. Hammoud, H.; Schmitt, M.; Blaise, E.; Bihel, F.; Bourguignon, J.-J., *N*-Heteroarylation of Chiral α-Aminoesters by Means of Palladium-Catalyzed Buchwald–Hartwig Reaction. *The J. Org. Chem.* **2013,** *78* (16), 7930-7937.

10. Osinubi, A. D.; Izunobi, J. U.; Asekun, O. T.; Familoni, O. B.; Bao, X., Transition Metal-Free, Base-Induced Arylation of Amino Acids: Synthesis of *N*-(para-Substituted phenyl)amino-2-carboxylic acids. *ChemistrySelect* **2020,** *5* (28), 8644-8648.

11. Sharma, K. K.; Mandloi, M.; Rai, N.; Jain, R., Copper-catalyzed *N*-(hetero)arylation of amino acids in water. *RSC Adv.* **2016,** *6* (99), 96762-96767.

12. Jiang, Q.; Jiang, D.; Jiang, Y.; Fu, H.; Zhao, Y., A Mild and Efficient Method for Copper-Catalyzed Ullmann-Type *N*-Arylation of Aliphatic Amines and Amino Acids. *Synlett* **2007,** *2007* (12), 1836-1842.

13. King, S. M.; Buchwald, S. L., Development of a method for the *N*-arylation of amino acid esters with aryl triflates. *Org. Lett.* **2016,** *18* (16), 4128-4131.

14. Ma, F.; Xie, X.; Ding, L.; Gao, J.; Zhang, Z., Palladium-Catalyzed Coupling Reaction of Amino Acids (Esters) with Aryl Bromides and Chlorides. *Tetrahedron* **2011,** *67* (48), 9405-9410.

15. Fu, H.; Prats Lujan, A.; Bothof, L.; Zhang, J.; Tepper, P. G.; Poelarends, G. J., Biocatalytic Asymmetric Synthesis Of *N*-Aryl-Functionalized Amino Acids And Substituted Pyrazolidinones. *ACS Catal.* **2019,** *9* (8), 7292-7299.

16. Kürti, L. s.; Czakó, B., *Strategic Applications of Named Reactions in Organic Synthesis: Background and Detailed Mechanisms*. Elsevier Academic Press: Amsterdam, 2005.

17. Young, H. A.; Guthrie, Q. A. E.; Proulx, C., *N*-Arylation of Amino Acid Esters to Expand Side Chain Diversity in Ketoxime Peptide Ligations. *J. Org. Chem.* **2020,** *85* (3), 1748-1755.

18. Chen, Z.; Zeng, H.; Gong, H.; Wang, H.; Li, C.-J., Palladium-catalyzed reductive coupling of phenols with anilines and amines: efficient conversion of phenolic lignin model monomers and analogues to cyclohexylamines. *Chem. Sci.* **2015,** *6* (7), 4174-4178.

19. Qiu, Z.; Li, J.-S.; Li, C.-J., Formal Aromaticity Transfer for Palladium-Catalyzed Coupling Between Phenols and Pyrrolidines/Indolines. *Chem. Sci.* **2017,** *8* (10), 6954-6958.

20. Chen, Z.; Zeng, H.; Girard, S. A.; Wang, F.; Chen, N.; Li, C.-J., Formal Direct Cross-Coupling of Phenols with Amines. *Angew. Chem. Int. Ed.* **2015,** *54* (48), 14487-14491.

21. Girard, S. A.; Hu, X.; Knauber, T.; Zhou, F.; Simon, M.-O.; Deng, G.-J.; Li, C.-J., Pd-Catalyzed Synthesis of Aryl Amines via Oxidative Aromatization of Cyclic Ketones and Amines with Molecular Oxygen. *Org. Lett.* **2012,** *14* (21), 5606-5609.

22. Li, J.-S.; Qiu, Z.; Li, C.-J., Palladium-Catalyzed Synthesis of *N*-Cyclohexyl Anilines from Phenols with Hydrazine or Hydroxylamine via N-N/O Cleavage. *Adv. Synth. Catal.* **2017,** *359* (20), 3648-3653.

23. Choudhary, V. R.; Samanta, C., Role of Chloride or Bromide Anions and Protons for Promoting the Selective Oxidation Of H_2 By O_2 To H_2O_2 Over Supported Pd Catalysts in an Aqueous Medium. *J. Catal.* **2006,** *238* (1), 28-38.

24. Liu, H.; Jiang, T.; Han, B.; Liang, S.; Zhou, Y., Selective Phenol Hydrogenation to Cyclohexanone Over a Dual Supported Pd-Lewis Acid Catalyst. *Science* **2009,** *326* (5957), 1250-2.

25. Sutter, M.; Sotto, N.; Raoul, Y.; Metay, E.; Lemaire, M., Straightforward Heterogeneous Palladium Catalyzed Synthesis Of Aryl Ethers And Aryl Amines Via A Solvent Free Aerobic And Non-Aerobic Dehydrogenative Arylation. *Green Chem.* **2013,** *15* (2), 347-352.

26. Meng, Q.; Hou, M.; Liu, H.; Song, J.; Han, B., Synthesis Of Ketones From Biomass-Derived Feedstock. *Nat. Commun.* **2017,** *8* (1), 14190.

27. Benkhaled, M.; Descorme, C.; Duprez, D.; Morin, S.; Thomazeau, C.; Uzio, D., Study Of Hydrogen Surface Mobility And Hydrogenation Reactions Over Alumina-Supported Palladium Catalysts. *Appl. Catal. A* **2008,** *346* (1), 36-43.

Chapter 3. *N*-Cylohexylation of α-amino acids using phenol

3.1 Background

N-alkyl-α-amino acids have become increasingly popular as materials for surfactants,[1] as buffering agents in the pharmaceutical and cosmetic industries,[2] as peptide *N*-modifications,[3] as well as crucial building blocks for the manufacture of plastics and herbicides.[4] However, the mono-*N*-alkylation of α- or β-amino acids is challenging, especially if enantiomeric retention is being considered. Nevertheless, chemists have been able to circumvent these difficulties through the development of methodologies that may involve nucleophilic substitution, reductive conditions, or metal catalysts. A brief review of these methodologies, applied specifically for the synthesis of *N*-cyclohexylated amino acids, is herein described.

The first report for the preparation of *N*-cyclohexylaminoisobutiric acid was from Nelson and Sinclair in 1960 (Scheme 3.1).[5] Their aim was to synthesize a nitrogen containing analogue to naturally occurring estrogens. Their methodology consists of using cyclohexylamine as the starting material and condensing it to acetone cyanohydrin, later on hydrolyzing the nitrile to yield the corresponding *N*-cyclohexylated amino acid in quantitative yields. Evidently, this procedure is limited in scope and does not yield an optically active compound. Nonetheless, subsequently developed techniques maintained cyclohexylamine as the starting material.

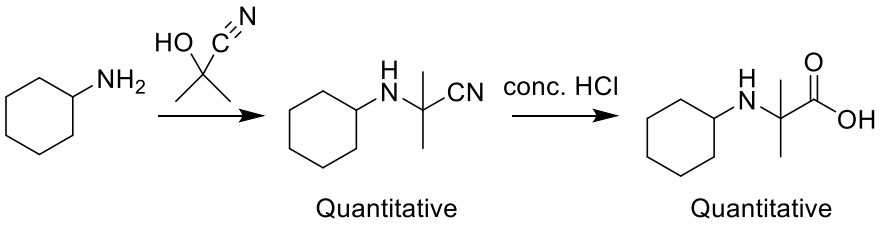

Scheme 3.1 Synthesis of *N*-cyclohexylaminoisobutyric acid from cyclohexylamine[5]

In 2004, Hu, Chen and Yang reported the synthesis of *N*-cyclohexylated glycine using a solid support (Scheme 3.2).[6] The PEG-bound product was prepared through an ester linkage using bromoacetyl bromide and PEG_{3400}. The polymer-supported product is obtained by precipitation and washing, followed by reacting with a variety of amines at room temperature to afford the corresponding PEG-bound *N*-modified amino acids. The advantage of this strategy is that no excess reagents are needed, and over alkylation of the corresponding amino acid is unlikely due to the steric bulk provided by the PEG support.

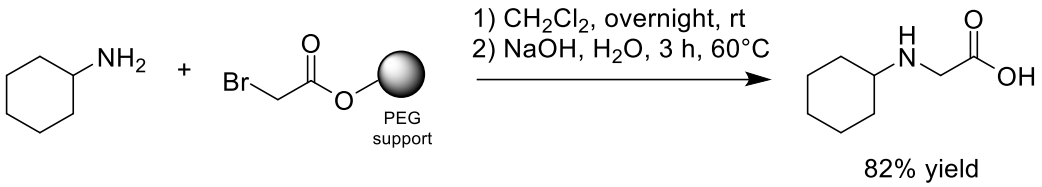

Scheme 3.2 Solid supported synthesis of *N*-cyclohexylated glycine[6]

The group of Tomkinson reported in 2007 a method for the formation of *N*-alkyl glycine derivatives using primary amines and glyoxylic acid (Scheme 3.3).[7] The reaction proceeds through a formylated intermediate, which is cleaved through the addition of 2 M hydrochloric acid, yielding the glycine derivatives as the chloride salts. The reaction scope included amines with different functionalities such as alkenes, carboxylic acids and substituted benzylic substrates. The proposed mechanism involves an imine intermediate upon condensation of the amine with glyoxylic acid, which then adds to a second molecule of glyoxylic acid to form, upon rearrangement, an *N*-formylated intermediate.

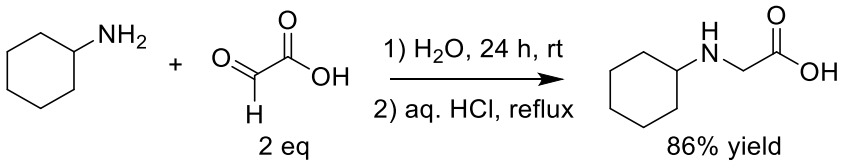

Scheme 3.3 Synthesis of *N*-alkyl glycine derivatives using primary amines and glyoxylic acid[7]

In 2015, inspired by our group's previous work,[8] Vaccaro *et al*.[9] published a hydrogenation-reductive amination of phenol in water-efficient at room temperature for 12 h or at 60 °C under microwave radiation for 20 min (Scheme 3.4). The protocol was adapted to work under continuous flow to yield different cyclohexylated amines in gram scale. The reaction scope includes 14 examples of various aliphatic amines and substituted phenols, with yields ranging from 35% to 85% yield. In particular, the *N*-cyclohexylation of phenylalanine methyl ester was achieved using this methodology, obtaining the *N*-cyclohexylated product in 64% yield. While no enantiomeric purity nor the diasteromeric ratio were reported, it set a precedent for the *N*-cyclohexylation of an aromatic α-amino acid ester under aqueous, reductive conditions.

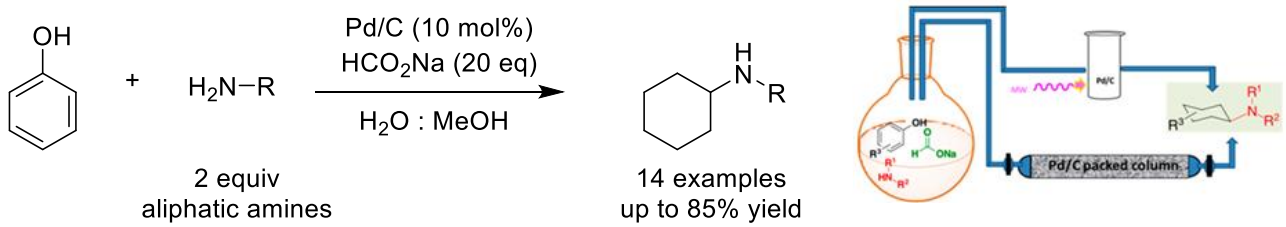

Scheme 3.4 Hydrogenation-reductive amination of phenol to yield substituted cyclohexylamines[9]

An *N*-alkylation of unprotected amino acids with alcohols was reported in 2017 by the group of Feringa.[10] This methodology uses a ruthenium catalyst which can oxidize the primary alcohols into its aldehyde form while generating a Ru-H species. The aldehyde and the *N*-terminus of the α-amino acid then condense to give an imine intermediate, which is reduced thanks to the Ru-H species, regenerating the catalyst and yielding the desired *N*-alkylated product. With the exception of isopropanol, the reaction yielded the di-*N*-alkylated products. The substrate scope included dipeptides and a tripeptide, and excellent retention of optical purity was observed in most cases.

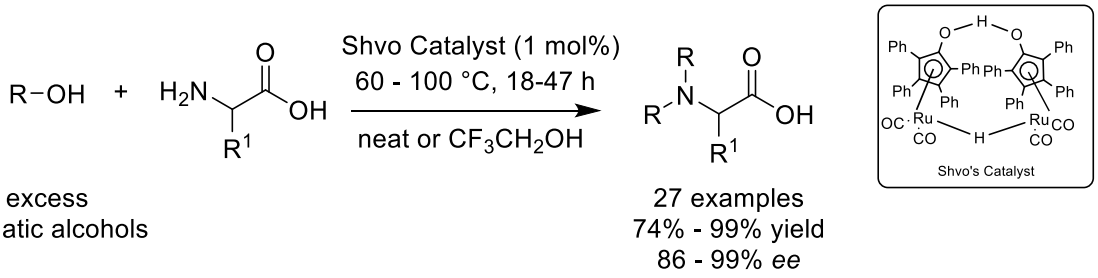

Scheme 3.5 *N*-alkylation of unprotected amino acids with alcohols[10]

3.2 Research objectives and plan

Given the harsh conditions required for the re-aromatization of the cyclohexyl ring, we envisioned favouring the formation of the fully hydrogenated product (Scheme 3.6). Ideally, this methodology would allow for (1) the use of phenol as the starting material, (2) the use of unprotected amino acids, (3) the use of a benign solvent, and (4) no heating to avoid racemization; while being applicable to a wide range of amino acids and peptides. In this case, the use of a hydride donor is necessary for the initial reduction of phenol into cyclohexenone or cyclohexanone for the condensation reaction to take place. Therefore, our study would begin with the screening of sodium formate before exploring the reaction scope. While the work of Vaccaro is similar in the sense that the reaction is run in water,[9] we envisioned a system where the amino acid is the limiting reagent, is broadly applicable to all amino acids as opposed to only phenylalanine, and without the use of microwave irradiation.

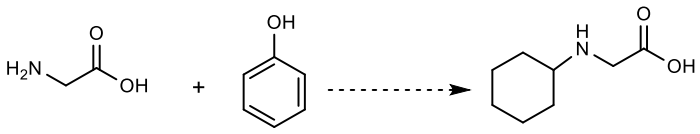

Scheme 3.6 Model reaction for the *N*-cyclohexylation of α-amino acids

3.3 Results and discussion

3.3.1 Condition Screening

We used glycine as the model substrate at room temperature in water, with a slight excess of phenol as the coupling reagent (1.5 equiv) and palladium on charcoal (10 mol%) as the catalyst. Each equivalent of sodium formate decomposes to give 1 equivalent of H^- which adsorbs to the palladium catalyst to give the PdH_2 intermediate. One equivalent of PdH_2 can react with phenol to give cyclohexenone, thus forming the desired reactive species. However, using 2 equiv of HCO_2Na with respect to phenol only produced the desired product in 11% yield with respect to glycine (Table 3.1, entry 1), and by increasing the loading to 4 equiv, the yield dramatically improved to 96% (Table 3.1, entry 2). Further increasing the loading to 6 equiv led the reaction to proceed quantitatively (Table 3.1, entry 3). Attempts to reduce the amount of phenol (Table 3.1, entry 4) or Pd/C (Table 3.1, entry 5) resulted in lower yields of *N*-cyclohexylglycine (**3**). Nonetheless, we were pleasantly surprised to find that the Pd/C catalyst could be recovered and reused for up to three cycles upon filtration before a decrease in activity was observed (Table 3.1, entries 6-8).

Table 3.1 Optimization of the reaction conditions for the *N*-cyclohexylation of glycine using phenol

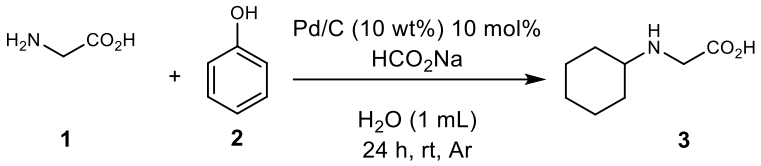

1 2 3

entry	**2** (equiv)	HCO_2Na (equiv)[a]	yield (%) 3[b]
1	1.5	2	11
2	1.5	4	96
3	1.5	6	>99
4	1	6	86
5 [c]	1.5	6	9
6 [d]	1.5	6	>99
7 [e]	1.5	6	>99
8 [f]	1.5	6	89

Reaction conditions: **1** (0.2 mmol, 1 equiv), **2**, HCO_2Na, Pd/C (10 wt%, 0.2 mmol), H_2O (1 mL), 24 h, rt.

[a] Equivalency respective to phenol.

[b] Yield determined by ^1H NMR using DMSO as the internal standard.

[c] 5 mol% of Pd/C (10 wt%) was used instead of 10 mol%.

[d] Pd/C recycled for the first time. [e] Pd/C recycled for the second time. [f] Pd/C recycled for the third time.

3.3.2 Substrate scope

The reaction scope was investigated under the optimized conditions, proving to be efficient in the *N*-cyclohexylation of 17 out of the 20 naturally occurring amino acids without protecting groups (Figure 3.1). Sulphur-containing compounds would deactivate the palladium catalyst, thereby making them inaccessible substrates for this methodology. Amino acids with nonpolar, aliphatic R^1 chains, including β-alanine (**3**, **3a**-**3d**), as well as those with polar uncharged (**3e**-**3i**), aromatic (**3j**-**3l**), and polar charged R^1 chains (**3m**-**3q**) were excellent substrates for the reaction and showed that functional groups such as alcohols, carboxylic acids and amides were compatible. In the case of *O*-unprotected tyrosine (**3k**), the phenol ring was also reduced, despite having only 2 eq of formate present in the reaction. This problem was circumvented by using *O*^{t}Bu-Tyr (**3l**) which prevents the formation of the ketone intermediate while adding steric bulk to the ring. Given that we were interested in mainting the natural functionality of the amino acids, more equivalents of sodium formate were not tested to further push the reaction towards the formation of **3k**. Lysine resulted in the doubly *N*-cyclohexylated product (**3o**), and for which reason the amount of phenol being added was required to be doubled. The case of tryptophan was particularly interesting, as the reaction's favoured product was the result of a Pictet-Spengler condensation (**3r**). Some substrates required the use of gentle heating at 50 °C or the addition of methanol to the reaction solvent in order to facilitate the reaction through the improvement of the substrate's solubility in water. With this in mind, we were set to test more challenging substrates such as di-, tri- and tetra- peptides which, if necessary, could be later on conjugated to longer amino acid chains through traditional coupling processes. Glycine peptide chains were chosen as model substrates and were successfully *N*-cyclohexylated (**3s**-**3u**), with solubility being the only limitation to the process. The solubility of these peptides can be readily tuned by modifying the different substituents in the R^1 chains, making this an efficient procedure for their *N*-modification. Finally, various phenolic compounds were examined as the coupling partners, with *para*-substituted compounds being well-tolerated (**3w**-**3x**), and di-substituted phenols leading to a lower yield due to steric effects (**3y**). When *para*-chlorophenol (**3z**) was used as the substrate, the product with the cleaved chlorine was obtained in quantitative yields, in agreement with observations of previous reports.[9] To test for enantiomeric retention we selected product **3j** since the α-proton could easily racemize due to its benzylic position. In addition, the reaction for phenylalanine (**3j**) was performed at 50 °C, making the conditions harsher than for most of the substrates. Upon running the reaction under the described conditions, we found that the *N*-cyclohexylated product **3j** was generated without any racemization.

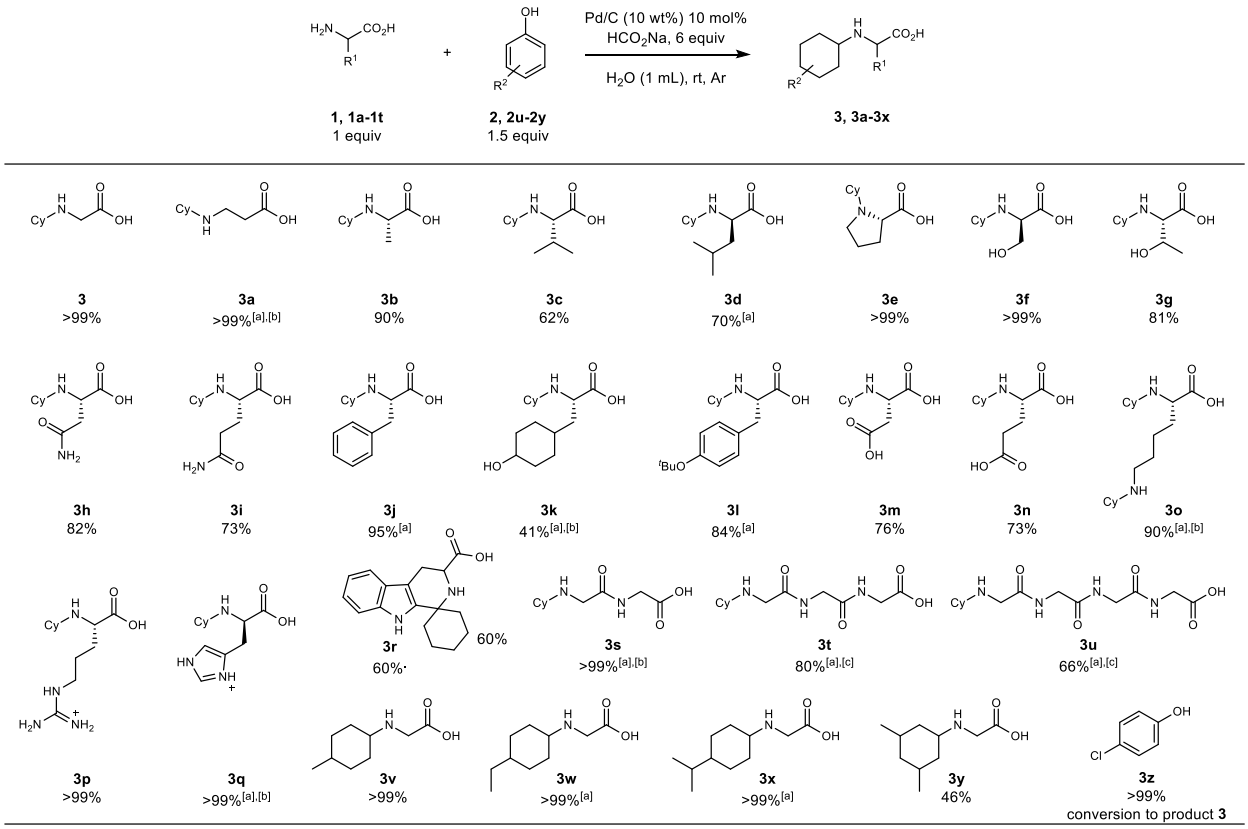

Figure 3.1 Amino acid and phenolic substrate scope for the *N*-cyclohexylation reaction. Reaction conditions: **1, 1a-1t** (0.2 mmol, 1 equiv), **2, 2u-2y** (0.3 mmol, 1.5 equiv), HCO_2Na (1.8 mmol, 6 equiv), Pd/C (10 wt%, 0.2 mmol), H_2O (1 mL), 24 h, rt. [a] Temperature increased to 50 °C to improve solubility. [b] 1 mL of a 1:1 MeOH:H_2O mixture was used as the solvent. [c] 1 mmol of starting material used in 0.3 mL of 20% MeOH in H_2O.

3.3.3 Mechanistic considerations

Following our group's results to probe this mechanism,[11] we tested cyclohexanol, cyclohexanone and 2-cyclohexen-1-one as coupling partners under the optimized conditions (Figure 3.2). As suspected, the alcohol was the only species unsuitable for the transformation since the imine formation cannot proceed. The mono *N*-cyclohexylation was observed when using both cyclohexanone and 2-cyclohexen-1-one. These results further support the mechanistic proposal that phenol is reduced *in-situ* to a ketone, aminated, and also reduced to yield product **3**.

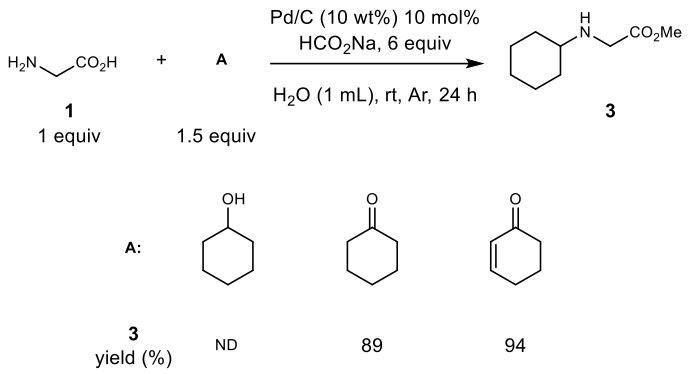

Figure 3.2 Different coupling partners for the *N*-cyclohexylation of glycine. Reaction conditions: **1** (0.2 mmol, 1 equiv), **A** (0.3 mmol, 1.5 equiv), HCO_2Na (1.8 mmol, 6 equiv), Pd/C (10 wt%, 0.2 mmol), H_2O (1 mL), 24 h, rt. Yield determined by ^1H NMR using DMSO as the internal standard. ND: not detected.

3.4 Conclusion and outlook

The *N*-alkylation of amino acids and peptides using phenol as a bio-renewable alkylation reagent was successfully achieved with Pd/C as the catalyst. While *N*-arylation requires high temperatures due to the high energy required to aromatize the cyclohexyl ring, the *N*-cyclohexylation was achieved for 17 out of the 20 naturally occurring amino acids under bio-compatible conditions without racemization. With this technique in hand, we hope to move towards the usage of more sustainable feedstocks to modify bio-compounds with applications in chemical biology, pharmaceuticals, and agrochemicals. Furthermore, this methodology could use tyrosine's side chain as a handle, without compromising the composition of the rest of the peptide sequence, to produce polymerization products, selective protein tagging, or macrocyclic peptides.

3.5 Contributions

Project conceptualization was realized by Prof. Chao-Jun Li. Methodology, experimentation and characterization were performed by myself with the assistance of Dr. Inna Perepichka. High-resolution mass spectrometry was performed by Dr. Nadim Saadeh and Dr. Alexander Wahba at the McGill University Department of Chemistry Mass Spectrometry Laboratory. The publication manuscript, which shares

common content with this thesis chapter, was written by myself, edited and proofread by Dr. Zoë Hearne, Dr. Wenbo Liu, and Dr. Zihang Qiu and Prof. Chao-Jun Li.

3.6 Experimental section

3.6.1 General Information

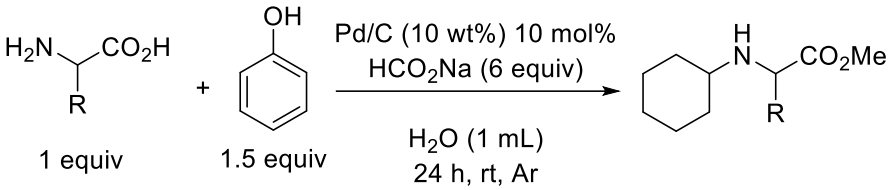

In a U-shaped microwave vial, charged with a stir bar, the amino acid (0.2 mmol, 1 equiv), phenol (0.3 mmol, 1.5 equiv), HCO_2Na (1.8 mmol, 6 equiv) and Pd/C (10% wt) (0.2 mmol, 25.5 mg) were added under air. The vial was flushed with argon three times, and 1 mL of distilled water was then added under an argon flow. The vial was capped with a rubber septum, and stirring was set at 500 rpm for 24 h at the indicated temperature. The septum was then removed, and the reaction was diluted using distilled water. The Pd/C was then removed by filtration through celite, followed by washing with additional water. The reaction was acidified to pH=0 with HCl to be able to remove formic acid in vacuo. The reaction mixture was then concentrated in vacuo and filtered with cold methanol to remove NaCl to obtain the pure product.

3.6.2 Analytical Data

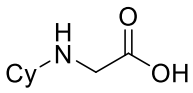

3

^{1}H NMR (500 MHz, D_2O) δ 3.94 (s, 2H), 3.28 (tt, *J* = 11.4, 3.7 Hz, 1H), 2.19 (d, *J* = 11.5 Hz, 2H), 1.95 (d, *J* = 13.2 Hz, 2H), 1.80 – 1.69 (m, 1H), 1.58 – 1.36 (m, 4H), 1.34 – 1.17 (m, 1H). ^{13}C NMR (126 MHz, D_2O) δ 170.4, 57.6, 45.6, 28.9, 24.6, 24.1.

HRAPCI-MS calc. for $C_8H_{14}NO_2$ $[M-H]^-$ 156.1019, found 156.1018

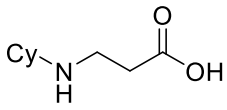

3a

^{1}H NMR (500 MHz, D_2O) δ 3.47 (t, *J* = 6.7 Hz, 2H), 3.33 – 3.24 (m, 1H), 2.96 (t, *J* = 6.7 Hz, 2H), 2.20 (d, *J* = 11.3 Hz, 2H), 1.94 (d, *J* = 13.0 Hz, 2H), 1.82 – 1.73 (m, 1H), 1.55 – 1.37 (m, 4H), 1.35 – 1.24 (m, 1H). ^{13}C NMR (126 MHz, D_2O) δ 172.8, 56.4, 38.6, 29.1, 27.5, 23.2, 22.7.

HRESI-MS calc. for $C_9H_{18}NO_2$ $[M+H]^+$ 172.1332, found 172.1340

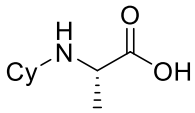

3b

^{1}H NMR (500 MHz, MeOD) δ 4.18 (q, *J* = 7.2 Hz, 1H), 3.21 – 3.11 (m, 1H), 2.18 – 2.03 (m, 2H), 1.88 (d, *J* = 11.8 Hz, 2H), 1.71 (d, *J* = 13.1 Hz, 1H), 1.59 (d, *J* = 7.2 Hz, 3H), 1.46 – 1.26 (m, 5H). ^{13}C NMR (126 MHz, MeOD) δ 172.0, 57.1, 53.3, 30.3, 30.2, 26.0, 25.5, 16.3, 15.6.

HRESI-MS calc. for $C_9H_{17}NO_2Na$ $[M+Na]^+$ 194.1151, found 194.1149

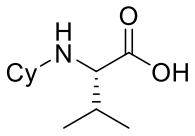

3c

^{1}H NMR (500 MHz, MeOD) δ 3.47 (d, *J* = 4.1 Hz, 1H), 3.04 – 2.96 (m, 1H), 2.21 (dtd, *J* = 14.0, 7.0, 4.1 Hz, 1H), 2.16 – 2.06 (m, 2H), 1.86 (d, *J* = 12.0 Hz, 2H), 1.70 (d, *J* = 12.8 Hz, 1H), 1.46 (ddd, *J* = 24.3, 12.2, 3.4 Hz, 1H), 1.40 – 1.27 (m, 3H), 1.26 – 1.15 (m, 1H), 1.06 (dt, *J* = 16.6, 8.3 Hz, 6H). ^{13}C NMR (126 MHz, MeOD) δ 172.6, 67.0, 59.3, 31.2, 31.0, 29.7, 26.1, 25.8, 25.7, 19.1, 18.6.

HRESI-MS calc. for $C_{11}H_{21}NO_2Na$ $[M+Na]^+$ 222.1464, found 222.1476

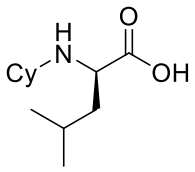

3d

^{1}H NMR (500 MHz, MeOD) δ 3.86 (t, *J* = 6.8 Hz, 1H), 3.12 – 3.03 (m, 1H), 2.19 – 2.02 (m, 2H), 1.93 – 1.77 (m, 4H), 1.72 (d, *J* = 12.7 Hz, 1H), 1.67 – 1.58 (m, 1H), 1.46 – 1.30 (m, 4H), 1.27 – 1.17 (m, 1H), 1.02 (dd, *J* = 12.0, 6.3 Hz, 6H). ^{13}C NMR (126 MHz, MeOD) δ 172.5, 58.1, 40.7, 31.1, 29.9, 26.1, 26.0, 25.6, 25.5, 23.3, 22.1.

HRESI-MS calc. for $C_{12}H_{24}NO_2$ $[M+H]^+$ 214.1802, found 214.1806

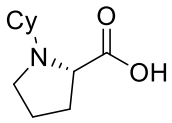

3e

^{1}H NMR (500 MHz, $CDCl_3$) δ 3.85 (ddd, *J* = 10.4, 7.8, 4.3 Hz, 2H), 3.13 (tt, *J* = 11.7, 3.2 Hz, 1H), 2.92 (td, *J* = 10.4, 7.4 Hz, 1H), 2.34 (dt, *J* = 10.9, 5.9 Hz, 1H), 2.20 (dtd, *J* = 11.4, 9.5, 4.5 Hz, 1H), 2.15 – 2.04 (m, 2H), 1.97 – 1.83 (m, 4H), 1.69 (d, *J* = 13.1 Hz, 1H), 1.57 – 1.38 (m, 2H), 1.35 – 1.21 (m, 2H), 1.19 – 1.08 (m, 1H). ^{13}C NMR (126 MHz, $CDCl_3$) δ 170.8, 66.5, 63.4, 51.6, 30.2, 29.1, 28.5, 25.2, 25.0, 24.9, 24.3.

HRESI-MS calc. for $C_{11}H_{19}NO_2Na$ $[M+Na]^+$ 220.1308, found 220.1300

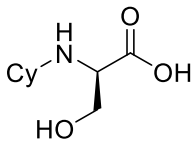

3f

^{1}H NMR (500 MHz, D_2O) δ 4.61 (t, *J* = 3.4 Hz, 1H), 4.45 – 4.37 (m, 2H), 3.59 (ddd, *J* = 15.5, 7.7, 3.8 Hz, 1H), 2.40 (t, *J* = 14.3 Hz, 2H), 2.13 (d, *J* = 13.1 Hz, 2H), 1.94 (d, *J* = 12.9 Hz, 1H), 1.79 – 1.67 (m, 2H), 1.60 (qd, *J* = 12.9, 2.9 Hz, 2H), 1.52 – 1.40 (m, 1H). ^{13}C NMR (126 MHz, D_2O) δ 170.7, 59.1, 56.9, 29.1, 29.0, 24.6, 24.2.
HRESI-MS calc. for $C_9H_{17}NO_3K$ $[M+K]^+$ 226.0840, found 226.0839

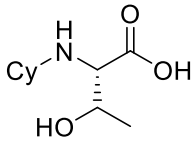

3g

^{1}H NMR (500 MHz, MeOD) δ 4.16 (p, *J* = 6.4 Hz, 1H), 3.90 (d, *J* = 6.6 Hz, 1H), 3.12 (tt, *J* = 11.7, 3.8 Hz, 1H), 2.11 (dd, *J* = 16.7, 14.0 Hz, 2H), 1.88 (d, *J* = 13.1 Hz, 2H), 1.69 (d, *J* = 12.8 Hz, 1H), 1.63 – 1.50 (m, 1H), 1.48 – 1.32 (m, 6H), 1.31 – 1.18 (m, 1H). ^{13}C NMR (126 MHz, D_2O) δ 170.1, 66.0, 65.4, 63.3, 58.6, 29.5, 28.4, 24.5, 24.3, 24.2, 19.4.
HRESI-MS found for $C_{10}H_{20}NO_3$ $[M+H]^+$ 202.1438, found 202.1426

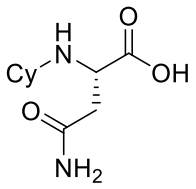

3h

^{1}H NMR (500 MHz, D_2O) δ 4.44 (t, *J* = 5.6 Hz, 1H), 3.23 (tt, *J* = 11.5, 3.8 Hz, 1H), 3.08 – 2.98 (m, 2H), 2.07 (t, *J* = 14.4 Hz, 2H), 1.81 (d, *J* = 13.4 Hz, 2H), 1.63 (dd, *J* = 9.9, 3.1 Hz, 1H), 1.39 (qd, *J* = 11.8, 2.6 Hz, 2H), 1.34 – 1.22 (m, 2H), 1.21 – 1.09 (m, 1H). ^{13}C NMR (126 MHz, D_2O) δ 173.0, 170.7, 57.4, 53.4, 38.8, 33.4, 28.9, 28.8, 24.4, 24.0.
HRESI-MS calc. for $C_{10}H_{19}N_2O_3$ $[M+H]^+$ 215.1390, found 215.1390

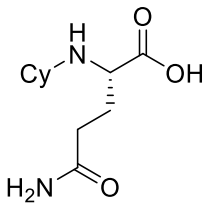

3i

^{1}H NMR (500 MHz, D_2O) δ 3.19 (dd, *J* = 8.5, 5.4 Hz, 1H), 2.31 (tt, *J* = 10.9, 3.5 Hz, 1H), 2.20 – 2.05 (m, 2H), 1.89 (d, *J* = 12.0 Hz, 1H), 1.77 (dtd, *J* = 16.8, 11.2, 5.7 Hz, 1H), 1.72 – 1.61 (m, 4H), 1.57 (d, *J* = 12.3 Hz, 1H), 1.29 – 1.02 (m, 4H), 0.93 (qd, *J* = 12.4, 3.4 Hz, 1H). ^{13}C NMR (126 MHz, D_2O) δ 182.6, 182.6, 60.4, 55.0, 34.3, 33.3, 31.1, 30.1, 25.6, 24.7, 24.4.

HRESI-MS calc. for $C_{11}H_{20}N_2O_3$ 228.1241, found 228.1237

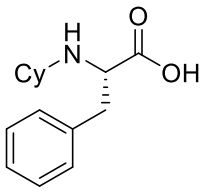

3j

^{1}H NMR (500 MHz, D_2O) δ 7.34 (t, *J* = 7.3 Hz, 2H), 7.30 – 7.21 (m, *J* = 15.5, 7.3 Hz, 3H), 3.52 (dd, *J* = 8.5, 5.4 Hz, 1H), 2.92 (dd, *J* = 13.2, 5.2 Hz, 1H), 2.76 (dd, *J* = 13.1, 8.8 Hz, 1H), 2.36 (t, *J* = 10.9 Hz, 1H), 1.92 (d, *J* = 11.6 Hz, 1H), 1.68 (d, *J* = 11.5 Hz, 3H), 1.59 (d, *J* = 11.8 Hz, 1H), 1.31 – 1.04 (m, 4H), 0.96 (dd, *J* = 22.4, 10.6 Hz, 1H). ^{13}C NMR (126 MHz, D_2O) δ 181.7, 138.1, 129.2, 128.5, 126.5, 62.1, 54.7, 39.3, 33.3, 30.9, 25.6, 24.7, 24.4.

HRESI-MS calc. for $C_{15}H_{21}NO_2Na$ $[M+Na]^+$ 270.1464, found 270.1469

HPLC analysis ((Chiralcel IC, 80:20:0.1 hexane:IPA:TFA 3.0 mL/min, 210 nm) no racemization. t_R (L-Phe) = 4.2 min, t_R (D-Phe) = 5.2 min.

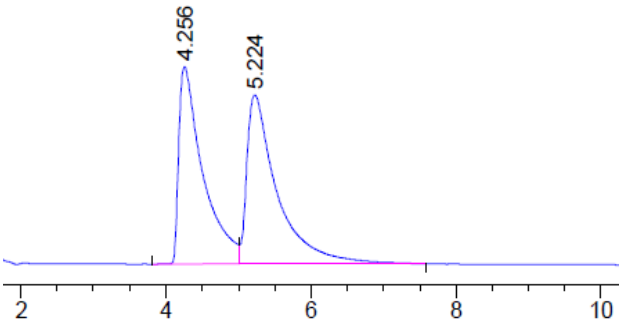

Reaction ran using D,L-phenyl alanine as the starting material according to described procedure

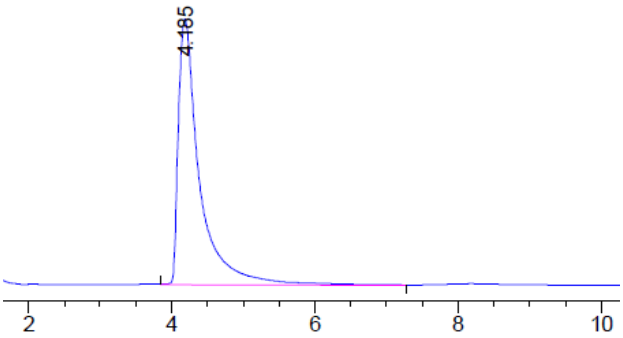

Reaction ran using L-phenyl alanine as the starting material according to described procedure

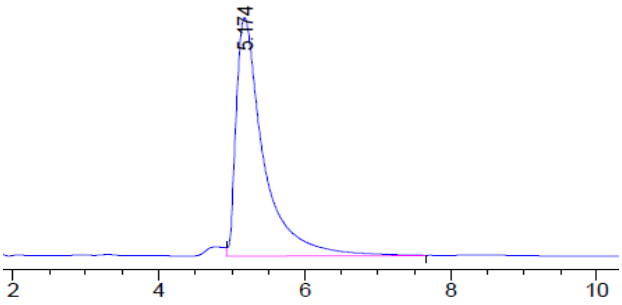

Reaction ran using D-phenyl alanine as the starting material according to described procedure

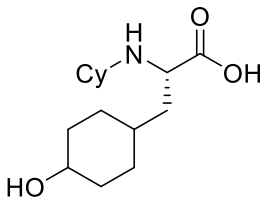

3k

^{1}H NMR (500 MHz, MeOD) δ 4.10 – 4.02 (m, 1H), 3.50 (tt, *J* = 10.8, 4.1 Hz, 1H), 3.15 – 3.05 (m, 1H), 2.11 (dd, *J* = 24.9, 11.8 Hz, 2H), 2.01 – 0.95 (m, 20H). ^{13}C NMR (126 MHz, MeOD) δ 171.5, 71.1, 58.2, 56.5, 38.1, 35.9, 35.7, 34.5, 32.7, 31.3, 30.9, 29.8, 25.9, 25.6, 25.5.

HRESI-MS calc. for $C_{15}H_{28}NO_3$ $[M+H]^+$ 270.2064, found 270.2066

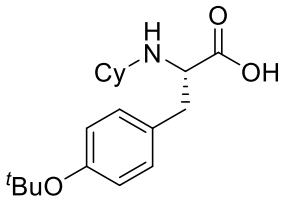

3l

^{1}H NMR (500 MHz, MeOD) δ 7.17 (d, *J* = 8.5 Hz, 2H), 6.87 (d, *J* = 8.5 Hz, 2H), 3.43 (dd, *J* = 7.7, 6.3 Hz, 1H), 2.82 (ddd, *J* = 19.6, 13.4, 7.0 Hz, 2H), 2.40 (tt, *J* = 10.6, 3.7 Hz, 1H), 1.94 (d, *J* = 12.3 Hz, 1H), 1.76 (d, *J* = 12.1 Hz, 1H), 1.68 (dd, *J* = 17.7, 8.4 Hz, 2H), 1.59 (d, *J* = 11.7 Hz, 1H), 1.34 – 1.06 (m, 13H), 0.96 (qd, *J* = 12.3, 3.5 Hz, 1H). ^{13}C NMR (126 MHz, MeOD) δ 181.6, 154.7, 135.6, 130.9, 125.0, 79.3, 64.0, 56.3, 40.8, 34.9, 32.9, 29.2, 27.2, 26.3, 26.0.

HRESI-MS calc. for $C_{19}H_{29}NO_3Na$ $[M+Na]^+$ 342.2040, found 342.2034

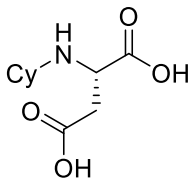

3m

^{1}H NMR (500 MHz, D_2O) δ 4.49 (dd, *J* = 6.2, 4.9 Hz, 1H), 3.23 (dt, *J* = 15.5, 3.8 Hz, 1H), 3.17 – 3.00 (m, 3H), 2.25 – 2.17 (m, 1H), 2.13 (d, *J* = 11.8 Hz, 1H), 1.88 (d, *J* = 13.1 Hz, 2H), 1.70 (d, *J* = 13.0 Hz, 1H), 1.53 – 1.30 (m, 4H), 1.30 – 1.17 (m, 1H). ^{13}C NMR (126 MHz, MeOD) δ 171.4, 170.2, 59.2, 54.5, 34.9, 30.5, 29.9, 25.9, 25.6, 25.5.

HRESI-MS calc. for $C_{10}H_{16}NO_4$ $[M-H]^-$ 214.1085, found 214.1095

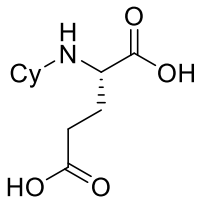

3n

^{1}H NMR (500 MHz, D_2O) δ 3.23 (dd, *J* = 8.1, 5.5 Hz, 1H), 2.35 (t, *J* = 10.8 Hz, 1H), 2.16 (pd, *J* = 14.7, 5.7 Hz, 2H), 1.93 (d, *J* = 11.0 Hz, 1H), 1.81 (dq, *J* = 17.1, 5.8 Hz, 1H), 1.76 – 1.65 (m, *J* = 16.4 Hz, 4H), 1.61 (d, *J* = 11.6 Hz, 1H), 1.33 – 1.06 (m, *J* = 41.0, 24.6, 12.4 Hz, 4H), 0.97 (dd, *J* = 22.2, 10.3 Hz, 1H). ^{13}C NMR (126 MHz, D_2O) δ 182.6, 60.4, 55.0, 34.3, 33.3, 31.1, 30.1, 25.6, 24.8, 24.4.

HRESI-MS calc. for $C_{11}H_{18}NO_4$ $[M-H]^-$ 228.1241, found 228.1233

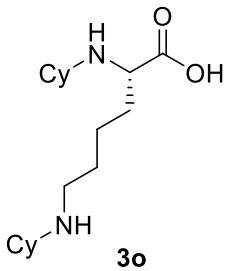

3o

^{1}H NMR (500 MHz, CD_3OD) δ 4.17 – 4.11 (m, 1H), 3.15 (t, *J* = 11.6 Hz, 1H), 3.11 – 3.01 (m, 3H), 2.21 – 1.94 (m, 6H), 1.87 (d, *J* = 8.8 Hz, 4H), 1.84 – 1.32 (m, 14H), 1.30 – 1.15 (m, 2H). ^{13}C NMR (126 MHz, CD_3OD) δ 171.1, 58.5, 58.4, 57.8, 45.2, 31.0, 30.8, 30.4, 30.3, 29.9, 26.9, 26.1, 26.0, 25.6, 25.5, 23.3. HRESI-MS calc. for $C_{18}H_{35}N_2O_2$ $[M+H]^+$ 311.2693, found 311.2687

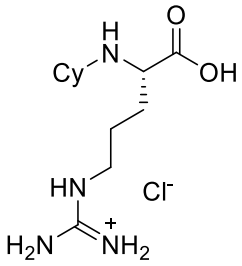

3p

^{1}H NMR (500 MHz, D_2O) δ 4.33 (dd, *J* = 7.3, 4.8 Hz, 1H), 3.35 (dd, *J* = 13.1, 6.2 Hz, 3H), 2.25 – 2.04 (m, 4H), 1.97 – 1.68 (m, 5H), 1.50 (qd, *J* = 12.0, 3.3 Hz, 2H), 1.44 – 1.32 (m, 2H), 1.32 – 1.15 (m, 1H). ^{13}C NMR (126 MHz, D_2O) δ 171.3, 156.8, 57.3, 56.5, 40.6, 29.3, 29.0, 26.4, 24.6, 24.3, 24.3, 23.9.

HRESI-MS calc. for $C_{12}H_{25}N_4O_2^+$ 257.1972, found 257.1971

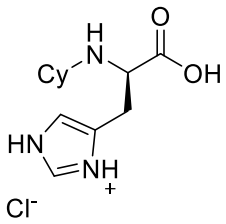

3q

^{1}H NMR (500 MHz, D_2O) δ 8.91 (s, 1H), 7.68 (s, 1H), 4.71 (dd, *J* = 8.0, 5.2 Hz, 1H), 3.75 (dd, *J* = 15.8, 5.0 Hz, 1H), 3.64 (dd, *J* = 15.8, 8.2 Hz, 1H), 3.48 (ddd, *J* = 11.6, 8.0, 3.9 Hz, 1H), 2.26 (t, *J* = 14.5 Hz, 2H), 1.98 (d, *J* = 12.8 Hz, 2H), 1.79 (d, *J* = 12.9 Hz, 1H), 1.65 – 1.53 (m, 2H), 1.46 (q, *J* = 13.0 Hz, 2H), 1.30 (q, *J* = 12.9 Hz, 1H). ^{13}C NMR (126 MHz, D_2O) δ 169.9, 134.4, 126.1, 118.6, 57.5, 55.7, 29.2, 29.0, 24.7, 24.6, 24.3.

HRESI-MS calc. for $C_{12}H_{20}N_3O_2^+$ 238.1550, found 238.1548

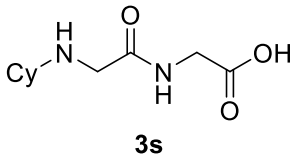

3s

^{1}H NMR (500 MHz, D_2O) δ 4.07 (s, 2H), 4.00 (s, 2H), 3.19 (tt, *J* = 11.3, 3.7 Hz, 1H), 2.09 (d, *J* = 11.6 Hz, 2H), 1.86 (d, *J* = 13.2 Hz, 2H), 1.75 – 1.64 (m, 1H), 1.47 – 1.26 (m, 4H), 1.25 – 1.09 (m, 1H). ^{13}C NMR (126 MHz, D_2O) δ 173.3, 166.9, 57.7, 45.0, 41.2, 40.4, 28.8, 28.7, 24.4, 23.9.

HRESI-MS calc. for $C_{10}H_{18}N_2O_3Na$ $[M+Na]^+$ 237.1210, found 237.1208

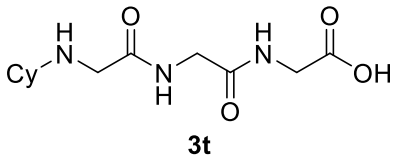

3t

^{1}H NMR (500 MHz, MeOD) δ 4.00 (s, 2H), 3.95(s, 2H), 3.929s, 2H), 3.18 – 3.09 (m, 1H), 2.12 (d, *J* = 10.0 Hz, 2H), 1.92 – 1.83 (m, 2H), 1.71 (d, *J* = 13.0 Hz, 1H), 1.48 – 1.31 (m, 4H), 1.31 – 1.18 (m, 1H). ^{13}C NMR (126 MHz, MeOD) δ 172.8, 171.6, 167.3, 58.6, 46.3, 43.2, 43.2, 41.8, 41.7, 30.2, 26.0, 25.5.

HRESI-MS calc. for $C_{12}H_{21}N_3O_4Na$ $[M+Na]^+$ 294.1424, found 294.1414

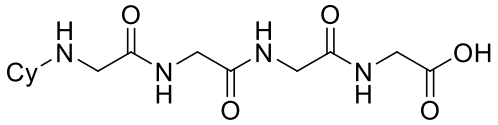

3u

^{1}H NMR (500 MHz, MeOD) δ 3.95 (s, 2H), 3.91 (s, 2H), 3.75 (s, 2H), 3.34 (s, 2H), 2.41 (tt, *J* = 10.6, 3.7 Hz, 1H), 1.94 – 1.86 (m, *J* = 6.3 Hz, 2H), 1.80 – 1.68 (m, 2H), 1.67 – 1.58 (m, 1H), 1.35 – 1.03 (m, 5H). Chemical HRESI-MS calc. for $C_{14}H_{24}N_4O_5Na$ [M+Na] 351.1639, found 351.1646

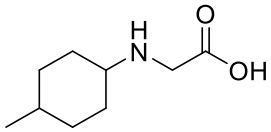

3v

^{1}H NMR Mixture of Isomers (500 MHz, D_2O) δ 3.51 – 3.44 (m, 1H), 3.35 (tt, *J* = 12.0, 3.8 Hz, 1H), 2.25 (dd, *J* = 14.1, 2.1 Hz, 2H), 2.04 – 1.87 (m, 8H), 1.77 (qd, *J* = 9.0, 4.2 Hz, 2H), 1.66 – 1.50 (m, 5H), 1.18 (qd, *J* = 13.6, 3.3 Hz, 2H), 1.11 (d, *J* = 7.0 Hz, 4H), 1.04 (d, *J* = 6.6 Hz, 3H). ^{13}C NMR Mixture of Isomers (126 MHz, D_2O) δ 169.4, 57.7, 57.3, 45.2, 44.9, 32.5, 31.1, 28.9, 28.8, 27.4, 24.4, 21.4, 18.3.

HRESI-MS calc. for $C_9H_{18}NO_2$ $[M+H]^+$ 172.1332, found 172.1327

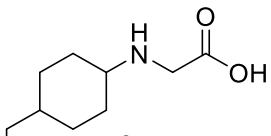

3w

^{1}H NMR Mixture of Isomers (500 MHz, D_2O) δ 3.42 – 3.36 (m, 1H), 3.25 (tt, *J* = 12.0, 3.9 Hz, 1H), 2.19 (dd, *J* = 14.2, 2.2 Hz, 2H), 1.98 (d, *J* = 12.0 Hz, 2H), 1.91 (ddd, *J* = 9.7, 9.2, 4.1 Hz, 3H), 1.85 – 1.74 (m, 3H), 1.72 – 1.55 (m, 7H), 1.50 (ddd, *J* = 24.9, 12.4, 3.5 Hz, 2H), 1.42 (p, *J* = 7.4 Hz, 3H), 1.35 – 1.22 (m, 3H), 1.07 (qd, *J* = 13.6, 3.2 Hz, 2H), 0.98 – 0.91 (m, 7H). ^{13}C NMR Mixture of Isomers (126 MHz, D_2O) δ 169.6, 169.6, 57.8, 57.2, 45.3, 44.9, 37.6, 34.5, 30.1, 28.8, 28.7, 26.6 24.8, 24.5, 11.4, 10.9.

HRESI-MS calc. for $C_{10}H_{19}NO_2Na$ $[M+Na]^+$ 281.1308, found 208.1309

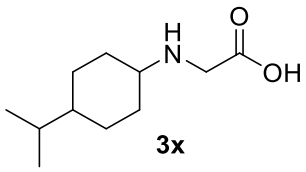

3x

^{1}H NMR Mixture of Isomers (500 MHz, D_2O) δ 3.51 – 3.43 (m, 1H), 3.25 (tt, *J* = 12.0, 3.9 Hz, 1H), 2.23 (dd, *J* = 12.9, 3.2 Hz, 1H), 1.99 – 1.83 (m, 5H), 1.74 – 1.62 (m, 5H), 1.59 – 1.46 (m, 1H), 1.34 – 1.27 (m, 1H), 1.23 – 1.13 (m, 1H), 0.98 (d, *J* = 6.7 Hz, 6H), 0.95 (d, *J* = 6.8 Hz, 3H). ^{13}C NMR Mixture of Isomers (126 MHz, D_2O) δ 169.6, 169.6, 57.8, 56.9, 45.5, 45.0, 42.3, 40.5, 31.8, 28.9, 28.4, 27.3, 25.2, 24.5, 20.0, 19.3. Chemical HRESI-MS calc. for $C_{11}H_{21}NO_2Na$ $[M+Na]^+$ 222.1464, found 222.1466

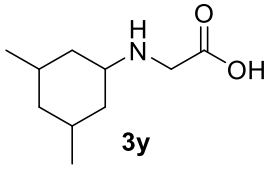

3y

^{1}H NMR Mixture of Isomers (500 MHz, MeOD) δ 3.61 – 3.56 (m, 1H), 3.20 (tt, *J* = 12.0, 3.8 Hz, 1H), 2.11 – 1.97 (m, 3H), 1.81 – 1.66 (m, 4H), 1.62 – 1.51 (m, 1H), 1.32 – 1.23 (m, 2H), 1.04 – 0.94 (m, 10H), 0.72 – 0.58 (m, 1H). ^{1}H NMR Mixture of Isomers (500 MHz, MeOD) δ 3.61 – 3.56 (m, 1H), 3.20 (tt, *J* = 12.0, 3.8 Hz, 1H), 2.11 – 1.97 (m, 3H), 1.81 – 1.66 (m, 4H), 1.62 – 1.51 (m, 1H), 1.32 – 1.23 (m, 2H), 1.04 – 0.94 (m, 10H), 0.72 – 0.58 (m, 1H).

HRESI-MS calc. for $C_{10}H_{19}NO_2Na$ $[M+Na]^+$ 208.1308, found 208.1311.

3.7 References

1. Li, Y.; Holmberg, K.; Bordes, R., Micellization of true amphoteric surfactants. *J. Colloid Interface Sci.* **2013,** *411*, 47-52.

2. Tripathy, D. B.; Mishra, A.; Clark, J.; Farmer, T., Synthesis, chemistry, physicochemical properties and industrial applications of amino acid surfactants: A review. *C. R. Chim.* **2018,** *21* (2), 112-130.

3. Hughes, A. B., *Amino Acids, Peptides and Proteins in Organic Chemistry, Analysis and Function of Amino Acids and Peptides*. John Wiley & Sons, Incorporated: Somerset, Germany, 2011.

4. Richard, T. J.; Miller, W. H. Preparation of *N*-alkylglycines from glyoxal and amines in the presence of sulfur dioxide. U.S. Patent US4684483A, 1987.

5. Nelson, N. A.; Sinclair, H. B., Steroidal hormone analogs. VIII. Amino acid analogs of some artificial estrogens. *J. Am. Chem. Soc.* **1960,** *82* (10), 2577-2580.

6. Hu, C.; Chen, Z.; Yang, G., Soluble polymer-supported synthesis of α-amino acid derivatives. *Synth. Commun.* **2004,** *34* (2), 219-224.

7. Gibbs, T. J.; Boomhoff, M.; Tomkinson, N. C., A mild and efficient method for the one-pot monocarboxymethylation of primary amines. *Synlett* **2007,** *2007* (10), 1573-1576.

8. Chen, Z.; Zeng, H.; Gong, H.; Wang, H.; Li, C.-J., Palladium-catalyzed reductive coupling of phenols with anilines and amines: efficient conversion of phenolic lignin model monomers and analogues to cyclohexylamines. *Chem. Sci.* **2015,** *6* (7), 4174-4178.

9. Jumde, V. R.; Petricci, E.; Petrucci, C.; Santillo, N.; Taddei, M.; Vaccaro, L., Domino hydrogenation–reductive amination of phenols, a simple process to access substituted cyclohexylamines. *Org. Lett.* **2015,** *17* (16), 3990-3993.

10. Yan, T.; Feringa, B. L.; Barta, K., Direct *N*-alkylation of unprotected amino acids with alcohols. *Sci. Adv.* **2017,** *3* (12), eaao6494/1-eaao6494/7.

11. Chen, Z.; Zeng, H.; Girard, S. A.; Wang, F.; Chen, N.; Li, C.-J., Formal Direct Cross-Coupling of Phenols with Amines. *Angew. Chem. Int. Ed.* **2015,** *54* (48), 14487-14491.

Chapter 4. Peptide stapling using tyrosine as a handle

4.1 Background

Proteins are responsible for complex and interrelated processes that constitute all living organisms. Proteins can be classified based on their (1) shape, (2) composition, or (3) function (Figure 1). Based on their shape, proteins are classified as fibrous or globular. Fibrous proteins are mainly structural and are not enzymatic, while globular proteins are mostly enzymatic with a compact and rounded aspect.[1] Based on composition, proteins can be classified as simple or conjugated. Simple proteins consist solely of amino acids, while conjugated proteins involve amino acids and a non-proteinic prosthetic group or co-factor.[1] Metalloproteins, chromoproteins, and glycoproteins are all part of the latter classification. Given that proteins have several functions within organisms, the classification by function is more extensive. Furthermore, proteins might be performing one or more functions within an organism.[1] Examples of structural proteins are collagen, actin and myosin. Myosin and actin are also classified as contractile proteins. Storage proteins include albumins and glutelins. Transporting proteins include myoglobin and hemoglobin. Antibodies are defense proteins, while insulin and the growth hormone are regulatory proteins.

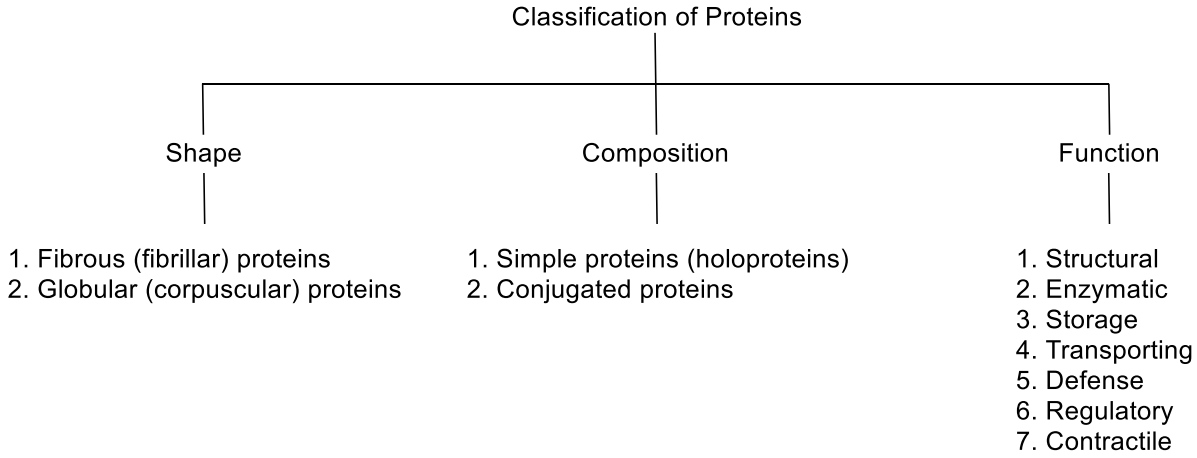

Figure 4.1. Different classifications of proteins

A protein's role is ultimately determined by the specific coding of the amino acid chain and its correct folding into its biologically active structure.[2] Thus, a protein's native state is essential to understanding its biological function and functional mechanism, making protein structure prediction a

coveted goal for biologists and computational scientists.[3] Anfinsen proposed that the three-dimensional structure of a protein is under thermodynamic control, stating that the biologically active conformation is the global minimum in Gibbs energy, causing the amino acid chain to fold spontaneously.[2] While the Gibbs energy hypothesis can only be studied computationally; it has been experimentally proven that the unfolded and native states exist in equilibrium with one another.[2]

Three main interactions control native protein stability: (1) the hydrophobic effect, (2) hydrogen bonding, and (3) configurational entropy.[2] The hydrophobic effect takes into account the high energy associated with the transfer of hydrophobic groups folded towards the protein's interior to water .[2] The energetical contribution of hydrogen bonding depends on the equilibrium between the intra- and intermolecular interactions.[2] In proteins, hydrogen donors and acceptors might solely involve amino acid chain residues - intramolecular hydrogen bonding - or the surrounding water molecules - intermolecular hydrogen bonding. Lastly, configurational entropy refers to the destabilizing energy from restricting the amino acid chain into its active state, causing the loss of rotational and torsional flexibility in the protein's backbone.[2] Given that several interactions are in balance, small changes in temperature, pH, or concentration can largely affect the equilibrium.[2]

These interactions will ultimately dictate the structure of a protein at four different levels. Each level of structure, primary, secondary, tertiary, and quaternary, examines a protein's structure with increasing complexity. The primary structure of a protein represents the sequence of amino acids held together through peptide bonds.[1] As previously mentioned, the primary structure does not give any insight regarding a protein's functionality. The secondary structure refers to the two main stabilized hydrogen bonding structures found in proteins: α-helixes and β-pleated sheets.[1] The tertiary structure of a protein refers mostly to globular proteins. This compact and rounded shape is obtained upon different amino acid side chains to establish different interactions upon acquiring their secondary structure, leading the chain to become multi-folded and acquire a three-dimensional and active conformation.[1] Lastly, the quaternary structure of a protein refers to oligomers that consist of two or more protein units that are joined together by non-covalent forces.[1]

4.1.1 Secondary protein structure

The α-helix is a single peptide chain coiled into a rigid, rod-like structure. The α-helix is established by hydrogen bonds between the amino (-NH), and carbonyl (-CO) groups situated 3.6 amino acid residues ahead in the linear sequence of the main peptide chain.[1] The distance between the points per turn, also known as the pitch, is 0.54 nm.[1] Certain amino acids such as alanine, glutamine, leucine and methionine are more commonly found in helical structures.[1] The α-helix may be right-handed or left-handed, but in most biological proteins, α-helixes are right-handed due to the innate presence of L-amino acids.[1] A helix may also contain both hydrophobic and hydrophilic ends, making it amphipathic in nature.[1]

While α-helixes only involve hydrogen bonding between residues of a single polypeptide chain, β-pleated sheets are formed by both intra- and intermolecular hydrogen bonds with two or more polypeptide chains lined side by side.[1] Each individual polypeptide chain is referred to as a β-strand. Rather than being coiled, pleated β-sheets are stabilized by hydrogen bonds formed between the -CO and -NH groups of the adjacent β-strands.[1] The functional groups of each amino acid in the β-strand alternately project above and below the plane of the sheet, leading to a two residue repeat unit.[1] β-Sheets may be parallel or antiparallel, with antiparallel sheets being more stable.[1] Parallel sheets have polypeptide chains arranged in the same direction, i.e. the N-terminus of all the chains lies on the same edge of the sheet, with the opposite being true for antiparallel sheets.[1] A comparison between the two secondary protein structures is presented in Table 1.[1]

Table 4.1. Characteristics of secondary protein structures[1]

Alpha helix	Beta pleated sheet
Coiled structure	Parallel or antiparallel sheets
Compact structures commonly found in globular proteins	Extended structures commonly found in fibrous proteins
Involves a single polypeptide chain	It involves two or more polypeptide chains
Axial distance between two residues is 0.15 nm	Axial distance between two residues is 0.35 nm
H bonds formed among residues of the same chain	H bonds formed among the residues of different chains

4.1.2 Peptide stapling

Modern therapeutics mostly rely on small molecules that can target enzyme pockets with high affinity.[4] Nonetheless, only 10% of all human-protein targets possess an accessible hydrophobic pocket on their surface.[4] Protein-protein interactions (PPIs) mediate many critical cellular functions and regulate metabolic pathways. However, they have traditionally been considered undruggable due to their large and shallow interfaces.[5, 6] Thus, considerable interest has arisen in protein therapeutics which could provide broad target recognition capabilities, high specificity and potency.[4, 5, 7] Despite these advantages, peptides possess several drawbacks such as low oral bioavailability, poor metabolic stability, poor membrane permeability, and rapid clearance.[5] Furthermore, there is a high entropic penalty for binding a peptide, which possesses a low intrinsic secondary structure in solution, in the specific conformation that mimics that of the target protein's binding partner.[5]

In order to circumvent these issues seen with native peptides, constrained peptides have been developed to lock the peptide strands into their bioactive conformation.[4, 7] This strategy can greatly improve the pharmacologic performance of peptides, increasing their target affinity, proteolytic resistance, and serum half-life while conferring on them high levels of cell penetration through endocytic vesicle trafficking.[4] Furthermore, additional chemical modifications can be introduced to improve the peptide's hydrophilicity and specificity.[7] Restricting the conformational freedom of a peptide can be achieved by different means. Among these strategies, there is head-to-tail, side chain-to-side chain, and side-chain-to-terminus macrocyclization; incorporation of a proline which fixes the dihedral angle, or incorporation of unnatural amino acids for chemical stapling.[8]

Stapled peptides possess multiple favourable properties, including reinforced helical conformation, resistance to proteolytic degradation, and enhanced cell permeability through an active transport mechanism, making them ideal for targeting PPIs of interest.[7] The term "peptide stapling" being first introduced by Verdine and co-workers, who expanded on the work by Grubb's ring-closing metathesis for stabilization of α-helices on peptides, demonstrating that stapled peptides are able to target PPIs effectively.[9] Since the α-helix is the most common secondary structure in PPIs, the introduction of a hydrocarbon staple has been found in numerous examples to confer high levels of α-helical content. This modification has been associated with a 5- to 5000-fold increase in target affinity, strong protection from proteolytic degradation, robust cell-penetration by endocytic vesicle trafficking, elongation of their *in vivo*

half-life, and specific antagonism of PPIs in cultured cells.[4] *In vivo* experiments on stapled peptides were investigated by Walensky *et al*., further establishing them as attractive therapeutics.[10]

Peptide stapling can be divided into one- or two-component coupling reactions. One-component reaction refers to staples that form between side-chains of unnatural amino acids incorporated into the sequence (Figure 2).[11] On the other hand, two-component staples require a separate bifunctional linker to bridge two unnatural amino acid residues (Figure 3).[11] In both cases, the secondary structural fold of the α-helix can be synthetically covalently reinforced. Depending on the distance at which the staple is placed, the staple may stabilize one or two helical turns. On average, there are 3.6 amino acid residues per helical turn in an α-helix.[1] Thus, a staple to stabilize one turn might be separated by three (i, i+3) or four (i, i+4) amino acids.[5, 11] On the other hand, two turns are more commonly spaced in an i, i+7 fashion. Three turns are less common but have also been reported at a distance of i, i+11.[5, 11]

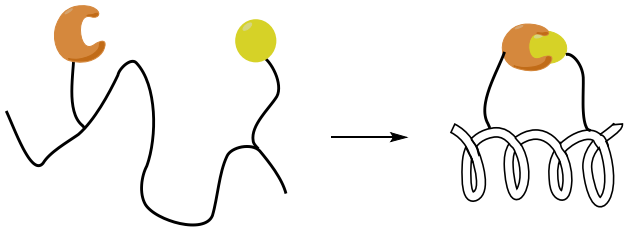

Figure 4.2. One-component peptide stapling[11]

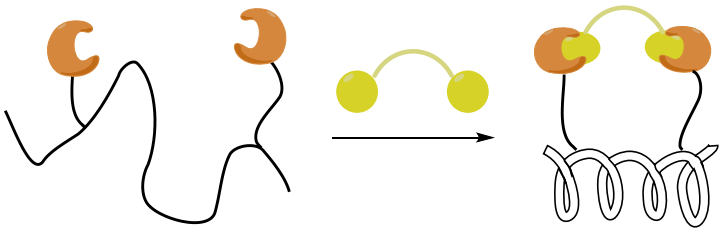

Figure 4.3. Two-component peptide stapling[11]

Various peptide stapling techniques have been investigated. One-component reactions include ring-closing metathesis, lactamisation, cycloadditions, disulphide, oxime, and thioether stapling.[11] On the other hand, two-component staples include photo-switchable linkers and functionalized double-click linkers.[11] However, the hydrocarbon and the triazole staples have been among the most chemically and biologically stable linkages.[5] The seminal work by Blackwell and Grubbs's on stapled peptides describes a

ruthenium-catalyzed ring-closing metathesis between *cis*-olefinic amino acid chains (Scheme 1).[12] In this report, α,α-disubstitution and macrocyclic bridge formation between the olefin side chains are introduced into the peptide to induce an α-helix upon ring-closing metathesis. Triazoles staples, on the other hand, are formed by the Cu(I)-catalyzed "click" cycloaddition between azido and alkynyl functionalities on the side chains of the amino acid residues. One-component[12] (Scheme 2) and two-component[13] (Scheme 3) click reactions have been used to enhance helicity in peptides. These reactions allow for a more comprehensive exploration of chemical space than hydrocarbon staples, as different dialkynyl linkers can be installed.[5]

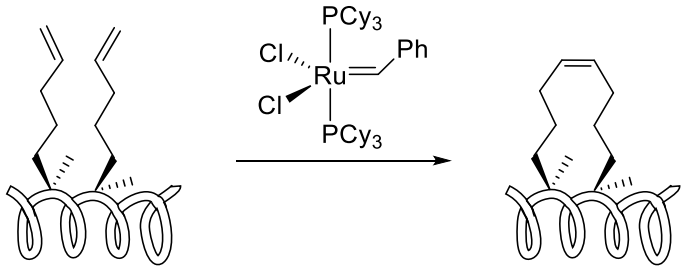

Scheme 4.1. Ruthenium-catalyzed hydrocarbon staple[12]

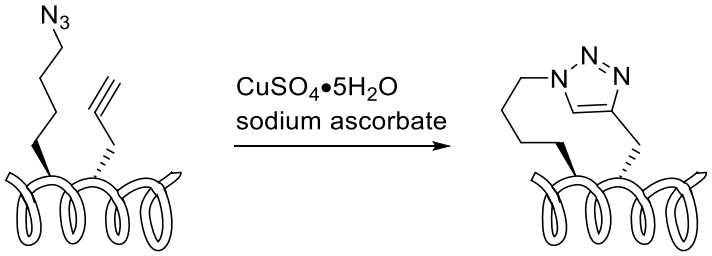

Scheme 4.2. Cu(I) catalyzed azide-alkyne cycloaddition[13]

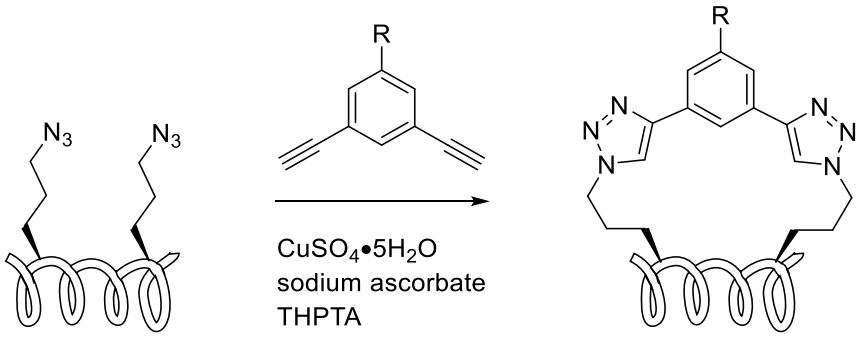

Scheme 4.3. Double click Cu(i) catalyzed azide-alkyne cycloaddition[14]

Several considerations must be taken into account when designing a peptide staple. For instance, the staple position must be placed on the same side of the helix for the macrocyclization reaction to proceed efficiently, with i, i+3 staples being most favourable with an (*R,S*) stereochemistry; i, i+4 staples having an optimal stereochemical combination at (*S,S*), and i, i+7 favouring the (*R,S*) configuration.[5] The lengths for hydrocarbon staples also have to be optimized for maximal crosslinking efficiency and helicity. If the linker is too short, the reaction cannot proceed efficiently, while if the linker is too long, it might not provide sufficient helix stabilization. Staples of type i, i+3 usually contain either six or eight carbon atoms in length, depending on the hydrophobicity desired.[5] The staple's position must be such that it does not interfere with any critical interacting residues, which might weaken its affinity.[5]

4.2 Research objectives and plan

Based on the results that we observed for the *N*-cyclohexylation of deprotected tyrosine and lysine,[15] we envisioned the possibility of using tyrosine as a handle for protein stapling (Figure 4.4). We hypothesized that given the unique phenolic functionality of tyrosine, we could selectively staple peptides through one- and two-component staples (Figure 4.5), without the need to introduce extrafunctional groups. Given that the reaction conditions had been previously optimized for the amino acid's modification at the *N*-terminus, we would commence our screening by using *N*-acetylated tyrosine as a model substrate and coupling it to an amine to see if the reaction yield could improve to quantitative yields as observed for other phenolic substrates. We would then focus on the one-component Lys-Tyr staple, followed by the possibility of having a two-component Tyr-Tyr staple. Based on these results, we would design a model peptide for testing these staples.

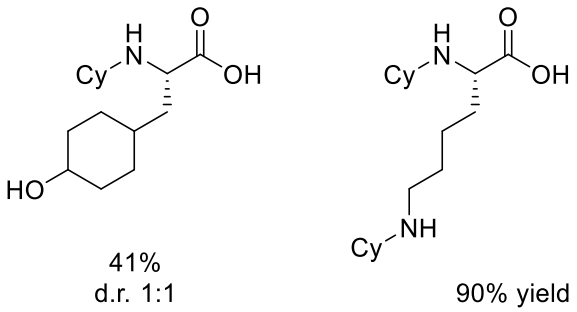

Figure 4.4 Tyrosine and lysine under optimized conditions for the *N*-cyclohexylation reaction using phenol and Pd/C as a catalyst. Reaction conditions: amino acid (0.2 mmol, 1 equiv), phenol (0.3 mmol, 1.5 equiv), HCO_2Na (1.8 mmol, 6 equiv), Pd/C (10 wt%, 0.2 mmol), MeOH:H_2O (1 mL, 1:1 mixture), 24 h, 50 °C.[15]

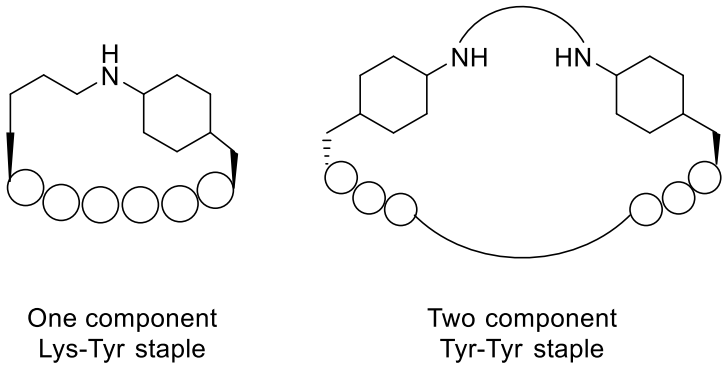

Figure 4.5 Model one- and two-component peptide staples using tyrosine as a handle

4.3 Results and discussion

4.3.1 Condition Screening

We began by testing glycine (**1**) and *N*-acetyl-L-tyrosine (**2**) under our previously reported conditions for amino acid *N*-cyclohexylation. We were delighted to see that the reaction proceeded in quantitative yields to give condensation product **3** in a 1:1 diastereomeric ratio. The diasteromeric center comes from the addition of the glycine in either a cis or trans conformation with respect to the amino acid moiety.

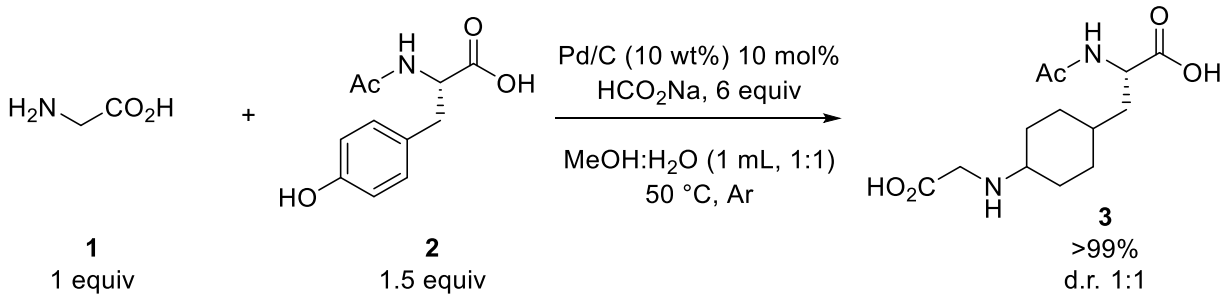

Scheme 4.4 Coupling of glycine at the *N*-terminus with the phenolic side chain of *N*-acetyl-L-tyrosine
Reaction conditions: **1** (0.2 mmol, 1 equiv), **2** (0.3 mmol, 1.5 equiv), HCO_2Na (1.8 mmol, 6 equiv), Pd/C (10 wt%, 0.2 mmol), MeOH:H_2O (1 mL, 1:1 mixture), 24 h, 50 °C.

With these results at hand, we proceeded to screen reaction conditions for the one-component Lys-Tyr staple model reaction (Table 4.2). Given that this methodology could be useful for the synthesis

and modification of biologically active compounds, we focused on testing milder conditions than those used in our model reaction to strengthen its applicability further. The amides proved to be more soluble in water than the free amino acids, only requiring 20% v/v of methanol for solvation. The reaction proceeded in 93% yield at room temperature (Table 4.2, entry 1), with slightly increased yields at 40 °C and 60 °C (Table 4.2 entries 2-3). Running the reaction under air instead of argon did not impact the formation of product **5** (Table 4.2, entry 4).

Table 4.2 Optimization of the one-component staple between *N*-acetyl-tyrosine and *N*-acetyl-lysine

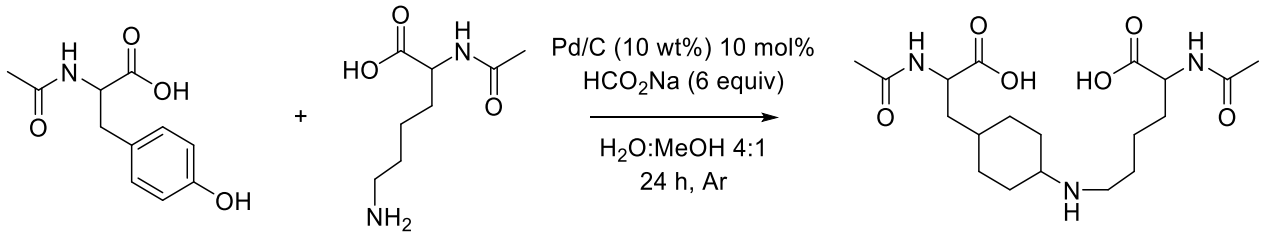

2 **4** **5**

entry	T (°C)	conversion (%)	yield **5**[a], [b] (%)
1	r.t.	99	93
2	40	99	95
3	60	99	96
4[c]	60	99	95

[a] Reaction conditions: *N*-acetyl tyrosine (0.2 mmol, 1 equiv), *N*-acetyl-lysine (0.2 mmol, 1 equiv), Pd/C (10 wt%, 0.2 mmol), HCO_2Na (1.2 mmol, 6 equiv), Ar, 24 h. r.t.= room temperature.

[b] Determined by ^1H NMR using dimethyl sulfoxide as the internal standard.

[c] Reaction was run in open air.

Encouraged by these results, we proceeded to screen the possibility of a two-component staple using tyrosine (**2**) and PEG-diamine (**6**) (Table 4.3). The reaction proceeded smoothly at 60 °C under argon after stirring for 24 hours, resulting in the formation of product **7** in 91% yield (Table 4.3, entry 1). Given this favourable result, we considered lowering the overall reaction concentration from 0.2 M to 0.1 M,

hoping to simulate biocompatible conditions. However, decreasing the concentration resulted in a lower yield of 80% (Table 4.3, entry 2). We considered increasing sodium formate amounts in the reaction, hoping to push the reductive amination at the lower concentration. Nonetheless, the reaction yield decreased even more than the standard conditions at 0.1 M (Table 4.3, entry 3). Given that this could result from the reaction's pH not favouring the imine formation due to the concentration of sodium formate present, we ran the reaction in sodium formate and formic acid buffer. However, no overall improvement was observed (Table 4.3, entry 4).

Table 4.3 Optimization of the two-component staple between *N*-acetyl-tyrosine 2,2'-(ethylenedioxy)bis(ethylamine)

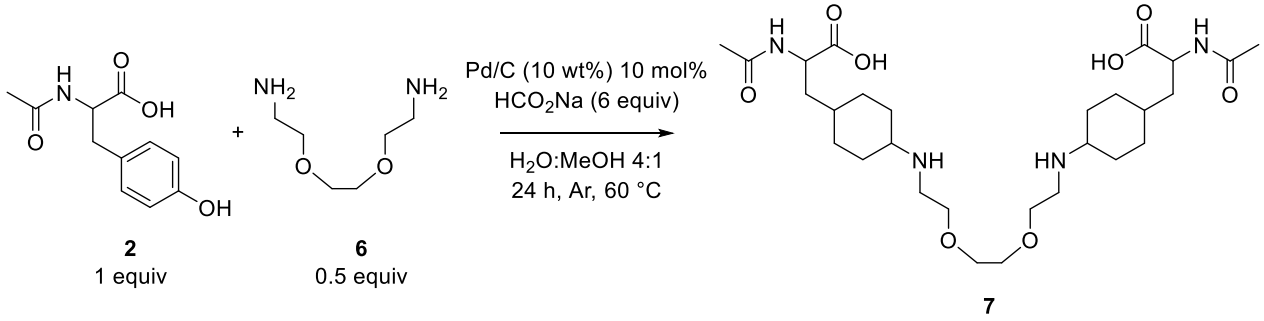

2
1 equiv

6
0.5 equiv

7

entry[a]	concentration [M]	HCO_2Na (equiv)	conversion (%)	yield **7**[b] (%)
1	0.2	6	98	91
2	0.1	6	82	80
3	0.1	12	70	50
4	0.1	Buffer	77	54

[a] Reaction conditions: *N*-acetyl-tyrosine (0.2 mmol, 1 equiv), PEG-diamine linker((2,2'-(Ethylenedioxy)bis (ethylamine)) (0.1 mmol, 0.5 equiv), Pd/C (10 wt%, 0.2 mmol), HCO_2Na (1.2 mmol, 6 equiv).

[b] Determined by ^1H NMR using dimethyl sulfoxide as the internal standard.

4.3.2 Substrate scope

The model compounds had been successfully obtained in high yields (Figure 4.6). However, several challenges arose when diastereomeric separation was assayed. Diastereomers co-eluted even when using prep-HPLC for purification. The free carboxylic acids significantly increased the compounds' polarity, requiring very polar solvent systems for the compounds to elute. This poses a significant impediment as separation will be necessary for the model peptides to be stapled through this methodology. Future steps in this project should consider the esterification of the model compounds at their *C*-terminus to facilitate the characterization of the products. Once this challenge is overcome, the model peptides **8** and **9** should be tested under the optimized reaction conditions to form the desired stapled peptides (Figure 4.7). However, the reaction will necessarily have to be run at a microscale due to the limited availability of these compounds.

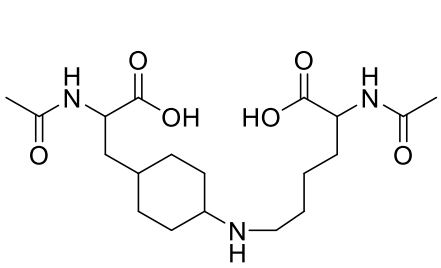

5
95% yield by NMR
99% Conversion of SM

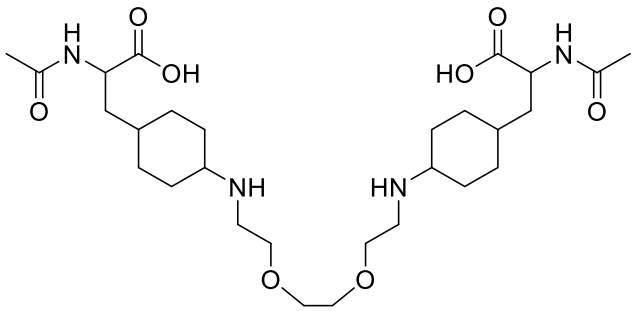

7
91% yield by NMR
98% Conversion of SM

Figure 4.6 Model compounds for the one- and two-component tyrosine staples

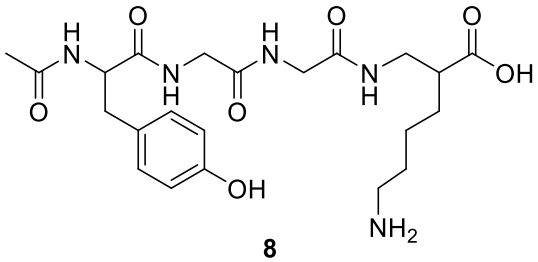

8

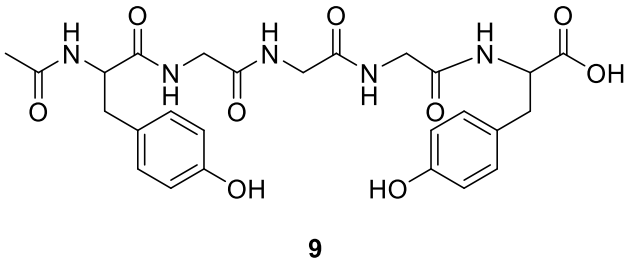

9

Figure 4.7 Model peptides for the Tyr-Lys one-component staple and the Tyr-Tyr two-component staple

4.3.4 Additional experiments

4.3.4.1 Protein tagging

In parallel, we envisioned using this methodology to target tyrosine in larger molecules such as proteins selectively. In this regard, we considered selectively tagging tyrosine using a fluorophore (Scheme 4.5). However, a brief screening of the reaction conditions at concentrations necessary for protein chemistry proved that the reaction did not proceed (Table 4.4). We speculate that these results might be linked to our catalyst's heterogeneous nature, preventing effective interactions from occurring at such low concentrations. Furthermore, three common fluorophores were surveyed as potential candidates for our tag (Scheme 4.6). Unfortunately, decomposition products were obtained when submitting the fluorophores to the standard reaction conditions.

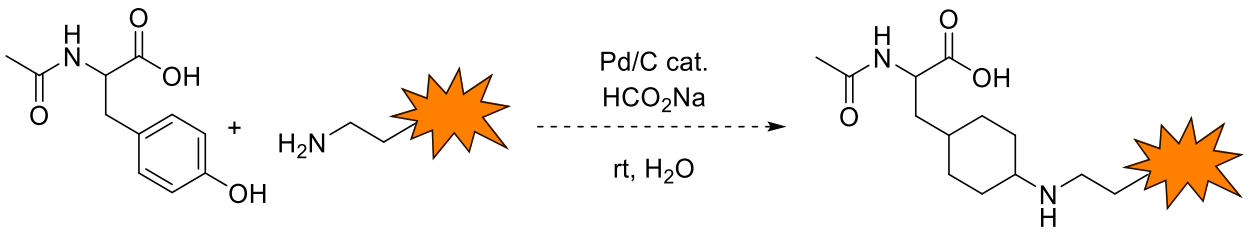

Scheme 4.5 Model reaction for the tagging of tyrosine residues in proteins

Table 4.4 Screening for the reduction of tyrosine at micromolar concentrations

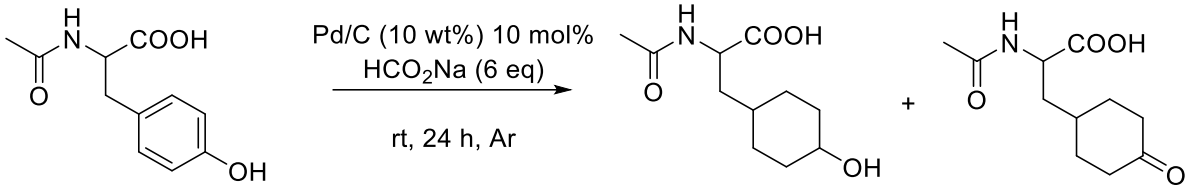

2

entry	[Ac-Tyr]	[HCO_2Na]	[Pd/C]	volume (mL)	conversion
1	0.2 mmol	1.2 mmol	0.2 mM	1	100%
2	100 µM	120 mM	100 µM	0.5	ND
3	100 µM	120 mM	1000 µM	0.5	ND

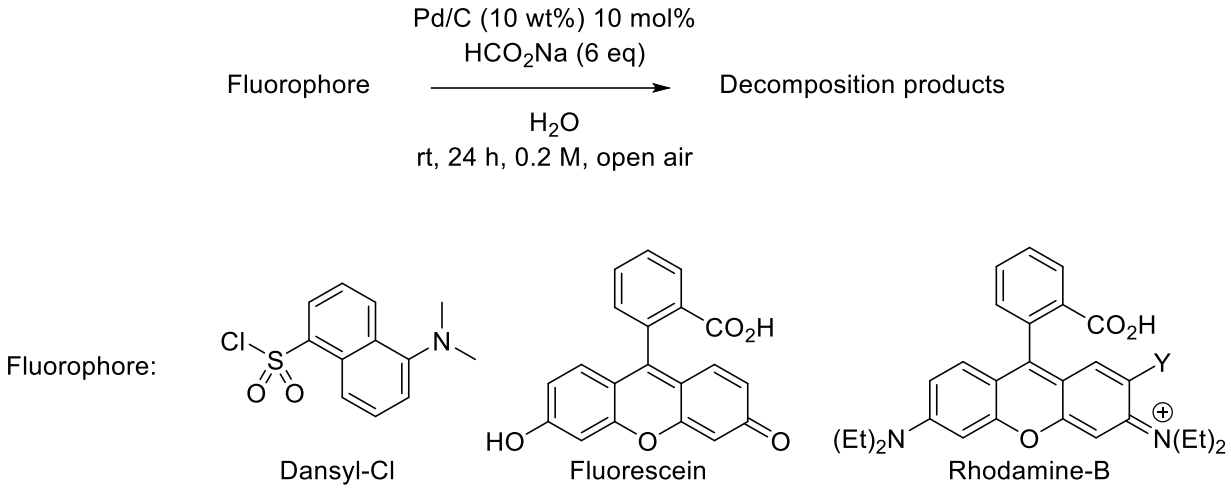

Scheme 4.6 Stability of common fluorophores used for protein tagging under standard reaction conditions

4.3.4.2 Tyrosine hydrogels

Since the reaction had proven ineffective at micromolar concentrations, we decided to focus on the possibility of self-polymerizing tyrosine to form hydrogels. Taking advantage of the chain's zwitterionic nature, we envisioned a material that could modify its characteristics based on pH (Figure 4.8). Furthermore, the reaction concentration would no longer be required to be maintained as low compared to protein substrates.

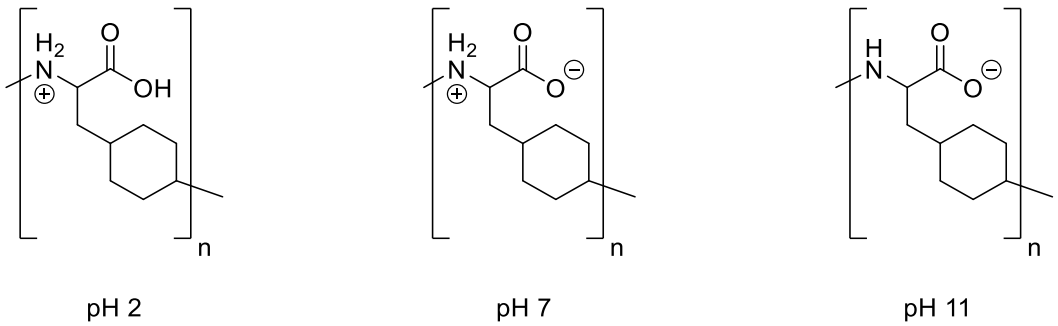

Figure 4.8 Polymerized tyrosine through C-N bonds between the *N*-terminus and the phenolic ring and the protonation at different pH

We began by testing the reaction under standard conditions (Table 4.5, entry 1). However, no product was detected. We then examined the impact of the temperature in the reaction (Table 4.5, entries 2-4). The reaction seemed to proceed most desirably at 80 °C, forming the desired C-N bond in 77% yield (Table 2.4, entry 3). Maintaining this temperature constant, we increased the sodium formate amounts in hopes that the yield would improve (Table 2.4, entries 5-6). However, a decrease in the reaction yield was observed most likely linked to the increase of the pH in the reaction mixture, inhibiting imine formation. The reaction time was then modified (Table 4.5, entries 7-8), with the best results obtained after leaving the reaction stir for 72 h. Once the reaction conditions had been optimized, the reaction mixture was analyzed by ESI in order to determine the chain length. Unfortunately, results showed only short chains forming (Figure 4.9), which might indicate that the polymerization is not preceding the hydrogenation.

Table 4.5 Screening of reaction conditions for the polymerization of tyrosine through reductive amination

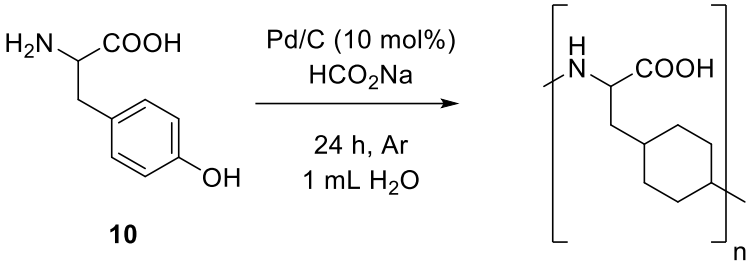

10

entry[a]	temperature (°C)	time (h)	HCO_2Na (equiv)	conversion[b] (%)
1	rt	24	6	ND
2	60	24	6	69
3	80	24	6	77
4	120	24	6	52
5	80	24	9	33
6	80	24	12	30
7	80	48	6	80
8	80	72	6	90

[a] Reaction conditions: tyrosine (0.2 mmol, 1 equiv), , Pd/C (10 wt%, 0.2 mmol), HCO_2Na (1.2 mmol, 6 equiv), 1 mL H_2O, Ar, 24 h.

[b] Determined by ^1H NMR using dimethyl sulfoxide as the internal standard.

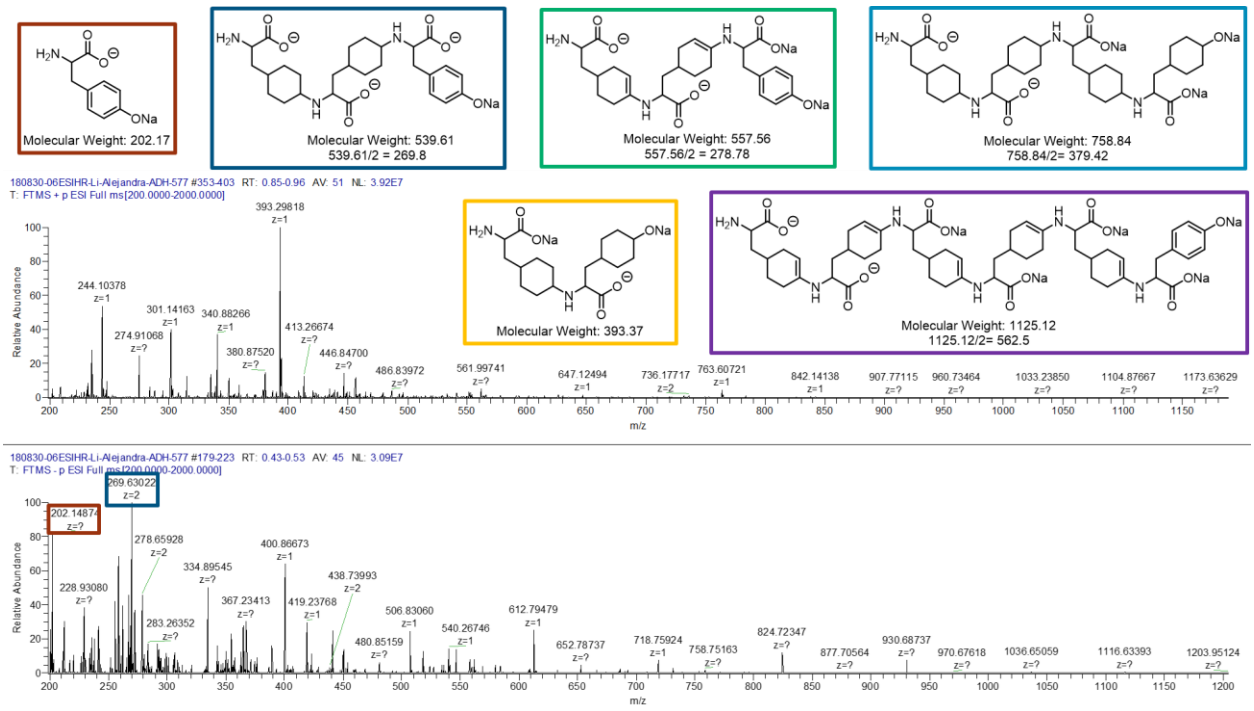

Figure 4.9 ESI results for the polymerization of tyrosine under optimized conditions

Other phenolic monomers were tested in hopes of increasing the polymer's length. Bisphenol F and Bisphenol A were both tested under optimized conditions. Given the high solubility of PEG-diamine, we used 2-methoxyethan-1-amine as a model substrate. While bisphenol F did not reduce under the standard reaction conditions (Scheme 4.7), bisphenol A gave moderate yields in the coupling with excess PEG-diamine (Table 4.6). It is worth noting that one of the biggest challenges was removing the Pd/C from the resulting reaction mixture. The standard workup for these reactions involved centrifuging, washing the pellet with DMF and hydrazine to sequester any leached palladium, followed by dialysis in tubing with a 3.5 kDa cut-off to remove remaining starting materials, in particular sodium formate.

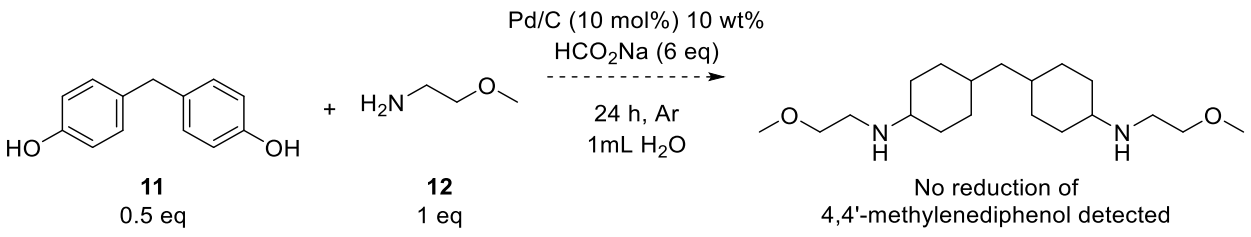

Scheme 4.7 Bisphenol F coupling with 2-methoxyethan-1-amine under optimized conditions

Table 4.6 Polymerization with BPA

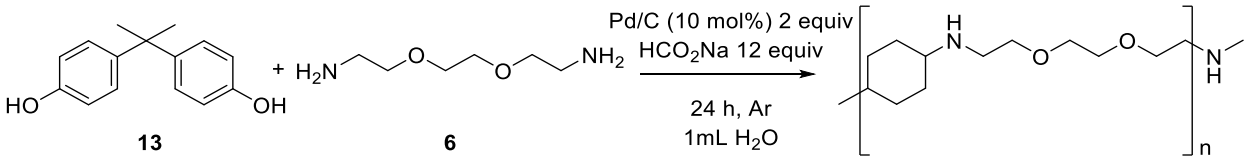

entry	BPA (equiv)	PEG-diamine (equiv)	conversion (%)
1	1	1	16
2	1	2	58
3	2	1	35

[a] Reaction conditions: BPA (0.1 mmol, 1 equiv), PEG-diamine indicated amount, Pd/C (10 wt%, 0.2 mmol), HCO_2Na (1.2 mmol, 12 equiv), 1 mL H_2O, Ar, 24 h.
[b] Determined by ^1H NMR using dimethyl sulfoxide as the internal standard.

Given that removing the excess of sodium formate from the reaction mixture proved problematic, we proceeded to test hydrogen as the reductant (Table 4.7). Phenol and 2-methoxyethan-1-amine were chosen as model substrates. While the reaction proceeds quantitatively under the standard reaction conditions (Table 4.7, entry 1), hydrogen still allows for the reaction to occur with a small decrease in the reaction yield (Table 4.7, entry 2). Nonetheless, this opens up the possibility of replacing sodium formate with hydrogen gas in future investigations.

Table 4.7 Hydrogen as a reductant in the model reaction between phenol and 2-methoxyethan-1-amine

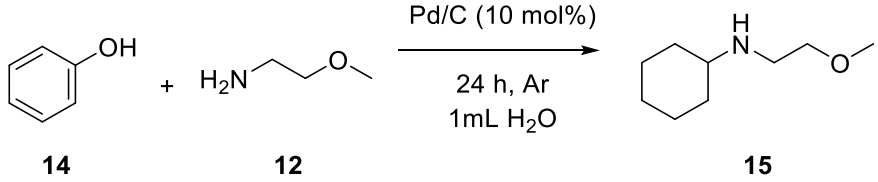

Entry[a]	reductant	yield **15**[b] (%)
1	HCO_2Na (6 equiv)	quantitative
2	H_2 (25 bar)	80

[a] Reaction conditions: phenol (0.2 mmol, 1 equiv), **12** (0.2 mmol, 1 equiv), Pd/C (10 wt%, 0.2 mmol), HCO_2Na (1.2 mmol, 6equiv), 1 mL H_2O, Ar, 24 h.
[b] Determined by ^1H NMR using dimethyl sulfoxide as the internal standard.

4.4 Conclusion and outlook

Benefiting from the phenolic moiety of tyrosine under our optimized conditions opens the possibility of applying this methodology for the synthesis of stapled peptides. We demonstrated the possibility of forming one- and two-component staples through the coupling of Lys-Tyr or Tyr-Tyr using a diamine as a linker, respectively. The coupling of model substrates was successfully achieved, resulting in the formation of the desired products in high yields. However, challenges regarding diastereomeric separation and concentration remain to be addressed for this methodology to be widely applicable. Additional transformations that could benefit from tyrosine's unique phenolic functionality under our reaction conditions, such as protein tagging and tyrosine hydrogel formation, were investigated. Nonetheless, several impediments were encountered. Research in homogeneous palladium catalysts that could accomplish the desired transformation would be highly beneficial, as it would help address most of the challenges that we faced.

4.5 Contributions

Project conceptualization was realized by Prof. Chao-Jun Li. Methodology, experimentation and characterization were performed by myself with the assistance of the summer student Anita Wang and Dr. Inna Perepichka. Protein tagging experiments were run with the aid of J.P. Daniel Therien. Jean-Louis Do performed GPC experiments for polymerization reactions. Mihai Mesko aided in the setup of the dialysis experiments. High-resolution mass spectrometry was performed by Dr. Nadim Saadeh and Dr. Alexander Wahba at the McGill University Department of Chemistry Mass Spectrometry Laboratory.

4.6 Experimental section

4.6.1 General Information

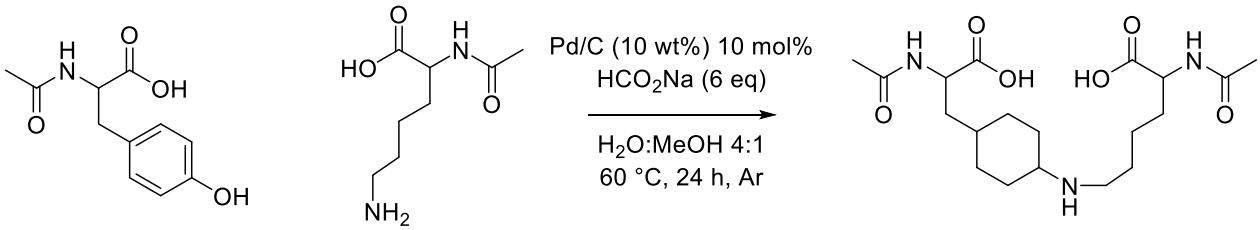

In a U-shaped microwave vial charged with a stir bar, *N*-acetyl tyrosine (0.2 mmol, 1 equiv) and *N*-acetyl lysine (0.2 mmol, 1 equiv), together with HCO_2Na (1.2 mmol, 6 equiv), and Pd/C (10 wt%) (0.2 mmol, 21.3 mg) were added under air. The vial was then flushed with argon three times, and 0.8 mL of distilled water plus 0.2 mL of methanol were injected under an argon flow. The reaction was stirred at

500 rpm for 24 h at 60 °C. Upon completion, the reaction was diluted using distilled water. The Pd/C was removed by filtering the reaction mixture through a celite plug, followed by washing with additional water and methanol. The reaction was acidified to pH=0 with HCl to be able to remove formic acid in vacuo. Upon evaporation of the solvents, the reaction residue was filtered with cold methanol to remove NaCl and to obtain the pure product.

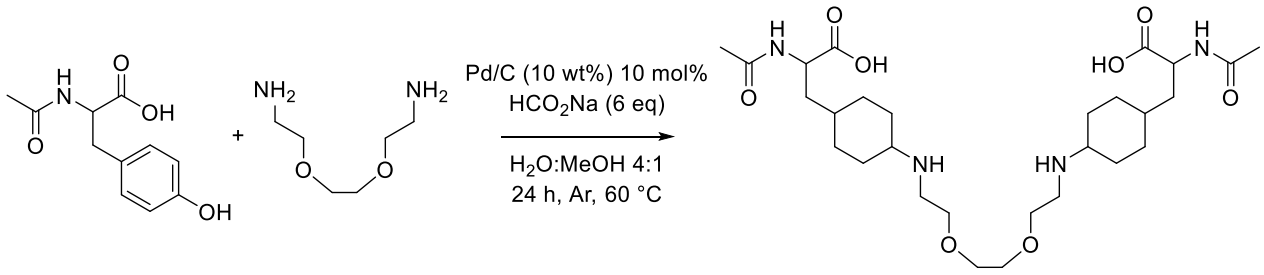

In a U-shaped microwave vial, charged with a stir bar, the *N*-acetyl tyrosine (0.2 mmol, 1 equiv), diamine PEG linker (0.1 mmol, 0.5 equiv), HCO_2Na (1.2 mmol, 6 equiv), and Pd/C (10 wt%) (0.2 mmol, 21.3 mg) were added under air. The vial was then flushed with argon three times, and 0.8 mL of distilled water, 0.2 mL of methanol were injected under an argon flow. The reaction was stirred at 500 rpm for 24 h at 60 °C. Upon completion, the reaction mixture was diluted using distilled water. The Pd/C was removed by filtering the reaction mixture through a celite plug, followed by washing with additional water and methanol. The reaction was acidified to pH=0 with HCl to be able to remove formic acid in vacuo. Upon evaporation of the solvents, the reaction residue was filtered with cold methanol to remove NaCl and obtain the pure product.

4.6.1 Analytical Data

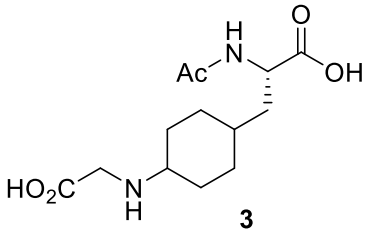

3

^{1}H NMR Mixture of Isomers (500 MHz, D_2O) δ 4.29 – 4.16 (m, 2H), 3.62 (s, 3H), 3.22 (br, 1H), 3.08 (t, *J* = 11.4 Hz, 1H), 2.61 – 2.46 (m, 1H), 2.45 – 2.37 (m, 1H), 2.19 – 2.04 (m, 10H), 2.01 – 1.82 (m, 5H), 1.81 – 1.59 (m, 8H), 1.59 – 1.49 (m, 2H), 1.48 – 1.36 (m, 3H), 1.21 – 1.00 (m, 2H).

^{13}C NMR Mixture of Isomers (126 MHz, D_2O) δ 180.1, 173.7, 162.9, 57.0, 56.0, 53.7, 53.5, 53.41, 47.3, 46.9, 40.2, 40.0, 38.3, 37.2, 33.1, 32.6, 32.1, 31.1, 31.0, 29.5, 29.1, 27.7, 25.6, 25.2, 22.0.

HRESI-MS calc. for $C_{13}H_{21}N_2O_5$ $[M-H]^-$ 285.1456, found 285.1443

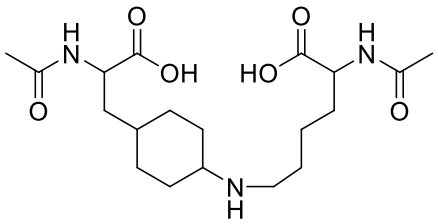

5

^{1}H NMR (500 MHz, D_2O) δ 4.14 – 4.05 (m, 2H), 2.51 – 2.48 (m, 3H), 2.38 – 2.33 (m, 1H), 1.98(s, 3H), 1.97(s, 3H), 1.87-1.84 (m, 1H), 1.78 – 1.70 (m, 2H), 1.65 – 1.59 (m, 2H), 1.56 – 1.38 (m, 7H), 1.35 – 1.24 (m, 3H), 1.02 – 0.88 (m, 2H).

^{13}C NMR (126 MHz, D_2O) Mixture of diastereomers δ 176.3, 176.3, 174.4, 174.3, 56.8, 55.8, 53.0, 52.5, 44.6, 44.2, 36.9, 32.6, 30.5, 29.9, 29.4, 29.2, 28.5, 28.3, 27.3, 25.3, 25.2, 25.0, 24.5, 24.2, 22.2, 22.2, 21.6

HRESI-MS calc. for $C_{19}H_{34}O_6N_3$ $[M+H]^+$ 400.2427, found 400.2442

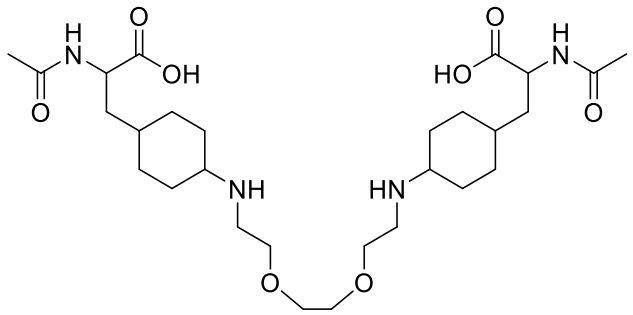

7

^{1}H NMR (500 MHz, D_2O) δ 4.29 – 4.19 (m, 2H), 3.86 – 3.83 (m, 4H), 3.80 (t, J = 3.0 Hz, 4H), 3.29 – 3.18 (m, 5H), 3.12 – 3.05 (m, 1H), 2.22 – 2.04 (m, 7H), 2.02 – 1.83 (m, 6H), 1.79 – 1.62 (m, 8H), 1.59 – 1.51 (m, 2H), 1.47 – 1.29 (m, 3H), 1.22 – 1.00 (m, 2H).

^{13}C NMR (126 MHz, D_2O) δ 176.0, 176.0, 174.5, 174.4, 69.6, 65.7, 65.6, 57.1, 56.2, 51.2, 51.1, 51.0, 50.9, 44.1, 36.8, 33.5, 32.6, 31.7, 30.5, 29.4, 29.2, 28.4, 28.3, 27.3, 25.4, 24.5, 24.2, 21.8.

HRESI-MS calc. for $C_{28}H_{51}O_8N_4$ $[M+H]^+$ 571.3701, found 571.3701

4.7 References

1. Agrawal, P. K., *Biology for chemists*; Global Media: Meerut, 2009.

2. Murphy, K. P., *Protein structure, stability, and folding*; Humana Press: Totowa, NJ, 2001.

3. Zaki, M. J.; Bystroff, C., *Protein structure prediction*, 2nd ed.; Humana Press: Totowa, N.J., 2008.

4. Wittrup, K. D.; Verdine, G. L. *Protein engineering for therapeutics. Part B*, 1st ed.; Academic: San Diego, Calif., 2012.

5. Tan, Y. S.; Lane, D. P.; Verma, C. S., Stapled peptide design: principles and roles of computation. *Drug Discov. Today* **2016,** *21* (10), 1642-1653.

6. Guarracino, D. A.; Bullock, B. N.; Arora, P. S. Mini review: protein-protein interactions in transcription: a fertile ground for helix mimetics. *Biopolymers* **2011,** *95* (1), 1-7.

7. *Next generation kinase inhibitors - moving beyond the ATP binding/catalytic sites*. Shapiro, P. Ed., Springer: Cham, Switzerland, 2020.

8. Koehnke, J.; Naismith, J.; Donk, W. A. *Cyclic peptides: from bioorganic synthesis to applications*. Royal Society of Chemistry: Cambridge, 2017.

9. Schafmeister, C. E.; Po, J.; Verdine, G. L., An All-Hydrocarbon Cross-Linking System for Enhancing the Helicity and Metabolic Stability of Peptides. *J. Am. Chem. Soc.* **2000,** *122* (24), 5891-5892.

10. Walensky, L. D.; Kung, A. L.; Escher, I.; Malia, T. J.; Barbuto, S.; Wright, R. D.; Wagner, G.; Verdine, G. L.; Korsmeyer, S. J., Activation of apoptosis in vivo by a hydrocarbon-stapled BH_3 helix. *Science* **2004,** *305* (5689), 1466.

11. Lau, Y. H.; de Andrade, P.; Wu, Y.; Spring, D. R., Peptide stapling techniques based on different macrocyclisation chemistries. *Chem. Soc. Rev.* **2015,** *44* (1), 91-102.

12. Blackwell, H. E.; Grubbs, R. H., Highly Efficient Synthesis of Covalently Cross-Linked Peptide Helices by Ring-Closing Metathesis. *Angew. Chem. Int. Ed.* **1998,** *37* (23), 3281-3284.

13. Scrima, M.; Le Chevalier-Isaad, A.; Rovero, P.; Papini, A. M.; Chorev, M.; D'Ursi, A. M., CuI-catalyzed azide–alkyne intramolecular i-to-(i+4) Side-chain-to-side-chain cyclization promotes the formation of helix-like secondary structures. *Eur. J. Org. Chem.* **2010,** *2010* (3), 446-457.

14. Torres, O.; Yüksel, D.; Bernardina, M.; Kumar, K.; Bong, D., Peptide tertiary structure nucleation by side-chain crosslinking with metal complexation and double "Click" cycloaddition. *ChemBioChem* **2008,** *9* (11), 1701-1705.

15. Dominguez-Huerta, A.; Perepichka, I.; Li, C.-J., Catalytic *N*-modification of α-amino acids and small peptides with phenol under bio-compatible conditions. *Commun. Chem.* **2018,** *1* (1), 1-7.

Chapter 5. Diphenylamines from phenol and ammonium formate

5.1 Background

Arylamines are valuable commodity chemicals, owing to their broad application as antioxidizers and as synthetically relevant building-blocks. Diphenylamine (DPA) is primarily used as a stabilizer for nitrocellulose explosives[1, 2] and the detection of oxidizers,[3]. In contrast, *C*-alkylated diphenylamines are widely used as antioxidants for the preservation of fruits,[4-6] oils,[7] and polymers (Figure 5.1).[8] Further uses of arylamines include being a precursor for the synthesis of (azo-)dyes,[9-11] and non-steroidal anti-inflammatory drugs.[12] Additionally, triphenylamines are important for the preparation of optoelectronic materials (Figure 5.1).[13-16] For a thorough review on the use of these compounds, please see reference articles by Drzyzga[17] and Layer.[18]

Diphenylamine Triphenylamine

Figure 5.1 Diphenyl and triphenylamine chemical structures

Arylamines are commonly prepared from amine precursors through metal-catalyzed C-N coupling reactions. Methods for the formation of these compounds include the Stille,[19] Chan-Evans-Lam,[20-24] Ullmann,[25-27] and Buchwald-Hartwig[28, 29] couplings (Scheme 5.1). In addition, other methods including P(III)/P(V)=O catalysis,[30] iodine,[31] sulfonium triflates,[32] various nanoparticle catalysts,[33, 34] and Pd/C for the formation of arylamines from aliphatic substrates,[35-37] have also been reported (Scheme 5.1). Similar developments for the formation of diaryl ethers have also been reported.[38, 39]

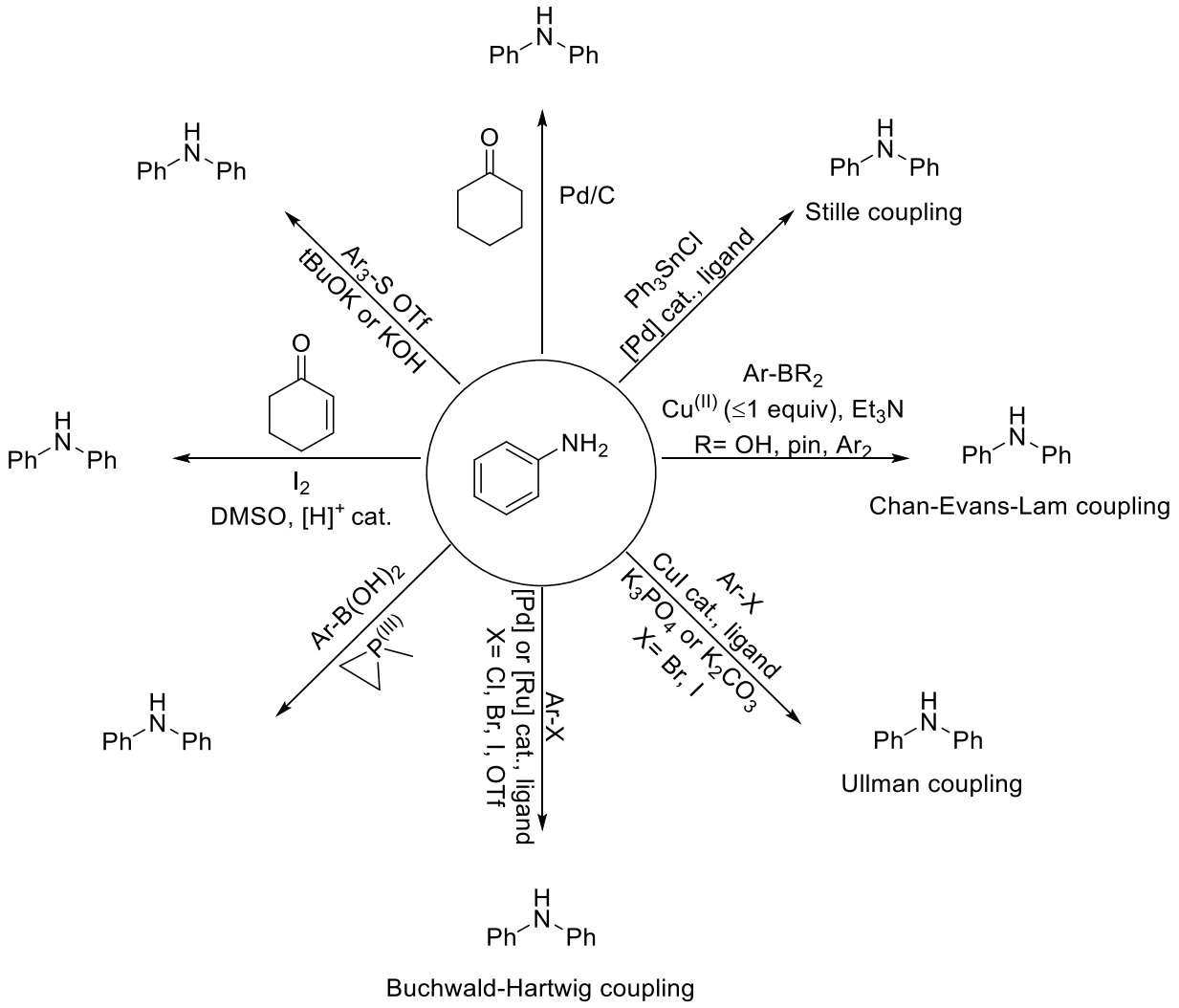

Scheme 5.1 Different methodologies for the synthesis of diphenylamine

Phenol can be obtained from natural sources as one of the basic units of lignin, making it an attractive bio-renewable feedstock for synthesis.[40] In an attempt to replace the use of aryl halides as starting materials, our group has investigated the possibility of using phenols as the coupling partner for the formation of C-N bonds through the use of heterogeneous palladium as a catalyst (Scheme 5.2).[41-43] In 2017, our group published a methodology to access *N*-cyclohexyl anilines from phenols using hydrazine or hydroxylamine[44] (Scheme 5.3). The latter is a deoxyamination process that involves a complex C−O bond and N−N/O bond-cleavage to yield *N*-substituted cyclohexyl anilines from an array of phenols by finely controlling the reaction conditions in moderate to good yields.

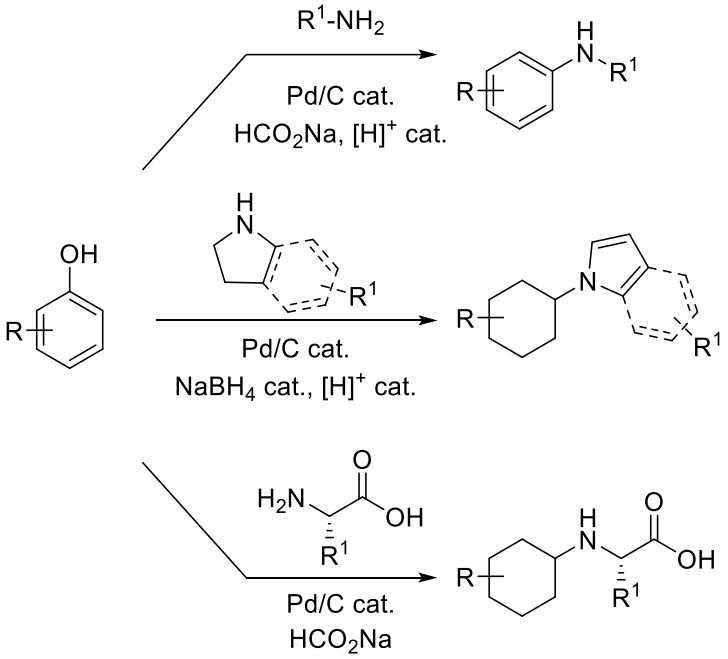

Scheme 5.2 Phenol as a coupling partner for C-N bond formation through (1) redox neutral pathway[41] (2) reductive aromaticity transfer[42] (3) reductive coupling.[43]

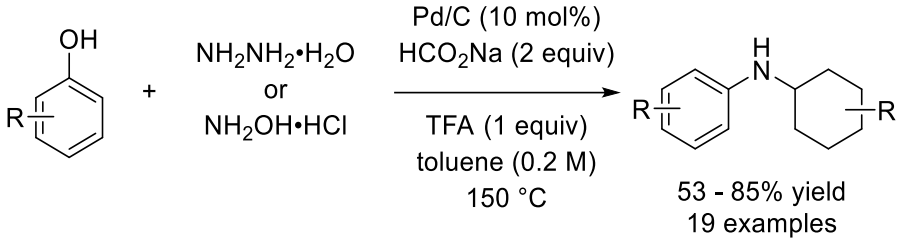

Scheme 5.3 Synthesis of *N*-cyclohexyl anilines from phenols with hydrazine or hydroxylamine[44]

5.2 Research objectives and plan

In our continuous drive to develop methodologies for the sustainable access to nitrogen-containing chemicals, we envisioned the synthesis of diphenylamines using phenol as the arylating reagent. The use of a safe and stable nitrogen source was also of high interest to us, as this would greatly expand the applicability of the process. Thus, we proposed using ammonium formate, a stable and non-corrosive salt, to generate ammonia in-situ (Scheme 5.4). Notably, the transformation would generate CO_2 and water as the only by-products. Based on our previous research,[44] the reaction conditions would be screened by first testing the required equivalencies of phenol required for the transformation, followed by the screening of temperature, reaction time, palladium sources, and basic additives. The optimal conditions would be then used to explore the reaction scope and the feasibility of synthesizing triaryl amines.

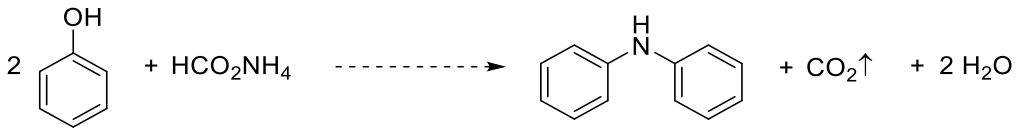

Scheme 5.4 Model reaction for the synthesis of diphenylamines using phenol and ammonium formate

5.3 Results and discussion

5.3.1 Condition Screening

We began by investigating the synthesis of diphenylamine using 4 equivalents of phenol (**1a**) and one equivalent of ammonium formate (**2**), with Pd/C as the catalyst at a loading of 20 mol%. *m*-Xylene was used as the solvent, and the reaction was run for 24 hours at 160 °C under an argon atmosphere. As opposed to the previous methodologies described, it is worth noting that since ammonium formate is the amine source, it is also the limiting reaget, therefore also limiting the amount of formate present in the reaction. To our delight, we were able to obtain the desired product (**3a**) in 54% yield (Table 5.1, entry 1). Upon increasing the loading of phenol (**1a**), we were able to obtain diphenylamine (**3a**) in 98% yield (Table 5.1, entries 2-4). While high amounts of phenol are required for the transformation to drive the equilibrium towards our desired product. Nonetheless, phenol can be recovered during the work-up through extraction at pH 14. The reaction was run neat using the optimized equivalencies of phenol, resulting in the formation of product **3a** in 95% yield (Table 5.1, entry 5). Although this experiment shows the feasibility of running the reaction without solvent, *m*-xylene was kept as part of the reaction system

to facilitate the stirring of the reagents. Upon optimizing reagent equivalencies and seeing that traces of triphenyl amine (**4**) were present, a lower loading of palladium at 10 mol% was tested. Unfortunately, the reaction yield dropped to 72%, which convinced us to keep the original loading (Table 5.1, entry 6). Palladium hydroxide on carbon was also tested at a 10 mol% loading. However, 20 mol% Pd/C still proved optimal (Table 5.1, entry 7). It is important to point out that the palladium catalyst had to be activated prior to the reaction in order to obtain optimal yields.

Table 5.1 Effect of the concentration of phenol for the formation of diphenylamine

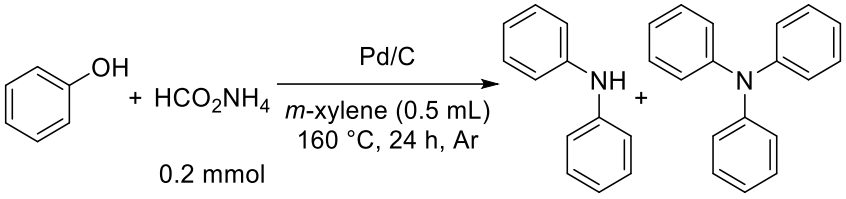

1a **2** **3a** **4**

Entry[a]	Conditions		Yield (%)[b]	
	1a (equiv)	Catalyst (mol%)	**3a**	**4**
1	4	Pd/C, 20	54	ND
2	6	Pd/C, 20	86	ND
3	8	Pd/C, 20	90	Traces
4	10	Pd/C, 20	98	Traces
5[c]	10	Pd/C, 20	95	Traces
6	10	Pd/C, 10	72	ND
7	10	$Pd(OH)_2$/C, 10	84	ND

[a] Reaction conditions: **1** (x equiv), **2** (0.2 mmol, 1 equiv), catalyst (x equiv), xylene (0.5 mL).

[b] NMR yield using CH_2Br_2 (0.2 mmol, 7 µL) as an internal standard and calculated based on HCO_2NH_4.

[c] Reaction was run neat. ND: not detected.

Aiming to see if we could push the reaction for the formation of triphenylamine, we analyzed the effect of temperature in the reaction (Table 5.2). Lowering the reaction temperature, even by 10 °C, caused a significant decrease in the yield of product **3a** (Table 5.2, entry 1). Increasing the temperature

barely impacted the yields of diphenylamine (**3a**) and triphenylamine (**4**) observed, prompting us to maintain 160 °C as the optimized temperature (Table 5.2, entries 2-4). Higher temperatures were not screened due to safety concerns regarding vial pressure build-up.

Table 5.2 Temperature effect on the reaction between phenol and ammonium formate

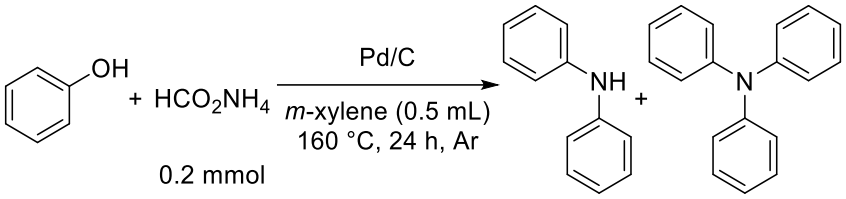

1a **2** **3a** **4**

Entry[a]	T [°C]	Yield (%)[b]	
		3a	**4**
1	150	65	ND
2	160	96	ND
3	170	87	Traces
4	180	96	Traces

[a] Conditions: **1** (2.0 mmol, 10 equiv), **2** (0.2 mmol, 1 equiv), Pd/C (10 wt%, 0.4 mmol), xylene (0.5 mL).

[b] NMR yield obtained using CH_2Br_2 (0.2 mmol, 7 µL) as an internal standard. ND: Not detected.

The reaction time was then investigated (Table 5.3). Short reaction times did not favour the formation of product **3a**, resulting in a significant drop in the reaction yield (Table 5.3, entries 1-4). The reaction proved to have an optimized yield when allowing the reaction to stir at 160 °C between 20 h and 28 h (Table 5.3, entries 5-7). Given that the yields were determined by NMR, these entries (Table 5.3, entries 5-7) can be considered to work with the same efficacy. Doubling or tripling the standard reaction time resulted in the decomposition of desired product **3a** without increasing triphenylamine formation (**4**).

Table 5.3 Time dependence of the reaction between phenol and ammonium formate

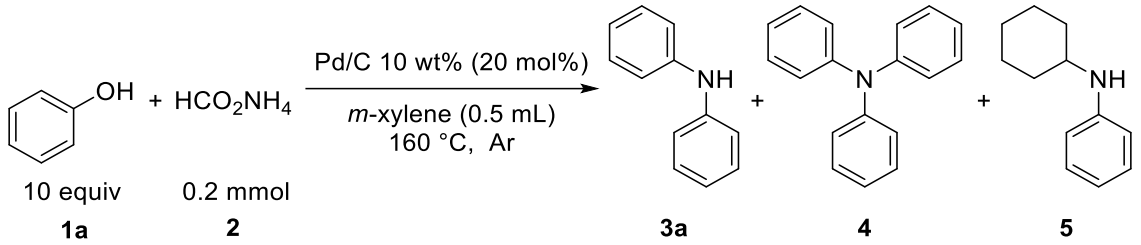

Entry[a]	Time (h)	Yield (%)[b]		
		3a	**4**	**5**
1	2	30	ND	15
2	4	46	ND	13
3	6	66	ND	14
4	9	71	ND	12
5	20	97	ND	ND
6	24	96	Traces	ND
7	28	>99	ND	ND
8	48	80	Traces	ND
9	72	82	Traces	ND

[a] Conditions: **1** (2.0 mmol, 10 equiv), **2** (0.2 mmol, 1 equiv), Pd/C (10 wt%, 0.4 mmol), xylene (0.5 mL).

[b] NMR yield obtained using CH_2Br_2 (0.2 mmol, 7 µL) as an internal standard. ND: Not detected.

Having found conditions we believed to be optimal, we proceeded to test the reaction scope. However, the reaction yield dropped considerably upon substitution of the phenolic ring. This prompted us to screen different palladium supports and additives in strive to resolve this difficulty. In order to find a broadly suitable catalyst or additive for all substrates, we decreased the reaction temperature while maintaining phenol (**1a**) as the model substrate. This was primarily done given that the reaction was already nearly quantitative, making it impossible to track any further improvements.

Different palladium supports were first screened at 150 °C, allowing the reaction to proceed for 20 h (Table 5.4). Using Pd/C as the catalyst in a concentration of 20 mol%, gave the product **3a** in 88% yield (Table 5.4, entry 1). Using basic supports such as MgO or $BaSO_4$ did not improve the reaction yield, even when doubling the catalyst's loading (Table 5.4, entries 2-3). Finally, using SiO_2 as an acidic support

also proved inefficient (Table 5.4, entry 4). Based on these results, Pd/C was maintained as the catalyst for the reaction.

Table 5.4 Effect of different supports on reaction yield

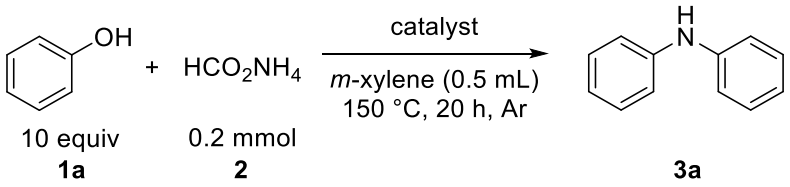

Entry[a]	Catalyst	Yield **3a**[b] (%)
1	10 wt% Pd/C (20 mol%)	88
2	5 wt% Pd/MgO (20 mol%)	80
3	5 wt% Pd/$BaSO_4$ (40 mol%)	22
4	5 wt% Pd/SiO_2 (40 mol%)	43

[a] Reaction conditions: **1** (2.0 mmol, 10 equiv), **2** (0.2 mmol, 1 equiv), catalyst, xylene (0.5 mL). Reaction was run at 150 °C in order to observe the effect of different catalyst supports on the reaction.

[b] NMR yield obtained using CH_2Br_2 (0.2 mmol, 7 µL) as an internal standard.

We further decreased the temperature to 140 °C to test additives that could favour the condensation between phenol and ammonium formate. At this temperature, the formation of **3a** decreased to 44% (Table 5.5, entry 1). Molecular sieves, MgO, and CaO, were screened as drying agents (Table 5.5, entries 2-4) to remove water produced during the condensation step, potentially competing with ammonia as a nucleophile. Although the reaction yield was improved in all three cases, we looked into using basic additives to improve ammonia formation, as the prevalence of NH_4^+ inevitably hinders product formation (Table 5.5, entries 5-6). We were pleased to find that at 40 mol% LiOH improved the reaction yield (Table 5.5, entry 5). We proceeded to compare CaO and LiOH as additives at different loadings (Table 5.5, entries 7-12). Finally, the optimal concentrations of these bases were compared at 150 °C (Table 5.5, entries 13-14). Although lithium hydroxide might act as a competing nucleophile, 40 mol% proved to be optimal and was kept for all further screening.

Table 5.5 Screening of additives at a lower temperature

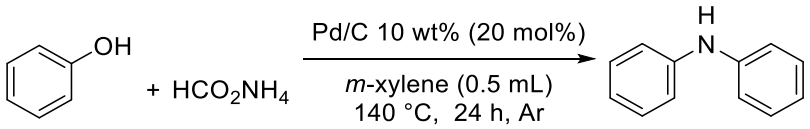

10 equiv **1a** 0.2 mmol **2** **3a**

Entry[a]	Additives	Yield **3a** (%)[b]
1	none	44
2	Molecular Sieves 100 mg	66
3	MgO (0.2 mmol)	62
4	CaO (0.4 mmol)	73
5	LiOH (0.08 mmol)	53
6	KOH (0.1 mmol)	ND
7	CaO (0.2 mmol)	55
8	CaO (0.4 mmol)	73
9	CaO (0.5 mmol)	69
10	LiOH (0.05 mmol)	43
11	LiOH (0.08 mmol)	53
12	LiOH (0.1 mmol)	44
13[c]	CaO (0.4 mmol)	75
14[c]	LiOH (0.08 mmol)	84

[a] Reaction conditions: **1** (2.0 mmol, 10 equiv), **2** (0.2 mmol, 1 equiv), catalyst, xylene (0.5 mL). The reaction was run at 140 °C in order to observe the effect of different additives on the reaction.

[b] NMR yield using CH_2Br_2 (0.2 mmol, 7 µL) as an internal standard and yield was calculated by HCO_2NH_4.

[c] Reaction ran at 150 °C. ND: not detected.

5.3.2 Substrate scope

With the optimized reaction conditions in hand, the reaction scope was tested using phenolic compounds **1a** – **1q** (Scheme 5.5). The reaction temperature was raised to 170 °C due to the sluggish reactivity of some substrates. Phenolic rings with a single methyl substitution at the *ortho*-, *meta*-, and *para*- positions proved to be successful substrates for the reaction (**3b** – **3d**). Ethyl, propyl, and *tert*-butyl substituents were well tolerated at the *ortho*- and *para*- positions (**3e** – **3i**). Having 2,6-dimethyl substitution proved to be a challenge due to the increased steric bulk, yielding only 27% of the desired product **3j**. On the other hand, rings with dimethyl substitution at the 3,6- and 3,4- positions gave the corresponding products **3k** and **3l** in good yields. Benzyl phenol (**1m**) gave the corresponding diarylated product **3m** in 68% yield without dearomatization of the benzyl ring. Using 2,3-dihydro-1H-inden-4-ol (**1n**) as the phenolic source gave the desired diarylated amine **3n** in 25% yield. We presume that the yield is lower due to the fused system, which might render both the hydrogenation and the rearomatization processes more sluggish. 1- and 2- naphthalenols (**1o** – **1p**) yielded the corresponding products **3o** and **3p** in 64% and 52% yield, respectively. Due to the fused ring system, which made the substrates more robust disfavouring the reduction step, an additional hydrogen source was necessary to reduce the phenolic ring to the corresponding enone. Thus, 1 equivalent of sodium formate was added for these substrates. Pyrocatechol (**1q**) also proved to be a successful substrate for the reaction, yielding phenazine (**3q**) as the reaction product in 49% yield.

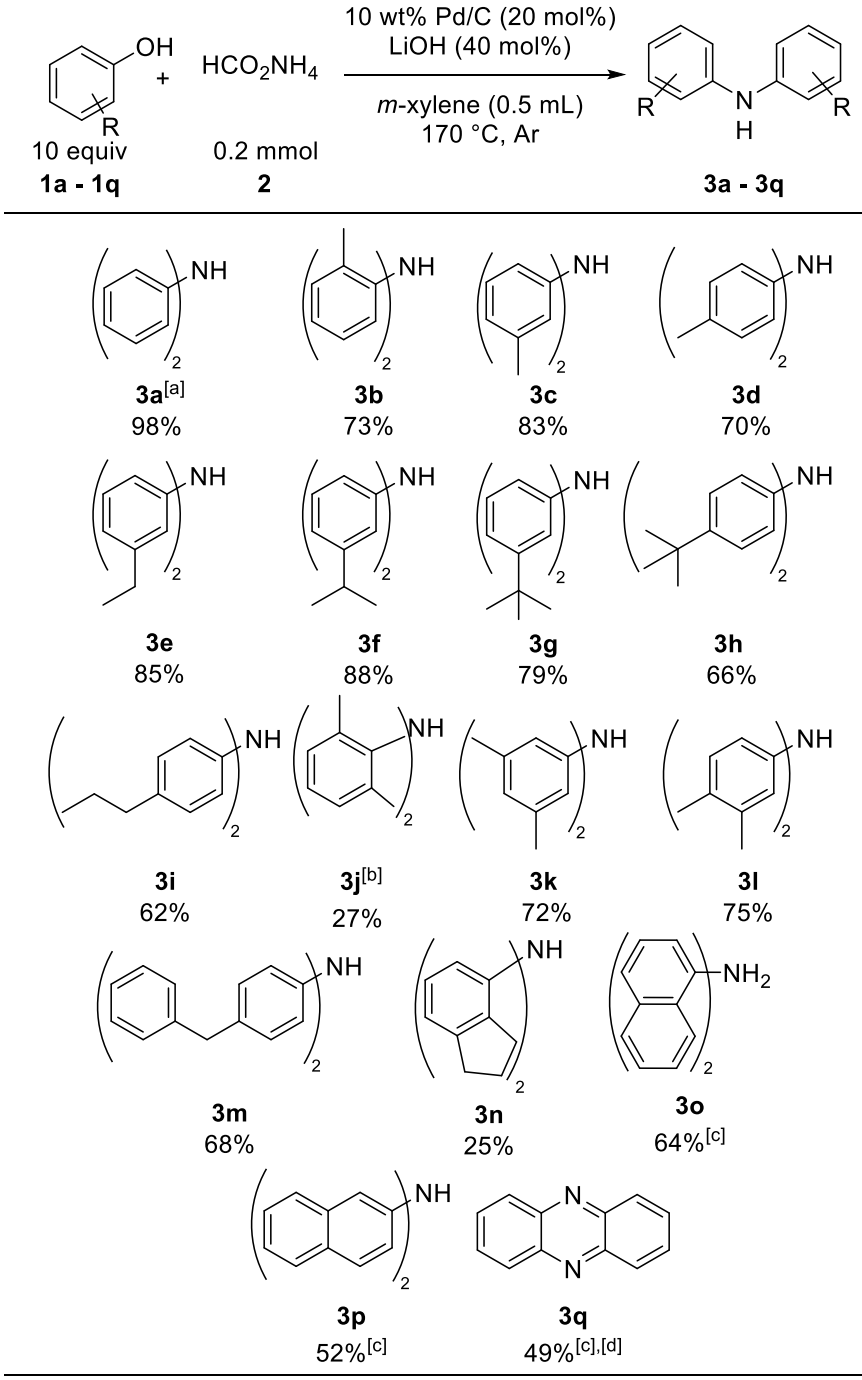

Scheme 5.5 Reaction scope using different substituted phenols and ammonium formate

[a] Reaction ran at 160 °C [b] NMR yield obtained using CH_2Br_2 (0.2 mmol, 7 µL) as an internal standard. [c] HCO_2Na (0.1 mmol, 6.8 mg) was used in the reaction. [d] Obtained from pyrocatechol as the starting material, reaction ran for 66 h.

Finally, we proceeded to test the feasibility of forming triphenylamine (**5**) from diphenylamine (**3a**). Unfortunately, resubmitting **3a** to the optimized reaction conditions did not yield **5** in sufficient amounts. Therefore, we decided to use 2-cylcohexen-1-one (**6**) as the coupling partner under our previously reported conditions in order to facilitate the condensation step,[43] yielding the desired compound **5** in 33% yield (Scheme 5.6).

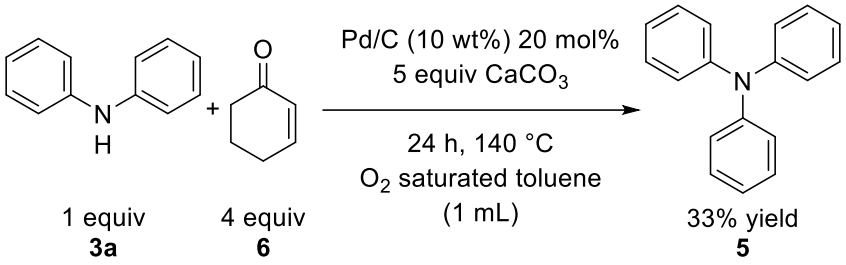

Scheme 5.6 Formation of triphenyl amine using our previous methodology

5.3.3 Mechanistic proposal

The proposed reaction mechanism for this reaction is shown in Scheme 5.7. Ammonium formate decomposes in the presence of Pd(0) to give a Pd(II) dihydride species, CO_2 and ammonia.[45] Phenol can then react with the Pd(II) dihydride to yield the corresponding cyclohexenone, which in turn can undergo condensation with the ammonia present in the reaction mixture. The resulting imine can undergo a second condensation, through enamine formation, to give intermediate **A**. Finally, intermediate **A** can dehydrogenate in the presence of Pd(0) to provide the corresponding product **3a**.

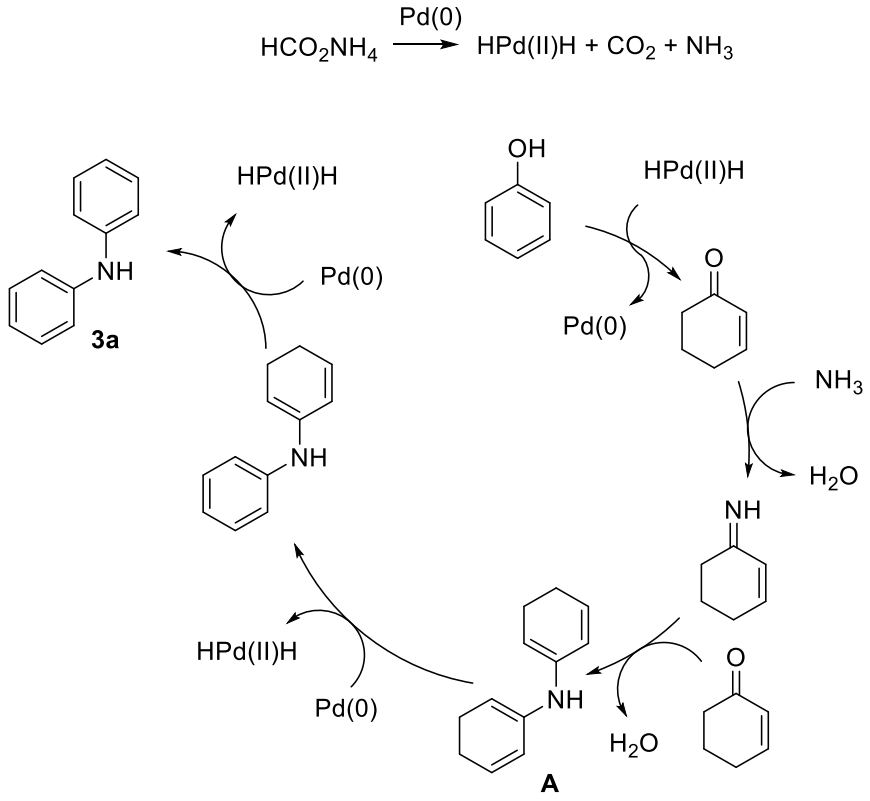

Scheme 5.7 Proposed reaction mechanism

5.3.4 Additional experiments

It is important to mention that the preparation of the palladium catalyst for the reaction had a significant impact on the reproducibility and overall yield of the reaction (Table 5.7). Using Pd/C without any pre-treatment resulted in 88% yield of diphenylamine (**3a**) under optimized conditions (Table 5.7, entry 1). Drying the catalyst under vacuum overnight resulted in a slight increase in the reaction yield (Table 5.7, entry 2). Best results were obtained when the catalyst was dried for 2 hours at 130 °C, making it our selected strategy for this transformation (Table 5.7, entry 3).

Table 5.6 Effect of pre-drying Pd/C on reaction yield

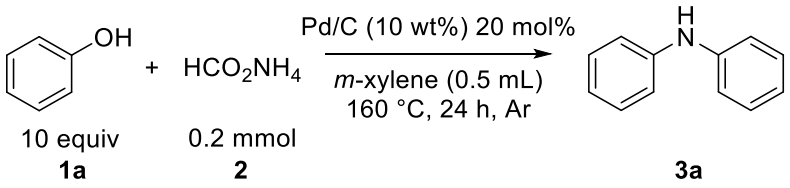

Entry[a]	Pd/C preparation	Yield **3**[b] (%)
1	Straight from the bottle	88
2	Dried with vacuum overnight	92
3	Dried for 2 h at 130 °C	98

[a] Conditions: **1** (2.0 mmol, 10 equiv), **2** (0.2 mmol, 1 equiv), Pd/C (10 wt%, 0.4 mmol), xylene (0.5 mL)

[b] NMR yield obtained using CH_2Br_2 (0.2 mmol, 7 µL) as an internal standard.

5.4 Conclusion and outlook

In conclusion, we were able to synthesize 17 different diarylated amines from a convenient ammonia source using phenols as arylating reagents and Pd/C as the catalyst. Yields for the reaction ranged from good to excellent, except for severely sterically hindered substrates bearing multiple ortho substituents. Furthermore, using our previously described arylating methodology with 2-cyclohexen-1-one, proved to be a viable synthetic route to triarylamines. This work demonstrates a pathway to synthesizing *N*-containing chemicals from reductive amination using biomass-derived compounds as arylating reagents and stable ammonia salts as the nitrogen source.

5.5 Contributions

Project conceptualization was realized by Prof. Chao-Jun Li. Methodology, experimentation and characterization were performed by myself with the assistance of Dr. Inna Perepichka. High-resolution mass spectrometry was performed by Dr. Nadim Saadeh and Dr. Alexander Wahba at the McGill University Department of Chemistry Mass Spectrometry Laboratory. The publication manuscript, which shares some shared content with this thesis chapter, was written by myself, edited and proofread by Dr. Zihang Qiu, Dr. Adam A. Elmehriki and Prof. Chao-Jun Li.

5.6 Experimental section

5.6.1 General Information

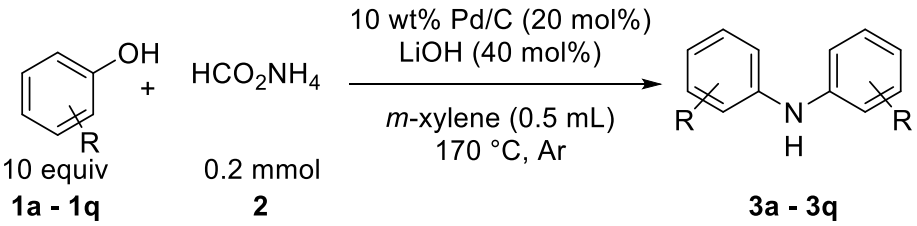

To a flame-dried Schlenk-type reaction flask (10.0 mL) equipped with a Teflon-coated magnetic stirring bar, phenol (2.0 mmol, 10 equiv), ammonium formate (**2**) (0.2 mmol, 1 equiv), lithium hydroxide (0.08 mmol, 0.4 equiv), and dry[a] 10 wt% Pd/C (0.2 mmol, 20 mmol%), were added. For substrates **1o** – **1q** sodium formate (0.1 mmol, 0.5 equiv) was added as an additional source for hydrogen. The resulting mixture was evacuated and backfilled with ultra-purified argon thrice, to which anhydrous *m*-xylene (0.5 mL) was added. The reaction flask was placed into an oil bath at 160 °C for phenol (**1a**), and 170 °C for all other substrates (**1b** – **1q**), with stirring. After 24 hours, the reaction mixture was diluted with EtOAc, filtered through a pad of silica gel and the organic solvent was evaporated. An aqueous solution of 2 N NaOH (100 mL) and EtOAc (20 mL) were added to the reaction crude, and the mixture was stirred for 15 mins. The organic layer was extracted with EtOAc (2 × 20 mL), and the combined organic phases were washed with brine and dried over sodium sulphate. The solvent was removed in vacuo, and the residue was purified by column chromatography on silica gel using hexane: ethyl acetate (5:1) as the eluent to give the corresponding pure product.

[a]Dried at 130 °C under vacuum for 2 h

5.6.2 Analytical Data

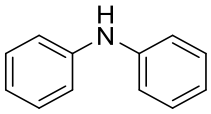

Diphenylamine (**3a**)

Use the general procedure described, compound **3a** was obtained from ammonium formate (0.20 mmol, 12.6 mg) and phenol (2.0 mmol, 188 mg) in 98% yield. R_f (hexane/EtOAc 5:1): 0.6.

^{1}H NMR (500 MHz, $CDCl_3$): δ 7.33-7.22 (m, 4H), 7.11 (dd, *J* = 8.4, 1.0 Hz, 4H), 6.95 (t, *J* = 7.4 Hz, 2H), 5.80 (br, 1H). ^{13}C NMR (126 MHz, $CDCl_3$) δ 143.06, 129.35, 121.01, 117.82.
HRMS (ESI) m/z: $[M + H]^+$ calculated for $C_{12}H_{12}N$ 170.09643, found 170.09660.

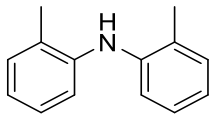

Di-*o*-tolylamine (**3b**)

Using the general procedure described, compound **3b** was obtained from ammonium formate (0.20 mmol, 12.6 mg) and *o*-cresol (2.0 mmol, 216 mg) in the presence of LiOH (0.08 mmol, 2 mg) in 73% yield.

^{1}H NMR (500 MHz, $CDCl_3$) δ 7.21 (d, *J* = 7.4 Hz, 2H), 7.15 (t, *J* = 7.7 Hz, 2H), 7.02 (d, *J* = 8.0 Hz, 2H), 6.93 (t, *J* = 7.4 Hz, 2H), 5.16 (br, 1H), 2.30 (s, 6H). ^{13}C NMR (126 MHz, $CDCl_3$) δ 141.9, 130.9, 127.6, 126.9, 121.5, 118.4, 17.9. HRMS (ESI) m/z: $[M + H]^+$ calculated for $C_{14}H_{16}N$ 198.12773, found 198.12796.

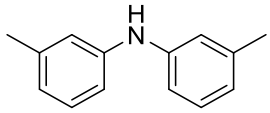

Di-*m*-tolylamine (**3c**)

Using the general procedure described, compound **3c** was obtained from ammonium formate (0.20 mmol, 12.6 mg) and *m*-cresol (2.0 mmol, 216 mg) in the presence of LiOH (0.08 mmol, 2 mg) in 83% yield.

^{1}H NMR (500 MHz, $CDCl_3$) δ 7.19 (dd, *J* = 8.7, 7.6 Hz, 2H), 6.97 – 6.86 (m, 4H), 6.79 (d, *J* = 7.3 Hz, 2H), 5.63 (br, 1H), 2.35 (s, 6H). ^{13}C NMR (126 MHz, $CDCl_3$) δ 143.3, 139.3, 129.3, 121.9, 118.7, 115.1, 21.7. HRMS (ESI) m/z: $[M + H]^+$ calculated for $C_{14}H_{16}N$ 198.12773, found 198.12797.

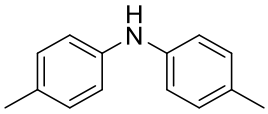

Di-*p*-tolylamine (**3d**)

Using the general procedure described, compound **3d** was obtained from ammonium formate (0.20 mmol, 12.6 mg) and *p*-cresol (2.0 mmol, 216 mg) in the presence of LiOH (0.08 mmol, 2 mg) in 70% yield.

^{1}H NMR (500 MHz, $CDCl_3$) δ 7.06 (d, *J* = 8.1 Hz, 4H), 6.95 (d, *J* = 8.4 Hz, 4H), 5.52 (br, 1H), 2.29 (s, 6H). ^{13}C NMR (126 MHz, $CDCl_3$) δ 141.3, 130.3, 130.0, 118.0, 20.8. HRMS (ESI) m/z: $[M + H]^+$ calculated for $C_{14}H_{16}N$ 198.12773, found 198.12801.

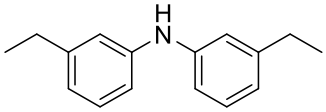

Bis(3-ethylphenyl)amine (**3e**)

Using the general procedure described, compound **3e** was obtained from ammonium formate (0.20 mmol, 12.6 mg) and 3-ethylphenol (2.0 mmol, 244 mg) in the presence of LiOH (0.08 mmol, 2 mg) in 85% yield.

^{1}H NMR (500 MHz, $CDCl_3$) δ 7.18 (t, *J* = 7.7 Hz, 2H), 6.93 – 6.88 (m, 4H), 6.77 (dd, *J* = 7.5, 0.5 Hz, 2H), 5.65 (br, 1H), 2.61 (q, *J* = 7.6 Hz, 4H), 1.23 (t, *J* = 7.6 Hz, 6H). ^{13}C NMR (126 MHz, $CDCl_3$) δ 145.7, 143.4, 129.4, 120.7, 117.5, 115.3, 29.1, 15.7. HRMS (APCI) m/z: $[M + H]^+$ calculated for $C_{16}H_{2o}N$ 226.15903, found 226.15936.

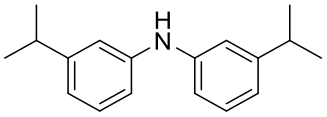

Bis(3-isopropylphenyl)amine (**3f**)

Using the general procedure described, compound **3f** was obtained from ammonium formate (0.20 mmol, 12.6 mg) and 3-isopropylphenol (2.0 mmol, 272 mg) in the presence of LiOH (0.08 mmol, 2 mg) in 88% yield.

^{1}H NMR (500 MHz, MeOD) δ 7.11 (dd, *J* = 9.9, 5.7 Hz, 2H), 6.95 (t, *J* = 1.8 Hz, 2H), 6.86 (ddd, *J* = 8.0, 2.2, 0.8 Hz, 2H), 6.70 (d, *J* = 7.6 Hz, 2H), 4.85 (s, 1H), 2.81 (hept, *J* = 6.9 Hz, 2H), 1.22 (d, *J* = 6.9 Hz, 12H). ^{13}C NMR (126 MHz, MeOD) δ 151.1, 145.4, 130.0, 119.3, 116.4, 116.0, 35.5, 24.5. HRMS (ESI) m/z: $[M + H]^+$ calculated for $C_{18}H_{24}N$ 254.1903, found 254.1897

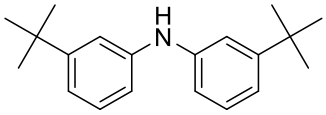

Bis(3-(tert-butyl)phenyl)amine (**3g**)

Using the general procedure described, compound **3g** was obtained from ammonium formate (0.20 mmol, 12.6 mg) and 3-(*tert*-butyl)phenol (2.0 mmol, 300 mg) in the presence of LiOH (0.08 mmol, 2 mg) in 79% yield.

^{1}H NMR (500 MHz, $CDCl_3$) δ 7.21 (t, *J* = 7.9 Hz, 2H), 7.15 (t, *J* = 1.9 Hz, 2H), 6.97 (d, *J* = 7.8 Hz, 2H), 6.89 (dd, *J* = 7.9, 1.5 Hz, 2H), 1.31 (s, 18H). ^{13}C NMR (126 MHz, $CDCl_3$) δ 152.6, 143.1, 129.1, 118.1, 115.2, 115.0, 34.9, 31.5. HRMS (ESI) m/z: $[M + H]^+$ calculated for $C_{20}H_{28}N$ 282.22163, found 282.22249.

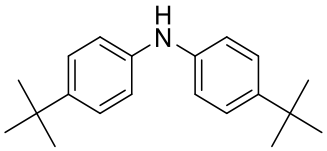

Bis(4-(tert-butyl)phenyl)amine (**3h**)

Using the general procedure described, compound **3h** was obtained from ammonium formate (0.20 mmol, 12.6 mg) and 4-(*tert*-butyl)phenol (2.0 mmol, 300 mg) in the presence of LiOH (0.08 mmol, 2 mg) in 66% yield.

^{1}H NMR (500 MHz, $CDCl_3$) δ 7.29 – 7.27 (m, 4H), 7.00 (s, 4H), 5.59 (br, 1H), 1.31 (s, 18H). ^{13}C NMR (126 MHz, $CDCl_3$) δ 143.7, 141.1, 126.2, 117.5, 34.3, 31.6. HRMS (ESI) m/z: $[M + H]^+$ calculated for $C_{20}H_{28}N$ 282.22163, found 282.22088

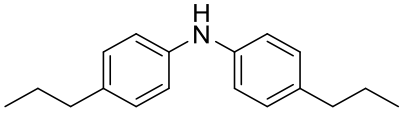

Bis(4-propylphenyl)amine (**3i**)

Using the general procedure described, compound **3i** was obtained from ammonium formate (0.20 mmol, 12.6 mg) and 4-propylphenol (2.0 mmol, 272 mg) in the presence of LiOH (0.08 mmol, 2 mg) in 62% yield.

^{1}H NMR (500 MHz, $CDCl_3$) δ 7.07 (d, *J* = 8.4 Hz, 4H), 6.97 (d, *J* = 8.3 Hz, 4H), 2.53 (t, *J* = 7.6 Hz, 4H), 1.61 (dt, *J* = 14.8, 7.4 Hz, 4H), 0.95 (t, *J* = 7.3 Hz, 6H). ^{13}C NMR (126 MHz, $CDCl_3$) δ 141.4, 135.3, 129.4, 118.0, 37.5, 24.9, 14.0. HRMS (ESI) m/z: $[M + H]^+$ calculated for $C_{18}H_{24}N$ 254.19033, found 254.19038.

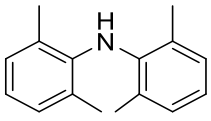

Bis(2,6-dimethylphenyl)amine (**3j**)

Using the general procedure described, compound **3j** was obtained from ammonium formate (0.20 mmol, 12.6 mg) and 2,6-dimethylphenol (2.0 mmol, 244 mg) in the presence of LiOH (0.08 mmol, 2 mg) in 27%

yield. Using our purification procedure, it was not possible to isolate compound **3j**. For this reason, only the crude ^{1}H NMR spectra is solely provided for this compound. ^{1}H NMR (500 MHz, $CDCl_3$) δ 7.11 (d, *J* = 7.5 Hz, 4 H), 6.90 (t, *J* = 7.5 Hz, 2 H), 2.37 (s, 12 H).

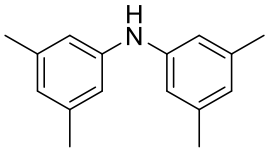

Bis(3,5-dimethylphenyl)amine (**3k**)

Using the general procedure described, compound **3k** was obtained from ammonium formate (0.20 mmol, 12.6 mg) and 3,5-dimehtylphenol (2.0 mmol, 244 mg) in the presence of LiOH (0.08 mmol, 2 mg) in 72% yield. ^{1}H NMR (500 MHz, $CDCl_3$) δ 6.70 (s, 4H), 6.58 (s, 2H), 5.53 (br, 1H), 2.27 (s, 12 H). ^{13}C NMR (126 MHz, $CDCl_3$) δ 143.4, 139.1, 122.9, 115.9, 21.6. HRMS (ESI) m/z: $[M + H]^+$ calculated for $C_{16}H_{20}N$ 226.15903, found 226.15847.

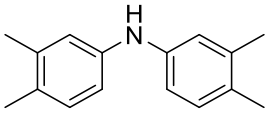

Bis(3,4-dimethylphenyl)amine (**3l**)

Using the general procedure described, compound **3l** was obtained from ammonium formate (0.20 mmol, 12.6 mg) and 3,4-dimethylphenol (2.0 mmol, 244 mg) in the presence of LiOH (0.08 mmol, 2 mg) in 75% yield.

^{1}H NMR (500 MHz, MeOD) δ 6.93 (d, *J* = 8.1 Hz, 2H), 6.81 (d, *J* = 2.2 Hz, 2H), 6.76 (dd, *J* = 8.0, 2.4 Hz, 2H), 2.19 (s, 6H), 2.17 (s, 6H). ^{13}C NMR (126 MHz, MeOD) δ 143.6, 138.0, 131.0, 128.9, 120.1, 116.0, 20.1, 19.0 HRMS (ESI) m/**z:** $[M + H]^+$ calculated for $C_{16}H_{20}N$ 226.1590, found 226.1582.

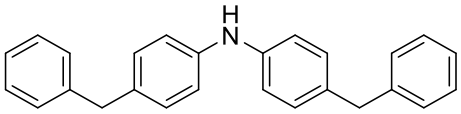

Bis(4-benzylphenyl)amine (**3m**)

Using the general procedure described, compound **3m** was obtained from ammonium formate (0.20 mmol, 12.6 mg) and 4-benzylphenol (2.0 mmol, 368 mg) in the presence of LiOH (0.08 mmol, 2 mg) in 68% yield.

^{1}H NMR (500 MHz, $CDCl_3$) δ 7.32 – 7.27 (m, 4H), 7.22 – 7.17 (m, 6H), 7.07 (d, *J* = 8.5 Hz, 4H), 6.98 (d, *J* = 8.4 Hz, 4H), 3.93 (s, 4H). ^{13}C NMR (126 MHz, $CDCl_3$) δ 141.7, 141.6, 133.7, 129.9, 129.0, 128.6, 126.1, 118.0, 41.4. HRMS (ESI) m/z: $[M + H]^+$ calculated for $C_{26}H_{24}N$ 350.1903, found 350.1892.

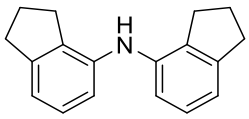

Bis(2,3-dihydro-1H-inden-4-yl)amine (**3n**)

Using the general procedure described, compound **3n** was obtained from ammonium formate (0.20 mmol, 12.6 mg) and 2,3-dihydro-1*H*-inden-4-ol (2.0 mmol, 268 mg) in the presence of LiOH (0.08 mmol, 2 mg) in 26% yield.

^{1}H NMR (500 MHz, MeOD) δ 7.02 (d, *J* = 8.0 Hz, 2H), 6.90 (d, *J* = 0.4 Hz, 2H), 6.79 (dd, *J* = 8.0, 2.1 Hz, 2H), 2.81 (q, *J* = 7.3 Hz, 8H), 2.04 (p, *J* = 7.4 Hz, 4H). ^{13}C NMR (126 MHz, MeOD) δ 146.1, 144.4, 136.7, 125.4, 117.1, 114.6, 34.0, 33.0, 26.8. HRMS (APCI) m/z: $[M + H]^+$ calculated for $C_{18}H_{20}N$ 250.15903, found 250.16005.

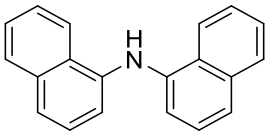

Di(naphthalen-1-yl)amine (**3o**)

Using the general procedure described, compound **3o** was obtained from ammonium formate (0.20 mmol, 12.6 mg) and naphthalene-1-ol (2.0 mmol, 288 mg) in the presence of LiOH (0.08 mmol, 2 mg) and HCO_2Na (0.1 mmol, 6.8 mg) in 64% yield.

^{1}H NMR (500 MHz, MeOD) δ 8.15 (d, *J* = 8.5 Hz, 2H), 7.85 (d, *J* = 8.1 Hz, 2H), 7.52 – 7.44 (m, 4H), 7.42 (ddd, *J* = 8.2, 6.8, 1.4 Hz, 2H), 7.31 – 7.25 (m, 2H), 6.86 (dd, *J* = 7.4, 0.9 Hz, 2H). ^{13}C NMR (126 MHz, MeOD) δ 142.9, 136.2, 129.3, 128.7, 127.1, 126.9, 126.8, 123.9, 122.9, 116.7. HRMS (ESI) m/z: $[M + H]^+$ calculated for $C_{20}H_{16}N$ 270.1277, found 270.1285.

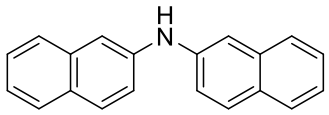

Di(naphthalen-2-yl)amine (**3p**)

Using the general procedure described, compound **3p** was obtained from ammonium formate (0.20 mmol, 12.6 mg) and naphthalene-2-ol (2.0 mmol, 244 mg) in the presence of LiOH (0.08 mmol, 2 mg) and HCO_2Na (0.1 mmol, 6.8 mg) in 52% yield.

^{1}H NMR (500 MHz, DMSO) δ 7.83 (d, *J* = 8.8 Hz, 2H), 7.76 (dd, *J* = 19.3, 8.1 Hz, 4H), 7.62 (s, 2H), 7.40 (dd, *J* = 14.5, 7.4 Hz, 4H), 7.29 (t, *J* = 7.3 Hz, 2H). ^{13}C NMR (126 MHz, DMSO) δ 141.0, 134.4, 128.9, 128.4, 127.4, 126.4, 126.3, 123.0, 120.2, 110.0. HRMS (ESI) m/z: $[M + H]^+$ calculated for $C_{20}H_{16}N$ 270.1277, found 270.1269.

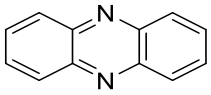

5,10-Dihydrophenazine (**3q**)

Using the general procedure described, compound **3q** was obtained from ammonium formate (0.20 mmol, 12.6 mg) and pyrocatechol (2.0 mmol, 220 mg) in the presence of LiOH (0.08 mmol, 2 mg) and HCO_2Na (0.1 mmol, 6.8 mg) in 49% yield.

^{1}H NMR (500 MHz, MeOD) δ 8.25 (dd, *J* = 6.7, 3.4 Hz, 4H), 7.95 (dd, *J* = 6.8, 3.4 Hz, 4H). ^{13}C NMR (126 MHz, MeOD) δ 144.5, 132.3, 130.2. HRMS (APCI) m/z: $[M + H]^+$ calculated for $C_{12}H_9N_2$ 181.0760, found 181.0752.

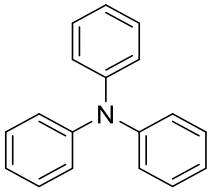

Triphenylamine (**4a**)

Using the general procedure described, compound **4a** was obtained from ammonium formate (0.20 mmol, 12.6 mg) and phenol (2.0 mmol, 188 mg) at 180 °C for 24h in 18% yield.

^{1}H NMR (500 MHz, $CDCl_3$) δ 7.28 – 7.23 (m, 6H), 7.11 (d, *J* = 7.6 Hz, 6H), 7.03 (t, *J* = 7.3 Hz, 3H). ^{13}C NMR (126 MHz, $CDCl_3$) δ 147.0, 129.2, 124.2, 122.7. HRMS (ESI) m/z: $[M + H]^+$ calculated for $C_{18}H_{16}N$ 246.12773, found 246.12774.

5.7 References

1. Shehata, A. B.; Hassan, M. A.; Nour, M. A., Effect of new poly 2-acryloyl-*N,N*'-bis (4-nitrophenyl) propandiamide and poly 2-acryloyl-*N,N*'-bis (4-methylphenyl) propandiamide and their synergistic action on the stability of nitrocellulose. *J. Hazard. Mater.* **2003,** *102* (2), 121-136.

2. Katoh, K.; Le, L.; Kumasaki, M.; Wada, Y.; Arai, M., Stabilization of nitrocellulose by diphenylamine and phenol compound. *Sci. Technol. Energetic Mater.* **2007,** *68* (1), 9-13.

3. Mutlu, M. M.; Erdoğdu, G., Selective detection of dopamine with poly(diphenylamine sulfonic acid) modified electrode in the presence of ascorbic acid. *J. Anal. Chem.* **2011,** *66* (7), 660-665.

4. Gapper, N. E.; Hertog, M. L. A. T. M.; Lee, J.; Buchanan, D. A.; Leisso, R. S.; Fei, Z.; Qu, G.; Giovannoni, J. J.; Johnston, J. W.; Schaffer, R. J.; Nicolaï, B. M.; Mattheis, J. P.; Watkins, C. B.; Rudell, D. R., Delayed response to cold stress is characterized by successive metabolic shifts culminating in apple fruit peel necrosis. *BMC Plant Biol.* **2017,** *17* (1), 77.

5. Lee, J.; Mattheis, J. P.; Rudell, D. R., Antioxidant treatment alters metabolism associated with internal browning in 'Braeburn' apples during controlled atmosphere storage. *Postharvest Biol. Tech.* **2012,** *68*, 32-42.

6. Leisso, R.; Buchanan, D.; Lee, J.; Mattheis, J.; Rudell, D., Cell Wall, Cell Membrane, and Volatile Metabolism Are Altered by Antioxidant Treatment, Temperature Shifts, and Peel Necrosis during Apple Fruit Storage. *J. Agric. Food Chem.* **2013,** *61* (6), 1373-1387.

7. Liping, W.; Dongya, Z.; Hongxing, W.; Youbai, X.; Guangneng, D., Effects of phosphorus-free antioxidants on oxidation stability and high-temperature tribological properties of lubricants. *P. I. Mech. Eng. J.-J. Eng.* **2017,** *231* (12), 1527-1536.

8. Chao, M.-R.; Li, W.-M.; Zhu, L.-L.; Ma, H.-H.; Wang, X.-B., Effect of alkylated diphenylamine on thermal-oxidative degradation behavior of poly-α-olefin. *Chem. Pap.* **2015,** *69* (7), 1004-1011.

9. Cui, J.; Zhang, S., Synthesis and application of a novel, triphendioxazine-based, phosphorus-containing acid dye for wool. *Color. Technol.* **2018,** *134* (5), 381-389.

10. Salimi Beni, A. R.; Karami, M.; Hosseinzadeh, B.; Ghahary, R., New organic dyes with diphenylamine core for dye-sensitized solar cells. *J. Mater. Sci.: Mater. Electron.* **2018,** *29* (8), 6323-6336.

11. Wang, X.; Zhong, Z.; Zhao, S.; Guo, T.; Jiang, J.-X.; Zou, J.; Ying, L.; Peng, J.; Cao, Y., An efficient blue emitter based on a naphthalene indenofluorene core. *Org. Electron.* **2018,** *55*, 157-164.

12. Janovec, L.; Janočková, J.; Matejová, M.; Konkoľová, E.; Paulíková, H.; Lichancová, D.; Júnošová, L.; Hamuľaková, S.; Imrich, J.; Kožurková, M., Proliferation inhibition of novel diphenylamine derivatives. *Bioorg. Chem.* **2019,** *83*, 487-499.

13. Naydyonov, V. P.; Syromyatnikov, V. G., Optical and electrical characteristics of triphenylamine composites. *Funct. Mater.* **2002,** *9* (3), 508-512.

14. Niu, H.; Kang, H.; Cai, J.; Wang, C.; Bai, X.; Wang, W., Novel soluble polyazomethines with pendant carbazole and triphenylamine derivatives: preparation, characterization, and optical, electrochemical and electrochromic properties. *Polym. Chem.* **2011,** *2* (12), 2804-2817.

15. Sannasi, V.; Jeyakumar, D., Synthesis of Porphyrin-Appended Poly(fluorene-alt-triphenylamine)s: Effect of Appending Groups on Optical and Electrochemical Properties. *ChemistrySelect* **2018,** *3* (4), 1004-1014.

16. Manifar, T.; Rohani, S., Synthesis and Analysis of Triphenylamine: A Review. *Can. J. Chem. Eng.* **2004,** *82* (2), 323-334.

17. Drzyzga, O., Diphenylamine and derivatives in the environment: a review. *Chemosphere* **2003,** *53* (8), 809-818.

18. Layer, R. W., Amines, Aromatic, Diarylamines. In *Kirk-Othmer Encyclopedia of Chemical Technology*, Wiley: 2000; Vol. Organic Chemicals.

19. Batmani, H.; Noroozi Pesyan, N.; Havasi, F., Synthesis and characterization of MCM-41-Biurea-Pd as a heterogeneous nanocatalyst and using its catalytic efficacy in C–C, C–N and C–O coupling reactions. *Appl. Organomet. Chem.* **2018,** *32* (8), e4419.

20. Lu, Z.; Yang, Y.-Q., Catalyst-Free Photodriven Reduction of α-Haloketones with Hantzsch Ester. *Synthesis* **2019,** *51* (02), 508-515.

21. Yang, Q.; Lei, X.; Yin, Z.; Deng, Z.; Peng, Y., Copper-Catalyzed NaBAr4-Based N-Arylation of Amines. *Synthesis* **2019,** *51* (02), 538-544.

22. Han, Y.; Zhang, M.; Zhang, Y.-Q.; Zhang, Z.-H., Copper immobilized at a covalent organic framework: an efficient and recyclable heterogeneous catalyst for the Chan–Lam coupling reaction of aryl boronic acids and amines. *Green Chem.* **2018,** *20* (21), 4891-4900.

23. Hardouin Duparc, V.; Bano, G. L.; Schaper, F., Chan–Evans–Lam Couplings with Copper Iminoarylsulfonate Complexes: Scope and Mechanism. *ACS Catal.* **2018,** *8* (8), 7308-7325.

24. Liu, S.; Xu, L., Copper-Catalyzed N-Arylation with Boronic Acid Pinacol Esters. *Asian J. Org. Chem.* **2018,** *7* (9), 1856-1863.

25. Yi, Z.; Huang, M.; Wan, Y.; Zhu, X., An Effective Heterogeneous Copper Catalyst System for C–N Coupling and Its Application in the Preparation of 2-Methyl-4-methoxydiphenylamine (MMDPA). *Synthesis* **2018,** *50* (19), 3911-3920.

26. Lo, Q. A.; Sale, D.; Braddock, D. C.; Davies, R. P., Mechanistic and Performance Studies on the Ligand-Promoted Ullmann Amination Reaction. *ACS Catal.* **2018,** *8* (1), 101-109.

27. Sonawane, R. B.; Rasal, N. K.; Bhange, D. S.; Jagtap, S. V., Copper-(II) Catalyzed *N*-Formylation and *N*-Acylation of Aromatic, Aliphatic, and Heterocyclic Amines and a Preventive Study in the C-N Cross Coupling of Amines with Aryl Halides. *ChemCatChem* **2018,** *10* (17), 3907-3913.

28. Crawford, S. M.; Wheaton, C. A.; Mishra, V.; Stradiotto, M., Probing the effect of donor-fragment substitution in Mor-DalPhos on palladium-catalyzed C–N and C–C cross-coupling reactivity. *Can. J. Chem.* **2018,** *96* (6), 578-586.

29. Mukherjee, A.; Hrovat, D. A.; Richmond, M. G.; Bhattacharya, S., A new diphosphine-carbonyl complex of ruthenium: an efficient precursor for C–C and C–N bond coupling catalysis. *Dalton Trans.* **2018,** *47* (30), 10264-10272.

30. Nykaza, T. V.; Cooper, J. C.; Li, G.; Mahieu, N.; Ramirez, A.; Luzung, M. R.; Radosevich, A. T., Intermolecular Reductive C–N Cross Coupling of Nitroarenes and Boronic Acids by PIII/PV═O Catalysis. *J. Am. Chem. Soc.* **2018,** *140* (45), 15200-15205.

31. Xiong, M.; Gao, Z.; Liang, X.; Cai, P.; Zhu, H.; Pan, Y., Iodine-catalyzed synthesis of N,N′-diaryl-o-phenylenediamines from cyclohexanones and anilines using DMSO and O_2 as oxidants. *Chem. Commun.* **2018,** *54* (69), 9679-9682.

32. Tian, Z.-Y.; Ming, X.-X.; Teng, H.-B.; Hu, Y.-T.; Zhang, C.-P., Transition-Metal-Free N-Arylation of Amines by Triarylsulfonium Triflates. *Chem.–Eur. J.* **2018,** *24* (52), 13744-13748.

33. Moghaddam, F. M.; Saberi, V.; Kalhor, S.; Veisi, N., Palladium(II) Immobilized Onto the Glucose Functionalized Magnetic Nanoparticle as a New and Efficient Catalyst for the One-pot Synthesis of Benzoxazoles. *Appl. Organomet. Chem.* **2018,** *32* (4), e4240.

34. Singh, G.; Kumar, M.; Bhalla, V., Ultrafine hybrid Cu2O–Fe2O3 nanoparticles stabilized by hexaphenylbenzene-based supramolecular assemblies: a photocatalytic system for the Ullmann–Goldberg coupling reaction. *Green Chem.* **2018,** *20* (23), 5346-5357.

35. Shimomoto, Y.; Matsubara, R.; Hayashi, M., Synthesis of Arylamines via Non-Aerobic Dehydrogenation Using a Palladium/Carbon-Ethylene System. *Adv. Synth. Catal.* **2018,** *360* (17), 3297-3305.

36. Girard, S. A.; Huang, H.; Zhou, F.; Deng, G.-J.; Li, C.-J., Catalytic dehydrogenative aromatization: an alternative route to functionalized arenes. *Org. Chem. Front.* **2015,** *2* (3), 279-287.

37. Qiu, Z.; Lv, L.; Li, J.; Li, C.-C.; Li, C.-J., Direct conversion of phenols into primary anilines with hydrazine catalyzed by palladium. *Chem. Sci.* **2019,** *10* (18), 4775-4781.

38. Maiti, D., Chemoselectivity in the Cu-catalyzed O-arylation of phenols and aliphatic alcohols. *Chem. Commun.* **2011,** *47* (29), 8340-8342.

39. Nejati, K.; Ahmadi, S.; Nikpassand, M.; Kheirollahi Nezhad, P. D.; Vessally, E., Diaryl ethers synthesis: nano-catalysts in carbon-oxygen cross-coupling reactions. *RSC Adv.* **2018,** *8* (34), 19125-19143.

40. Zeng, H.; Qiu, Z.; Domínguez-Huerta, A.; Hearne, Z.; Chen, Z.; Li, C.-J., An Adventure in Sustainable Cross-Coupling of Phenols and Derivatives via Carbon–Oxygen Bond Cleavage. *ACS Catal.* **2017,** *7* (1), 510-519.

41. Chen, Z.; Zeng, H.; Girard, S. A.; Wang, F.; Chen, N.; Li, C.-J., Formal Direct Cross-Coupling of Phenols with Amines. *Angew. Chem. Int. Ed.* **2015,** *54* (48), 14487-14491.

42. Qiu, Z.; Li, J.-S.; Li, C.-J.; Li, J.-S., Formal aromaticity transfer for palladium-catalyzed coupling between phenols and pyrrolidines/indolines. *Chem. Sci.* **2017,** *8* (10), 6954-6958.

43. Dominguez-Huerta, A.; Perepichka, I.; Li, C.-J., Catalytic *N*-modification of α-amino acids and small peptides with phenol under bio-compatible conditions. *Commun. Chem.* **2018,** *1* (1), 1-7.

44. Li, J.-S.; Qiu, Z.; Li, C.-J., Palladium-Catalyzed Synthesis of *N*-Cyclohexyl Anilines from Phenols with Hydrazine or Hydroxylamine via N-N/O Cleavage. *Adv. Synth. Catal.* **2017,** *359* (20), 3648-3653.

45. Dobrovolná, Z.; Červený, L., Ammonium formate decomposition using palladium catalyst. *Res. Chem. Intermed.* **2000,** *26* (5), 489-497.

Chapter 6. Summary and closing remarks

Motivated to shift chemistry towards the use of biorenewable starting materials, we envisioned developing a methodology to use phenol and amino acids as coupling partners to form C-N bonds. We have presented the possibility of using 2-cyclohexen-1-one for the *N*-arylation of α-amino acids and phenol for the *N*-cyclohexylation of α-amino acids and peptides. While the *N*-arylation requires high temperatures due to the high energy necessary to aromatize the cyclohexyl ring, the *N*-cyclohexylation was successfully achieved for 17 out of the 20 naturally occurring amino acids under bio-compatible conditions without racemization. Our initial efforts towards applying this methodology for the synthesis of stapled peptides were also studied. Lastly, a methodology for synthesizing diphenylamines with ammonium formate, a stable ammonia source, was established. Seventeen symmetric diarylated amines were synthesized using phenols as arylating reagents and Pd/C as the catalyst. Yields for the reaction ranged from good to excellent, except for severely sterically hindered substrates bearing multiple *ortho* substituents.

Developing safer and more sustainable chemical methodologies is an iterative process, whereby each innovation can improve on the previous state-of-the-art. Thus, while advantages can always be attributed to any given approach, there is still room for improvement. Palladium on charcoal has proven to be an effective catalyst for reducing and rearomatizing phenols. Rearomatization necessarily requires high temperatures and hydrocarbon solvents to proceed; however, the reduction can occur at room temperature in aqueous conditions. The retention of activity and stability of Pd/C in water is remarkable for a heterogeneous catalyst, especially if this methodology is later adapted for the valorization of lignin. The heterogeneous nature of Pd/C made it ideal for catalyst recyclability. However, undeniable challenges such as mass transfer, dispersion, and chemisorption to determine the available number of active sites remain to be addressed. This proved especially troublesome when proteins were tested as substrates. While one alternative to this problem could be the use of miniproteins or globular proteins with a side-chain to increase the local concentration of the catalyst at the desired site, it might be better to circumvent this problem altoghether by the investigation of other catalysts. In this regard, the development of water-tolerant homogeneous or heterogeneous catalysts with an improved pore structure to promote mass transfer becomes crucial. A complementary alternative to homogenous catalysts comes from the potential development of versatile ionic liquids, which could successfully promote the reaction.

Alternatively, the use of light for the activation of C-H bonds could prove extremely compelling. Solving these challenges becomes increasingly relevant as more complex substrates, such as lignin, are targeted. Given that we chose phenol as a model compound, subsequent methodologies could look into using more robust substrates to strike a fairer balance between synthetic efforts and lignocellulose fidelity.

The use of sodium formate as a hydrogen donor and ammonium formate as both the hydrogen donor and the nitrogen source presents a safe alternative for research and development laboratories, as it circumvents the need for the manipulation of both hydrogen gas and ammonia. The next improvement in lignin valorization may involve designing a hydrogen transfer system that could benefit from using lignin itself as the hydrogen source. This self-production would result in a high atom economy and would entirely remove desalination challenges upon reaction completion.

While simple innovations can be readily adopted on a short timescale, more profound innovation can have more economical and sustainable implications. Herein, we have reported three novel methodologies that shift from traditional chemistry, in the sense that they do not part from highly reduced starting materials' functionalization. Instead, they harness phenol’s intrinsic functionality. Furthermore, phenols can be found as monomers of naturally abundant lignocellulose. Some of the reactions reported in this thesis have already been adopted by other research groups, highlighting their utility. Finally, it is worth noting that while scientists might understand and accept this notion of continual improvement, it might confuse the general population, who often prefer definite answers. Based on this, I find it essential that scientists take a more active role in explaining emerging developments in their fields while becoming implicated in developing science-based policies or overlooking these processes' industrial implementation. Personally, I have also learned a lot from the development of these methodologies and hope other people will have as much growth shall they take it upon themselves to continue with the work presented herein.

Appendix 1. NMR Spectral Data for Chapter 2

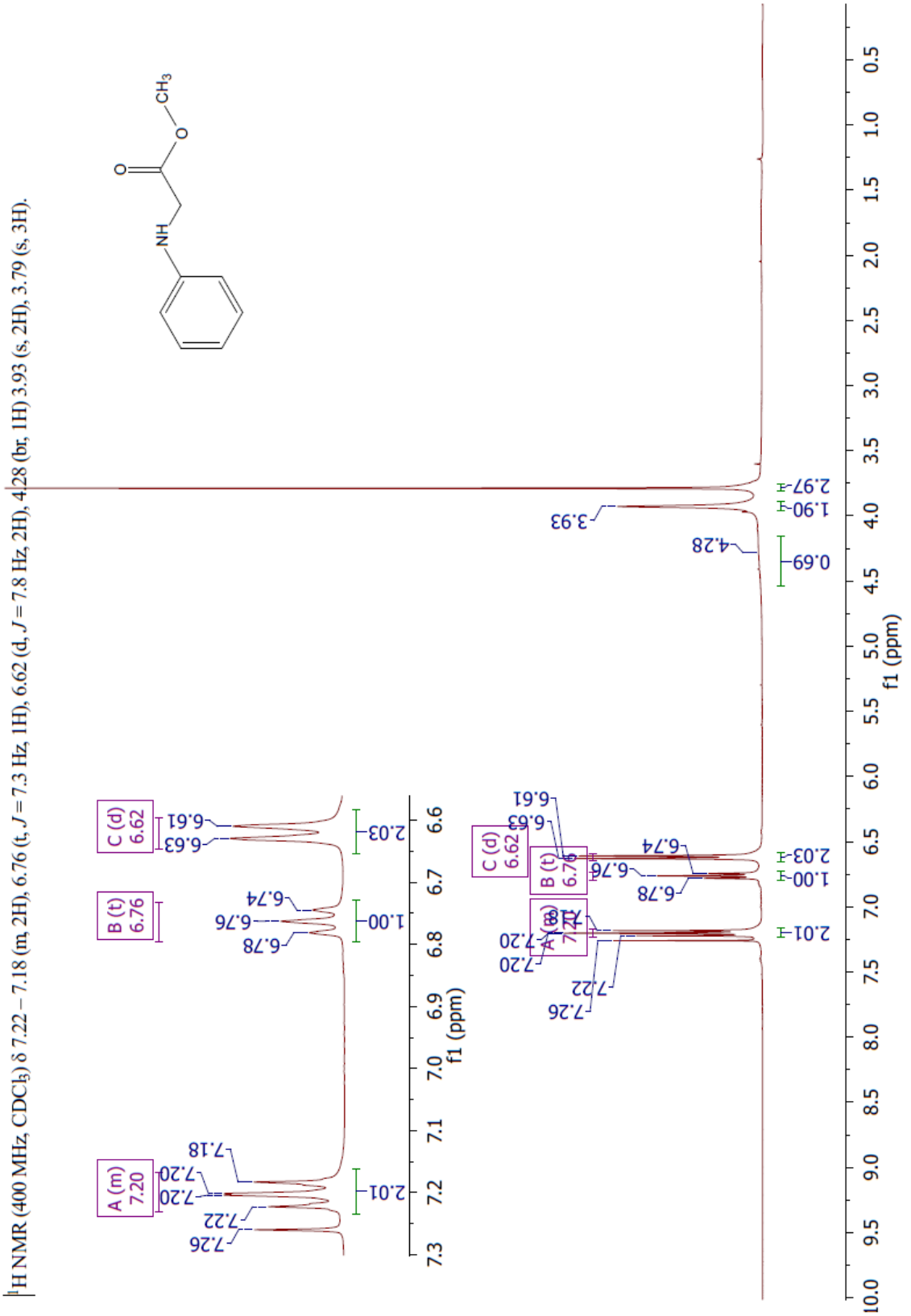

Figure 1. ^{1}H NMR spectra for compound **3**

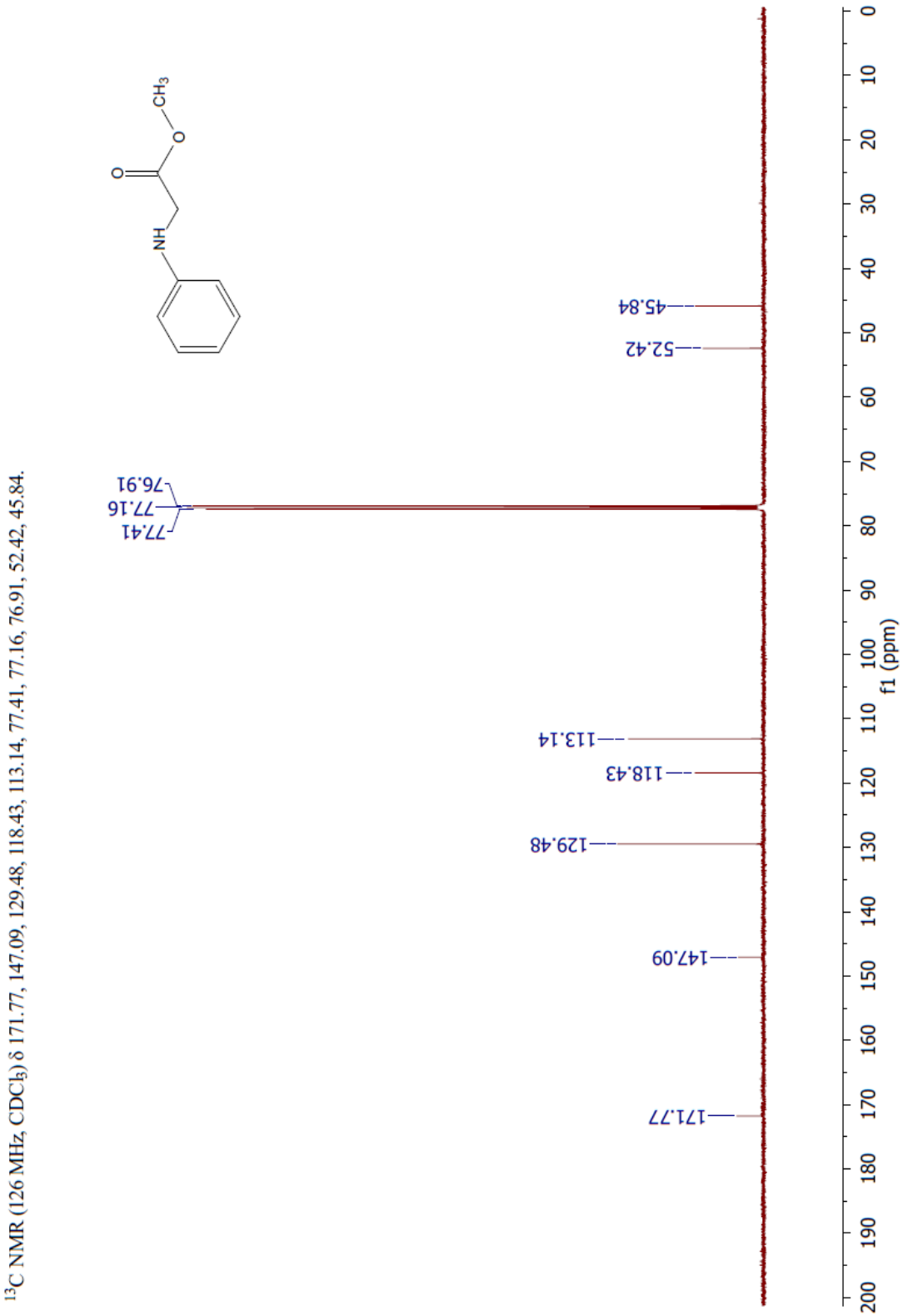

Figure 2. ^{13}C NMR spectra for compound **3**

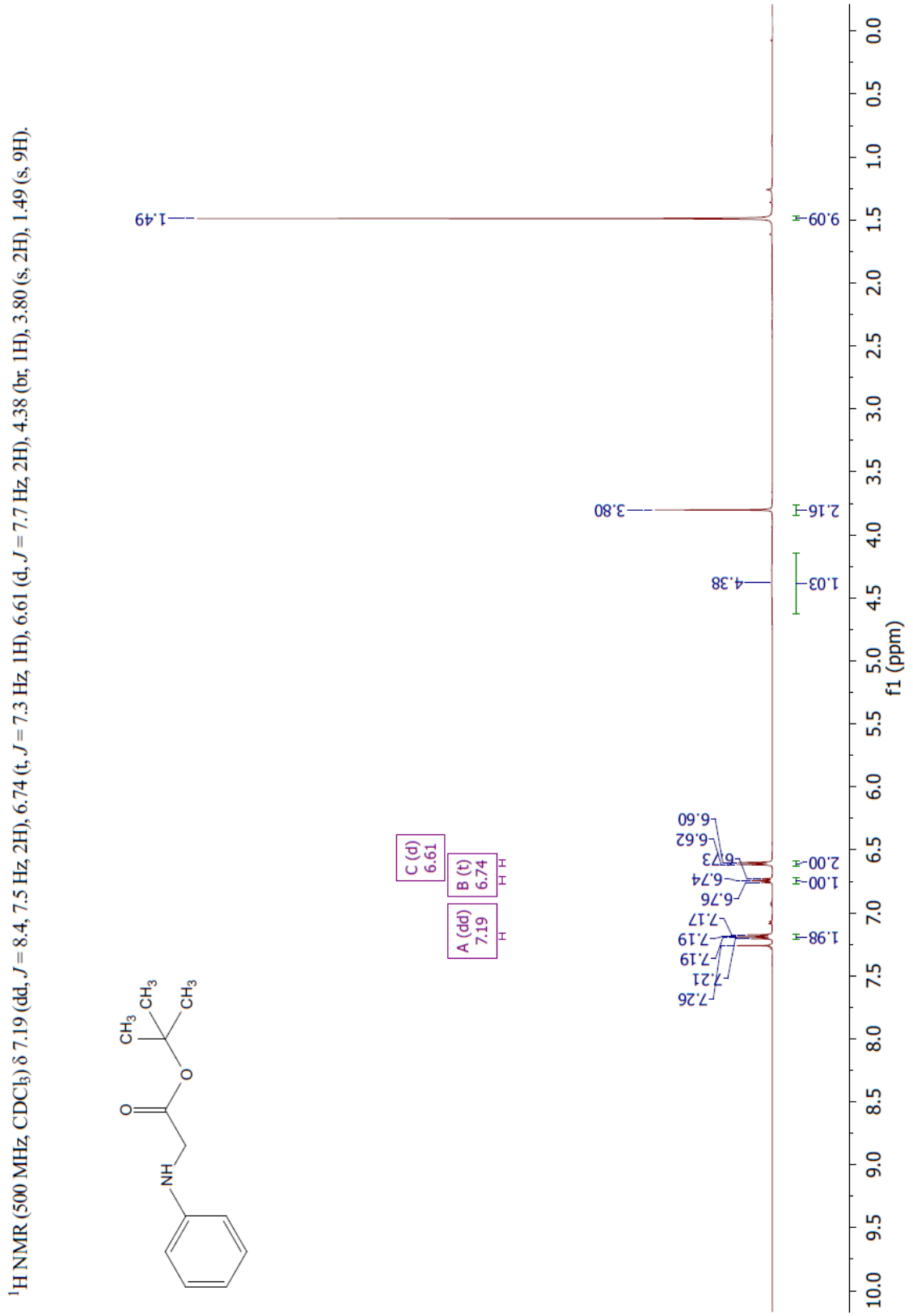

Figure 3. ^{1}H NMR spectra for compound **3a**

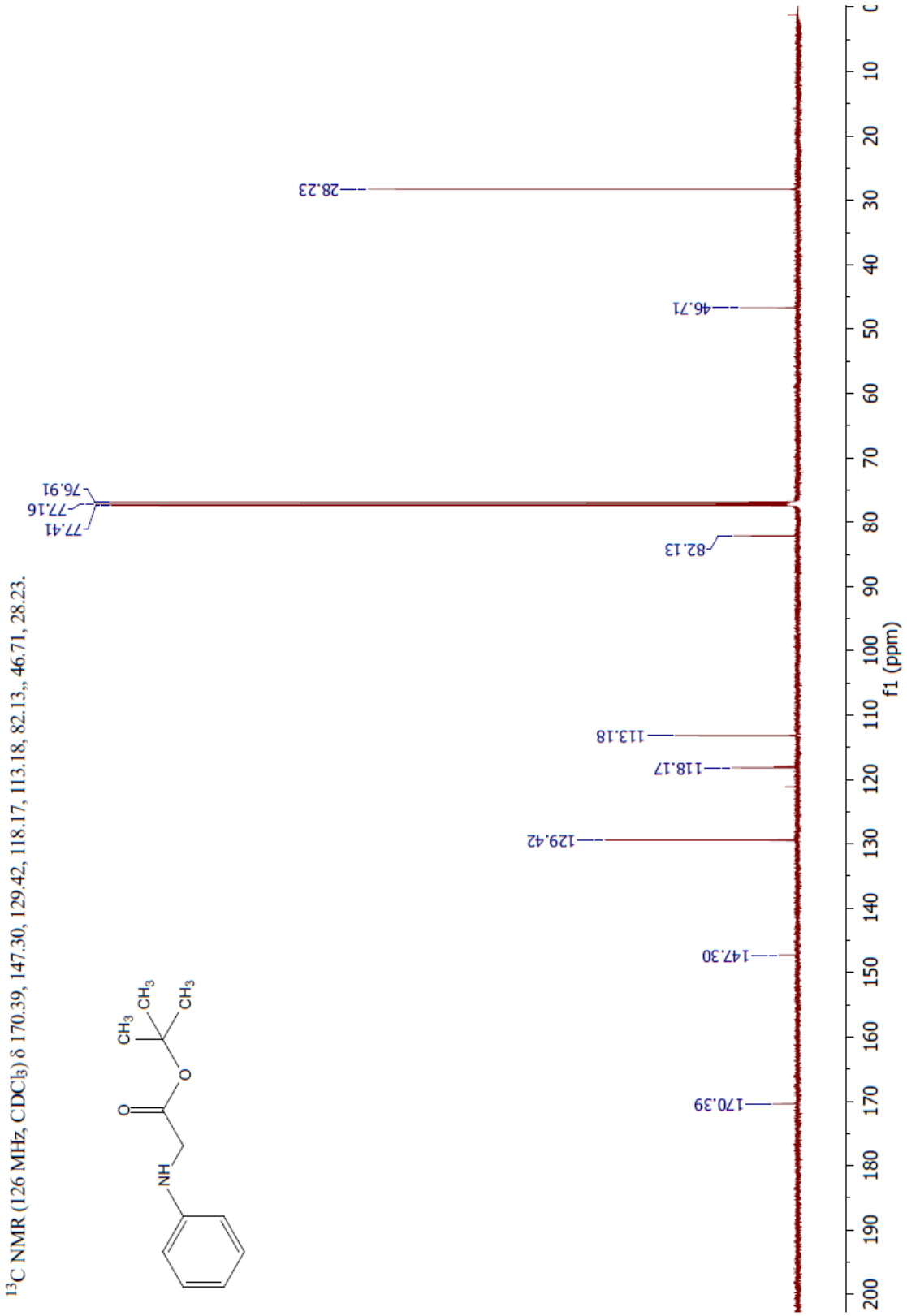

Figure 4. ^{13}C NMR spectra for compound **3a**

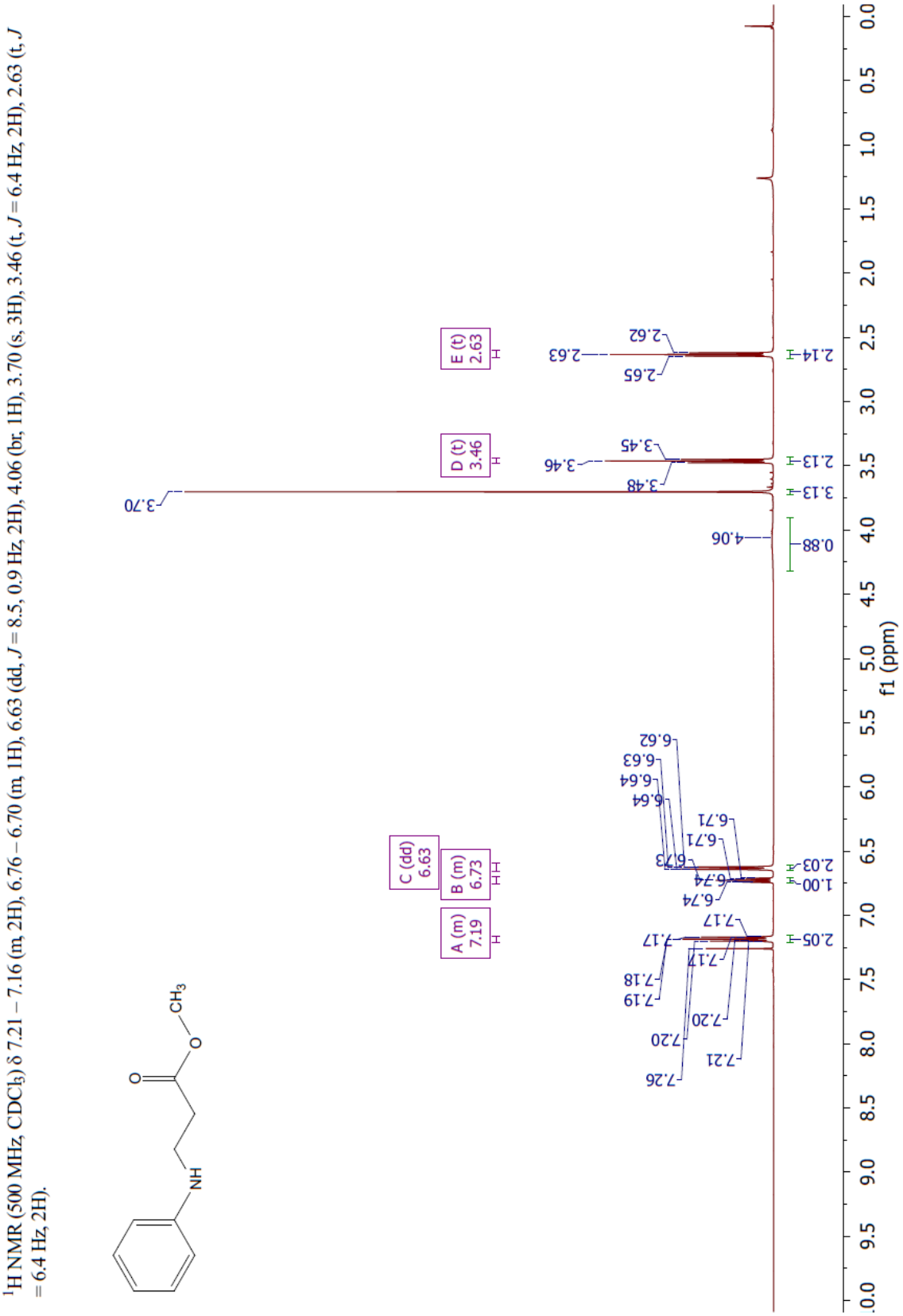

Figure 5. ^{1}H NMR spectra for compound **3b**

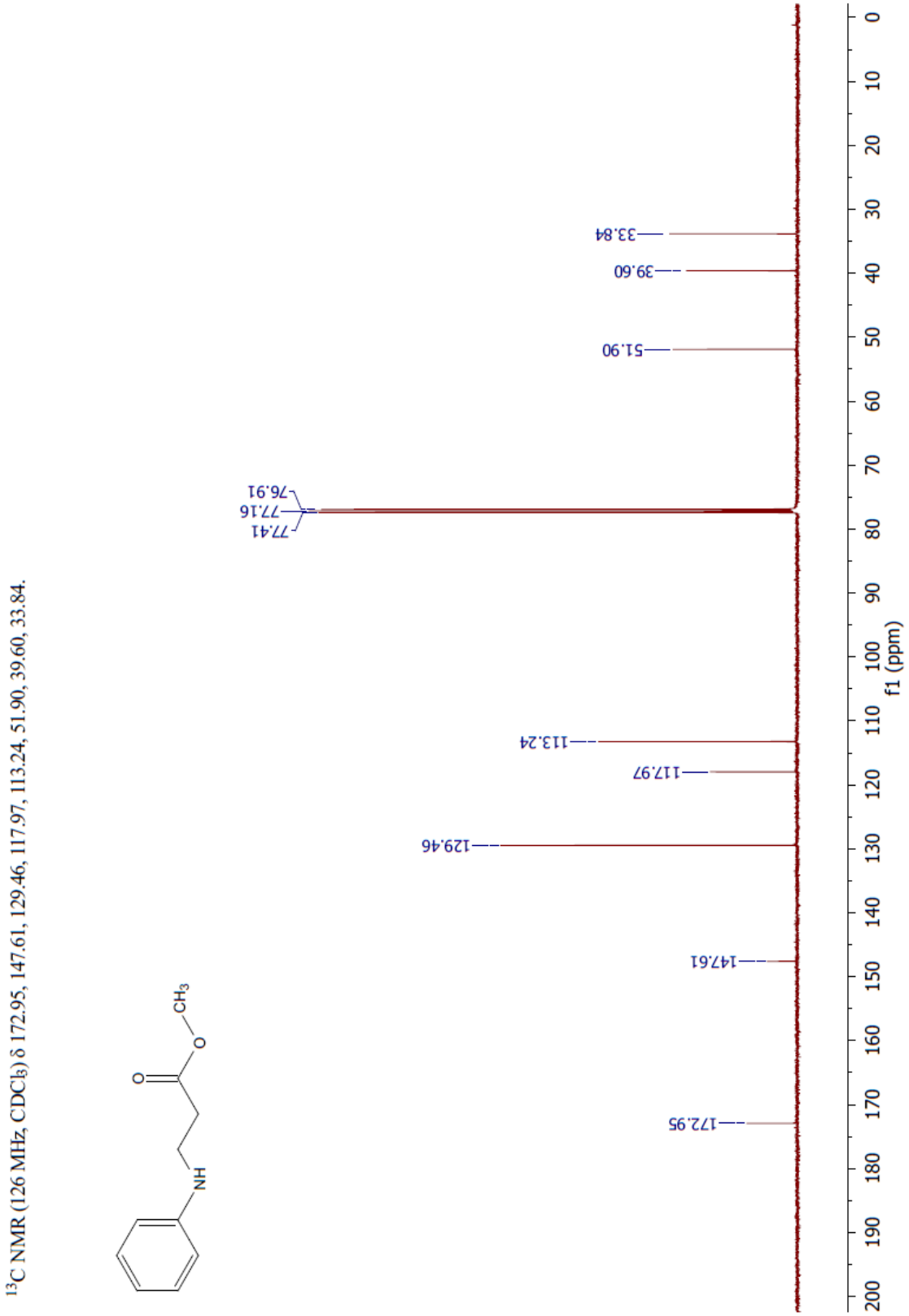

Figure 6. ^{13}C NMR spectra for compound **3b**

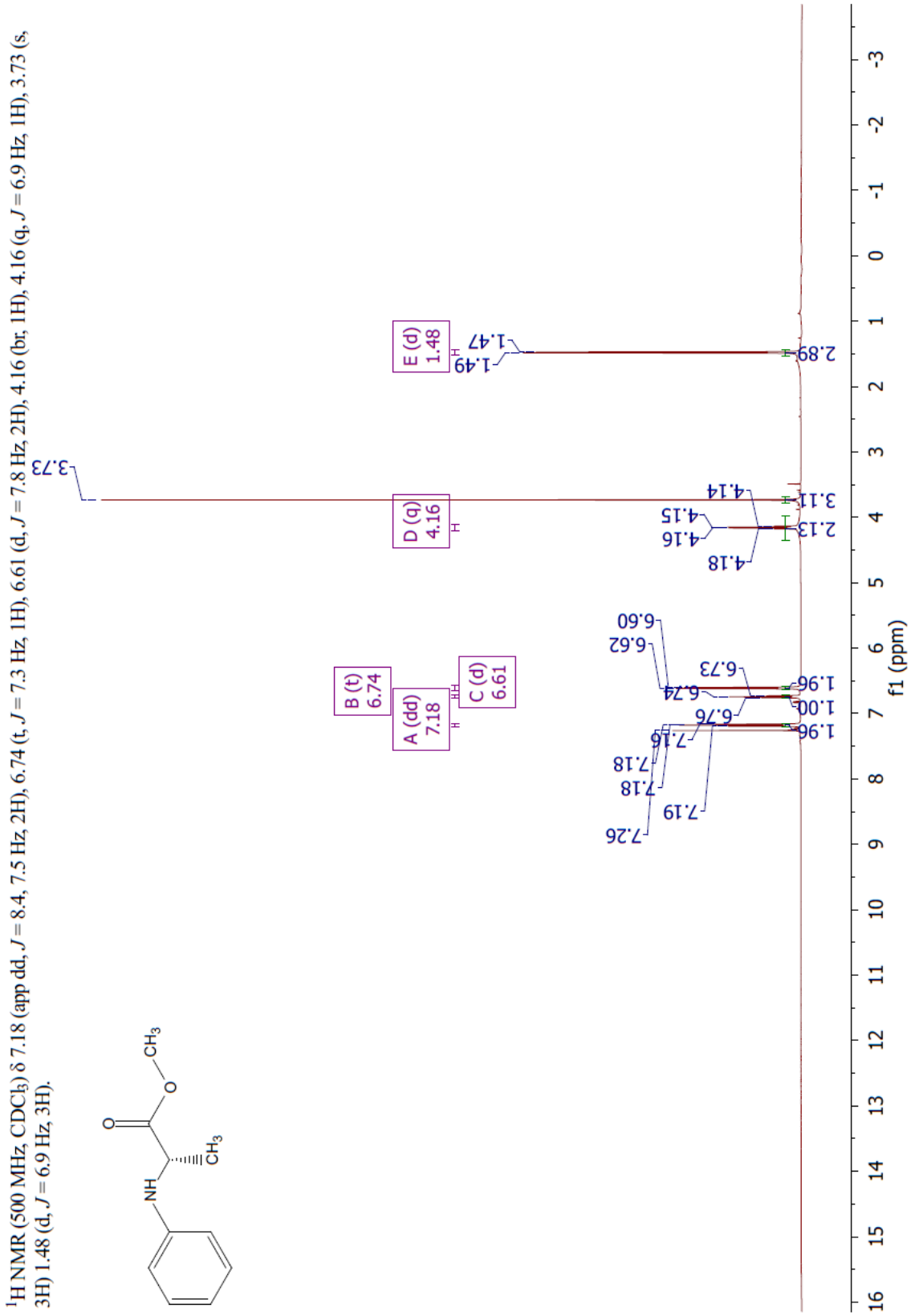

Figure 7. ^{1}H NMR spectra for compound **3c**

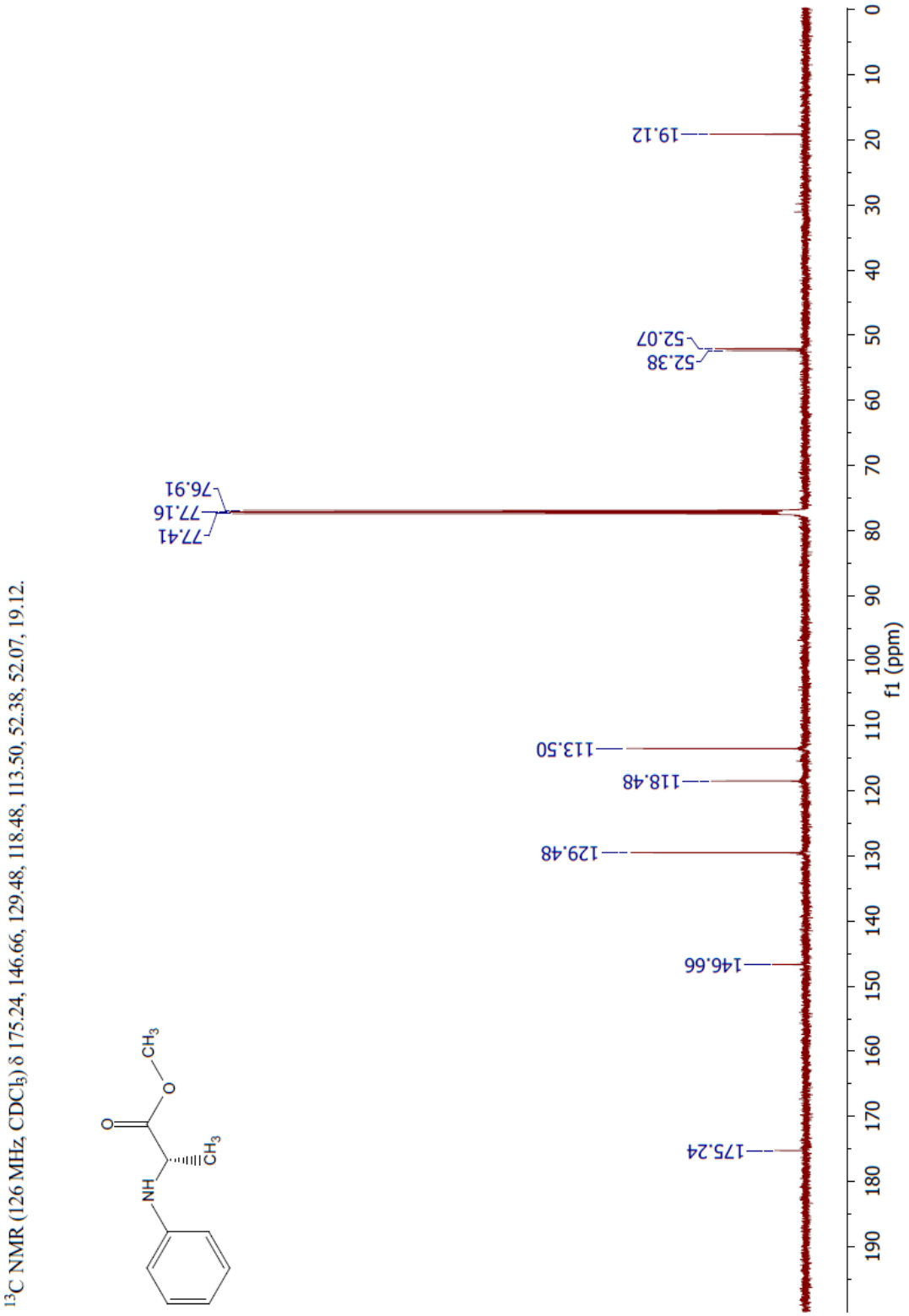

Figure 8. ^{13}C NMR spectra for compound **3c**

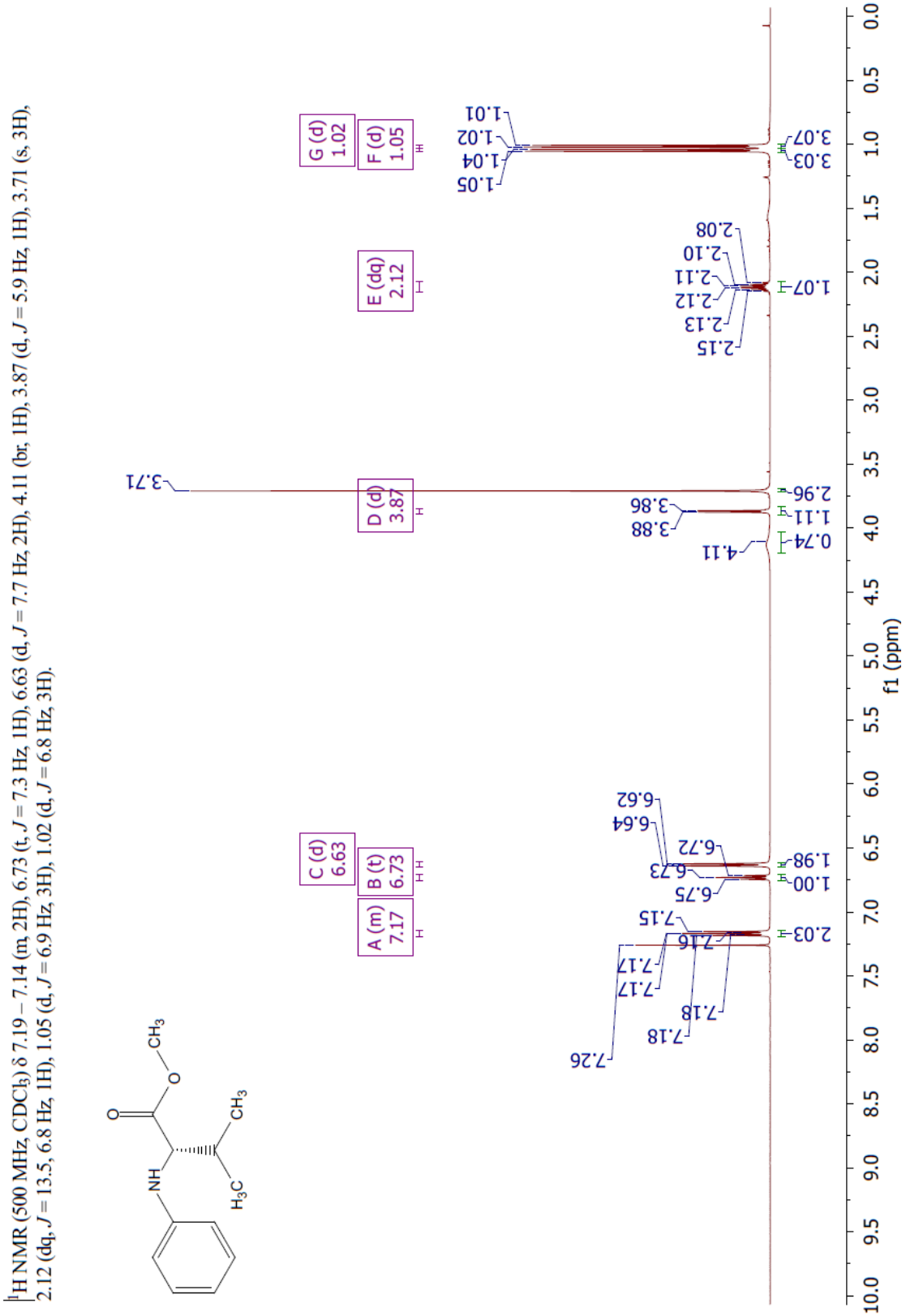

Figure 9. ^{1}H NMR spectra for compound **3d**

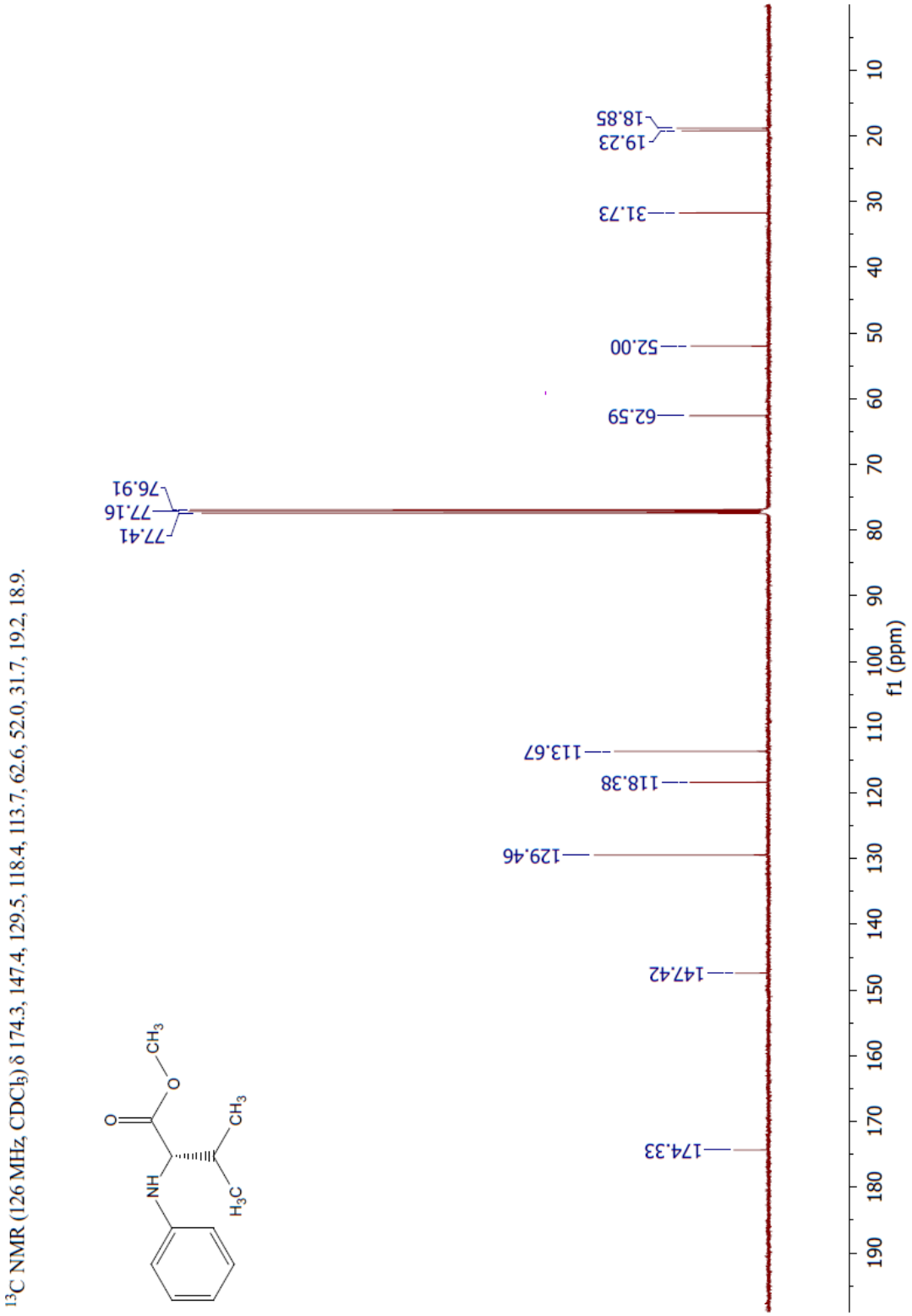

Figure 10. ^{13}C NMR spectra for compound **3d**

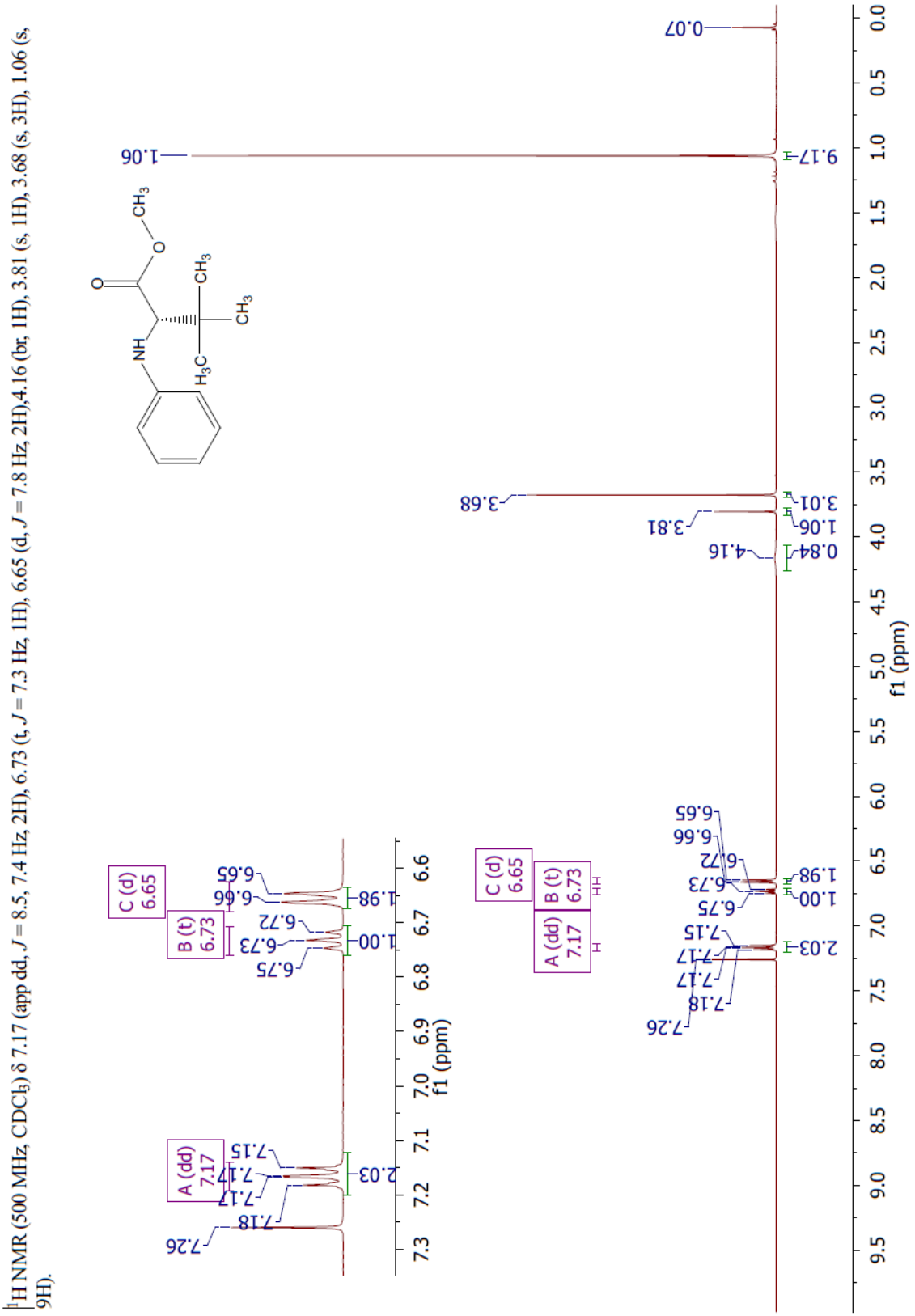

Figure 11. ^{1}H NMR spectra for compound **3e**

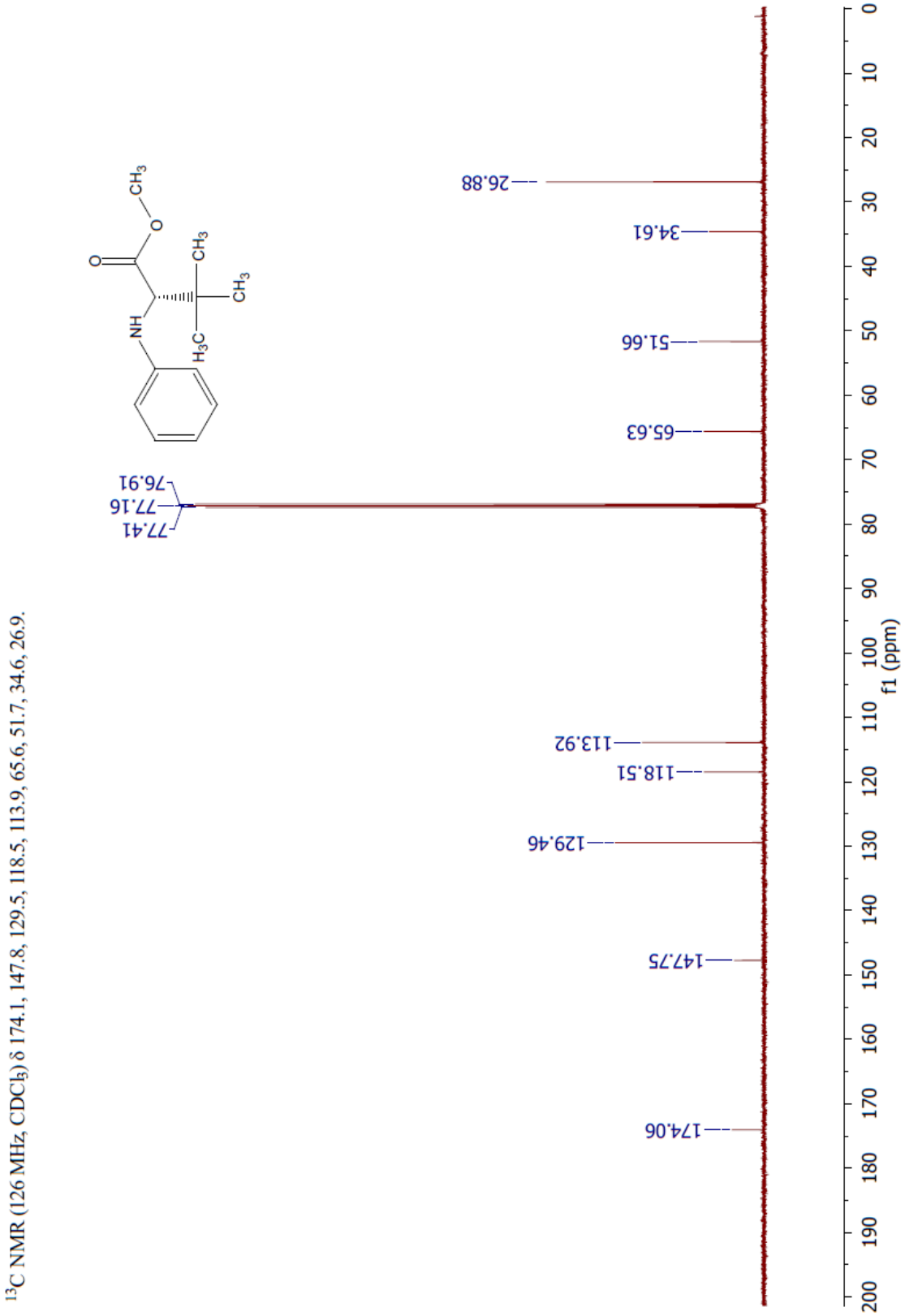

Figure 12. ^{13}C NMR spectra for compound **3e**

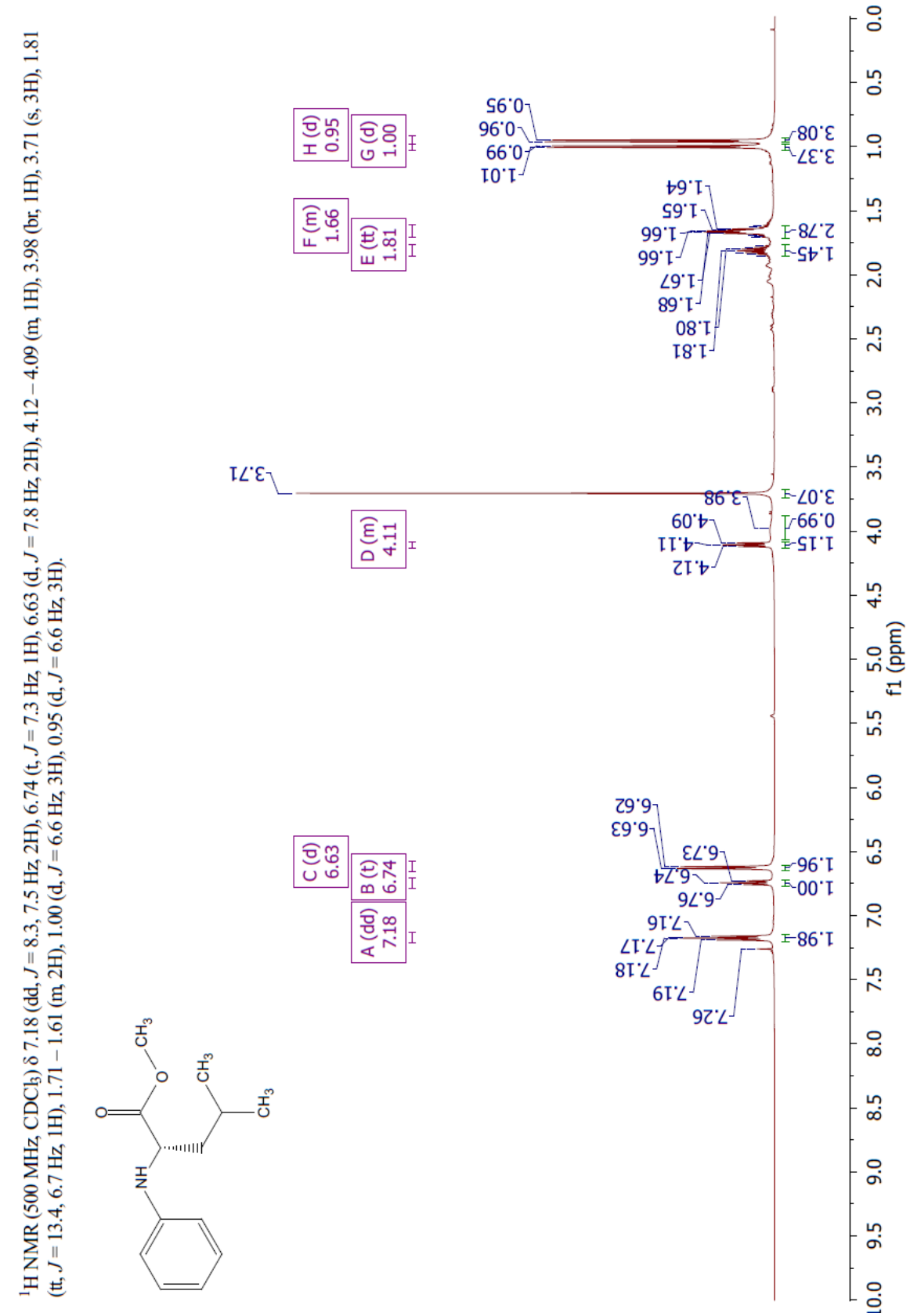

Figure 13. ^{1}H NMR spectra for compound **3f**

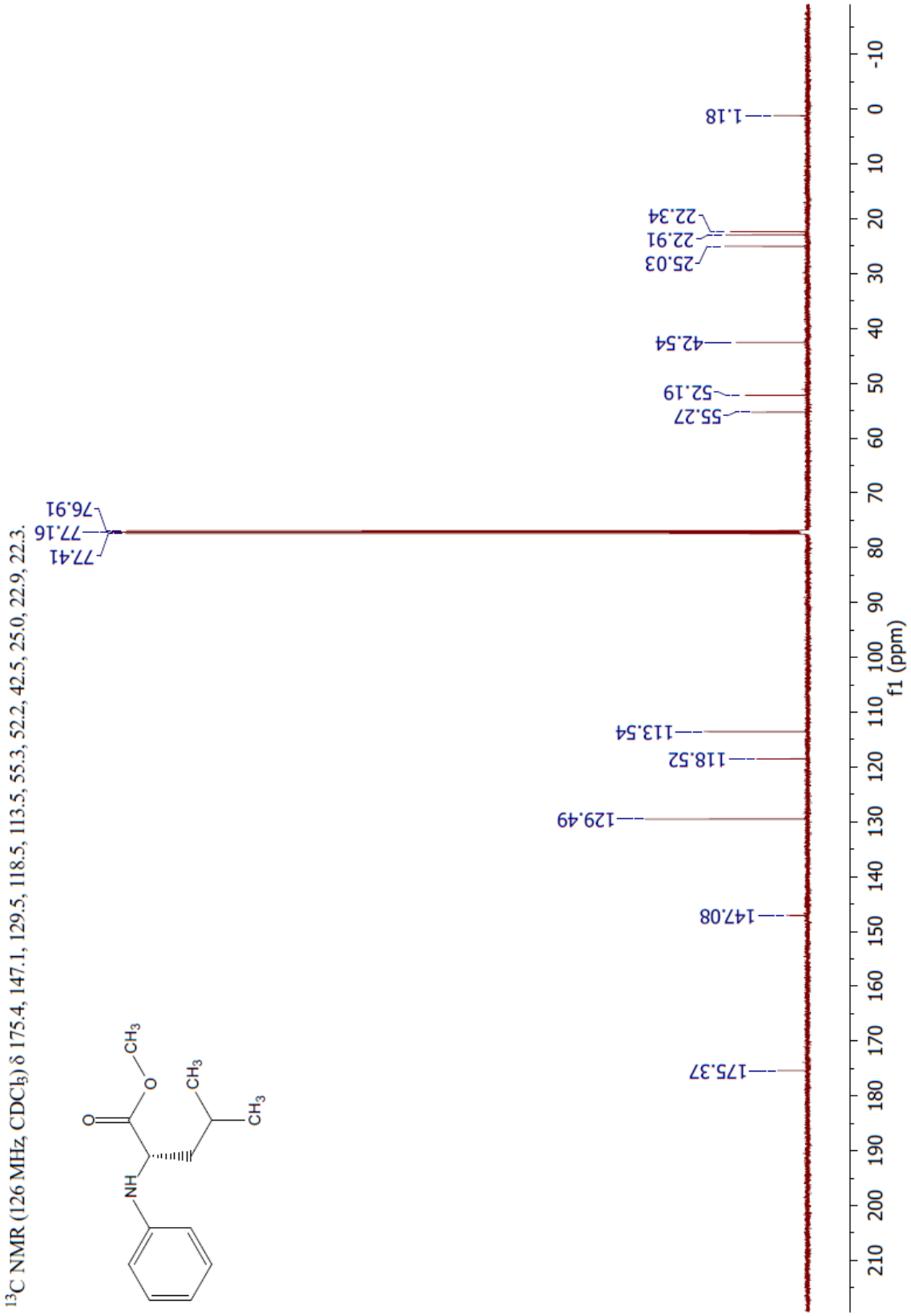

Figure 14. ^{13}C NMR spectra for compound **3f**

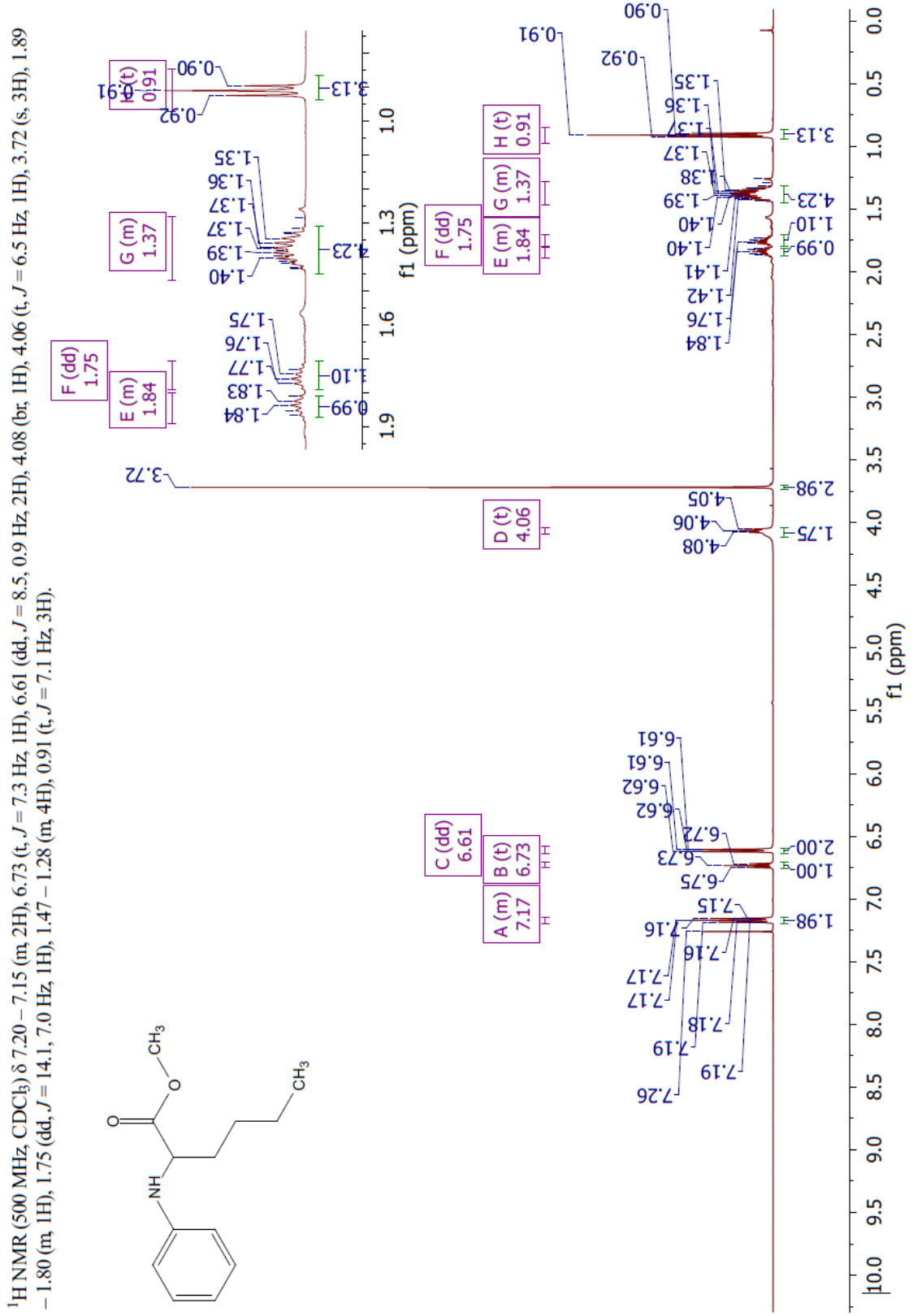

Figure 15. ^{1}H NMR spectra for compound **3g**

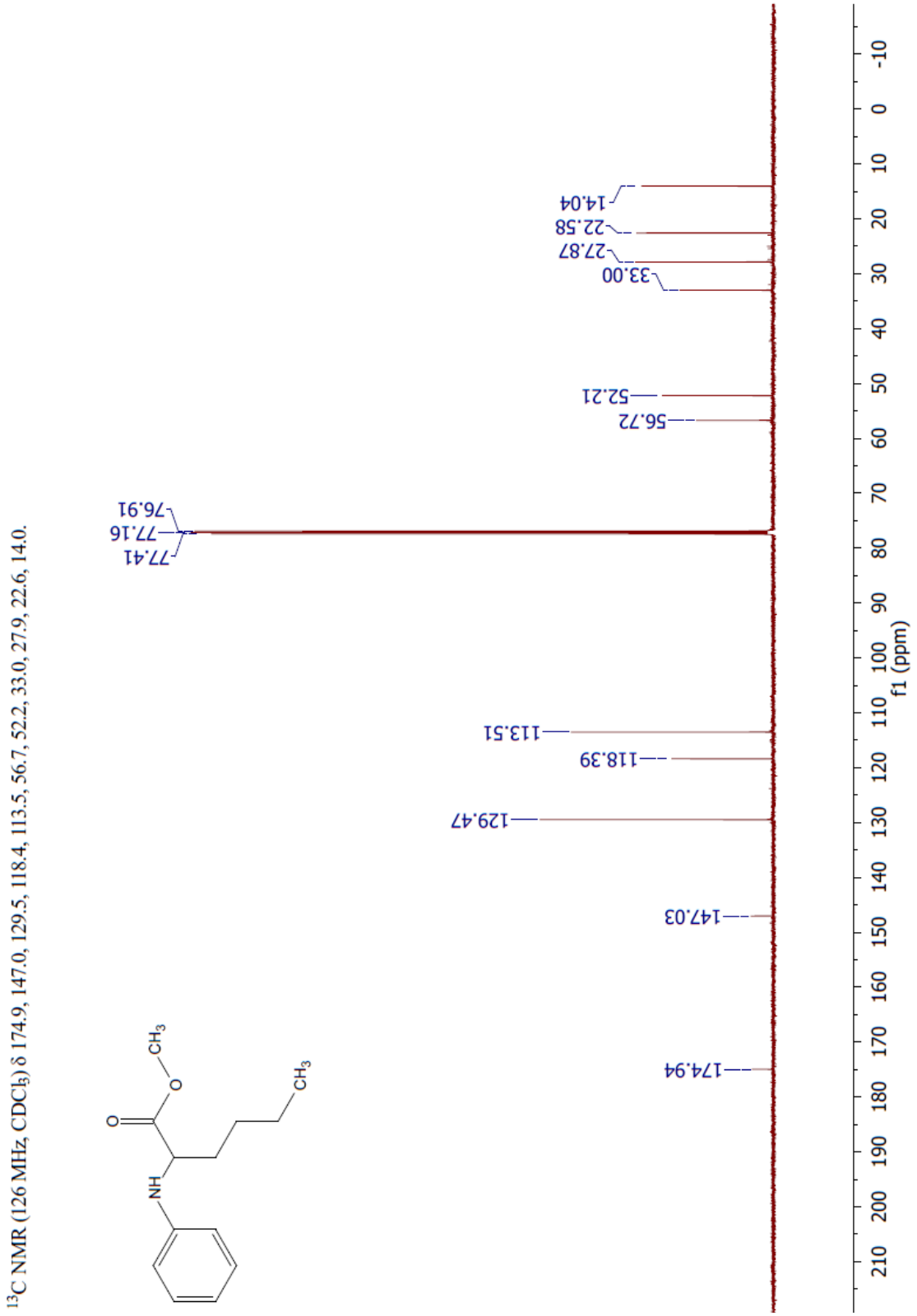

Figure 16. ^{13}C NMR spectra for compound **3g**

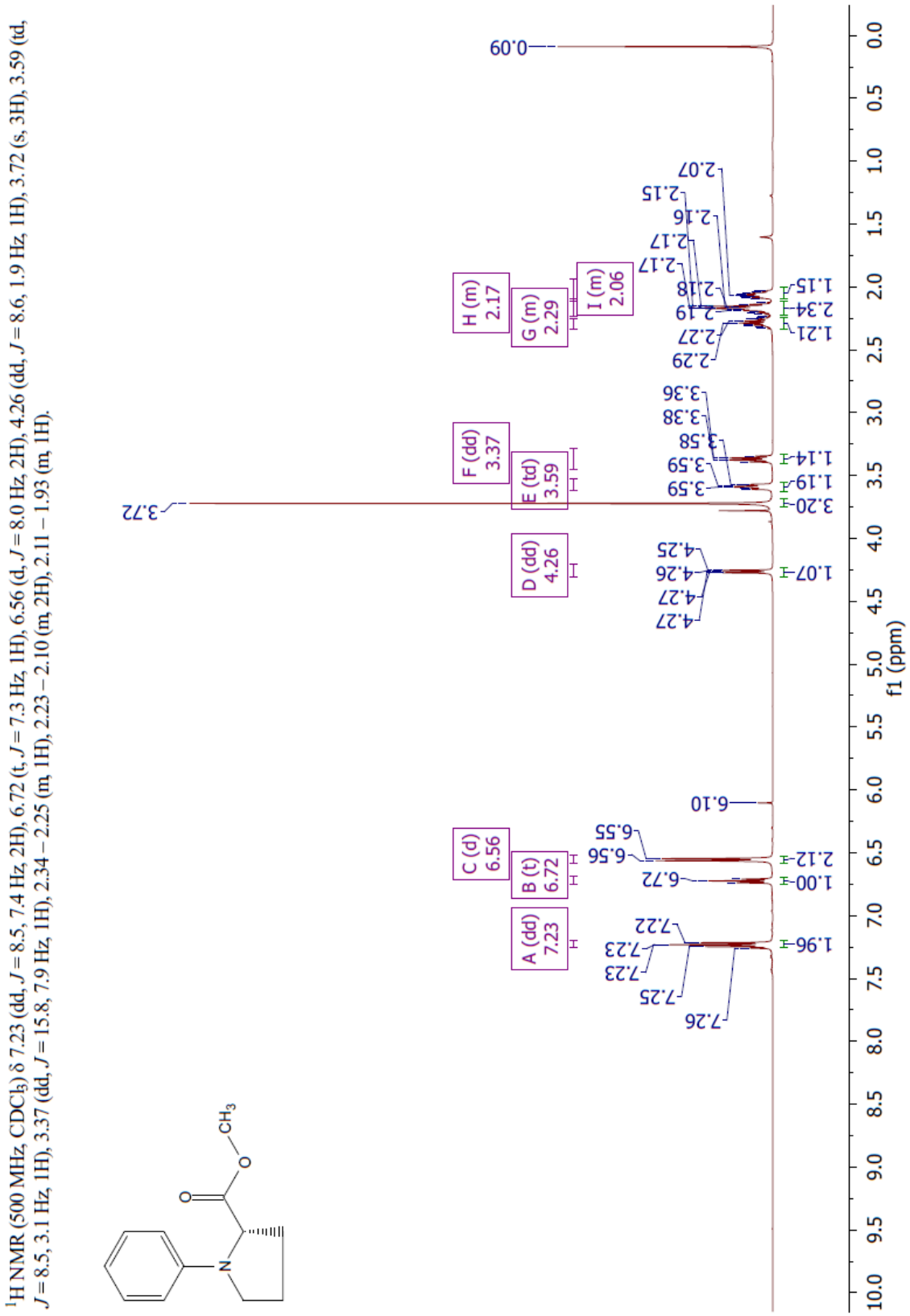

Figure 17. ^{1}H NMR spectra for compound **3h**

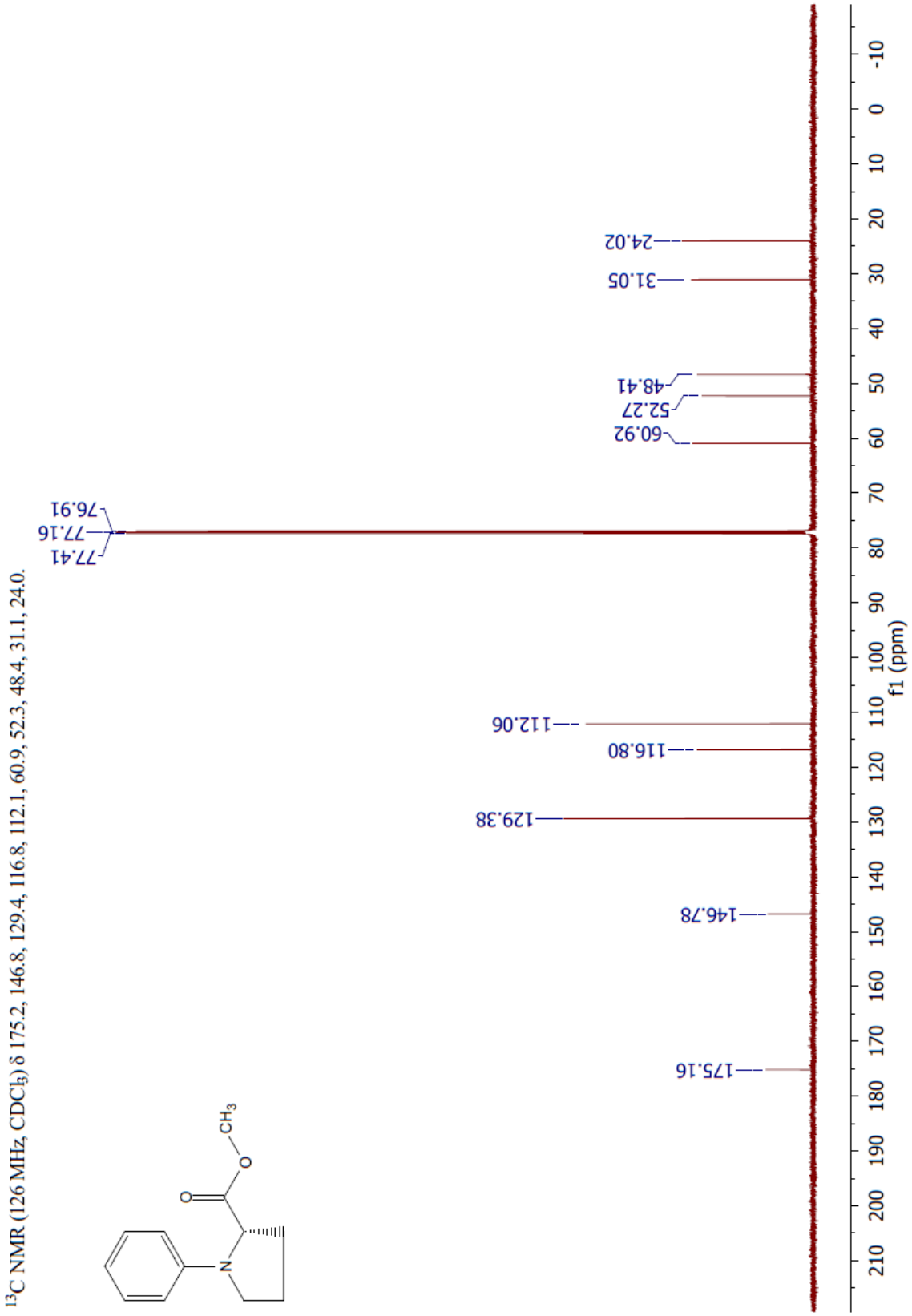

Figure 18. ^{13}C NMR spectra for compound **3h**

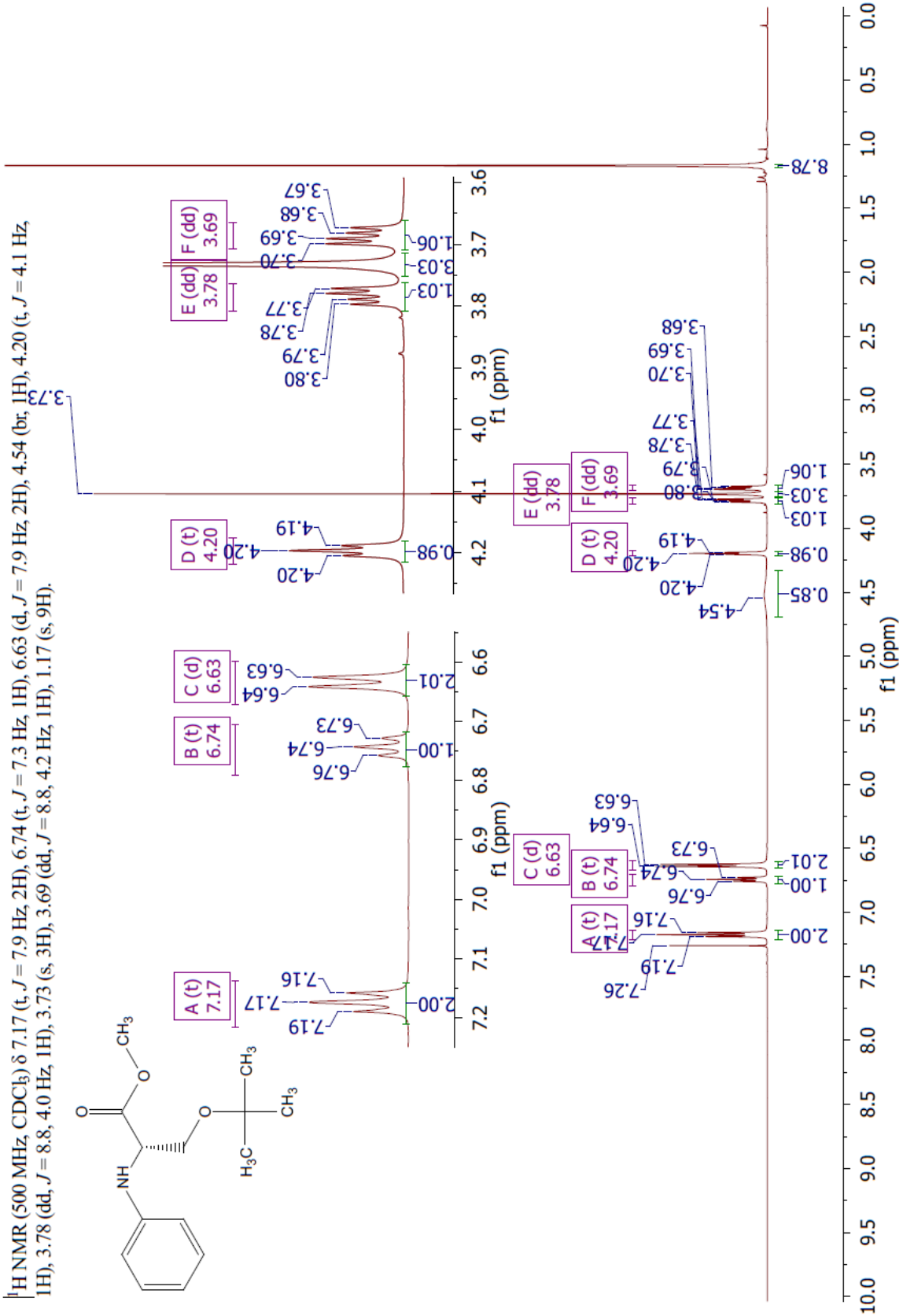

Figure 19. ^{1}H NMR spectra for compound **3i**

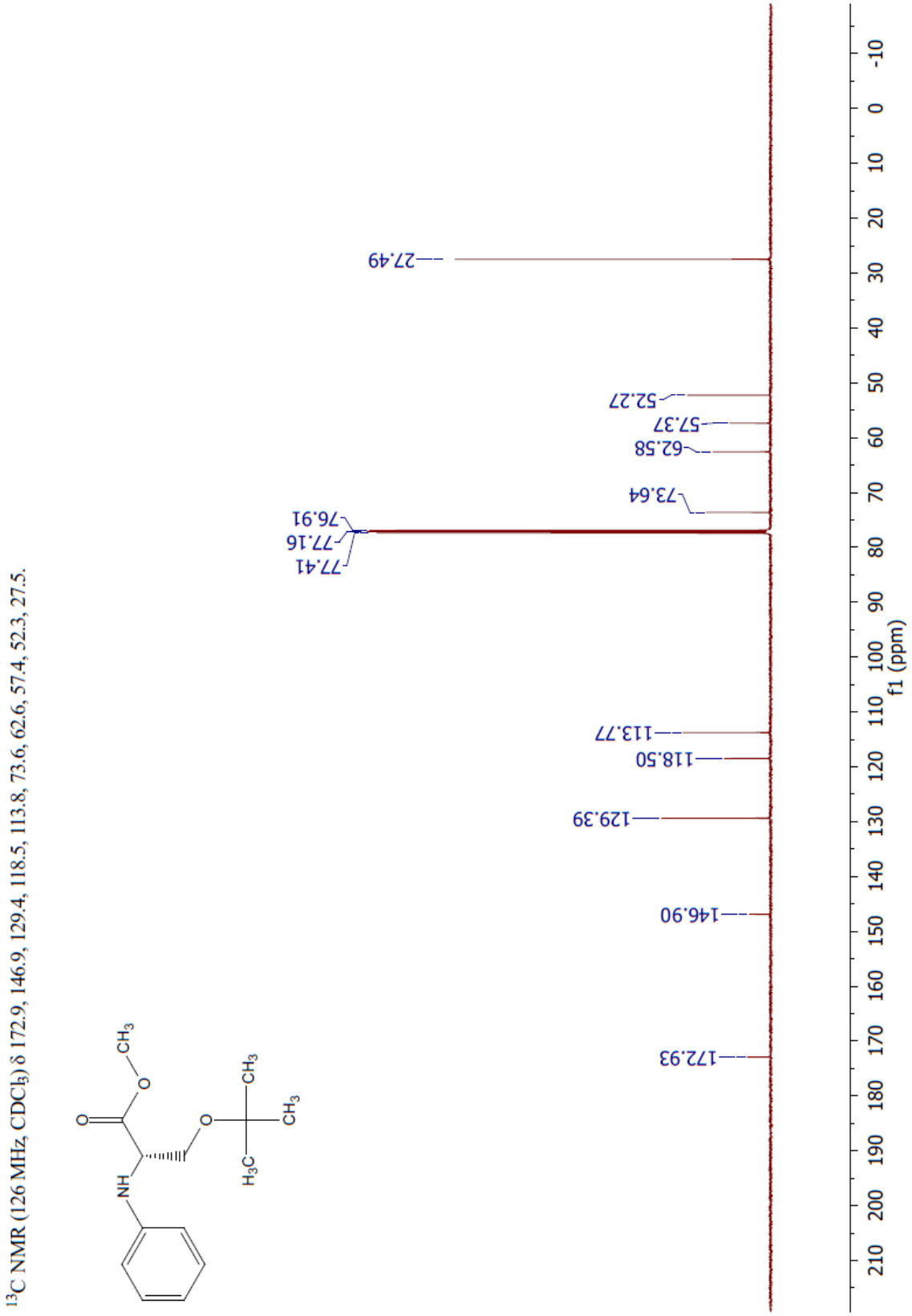

Figure 20. ^{13}C NMR spectra for compound **3i**

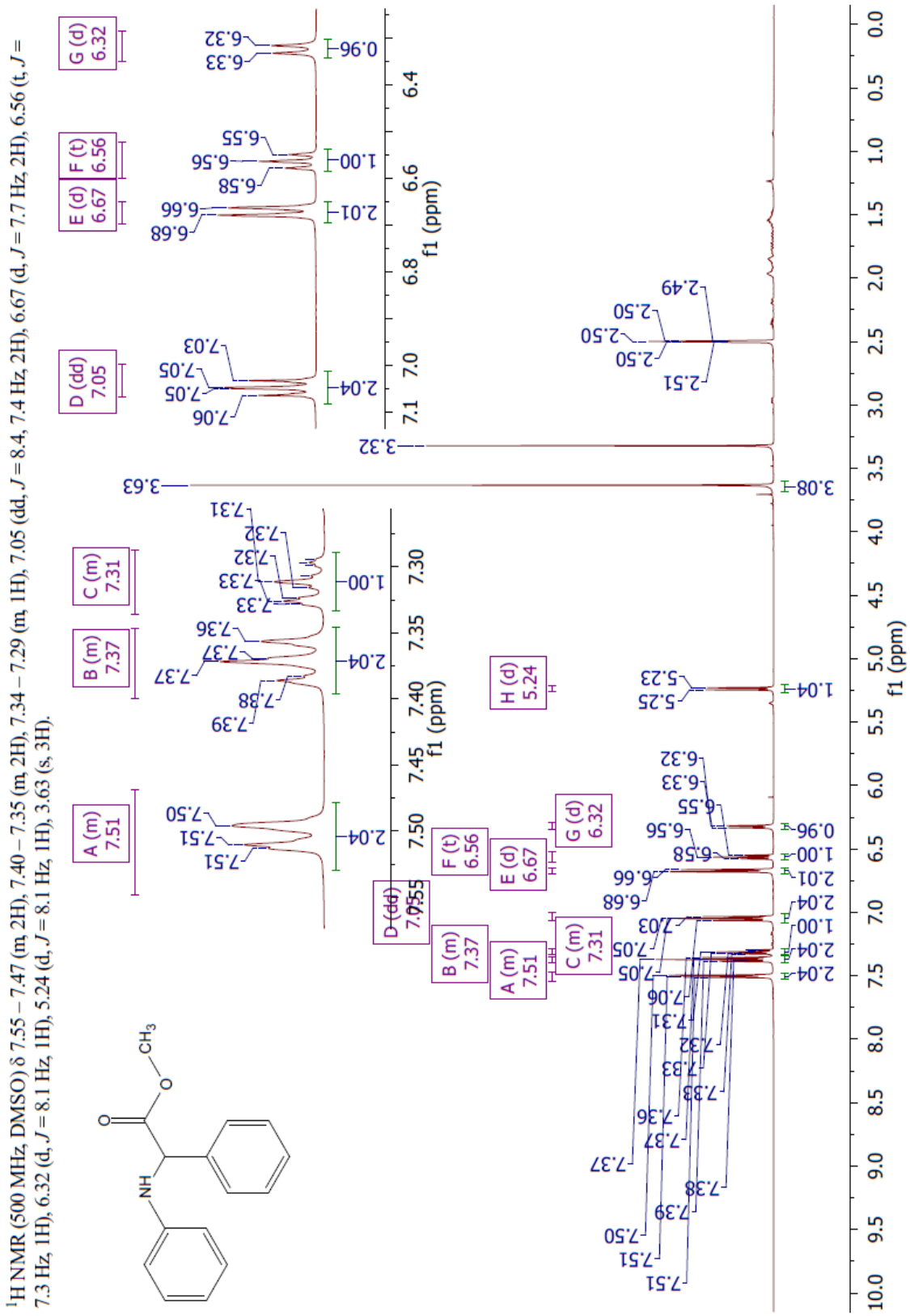

Figure 21. ^{1}H NMR spectra for compound **3j**

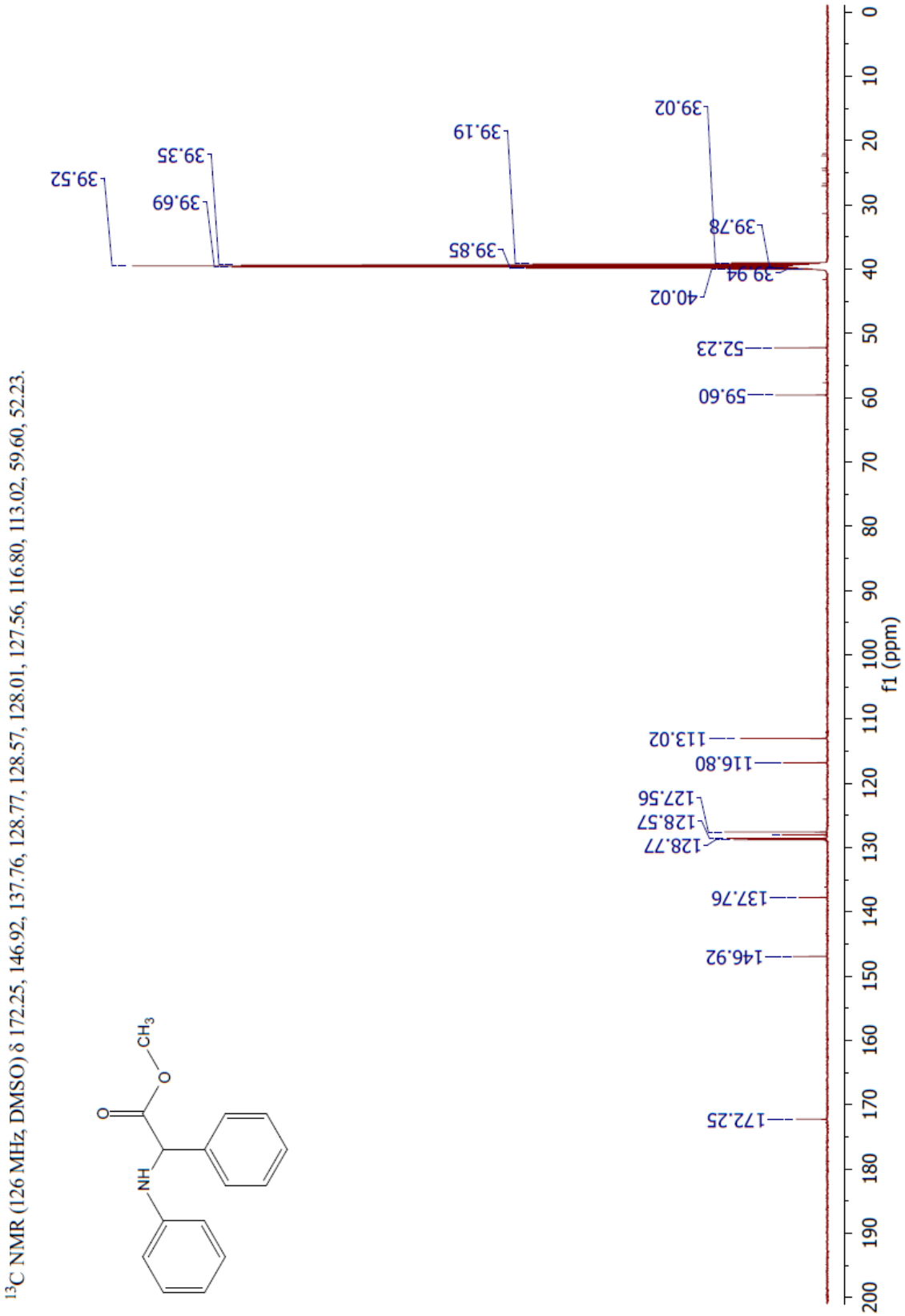

Figure 22. ^{13}C NMR spectra for compound **3j**

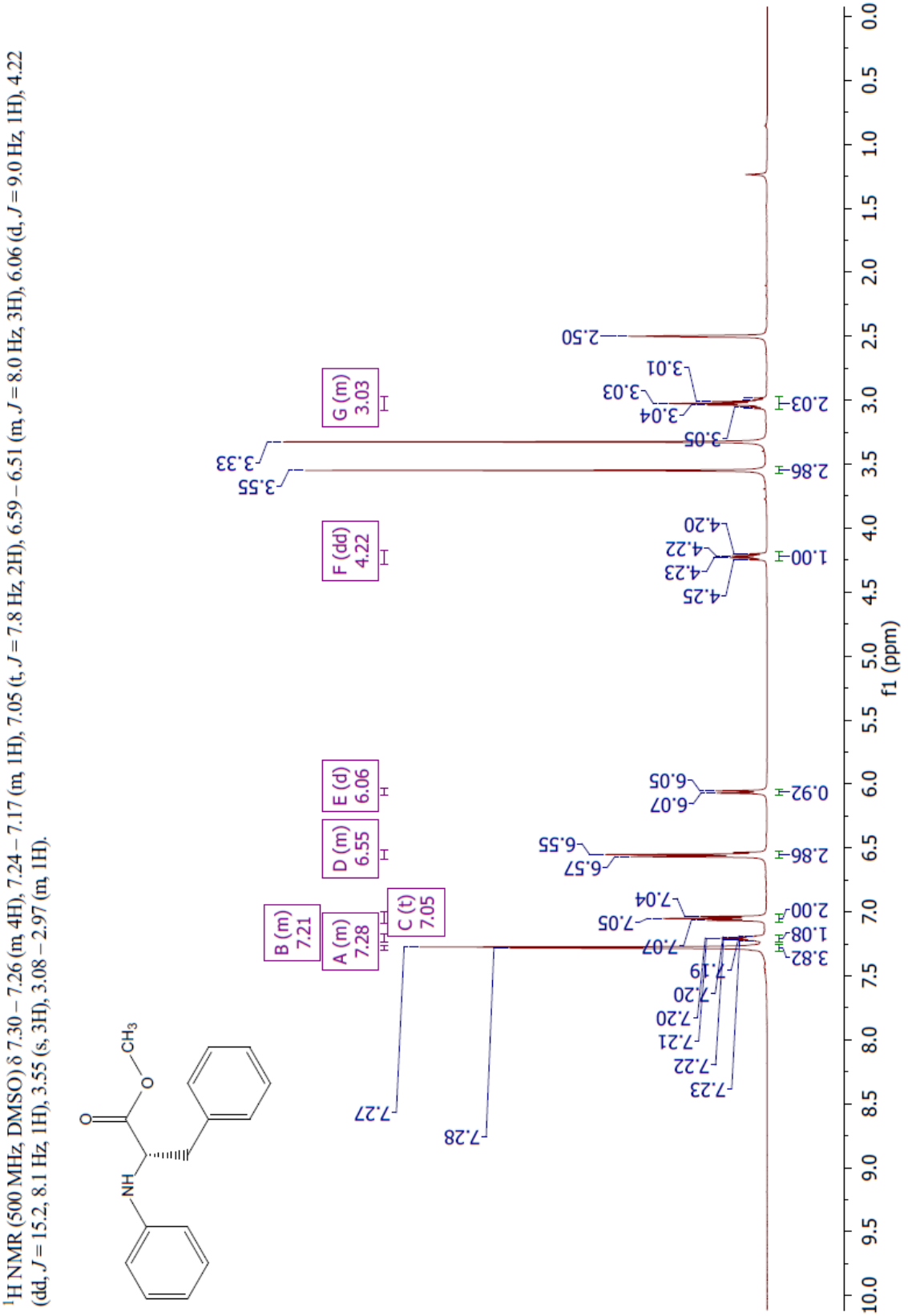

Figure 23. ^{1}H NMR spectra for compound **3k**

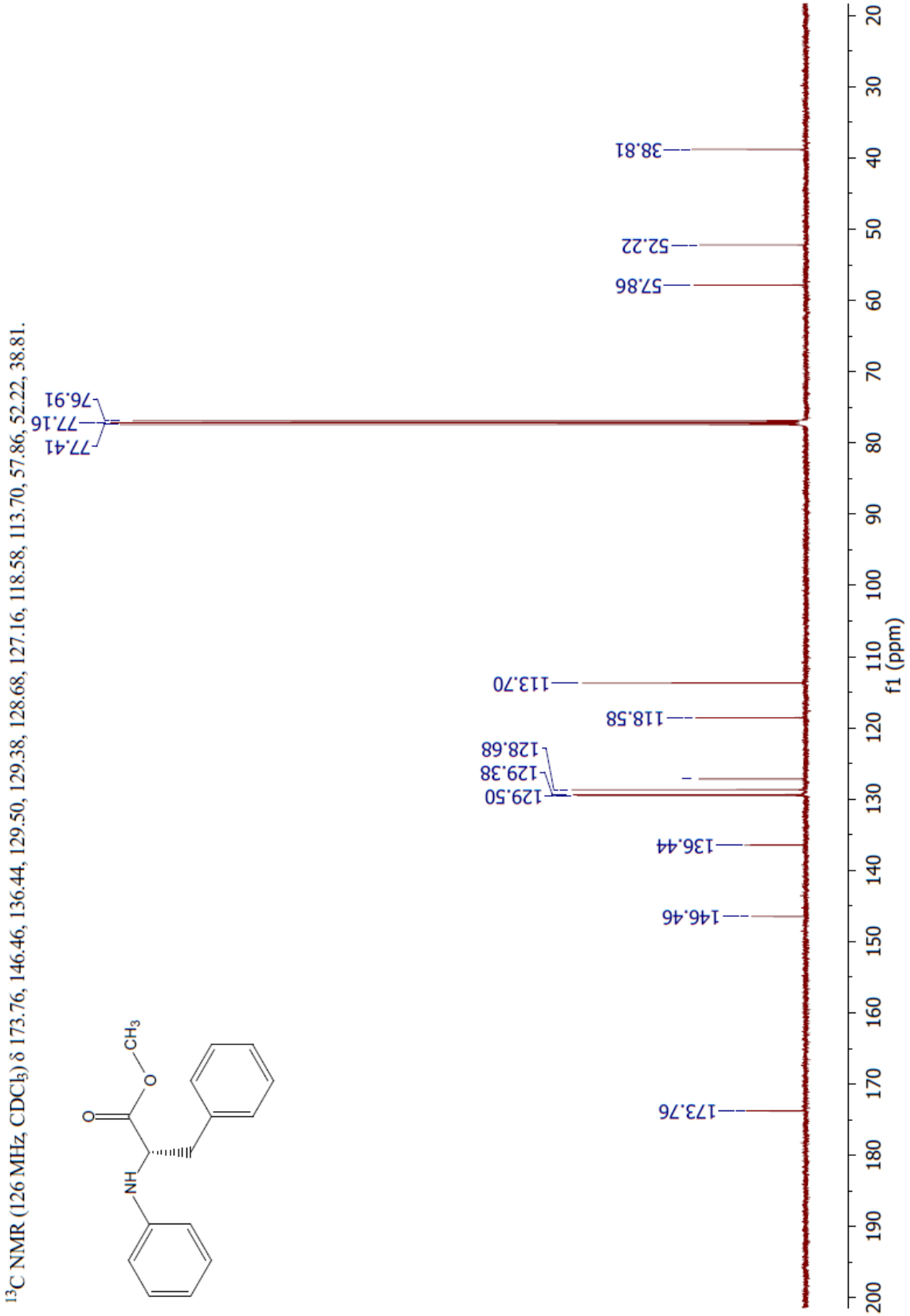

Figure 24. ^{13}C NMR spectra for compound **3k**

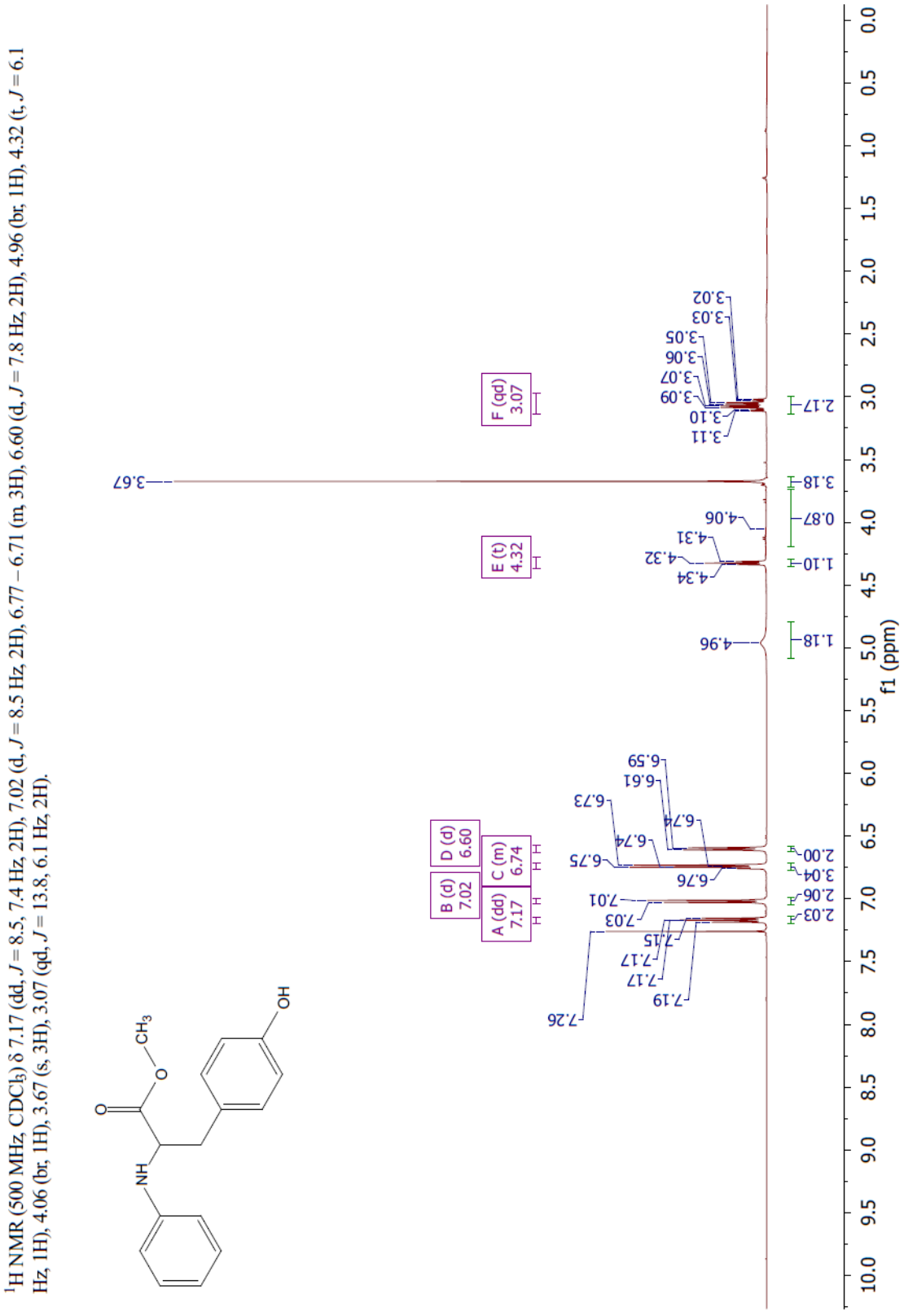

Figure 25. ^{1}H NMR spectra for compound **3l**

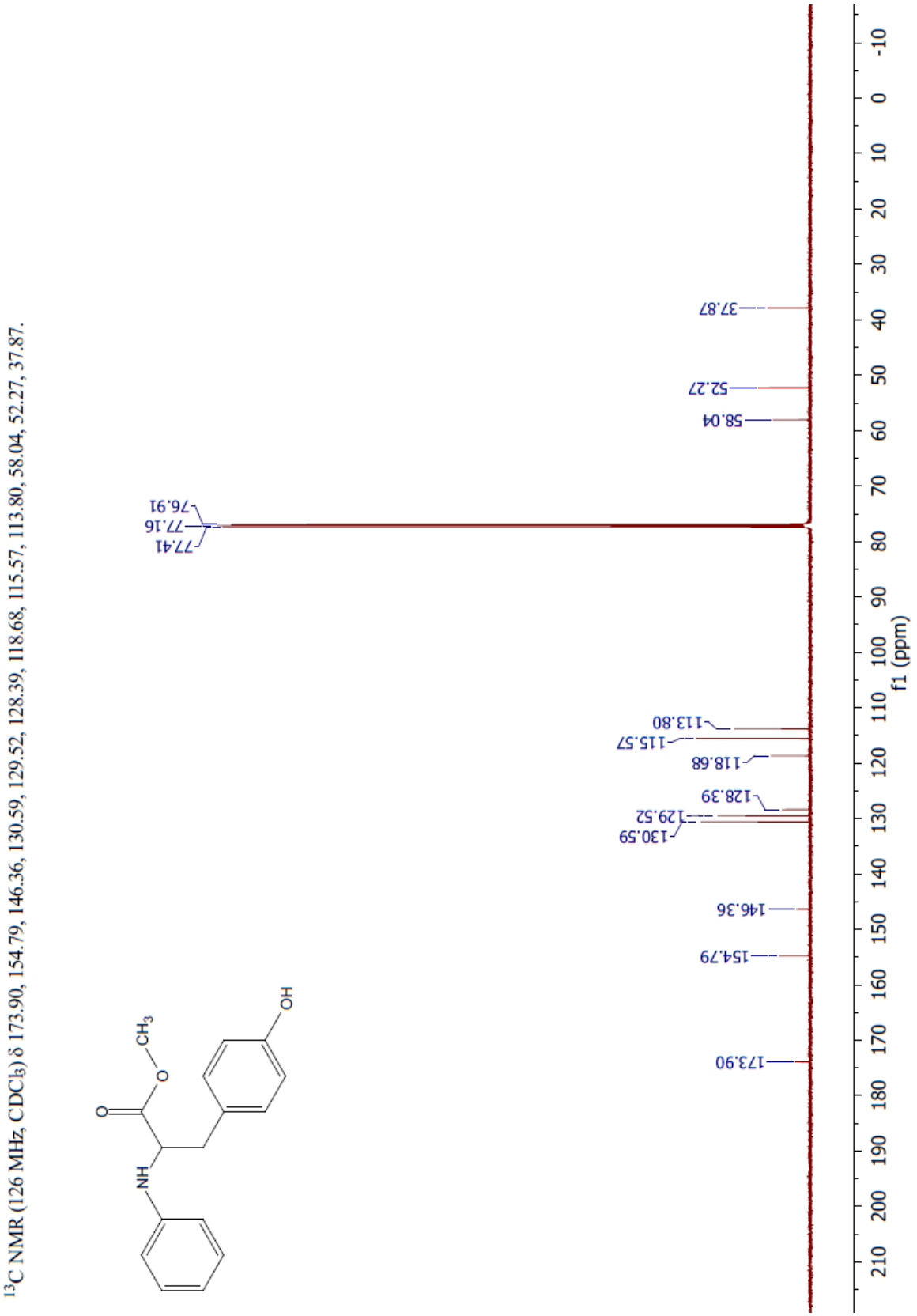

Figure 26. ^{13}C NMR spectra for compound **3l**

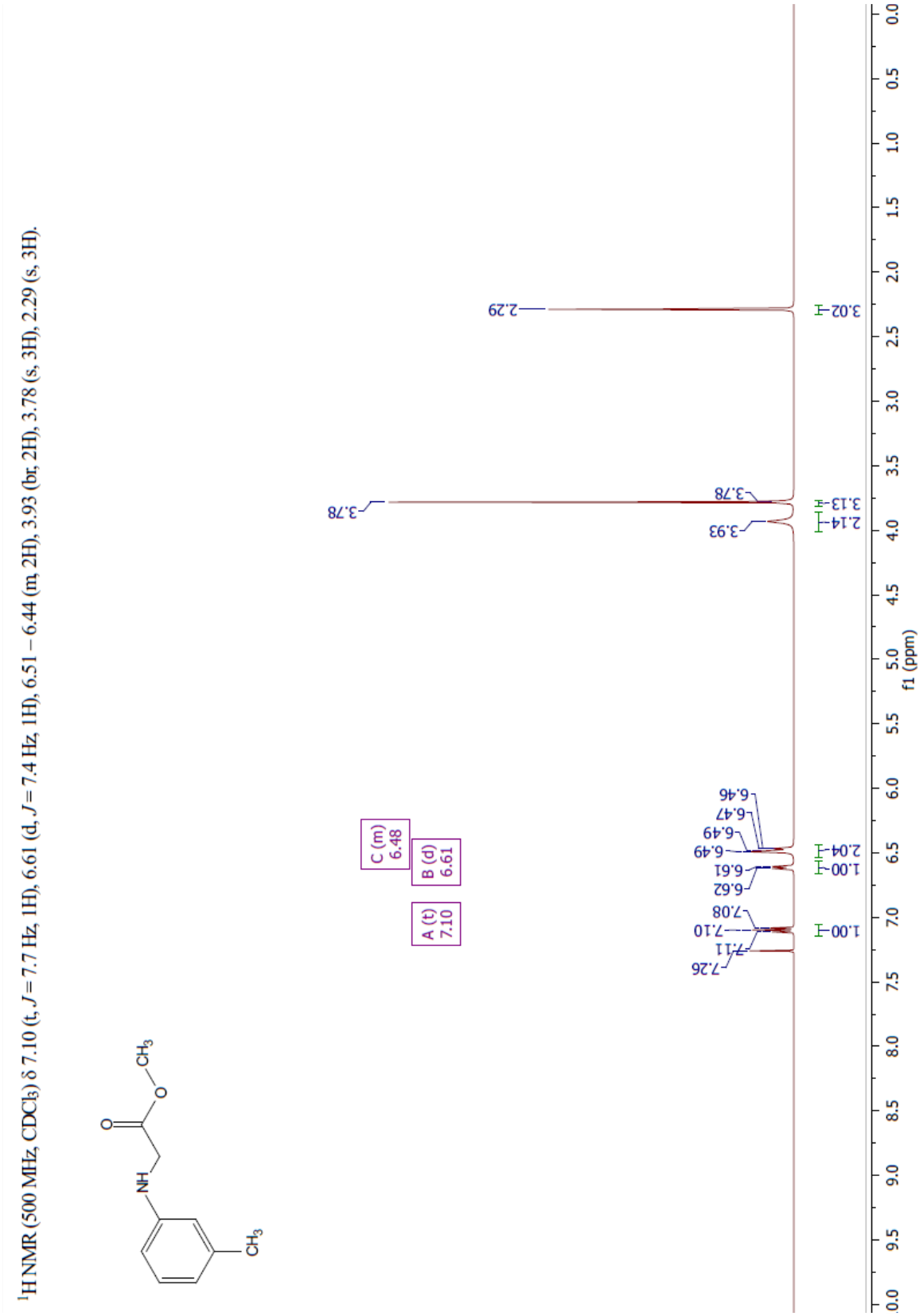

Figure 27. ^{1}H NMR spectra for compound **3m**

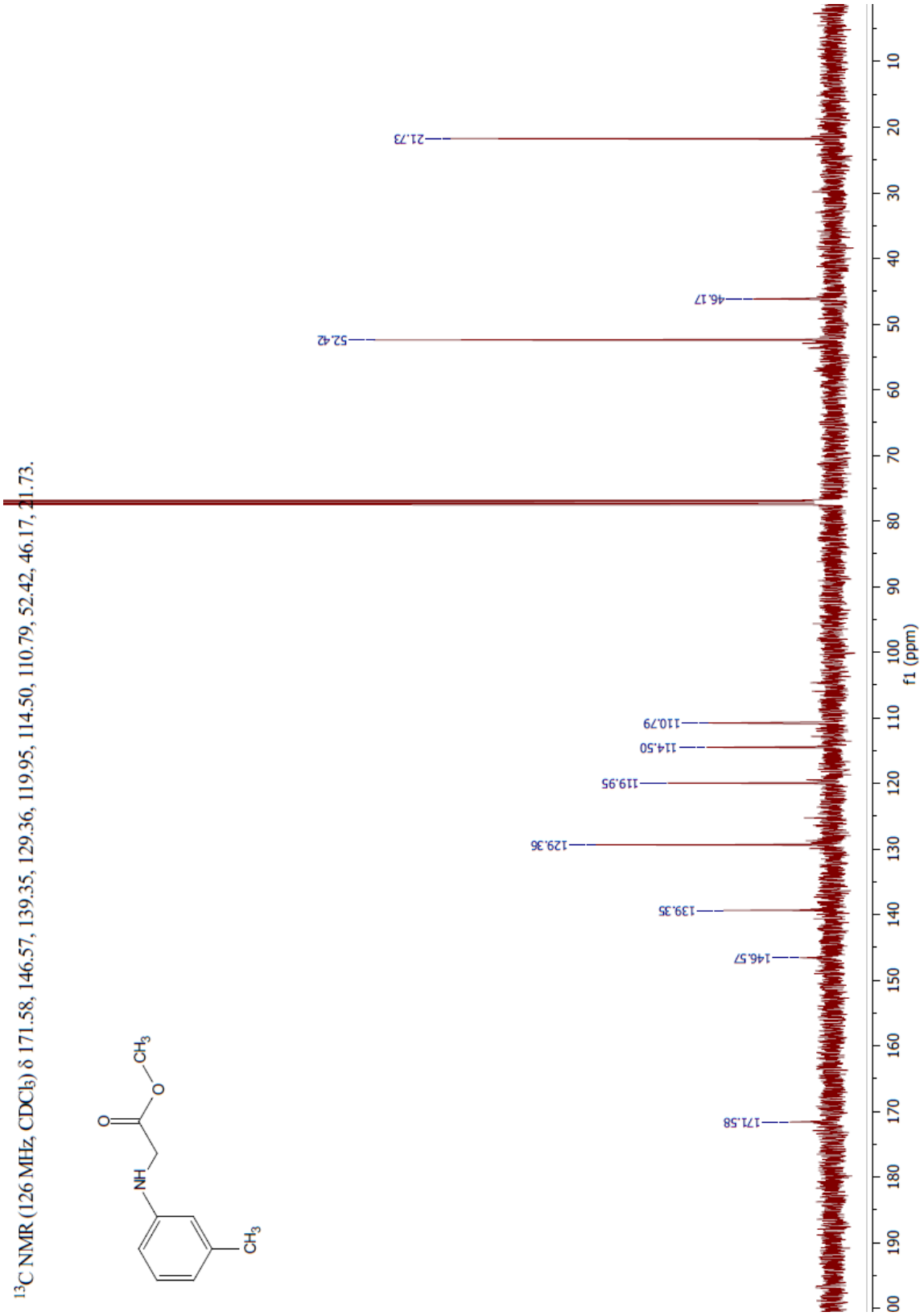

Figure 28. ^{13}C NMR spectra for compound **3m**

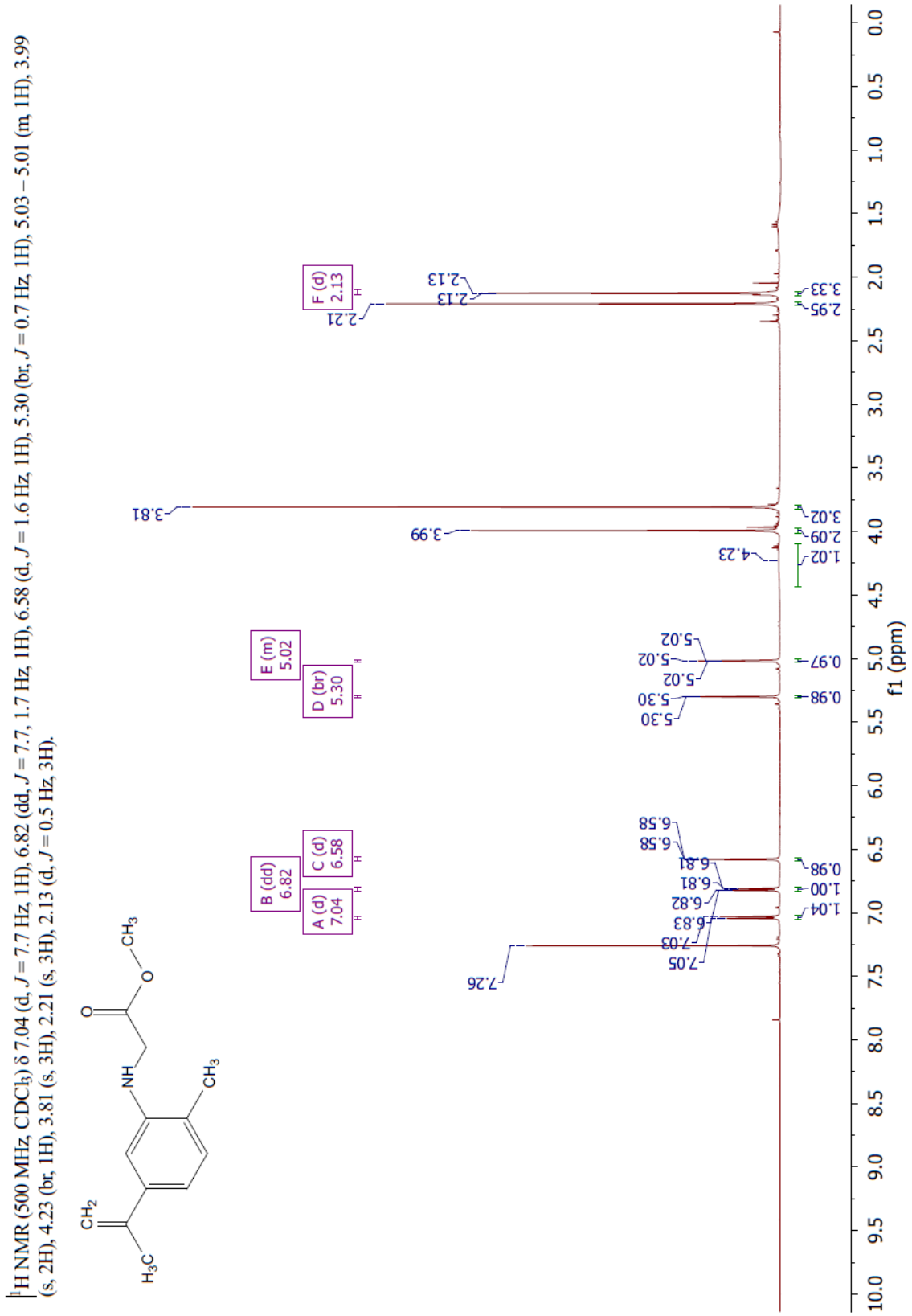

Figure 29. ^{1}H NMR spectra for compound **3n**

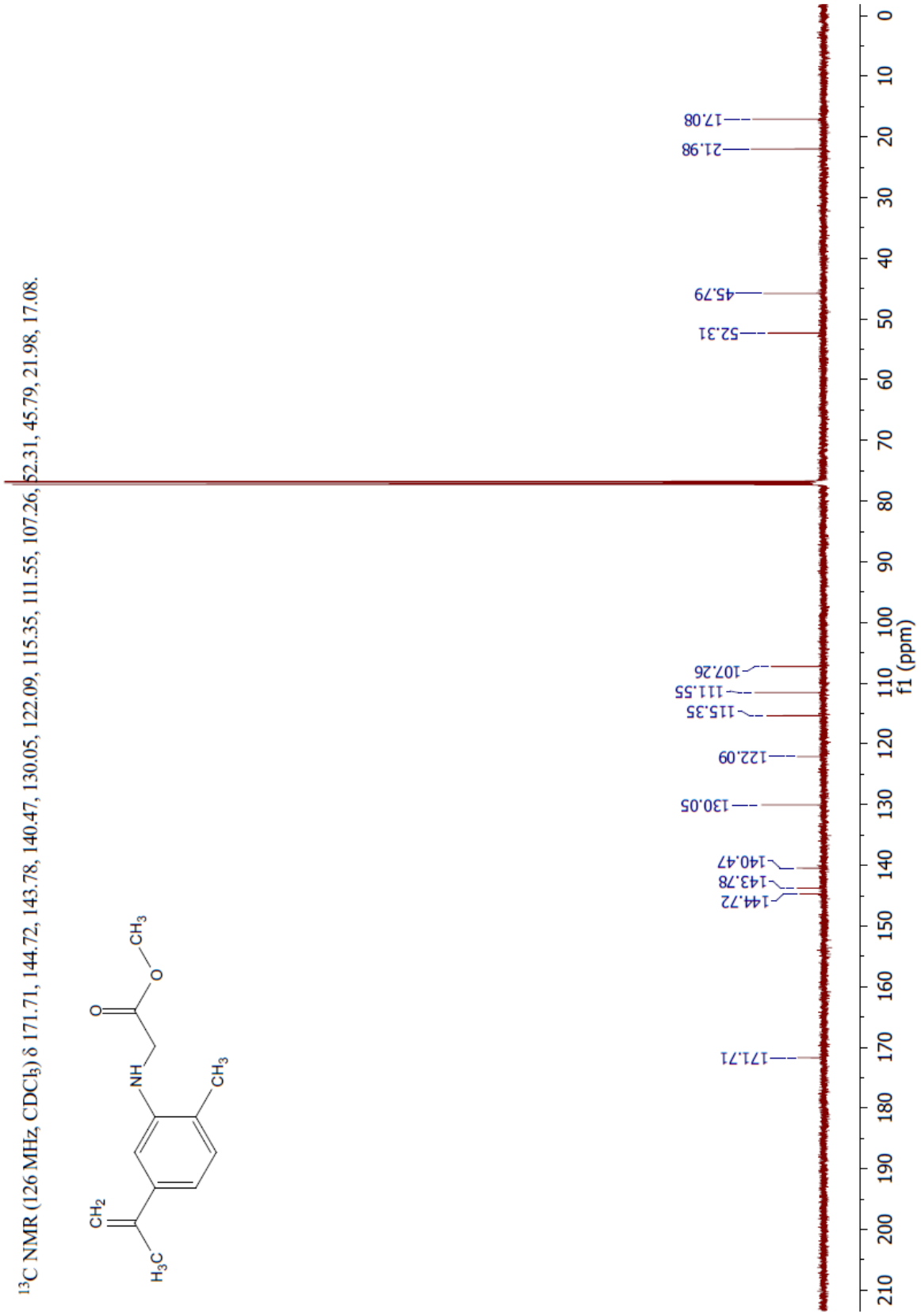

Figure 30. ^{13}C NMR spectra for compound **3n**

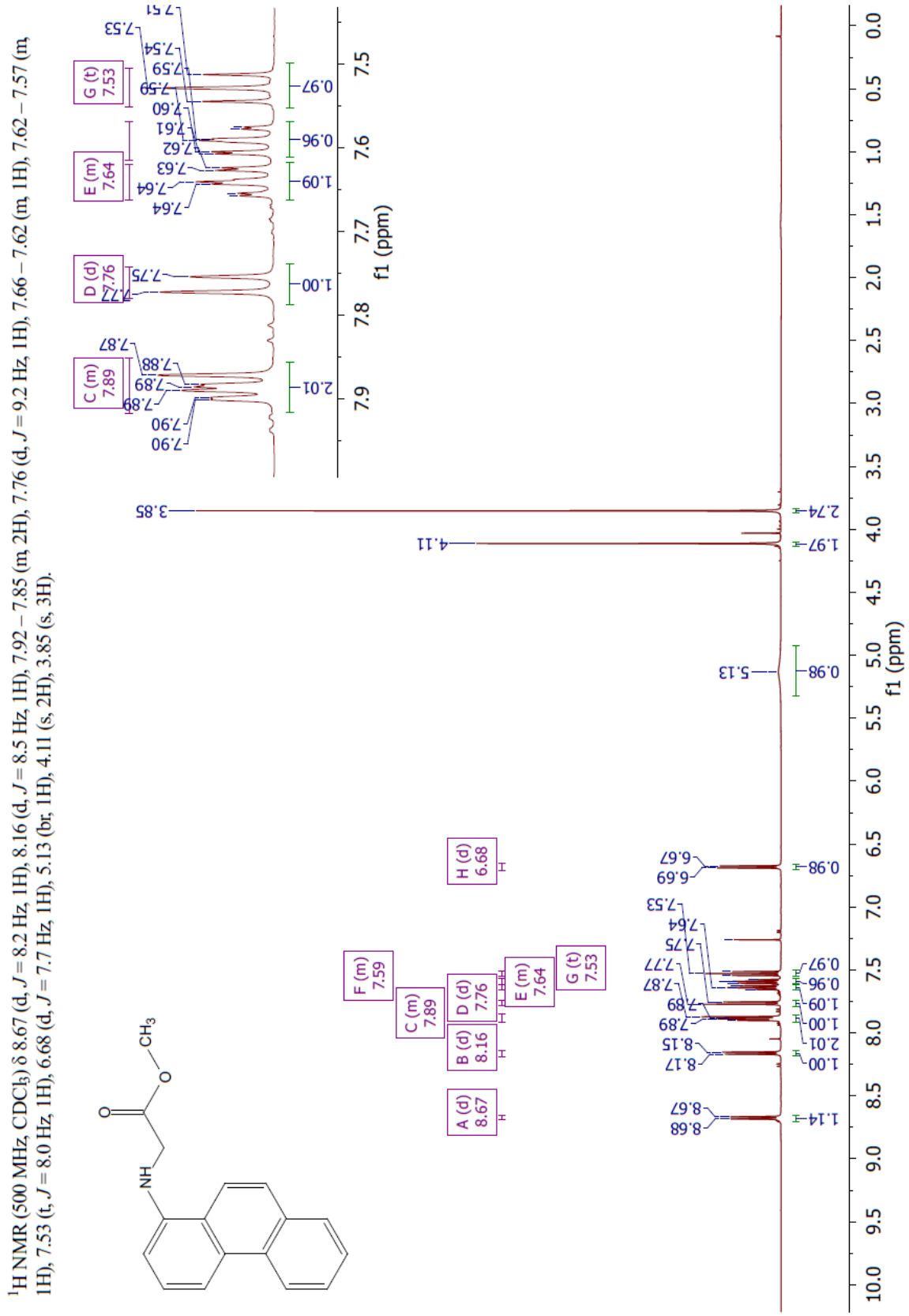

Figure 31. ^{1}H NMR spectra for compound **3o**

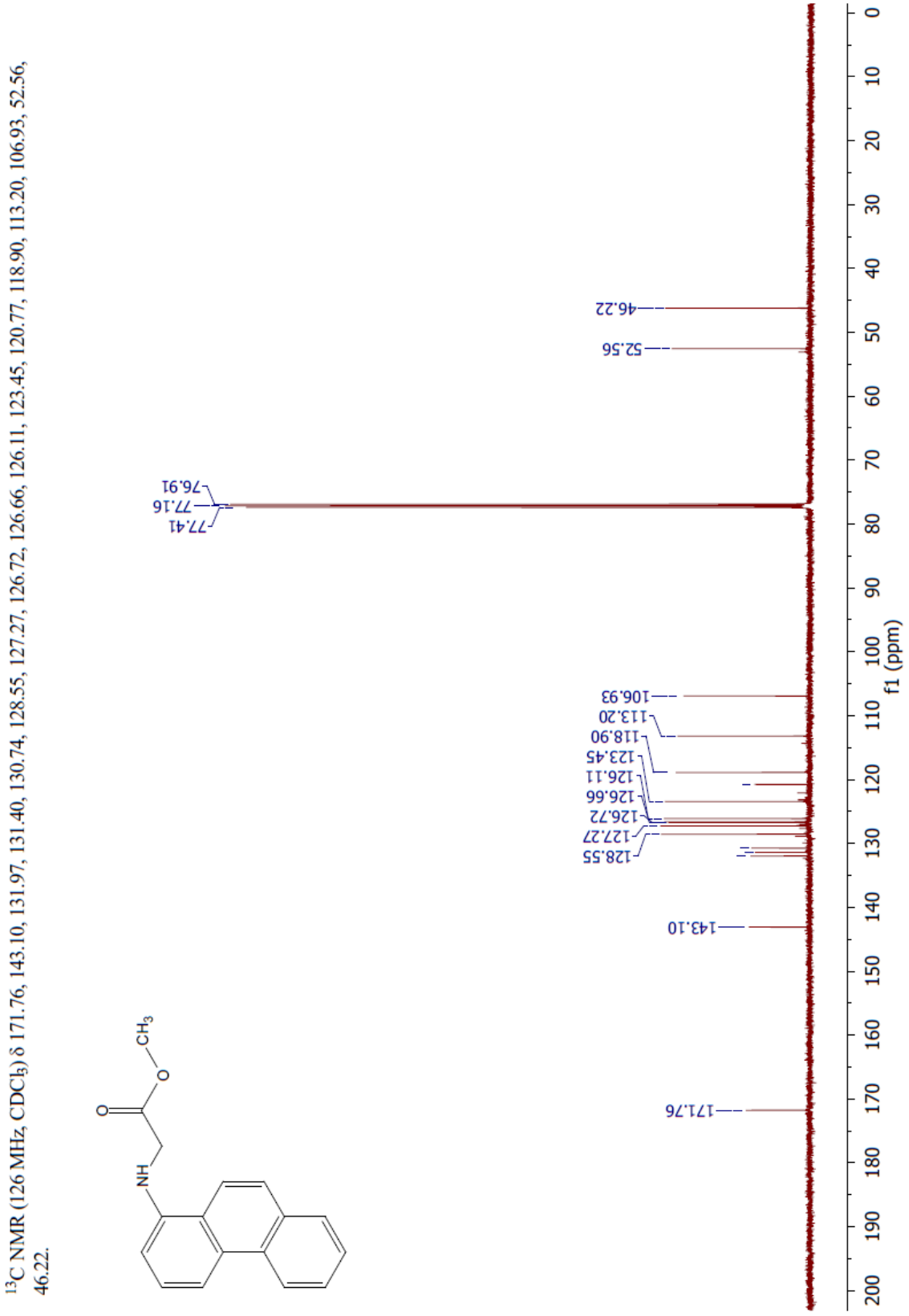

Figure 32. ^{13}C NMR spectra for compound **3o**

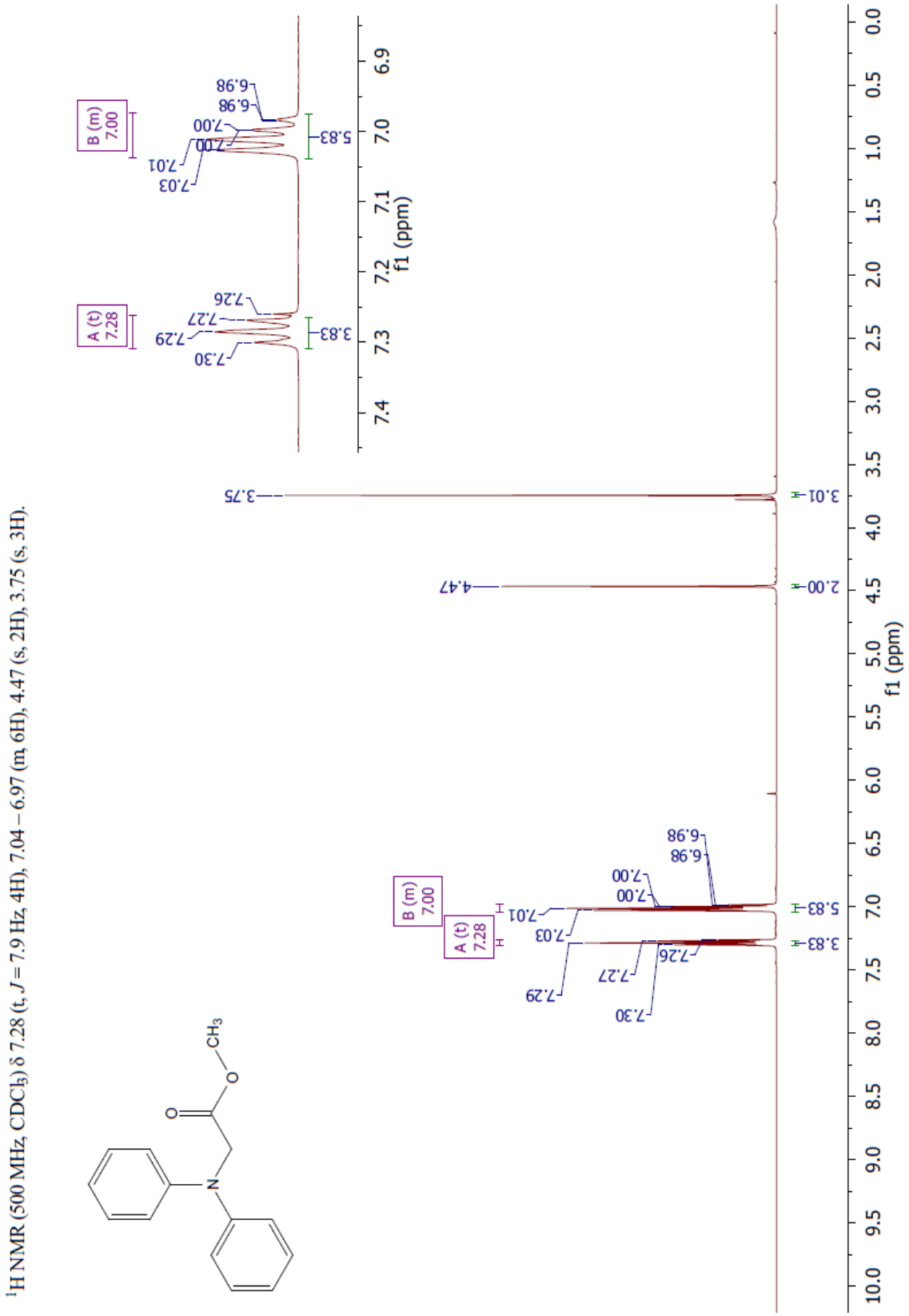

Figure 33. ^{1}H NMR spectra for compound **5**

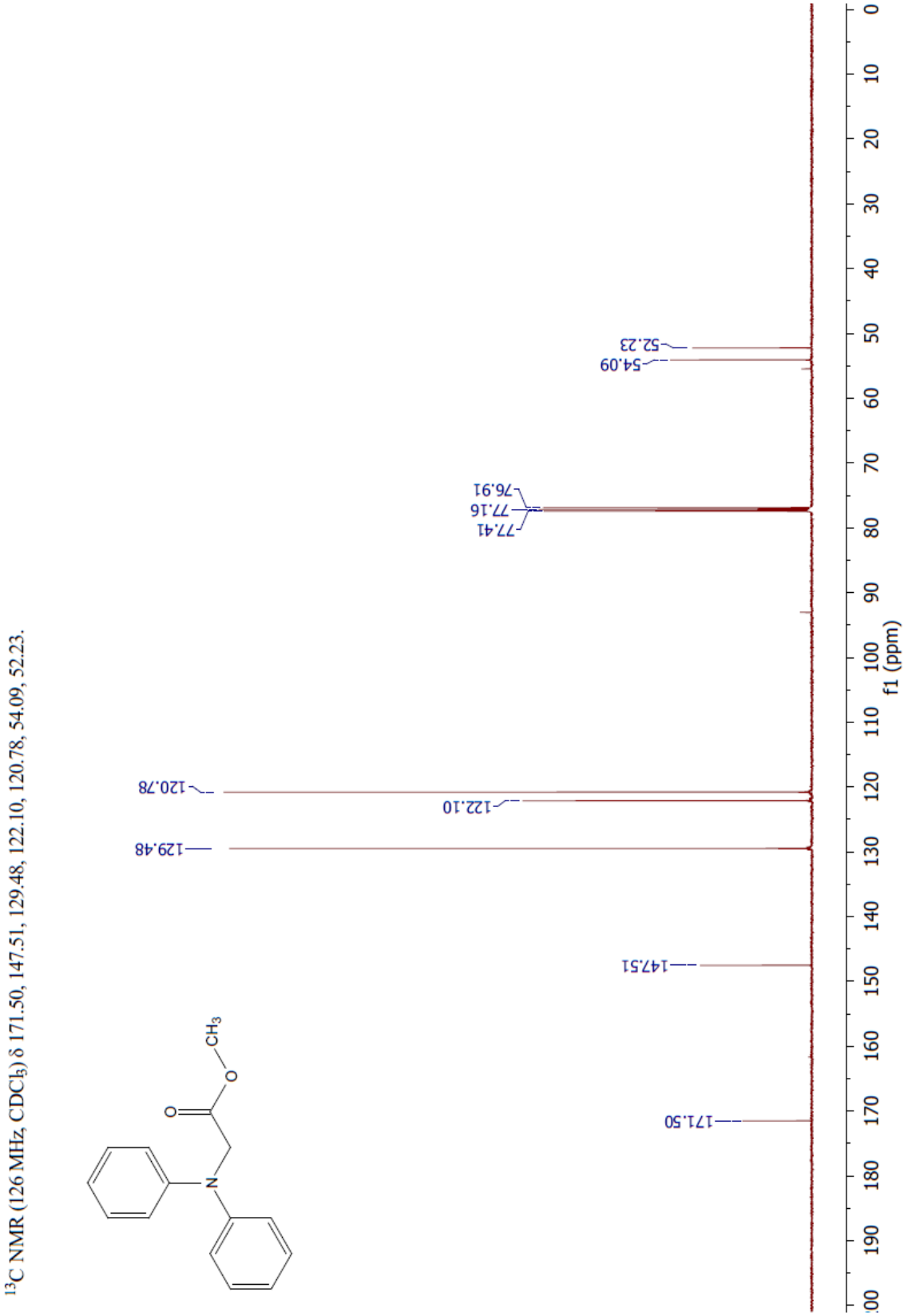

Figure 34. ^{13}C NMR spectra for compound **5**

Appendix 2. NMR Spectral Data for Chapter 3

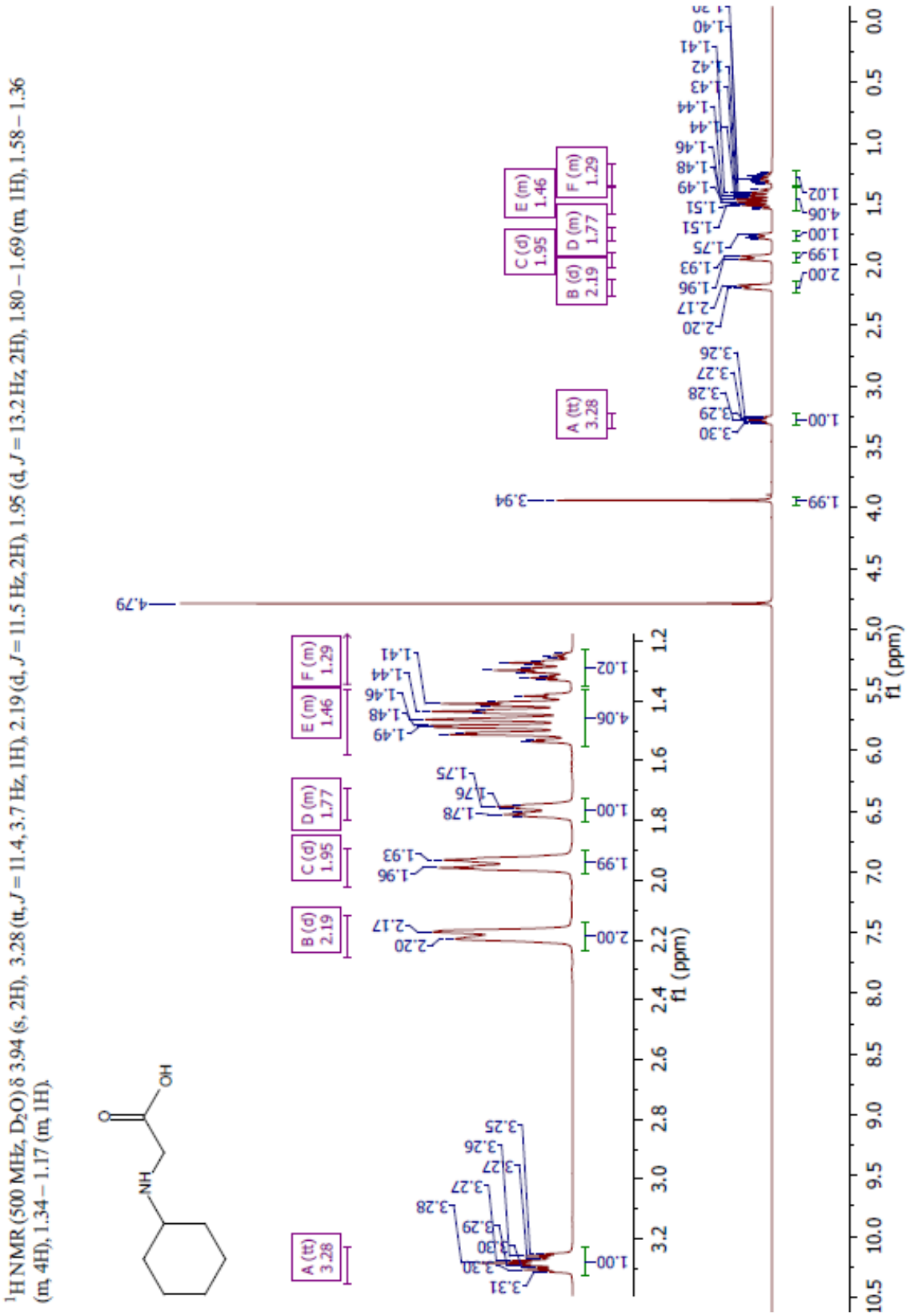

Figure 1. ^{1}H NMR spectra for compound **3**

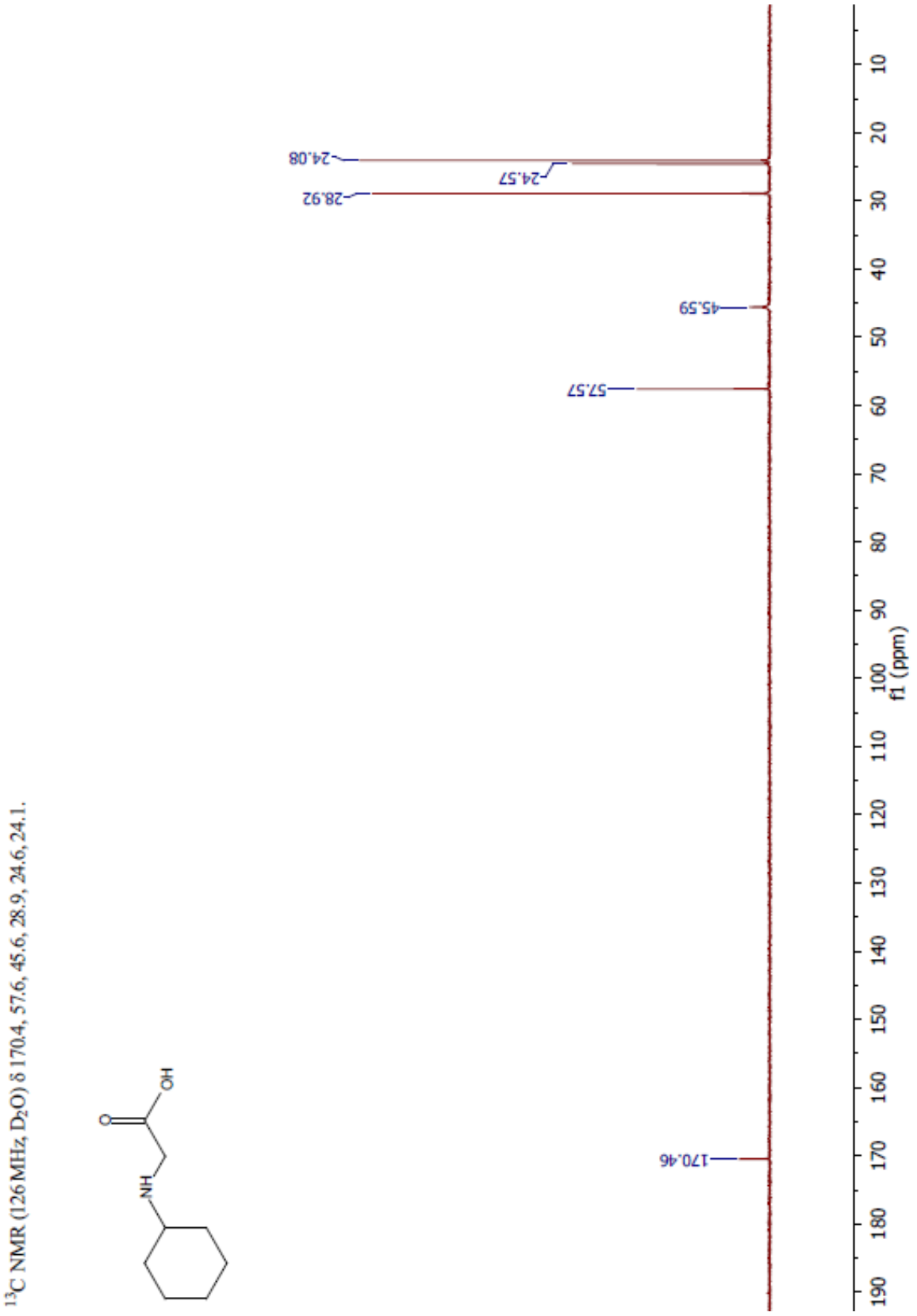

Figure 2. ^{13}C NMR spectra for compound **3**

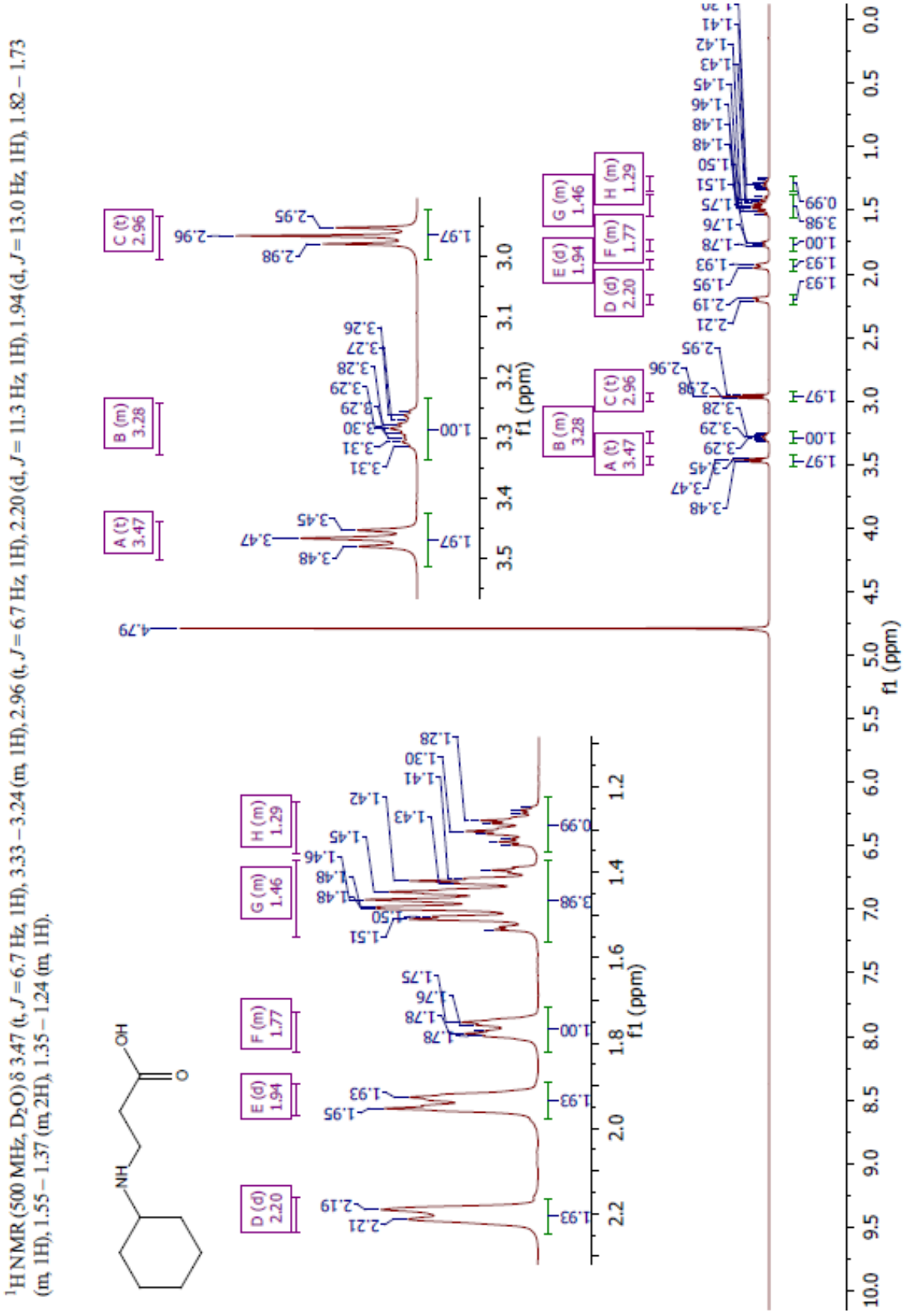

Figure 3. ^{1}H NMR spectra for compound **3a**

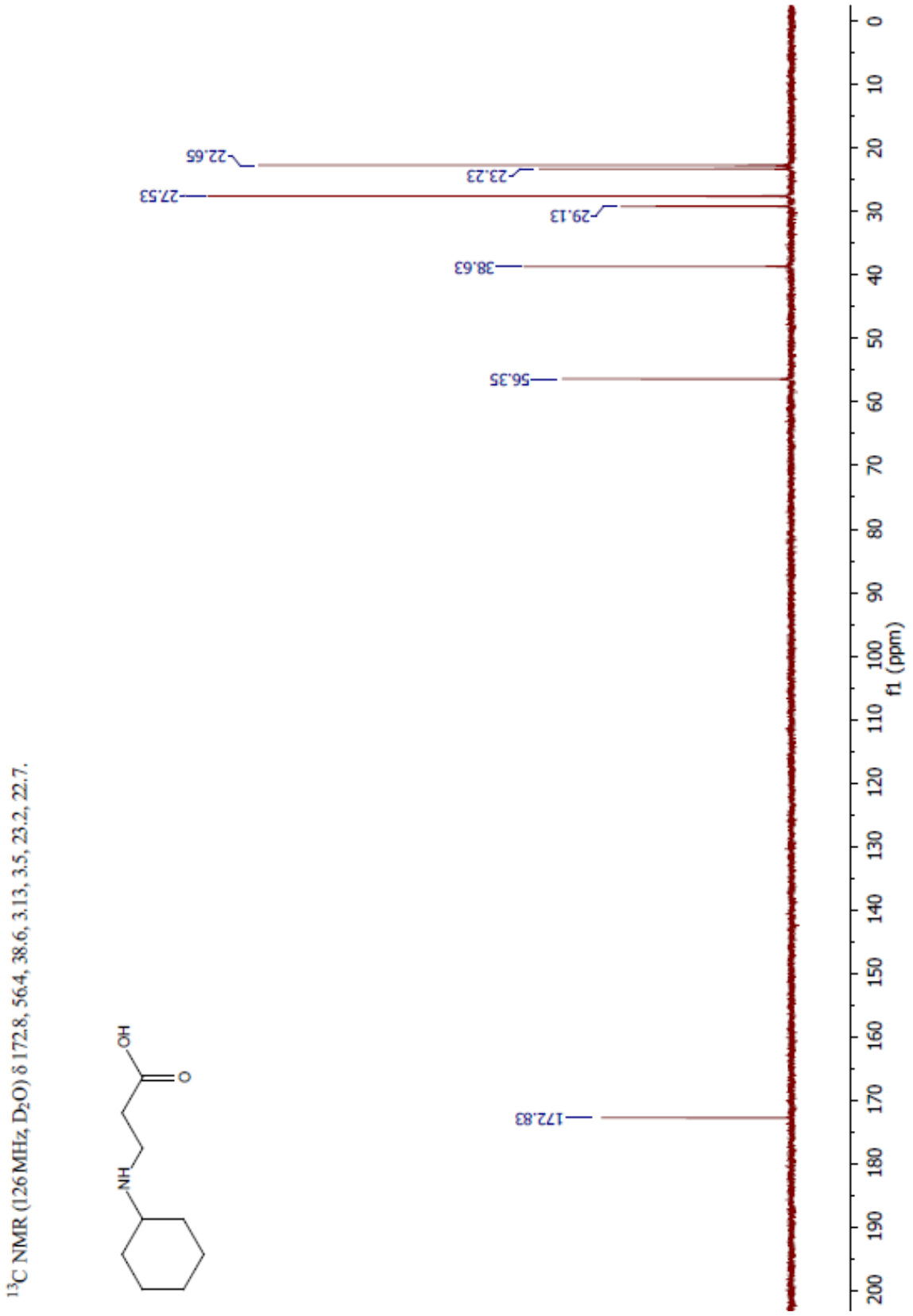

Figure 4. ^{13}C NMR spectra for compound **3a**

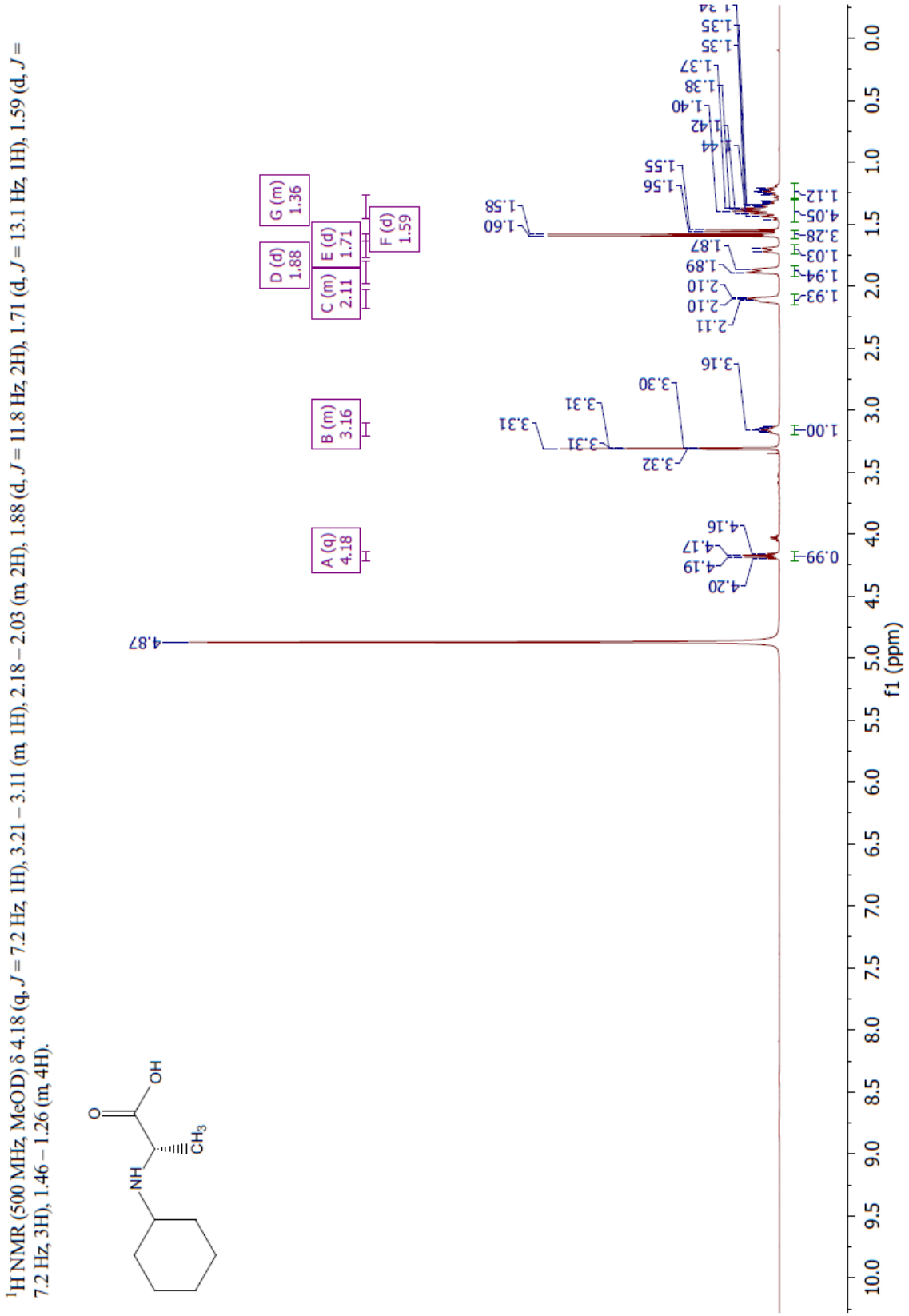

Figure 5. ^{1}H NMR spectra for compound **3b**

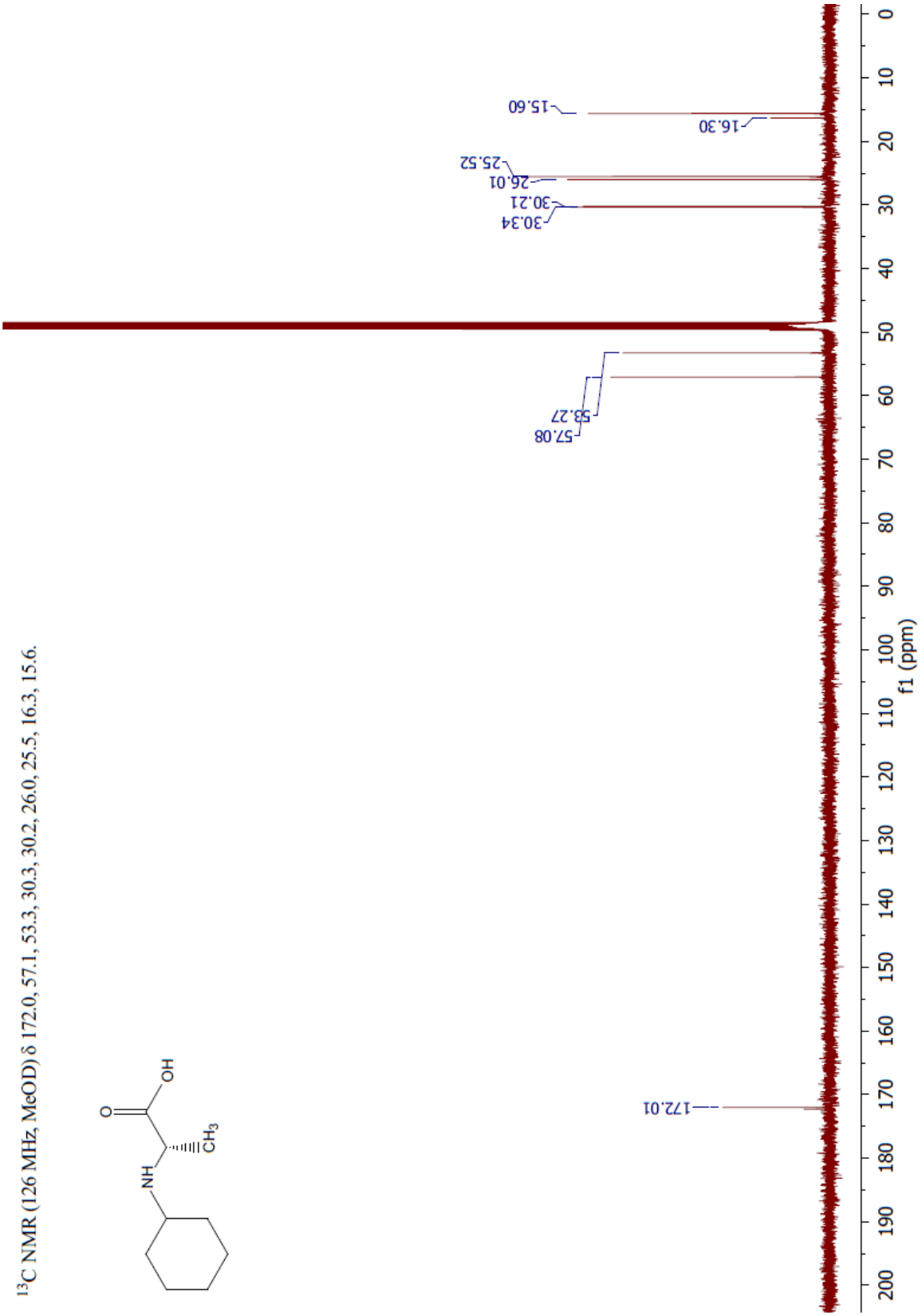

Figure 6. ^{13}C NMR spectra for compound **3b**

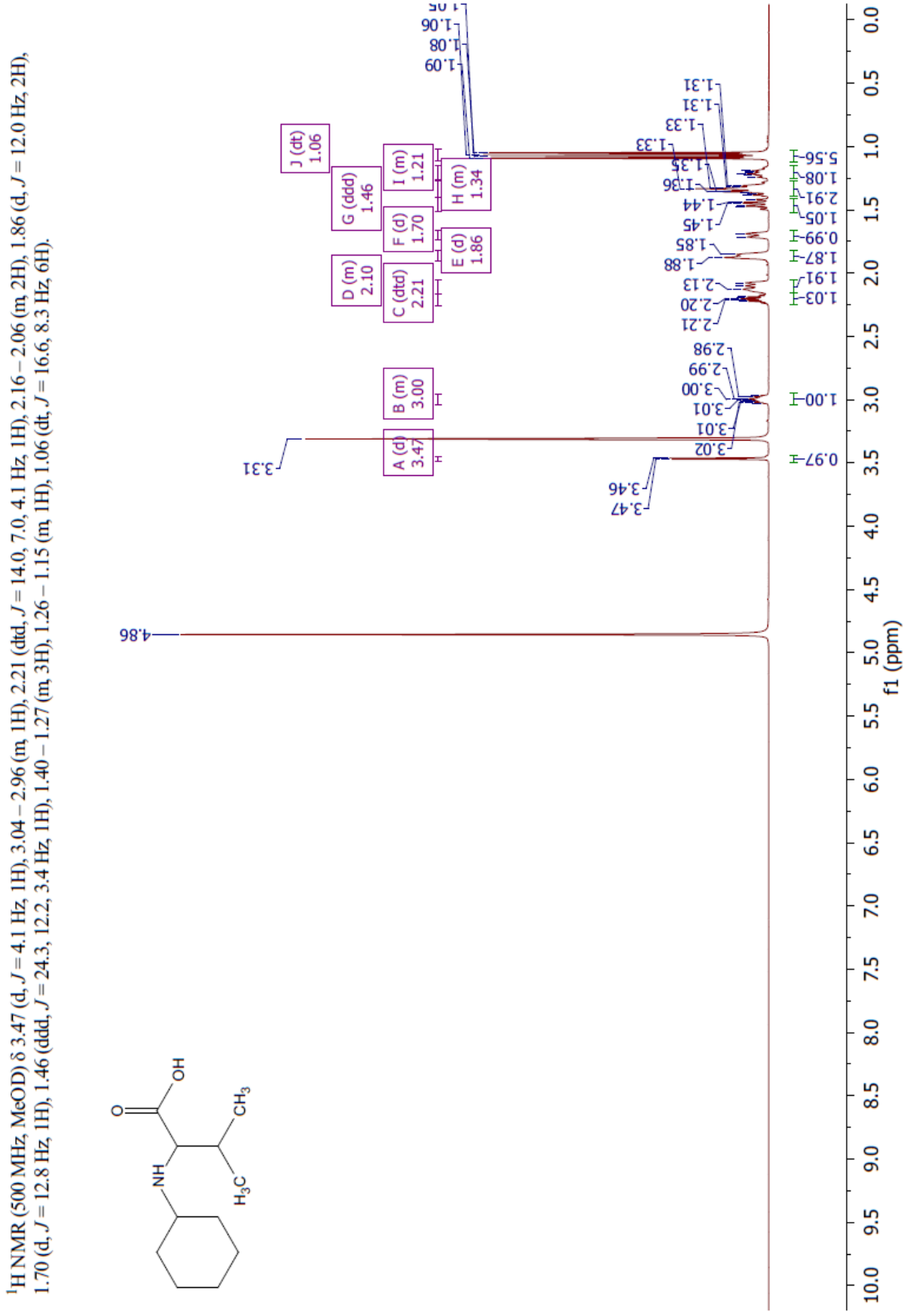

Figure 7. ^{1}H NMR spectra for compound **3c**

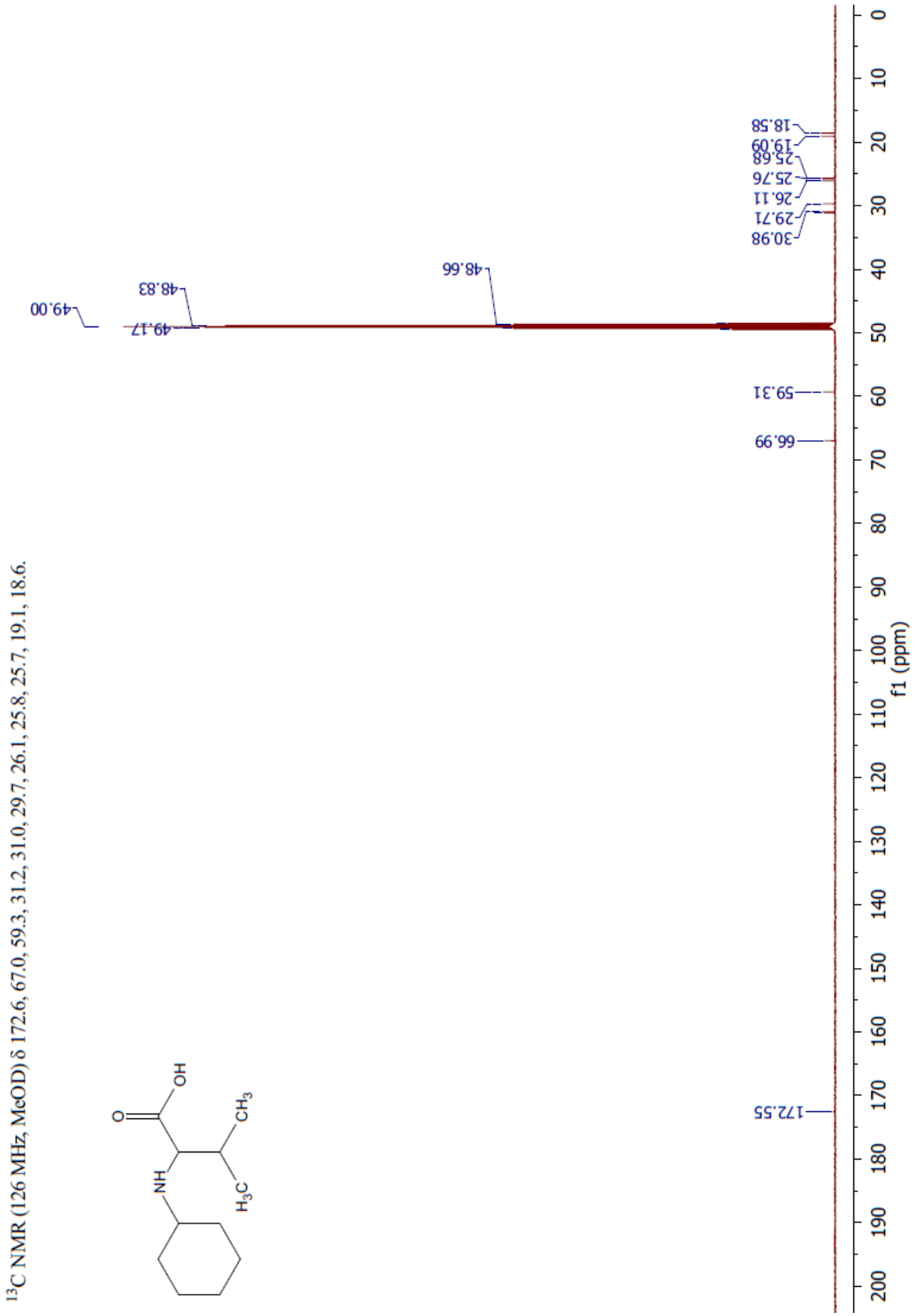

Figure 8. ^{13}C NMR spectra for compound **3c**

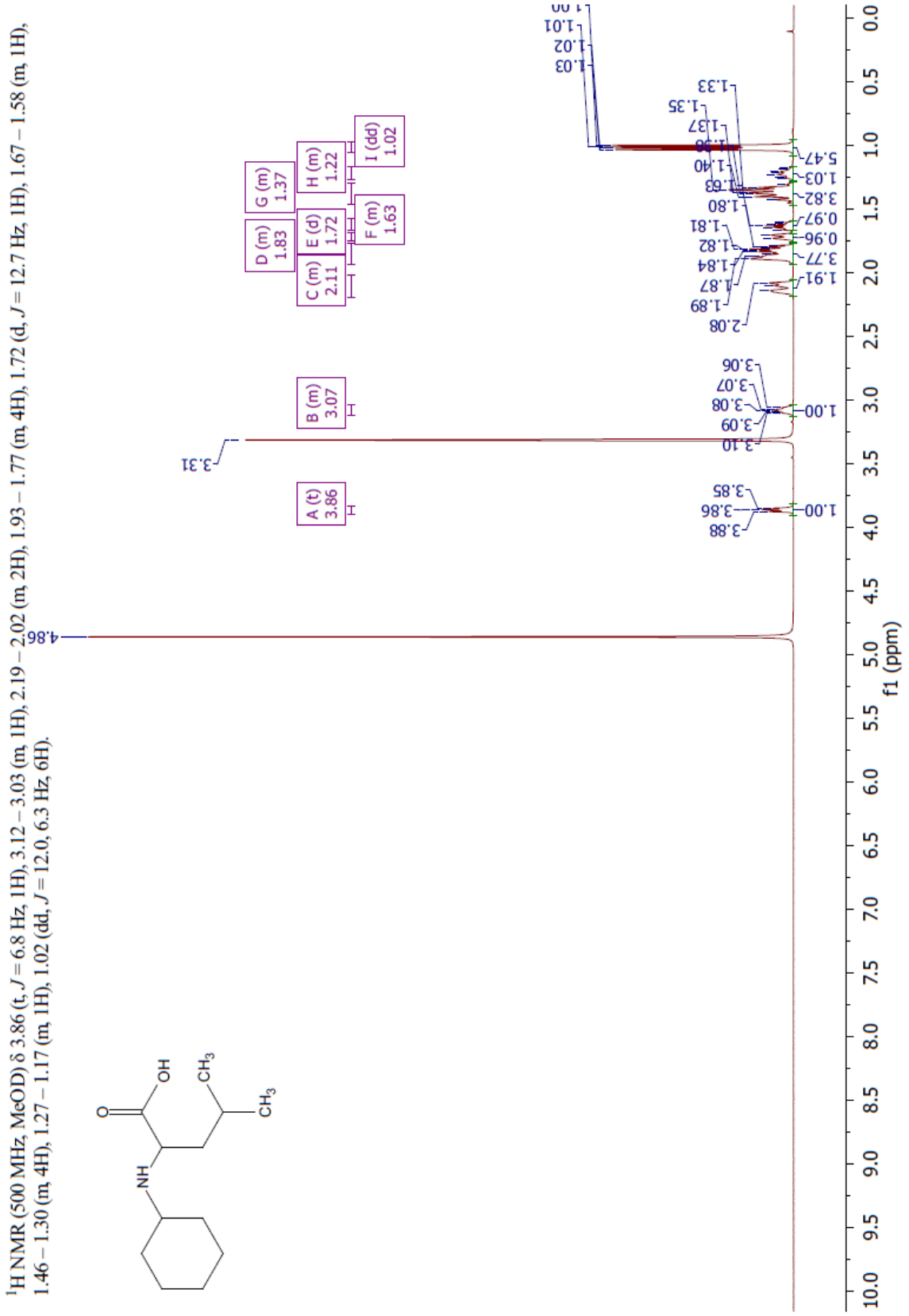

Figure 9. ^{1}H NMR spectra for compound **3d**

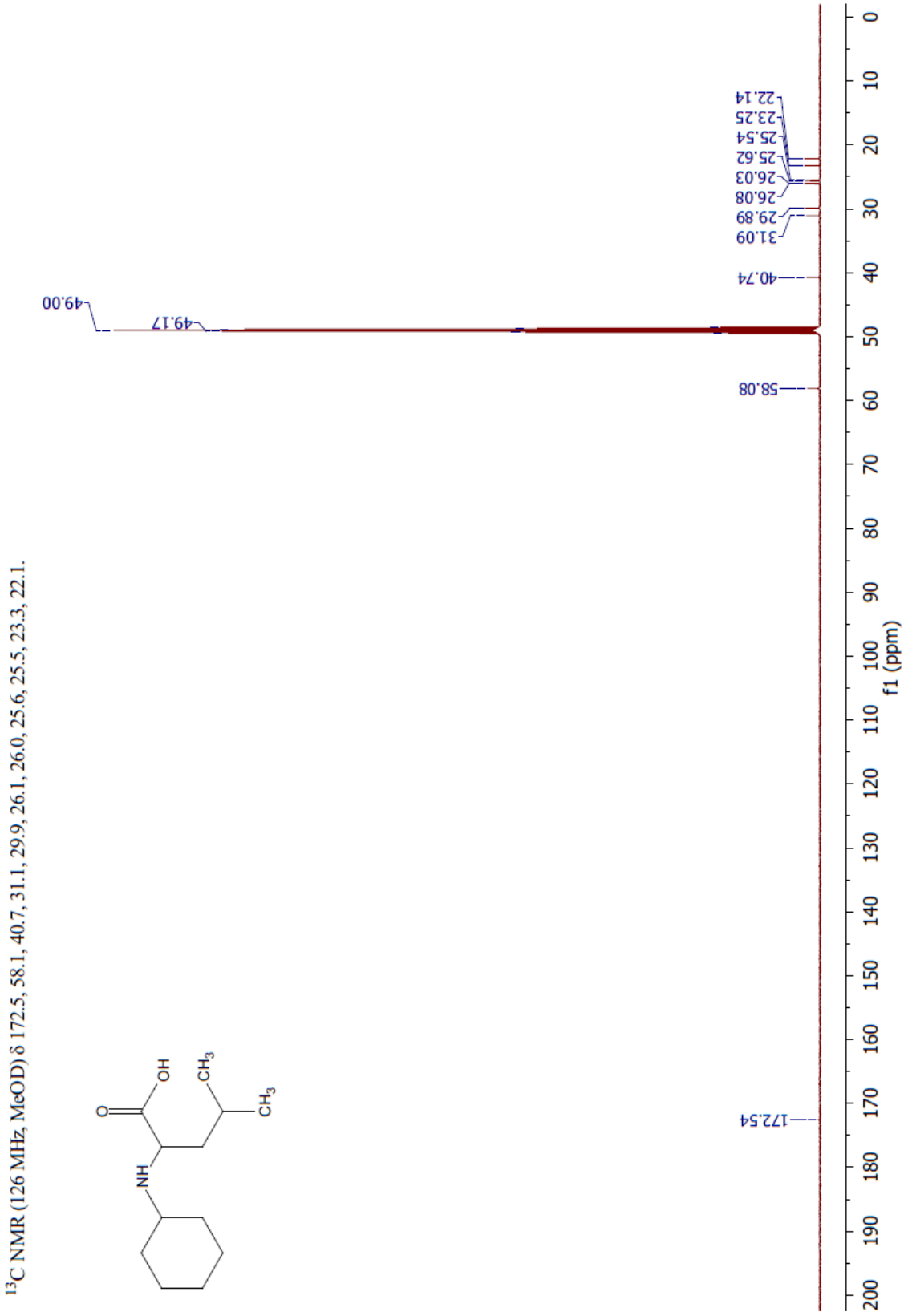

Figure 10. ^{13}C NMR spectra for compound **3d**

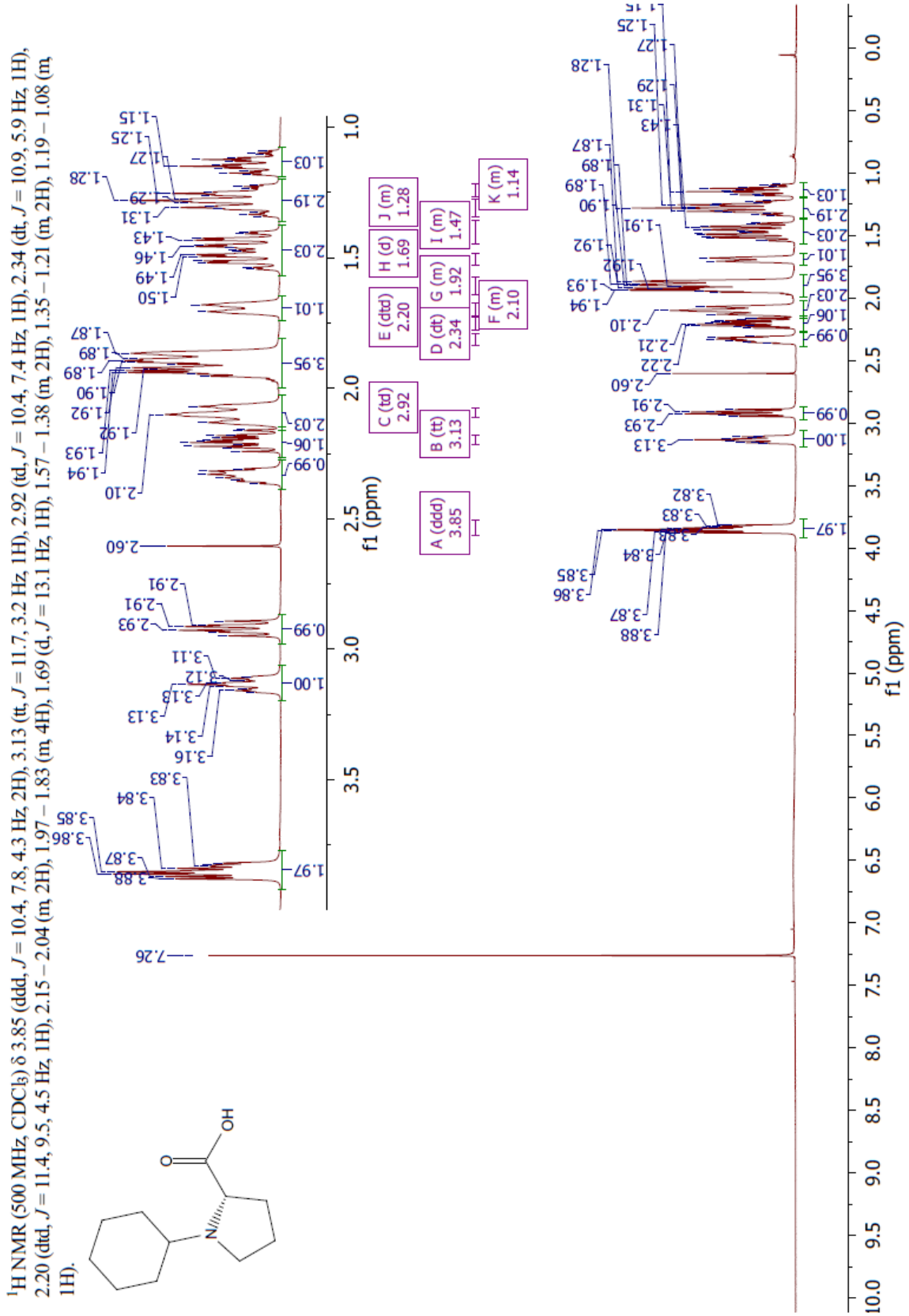

Figure 11. ^{1}H NMR spectra for compound **3e**

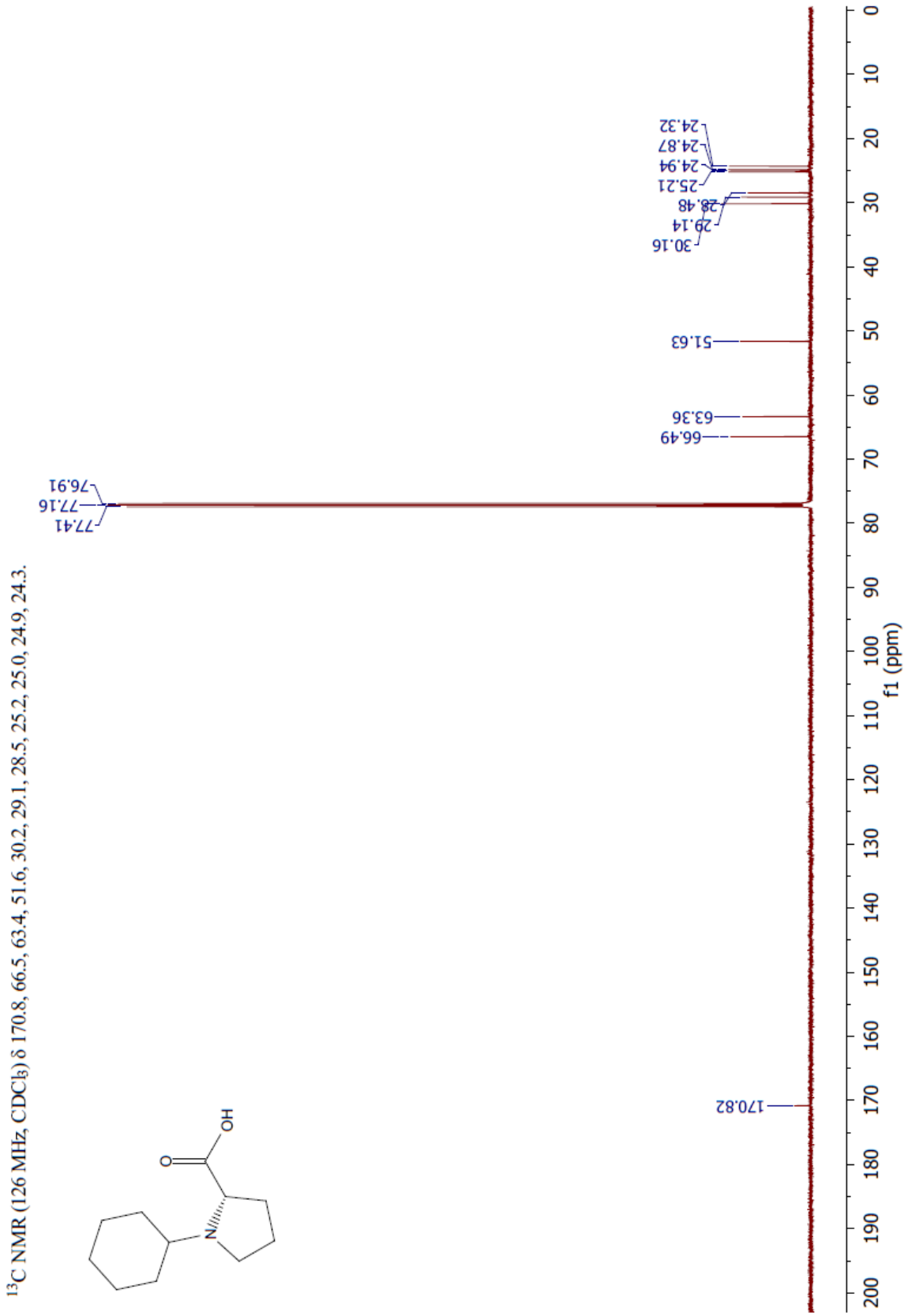

Figure 12. ^{13}C NMR spectra for compound **3e**

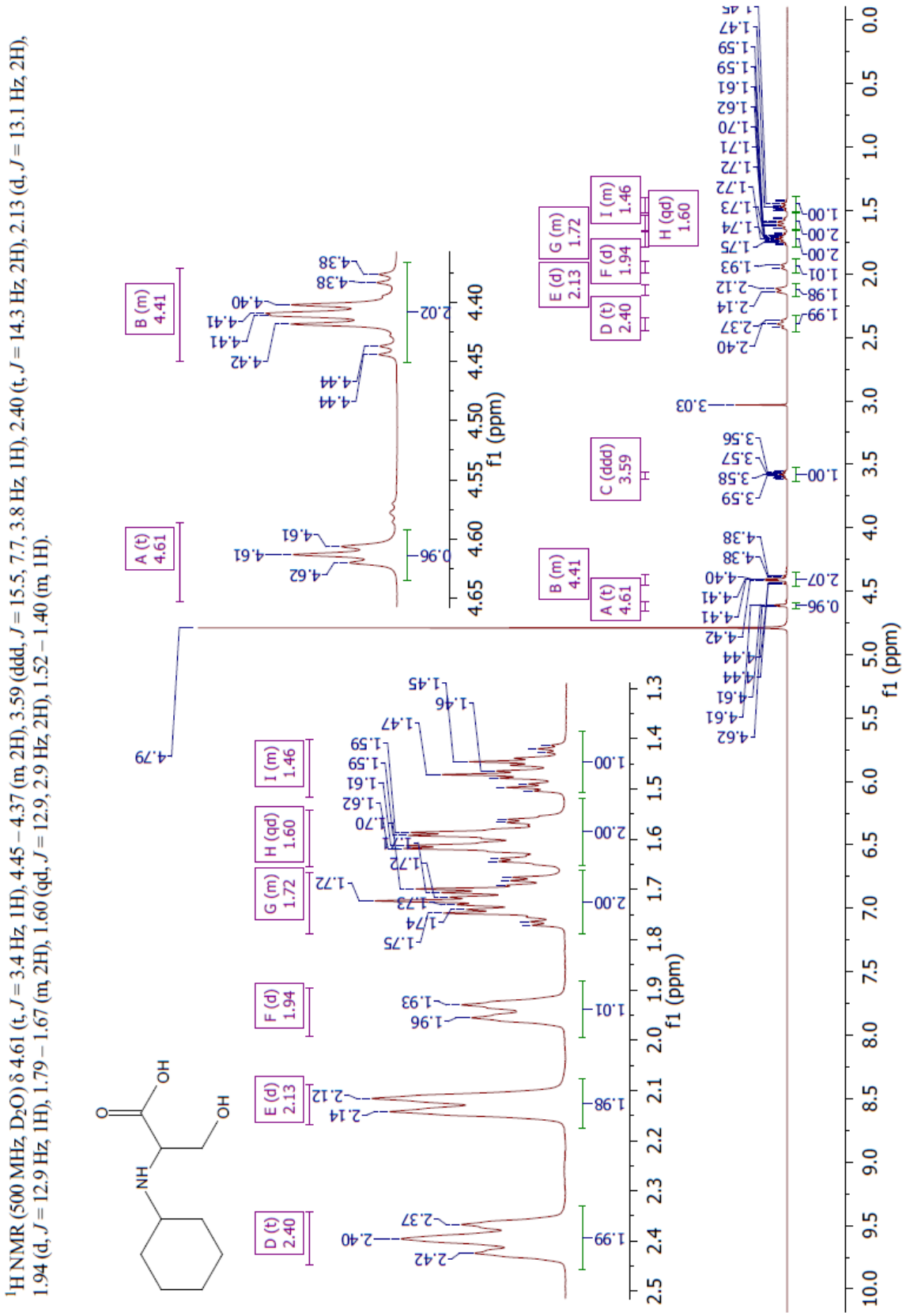

Figure 13. ^{1}H NMR spectra for compound **3f**

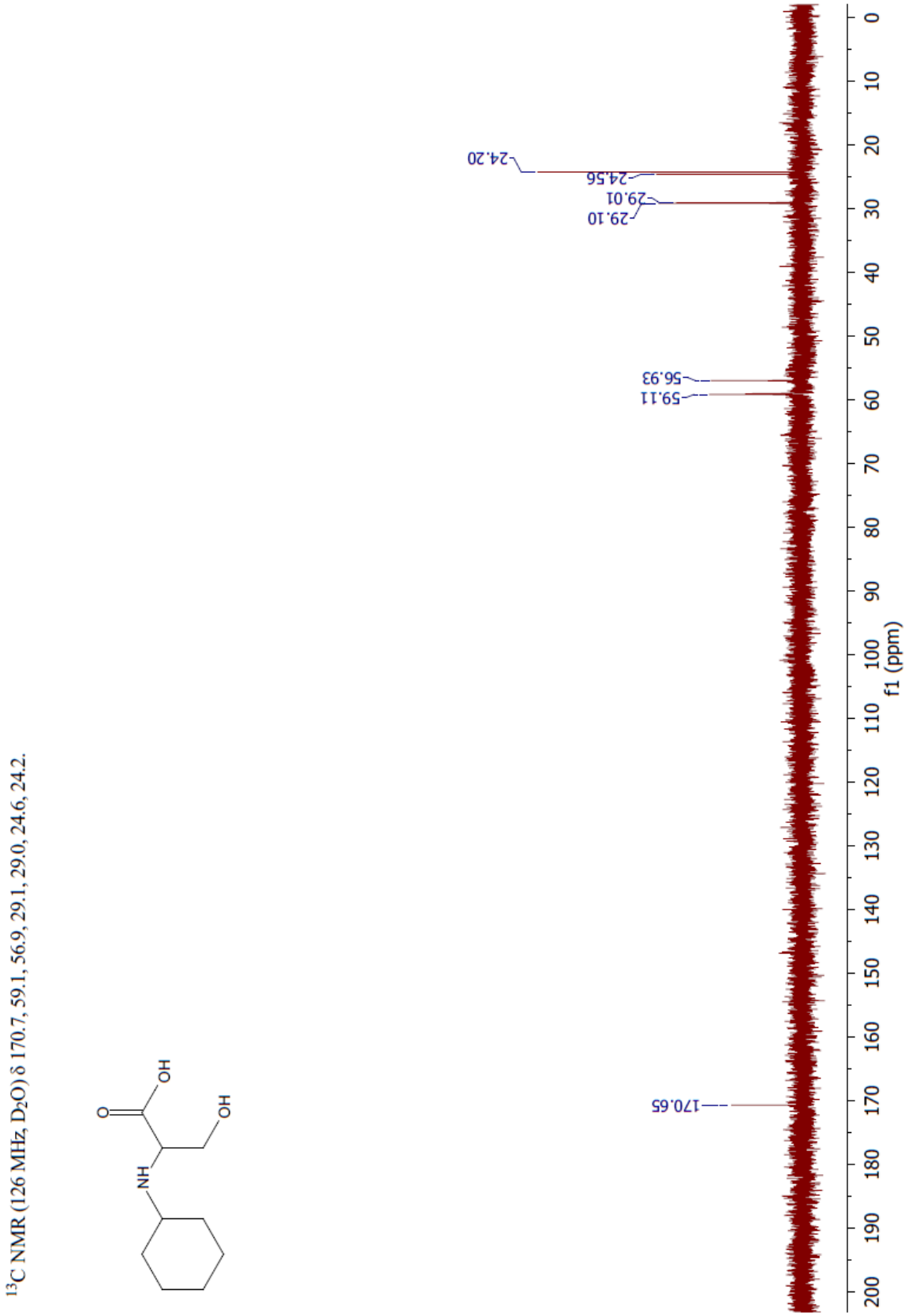

Figure 14. ^{13}C NMR spectra for compound **3f**

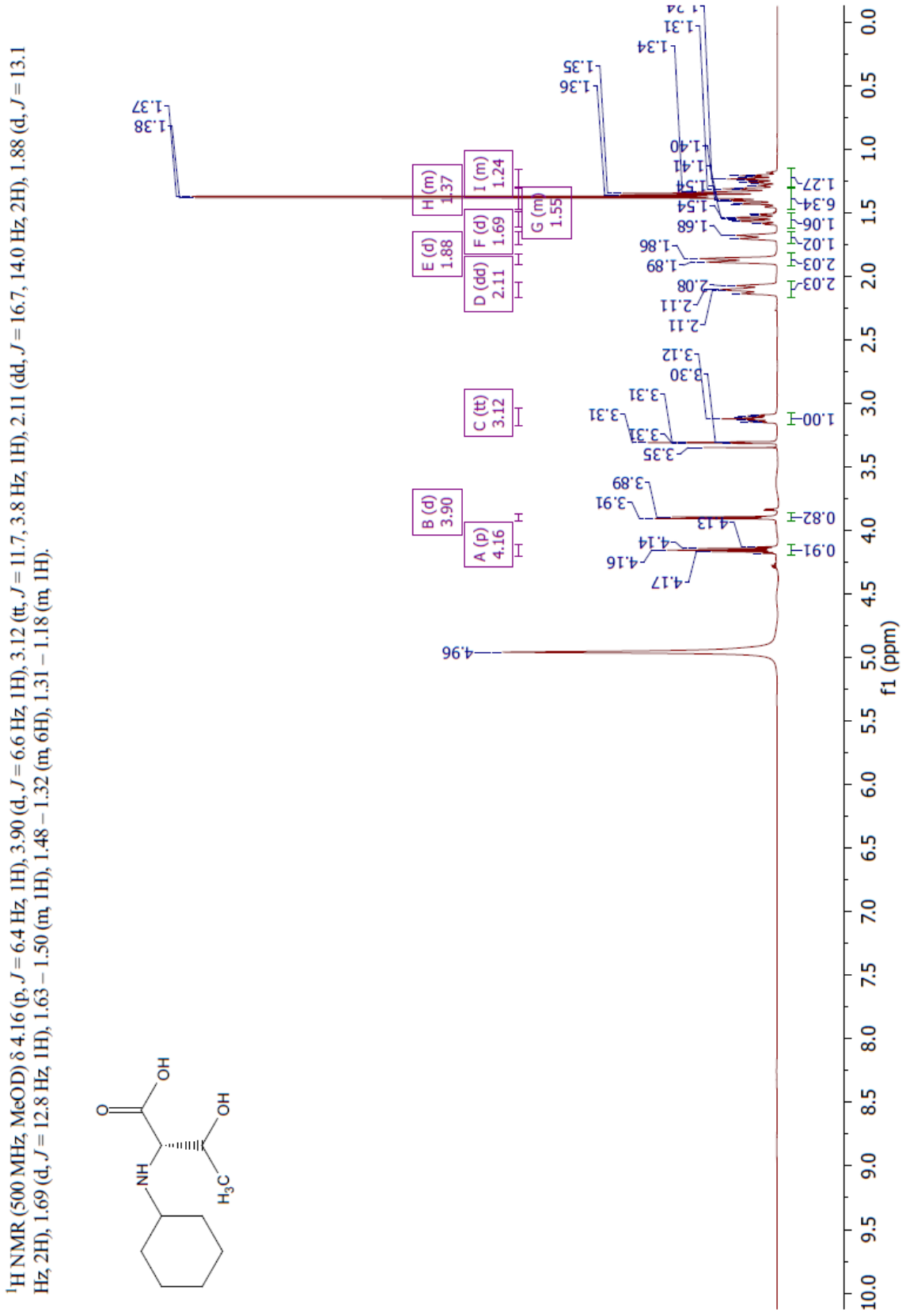

Figure 15. ^{1}H NMR spectra for compound **3g**

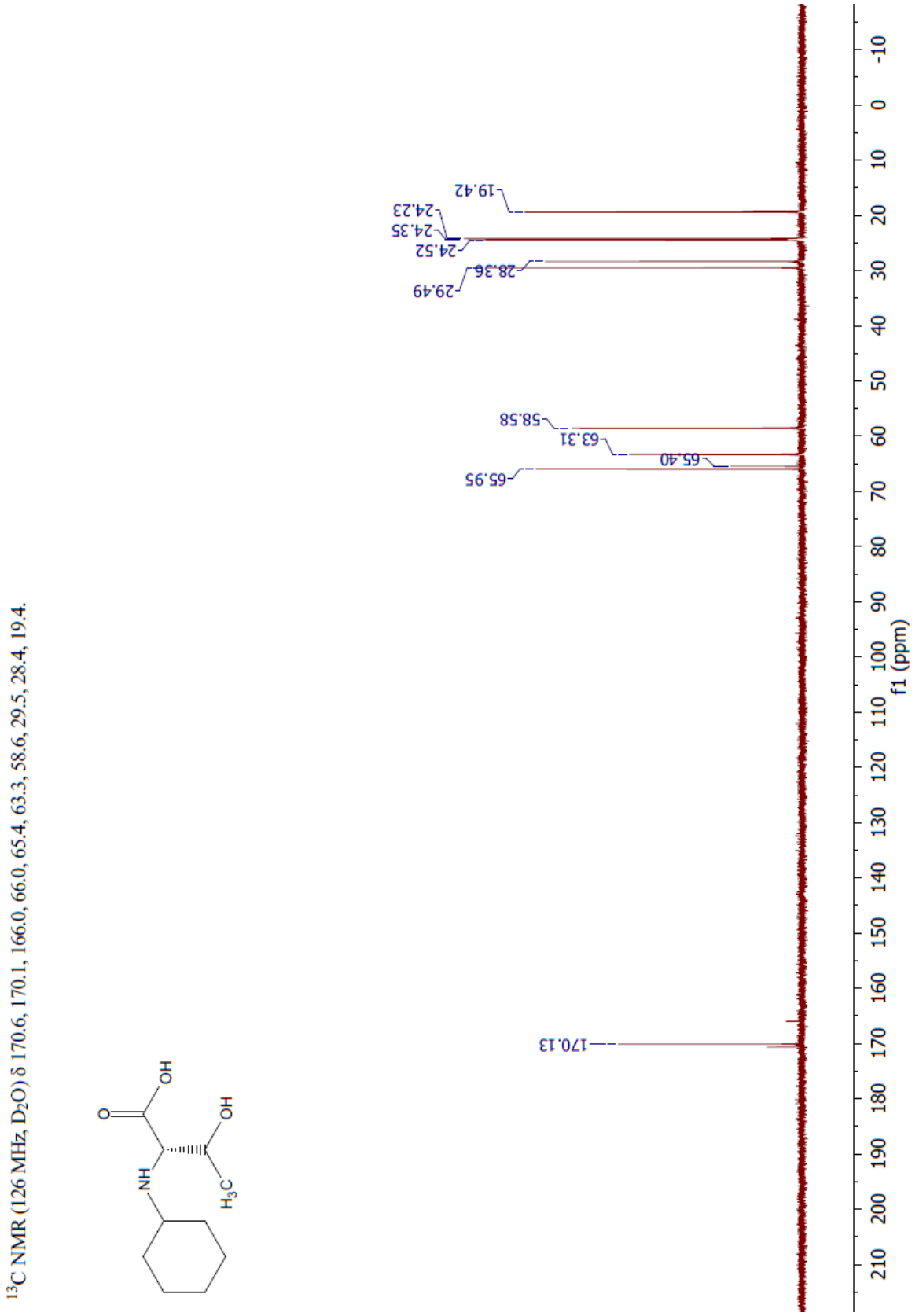

Figure 16. ^{13}C NMR spectra for compound **3g**

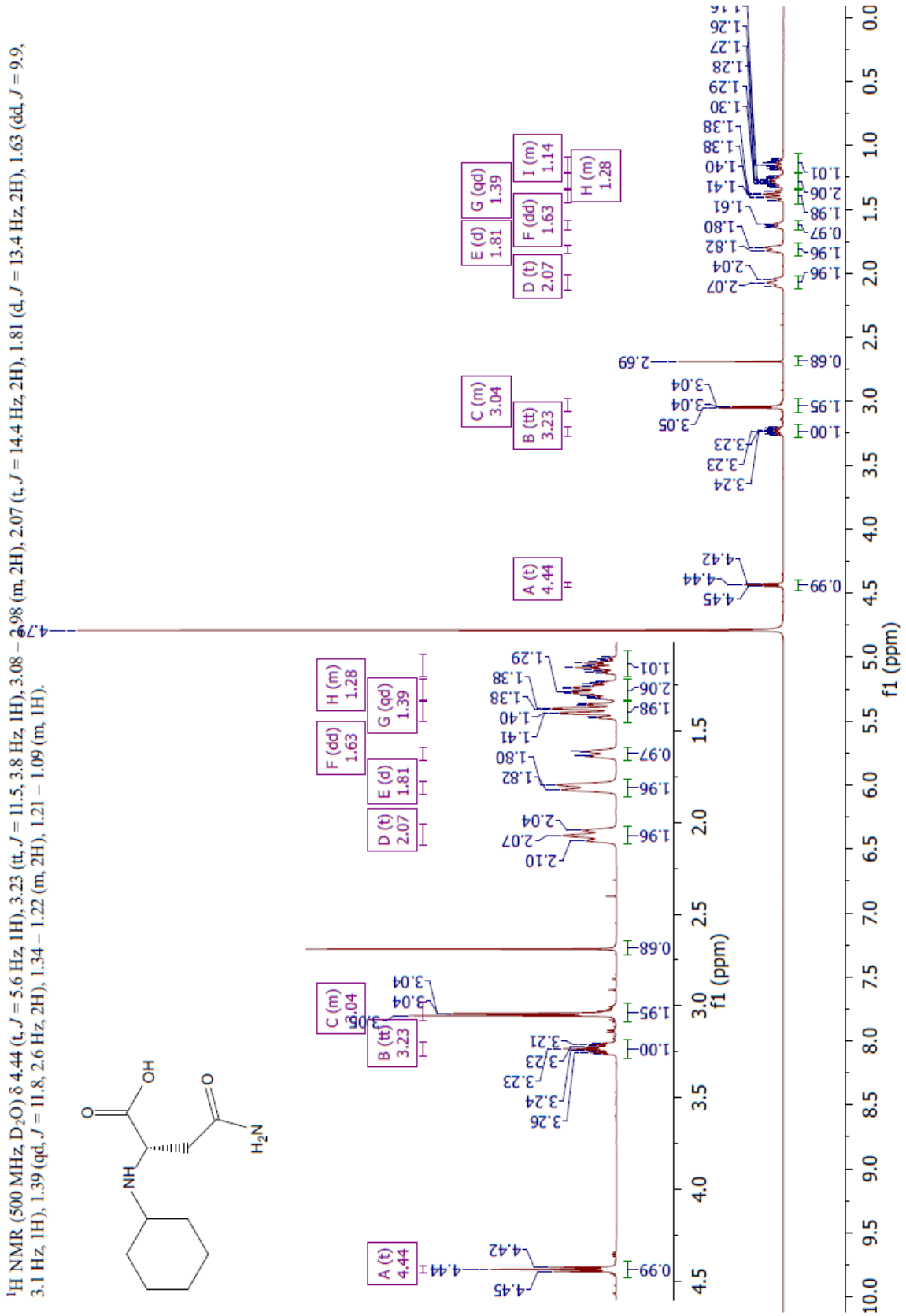

Figure 17. ^{1}H NMR spectra for compound **3h**

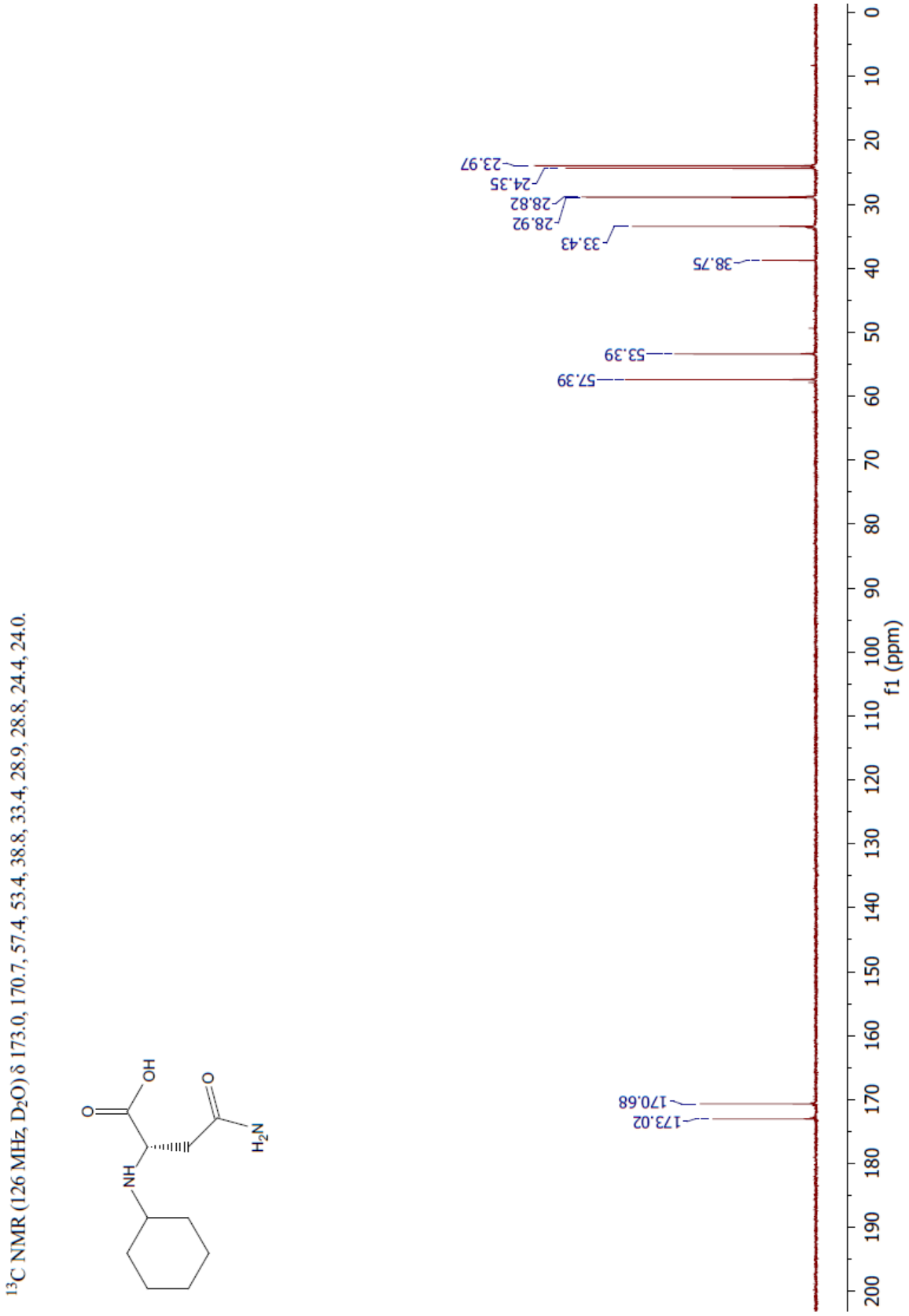

Figure 18. ^{13}C NMR spectra for compound **3h**

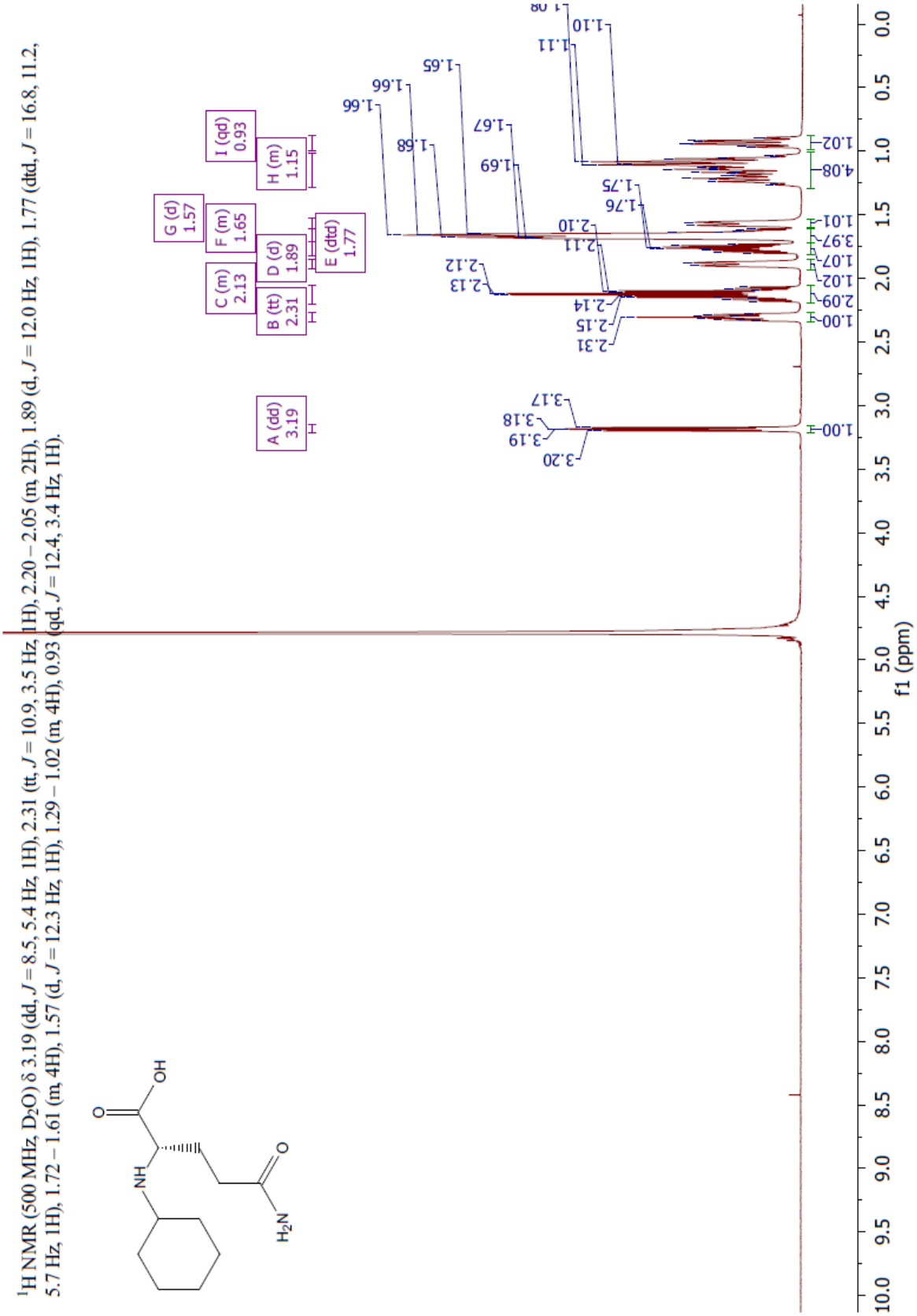

Figure 19. ^{1}H NMR spectra for compound **3i**

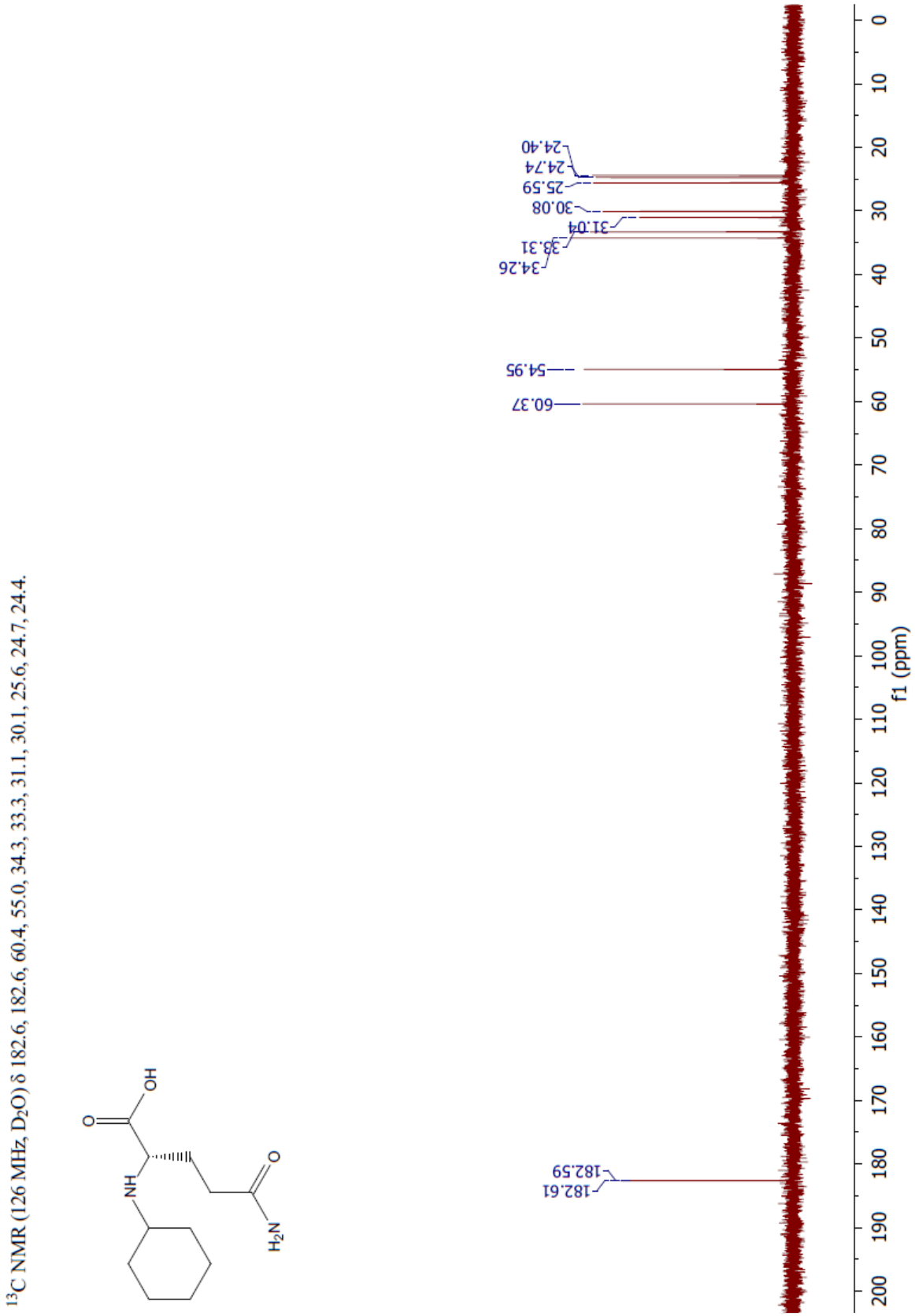

Figure 20. ^{13}C NMR spectra for compound **3i**

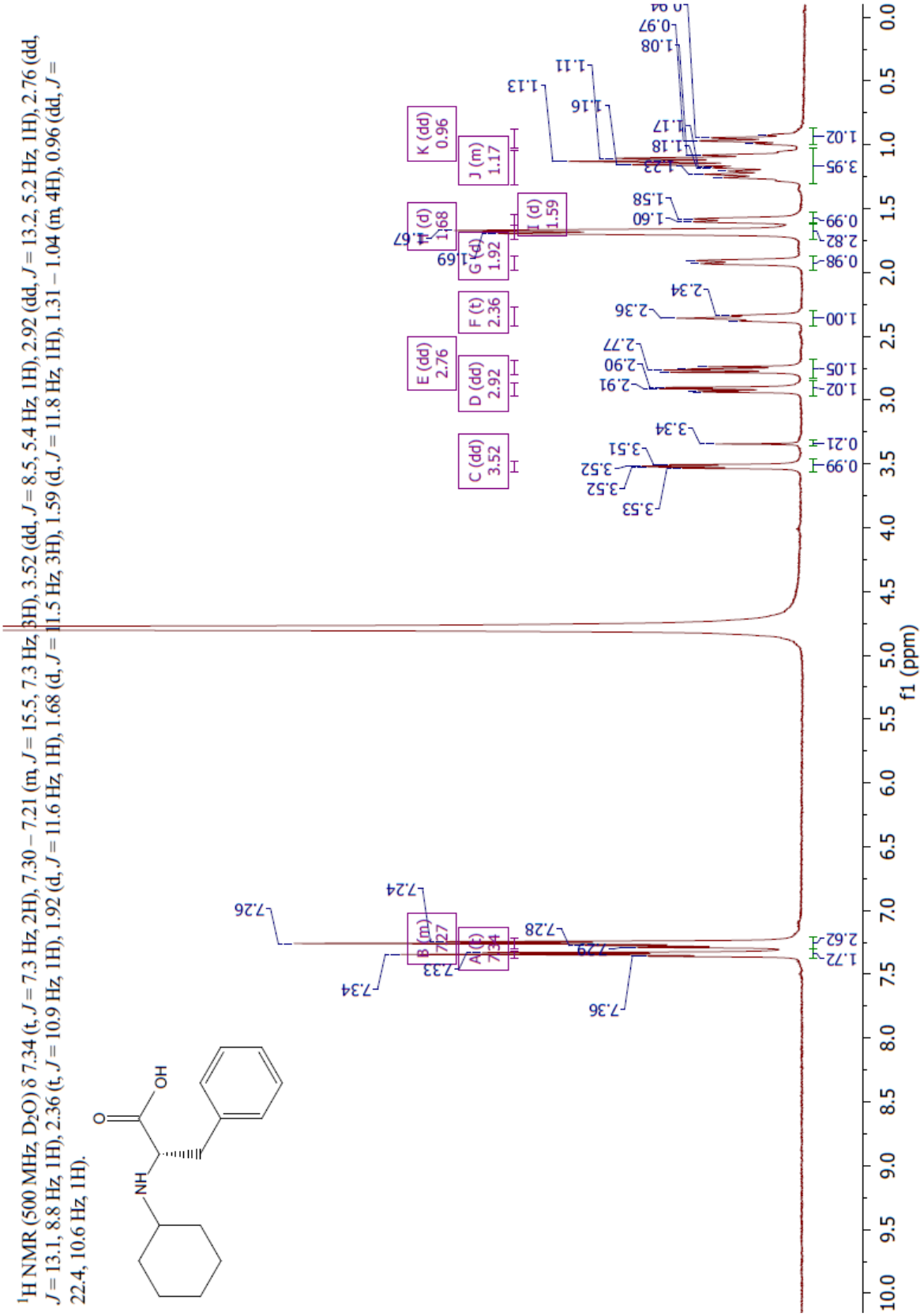

Figure 21. ^{1}H NMR spectra for compound **3j**

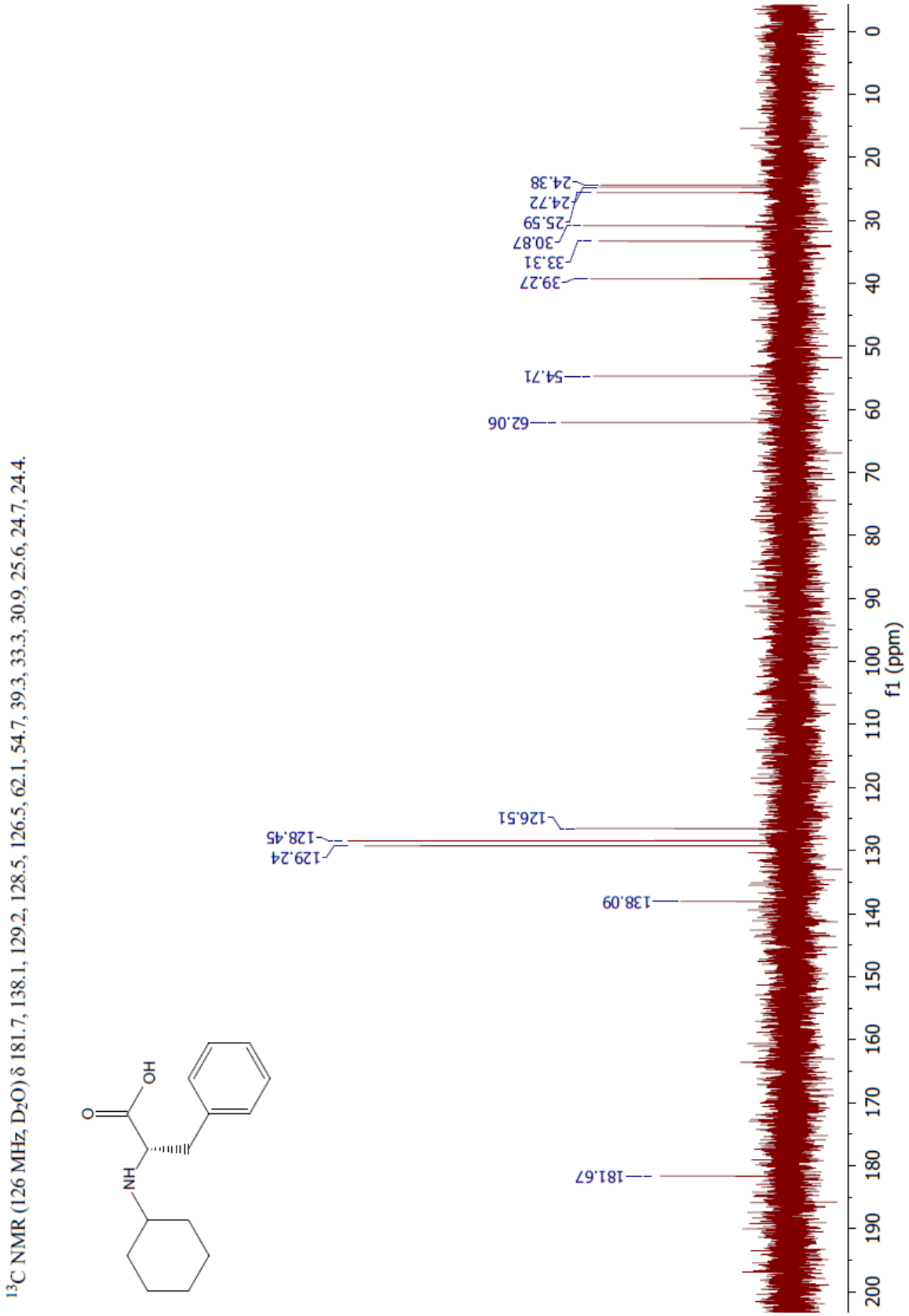

Figure 22. ^{13}C NMR spectra for compound **3j**

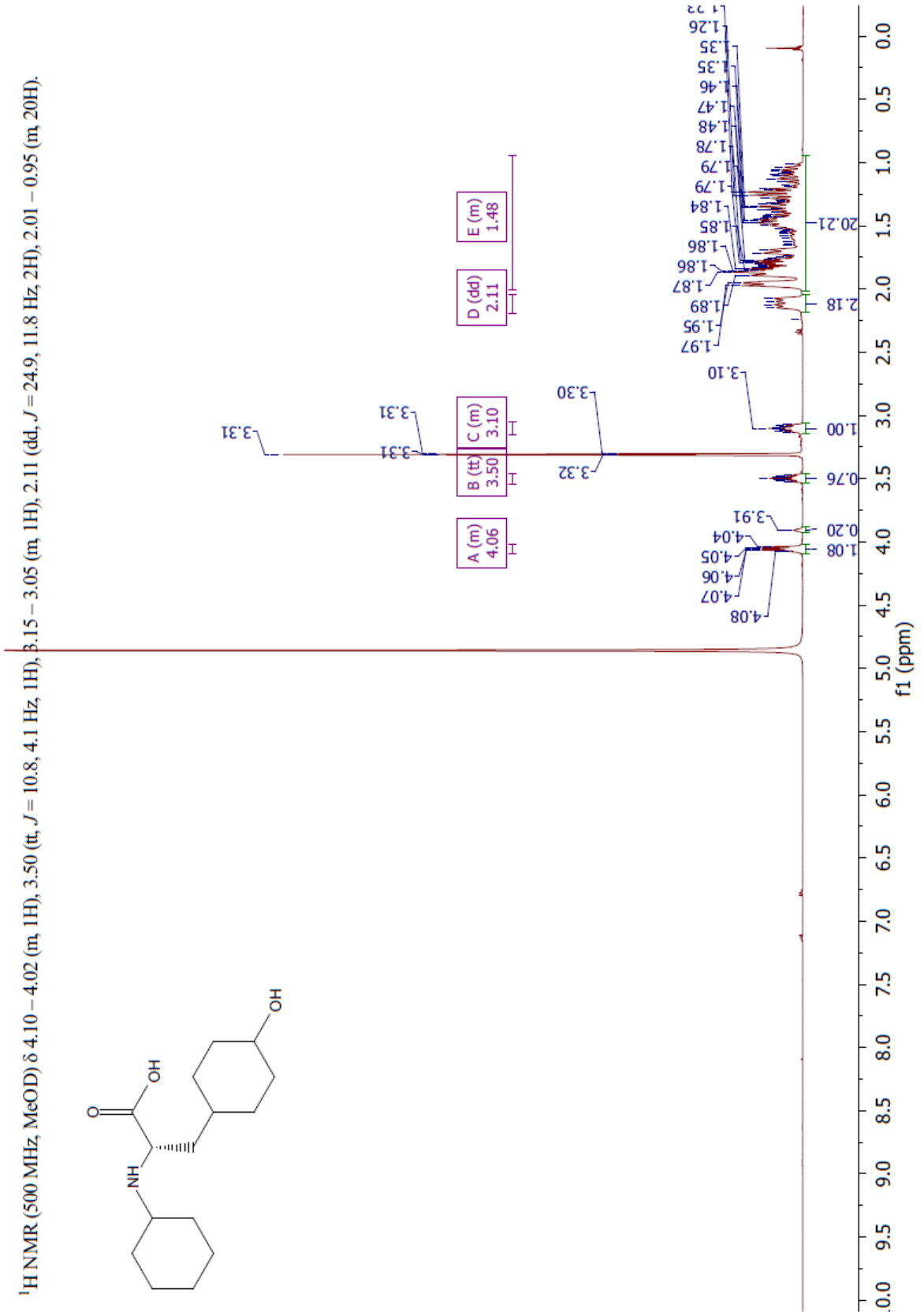

Figure 23. ^{1}H NMR spectra for compound **3k**

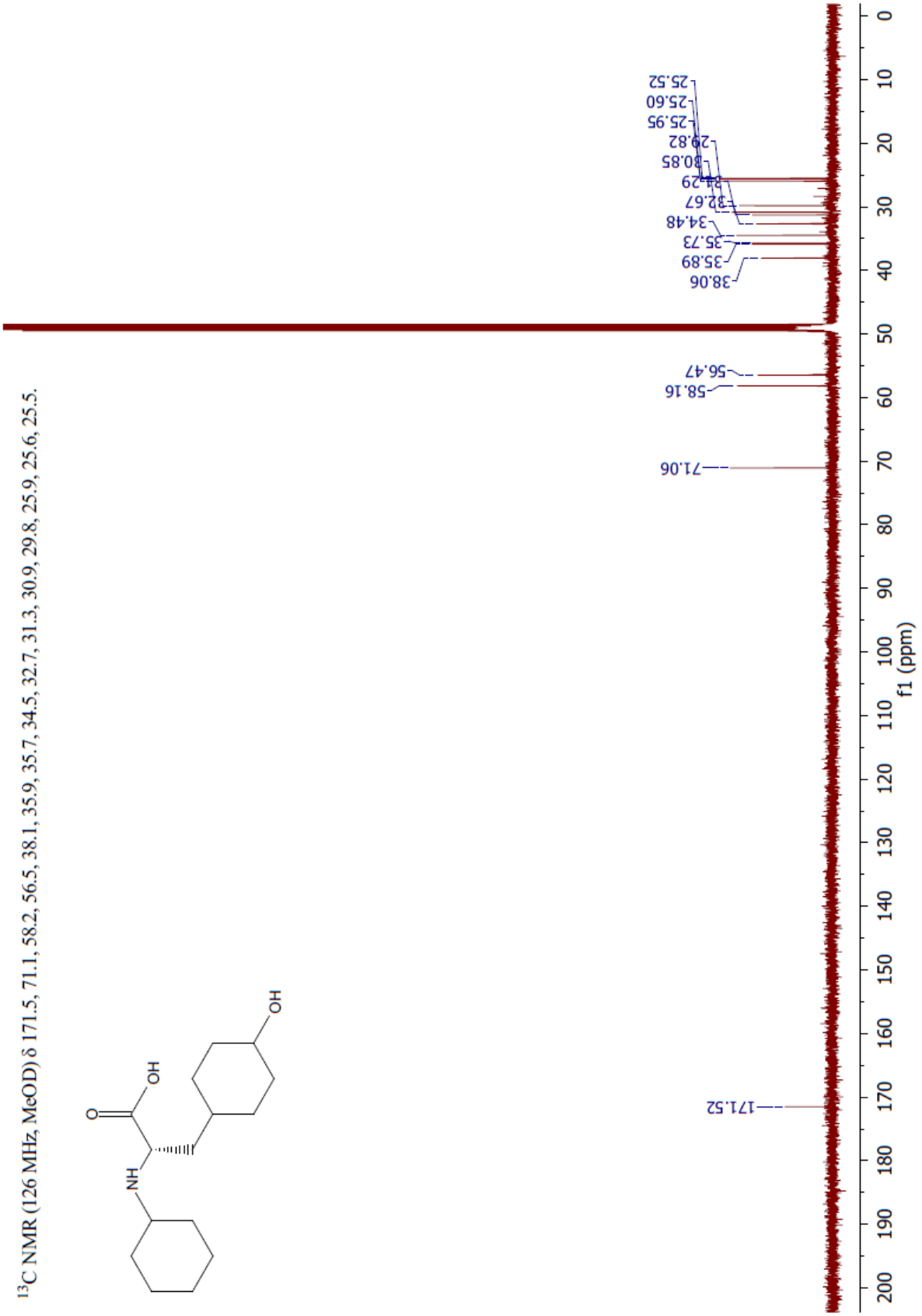

Figure 24. ^{13}C NMR spectra for compound **3k**

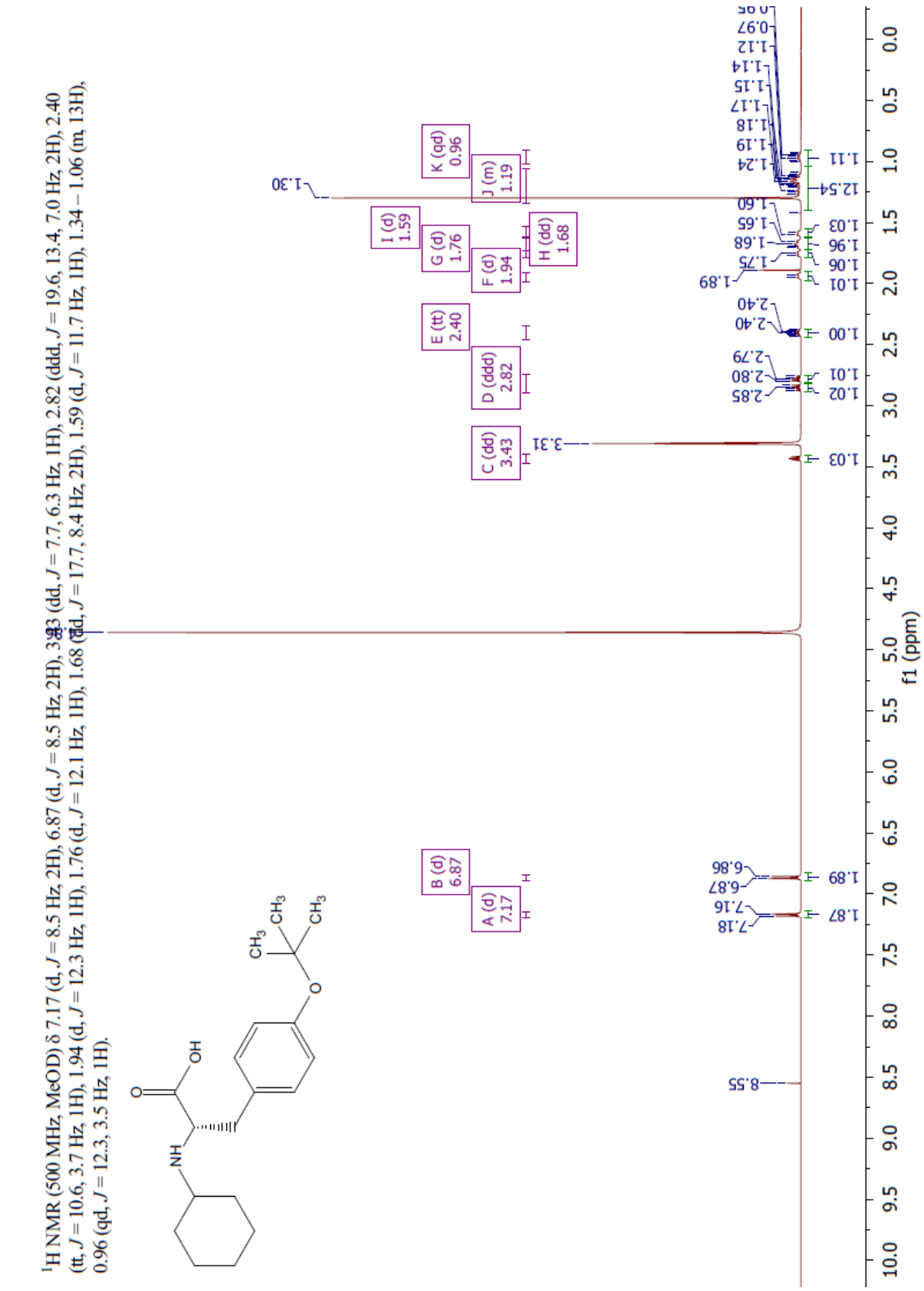

Figure 25. ^{1}H NMR spectra for compound **3l**

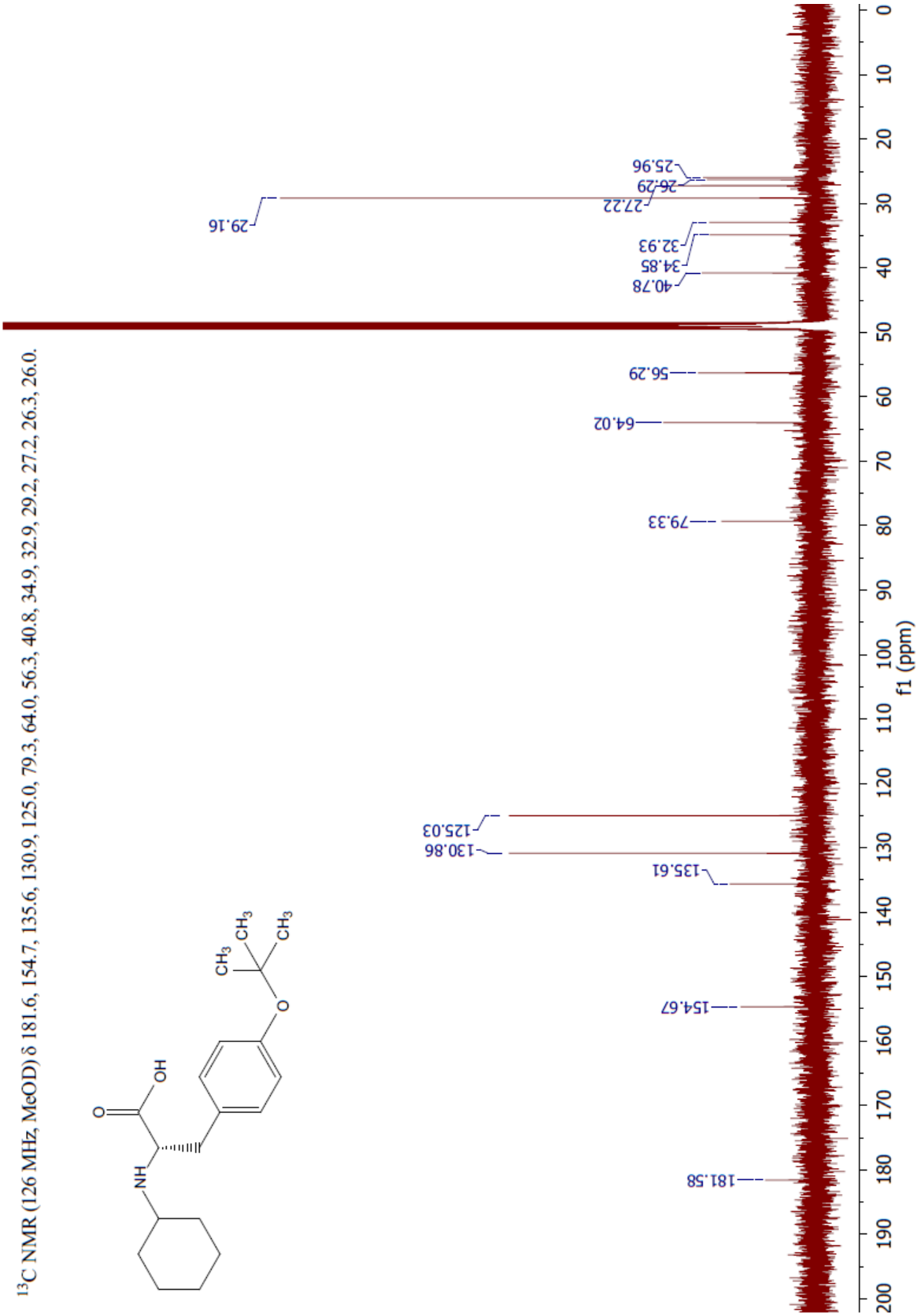

Figure 26. ^{13}C NMR spectra for compound **3l**

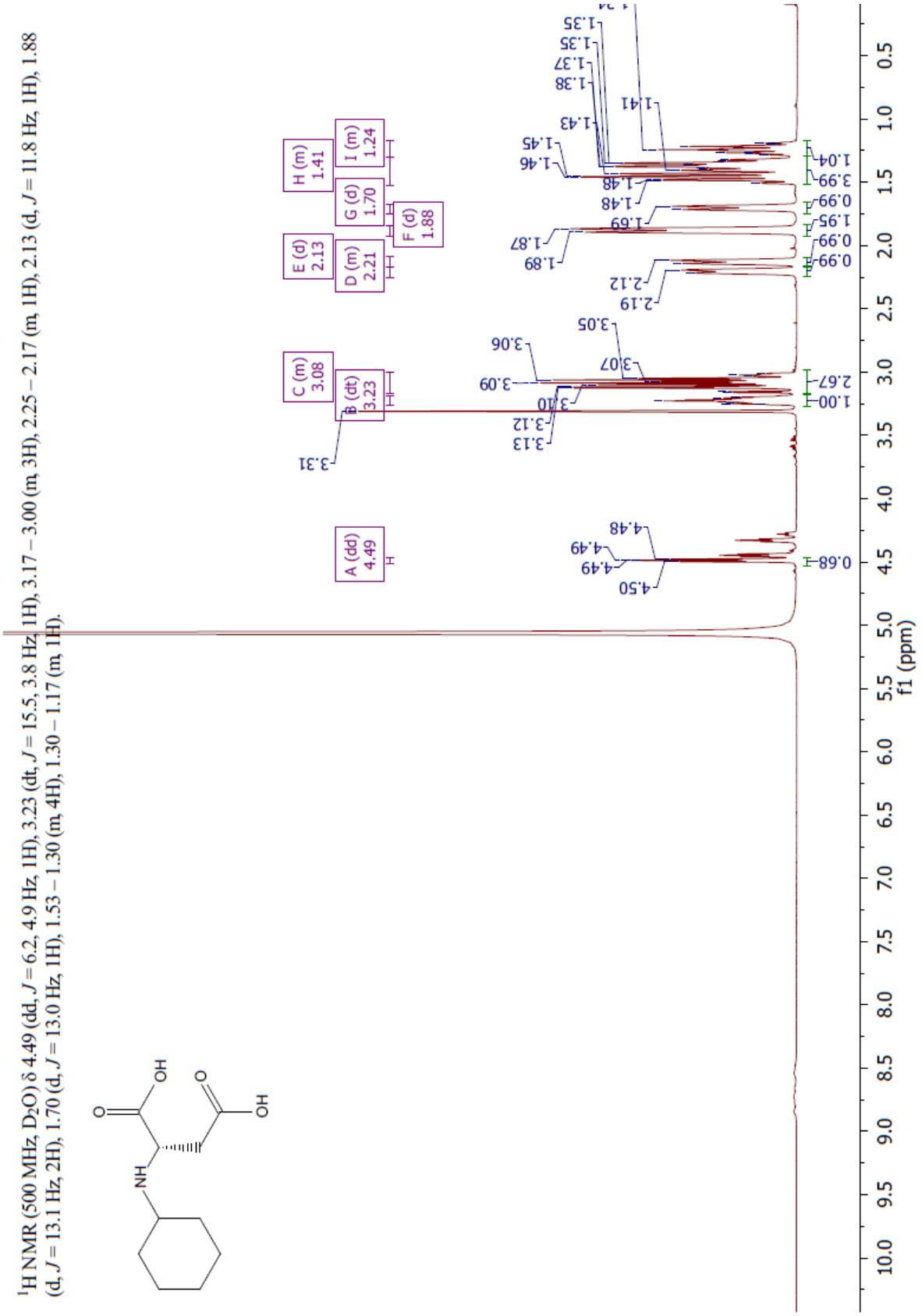

Figure 27. ^{1}H NMR spectra for compound **3m**

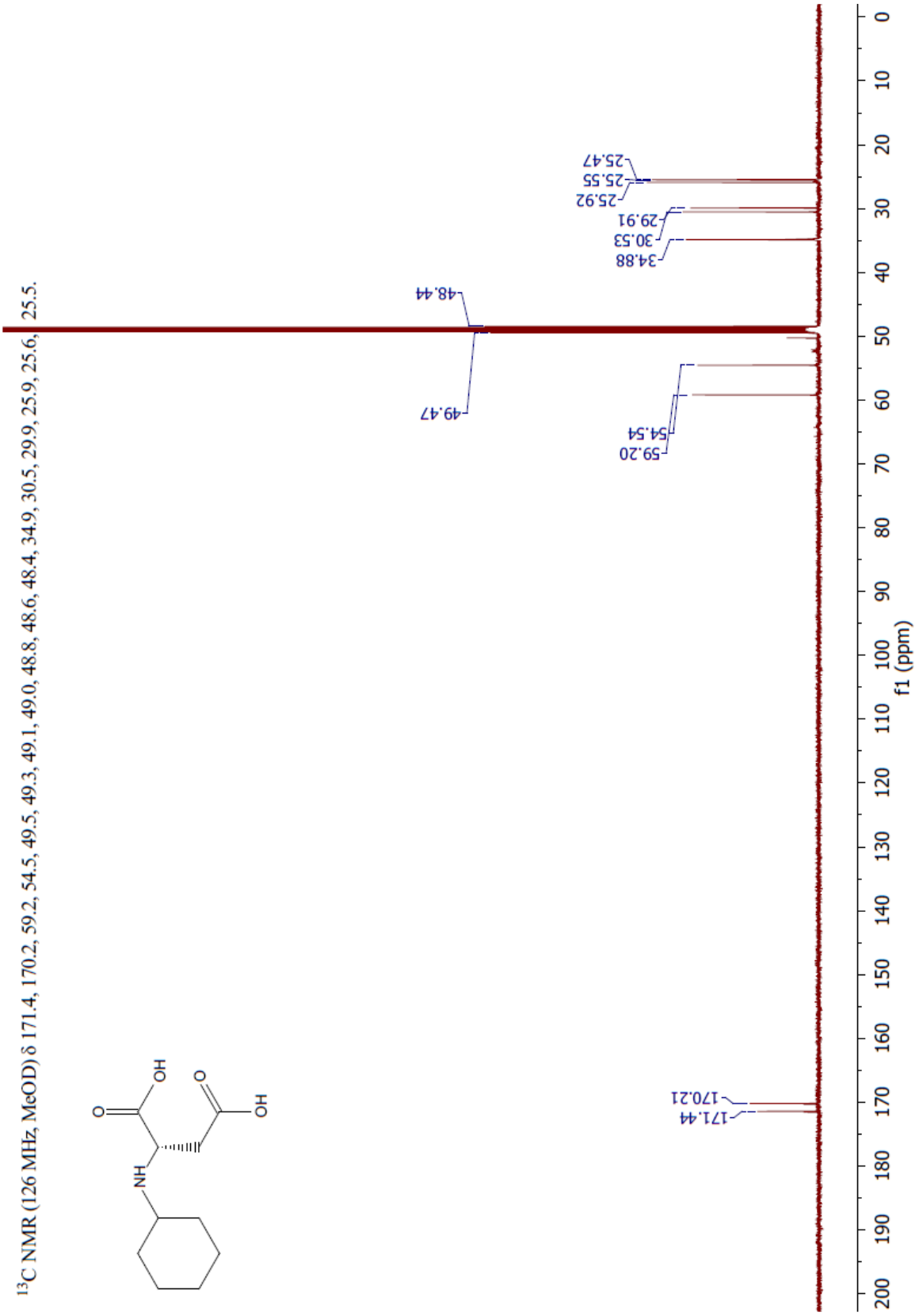

Figure 28. ^{13}C NMR spectra for compound **3m**

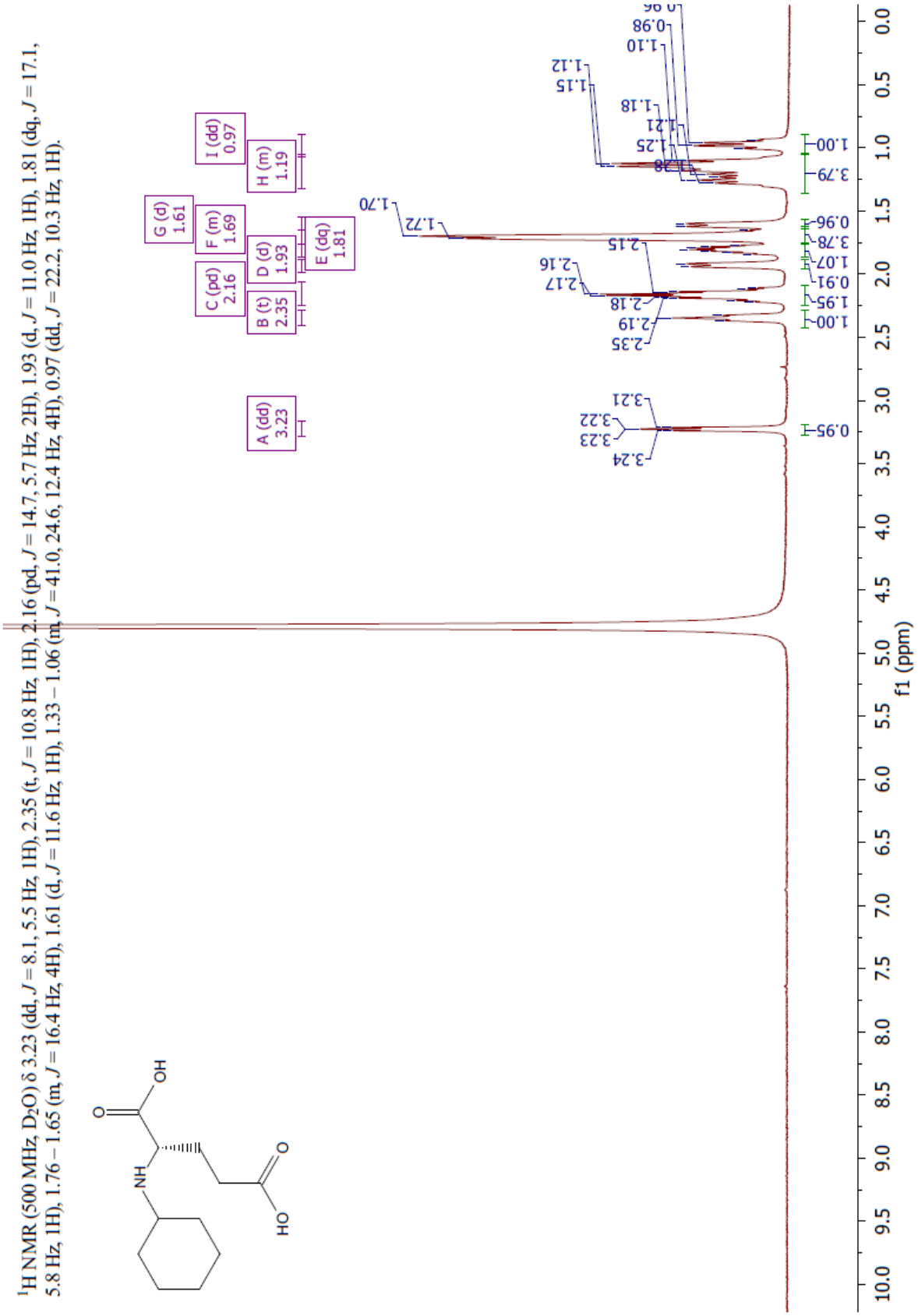

Figure 29. ^{1}H NMR spectra for compound **3n**

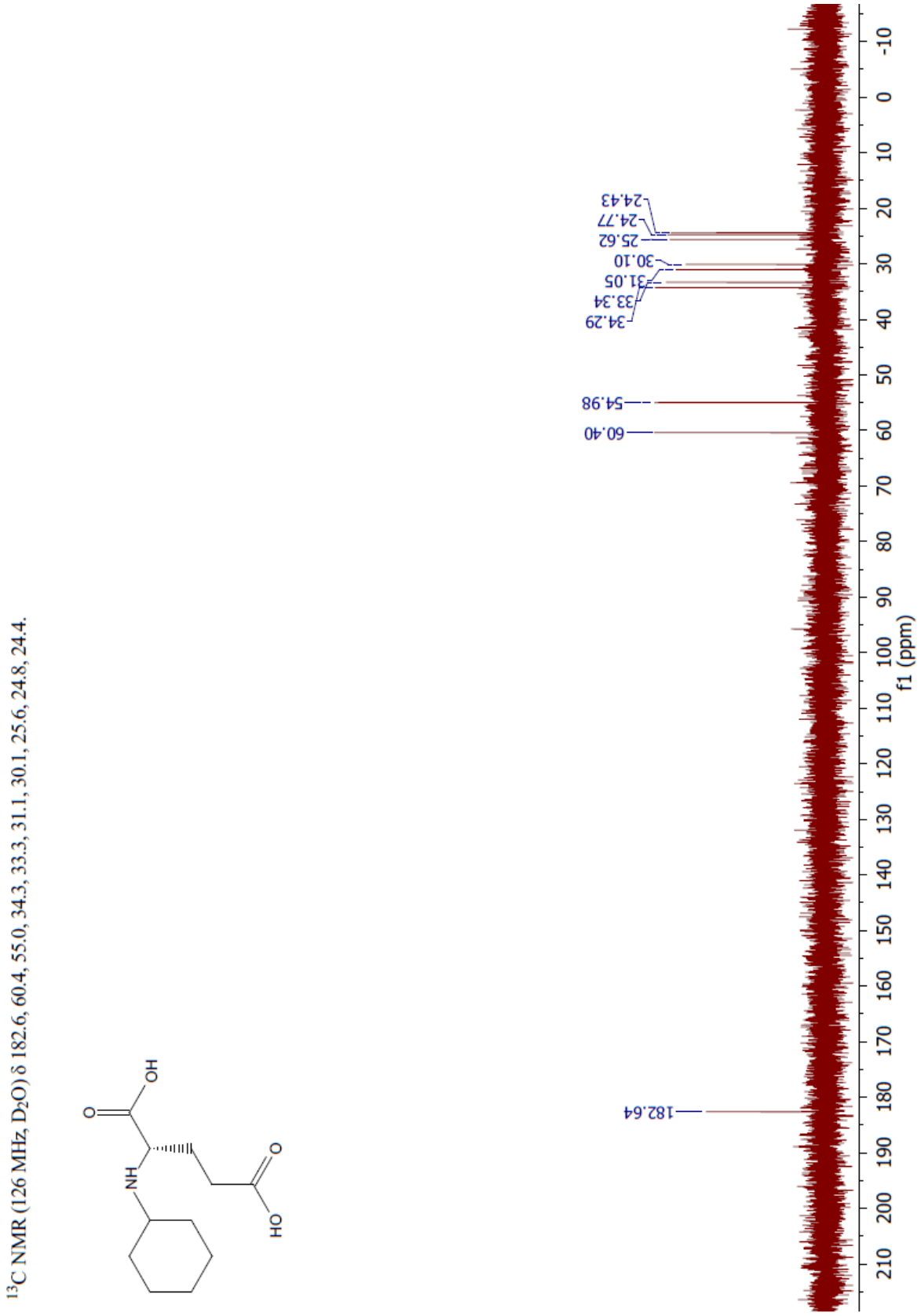

Figure 30. ^{13}C NMR spectra for compound **3n**

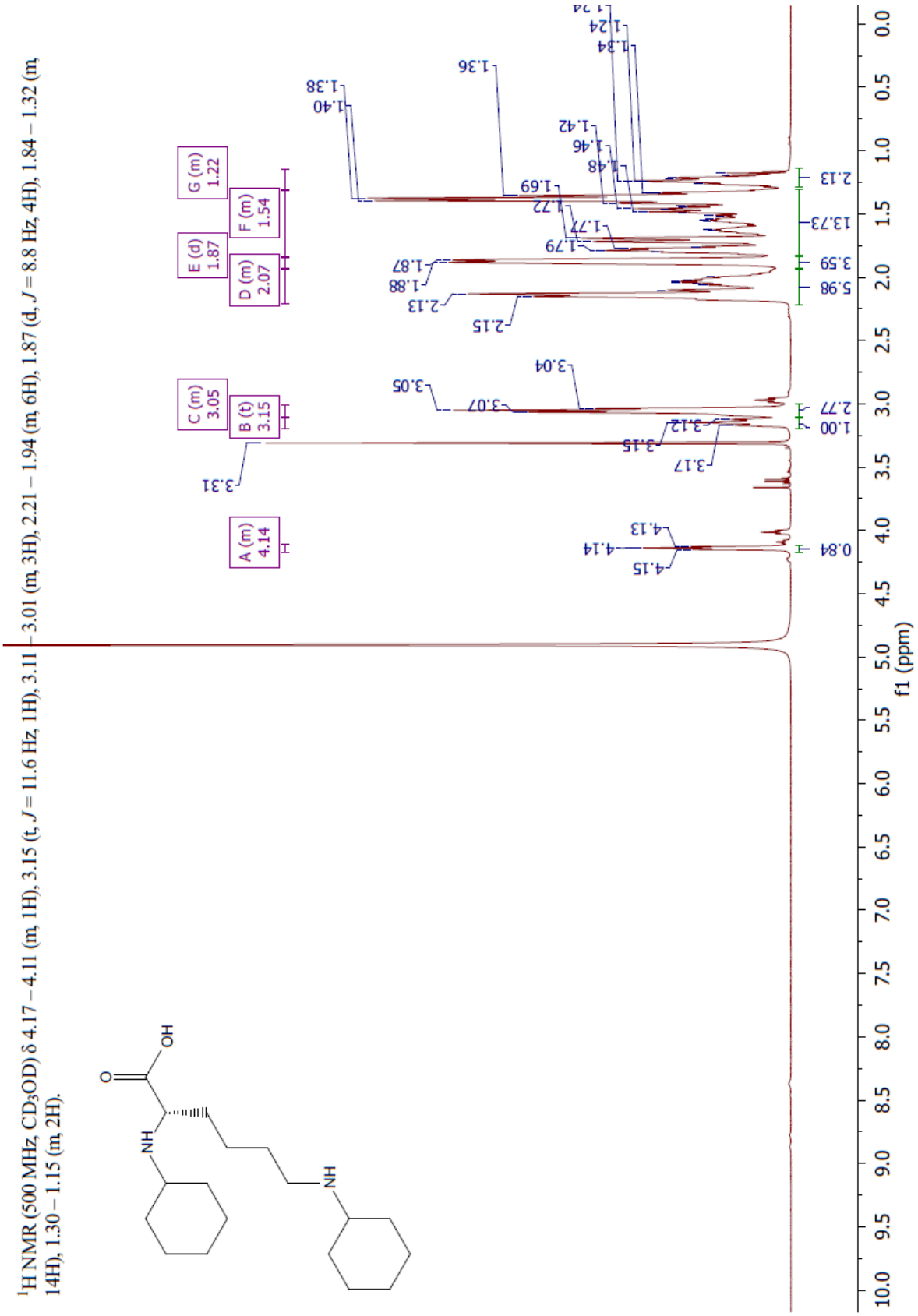

Figure 31. ^{1}H NMR spectra for compound **3o**

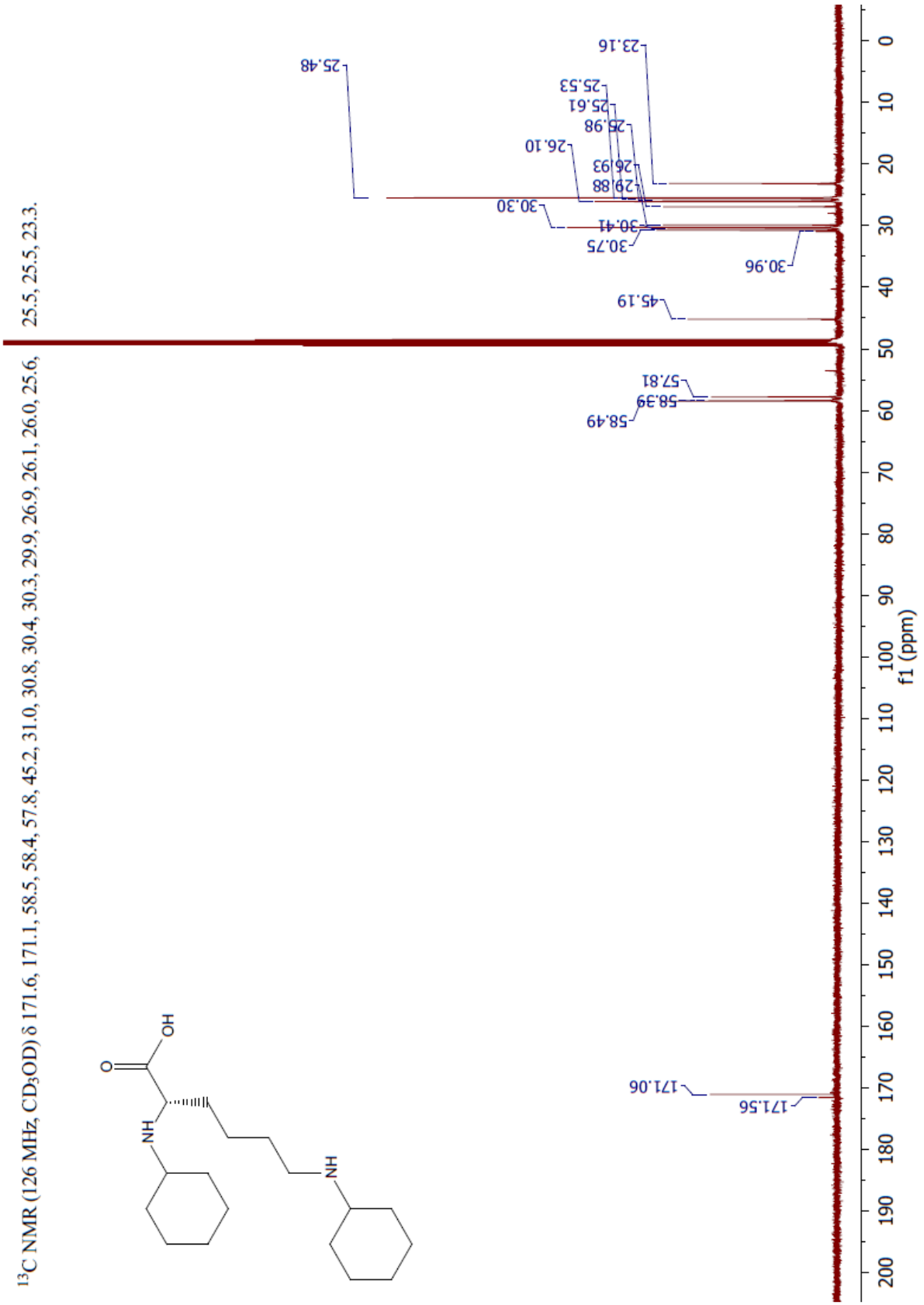

Figure 32. ^{13}C NMR spectra for compound **3o**

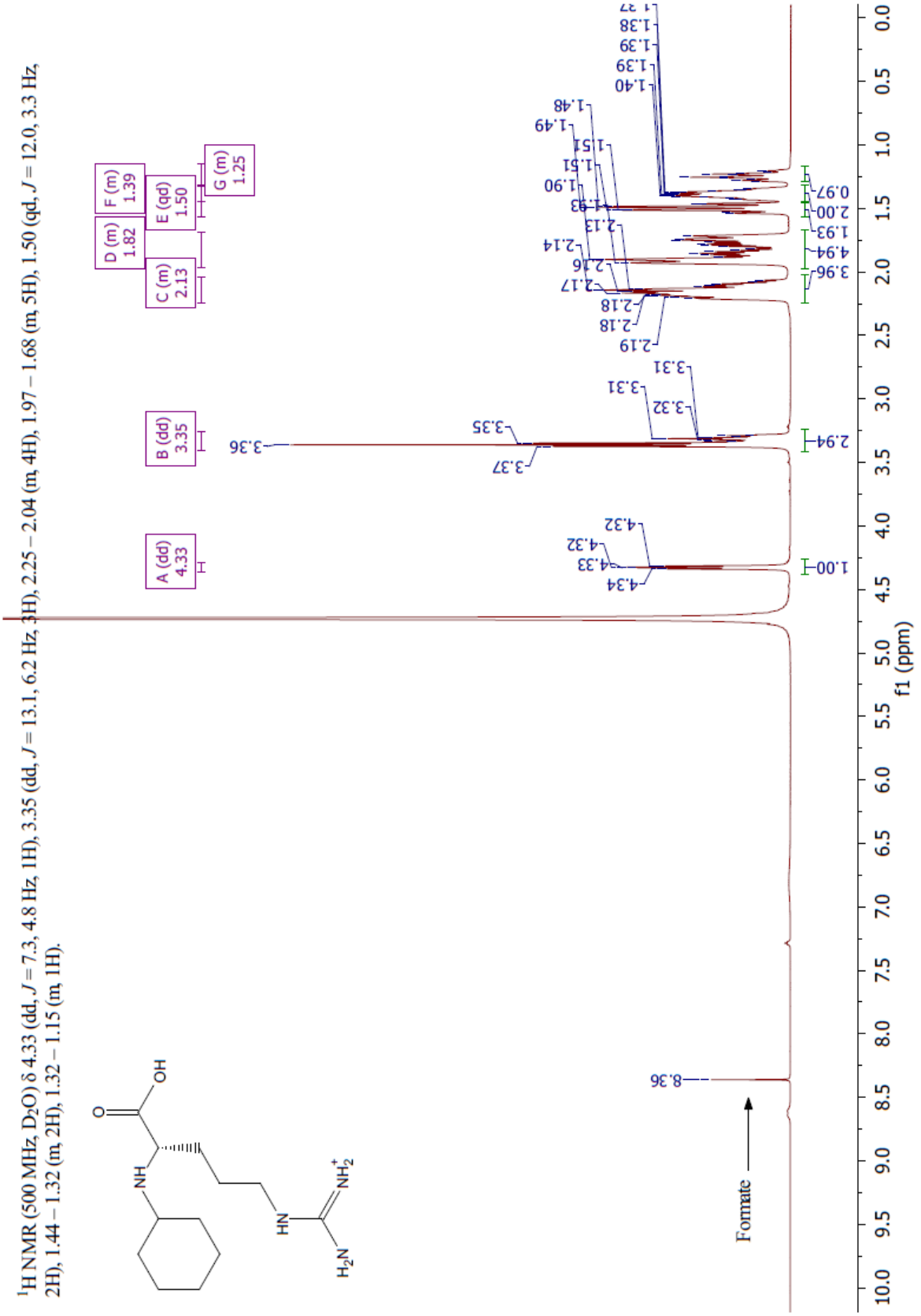

Figure 33. ^{1}H NMR spectra for compound **3p**

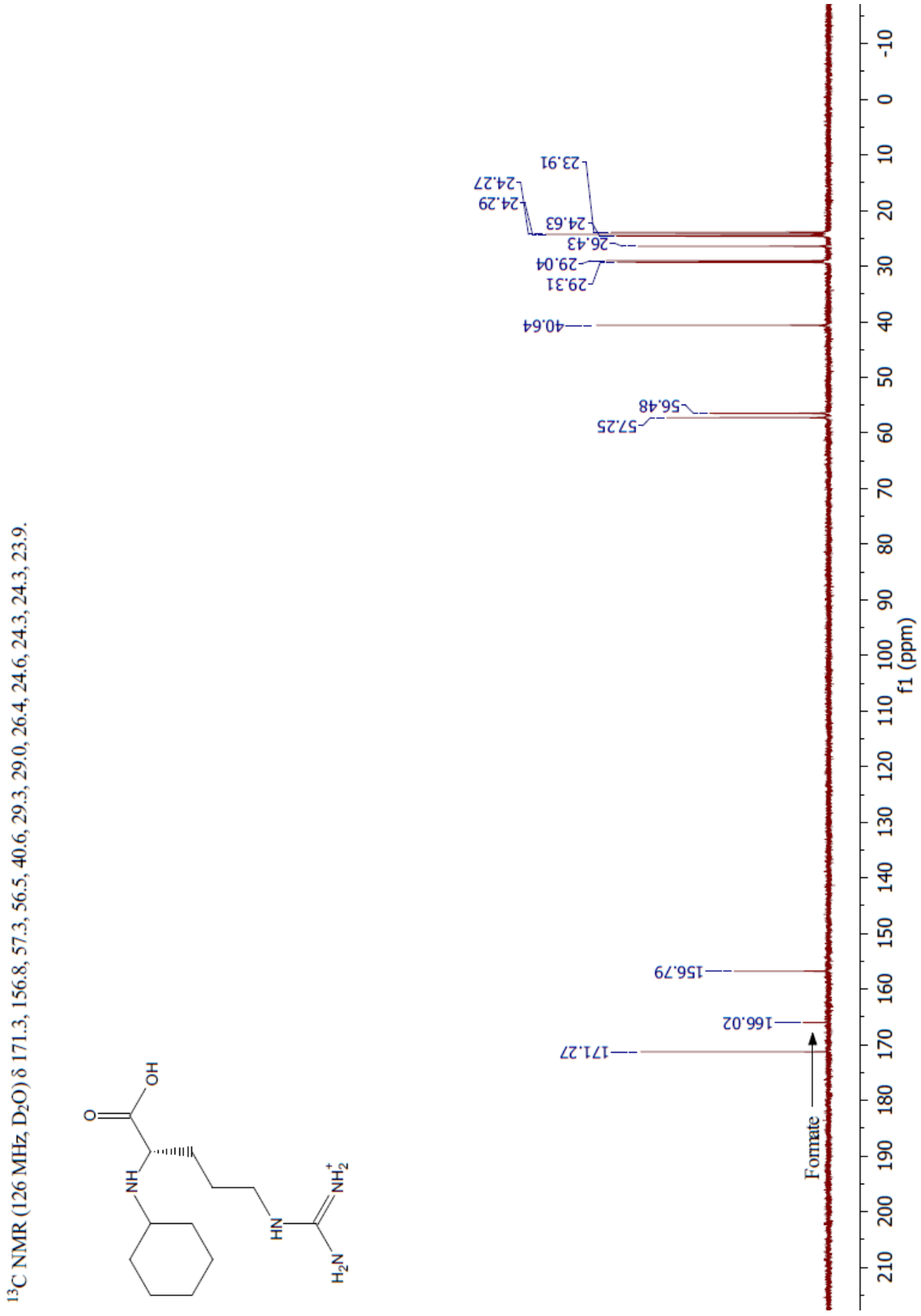

Figure 34. ^{13}C NMR spectra for compound **3p**

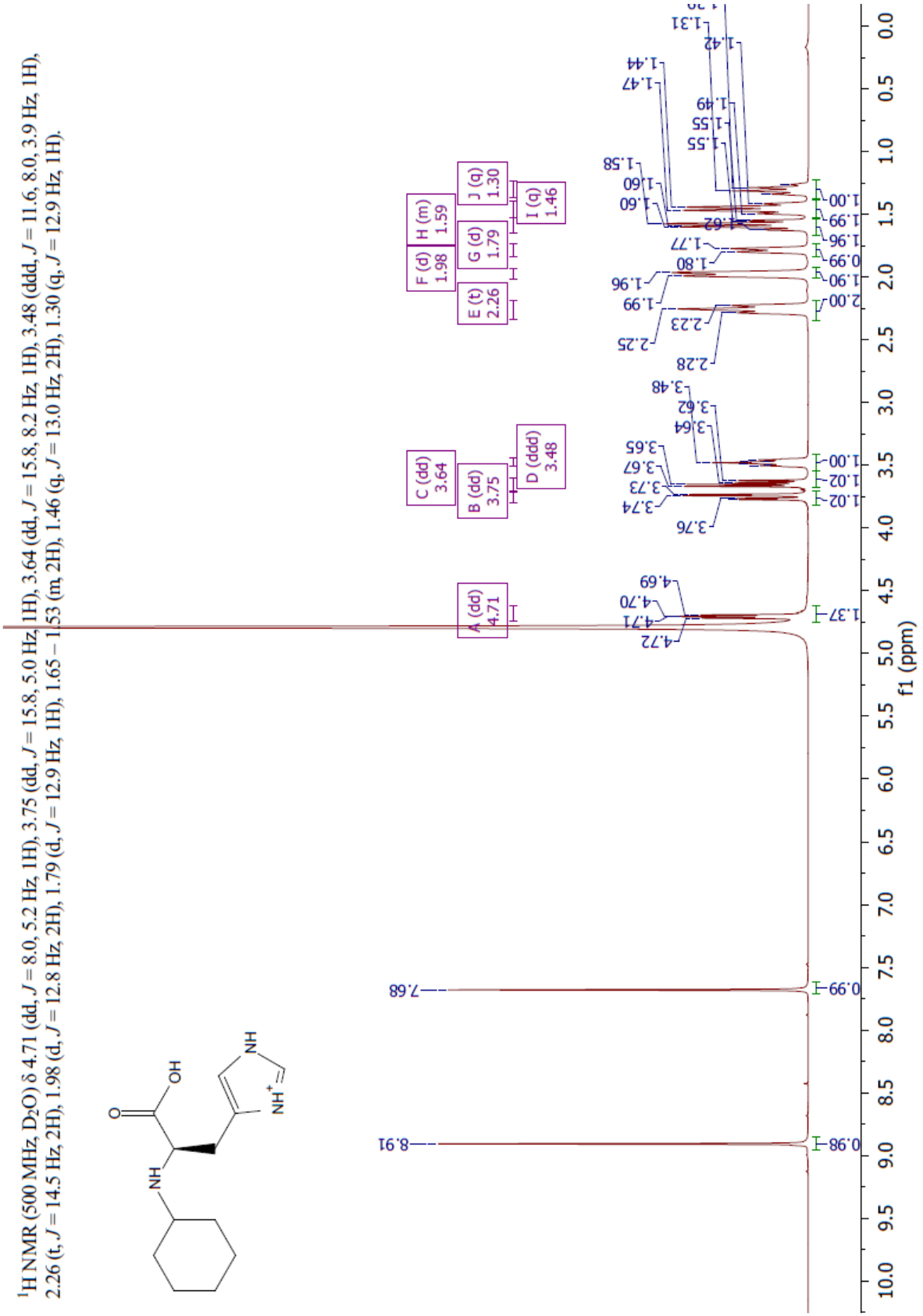

Figure 35. ^{1}H NMR spectra for compound **3q**

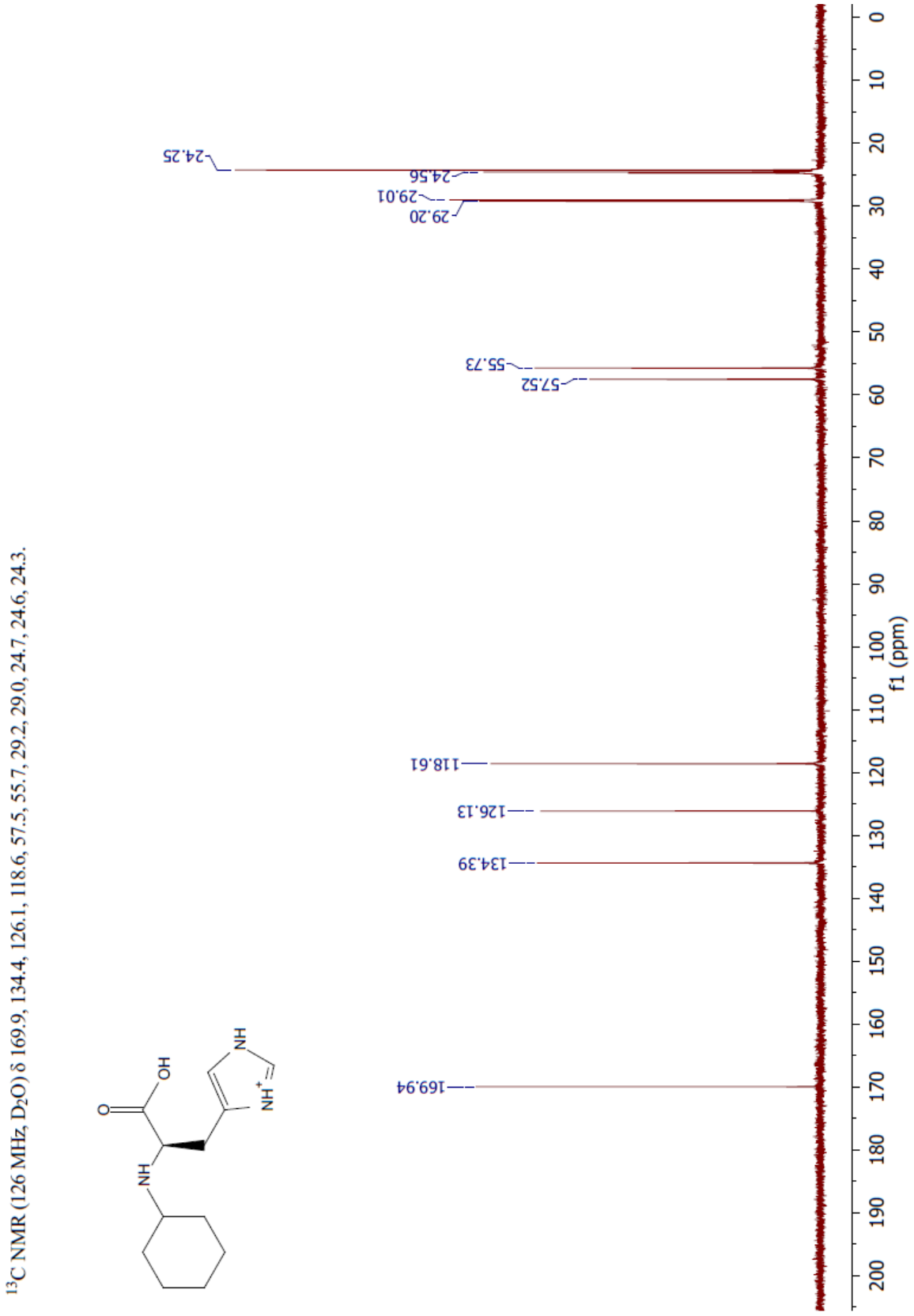

Figure 36. ^{13}C NMR spectra for compound **3q**

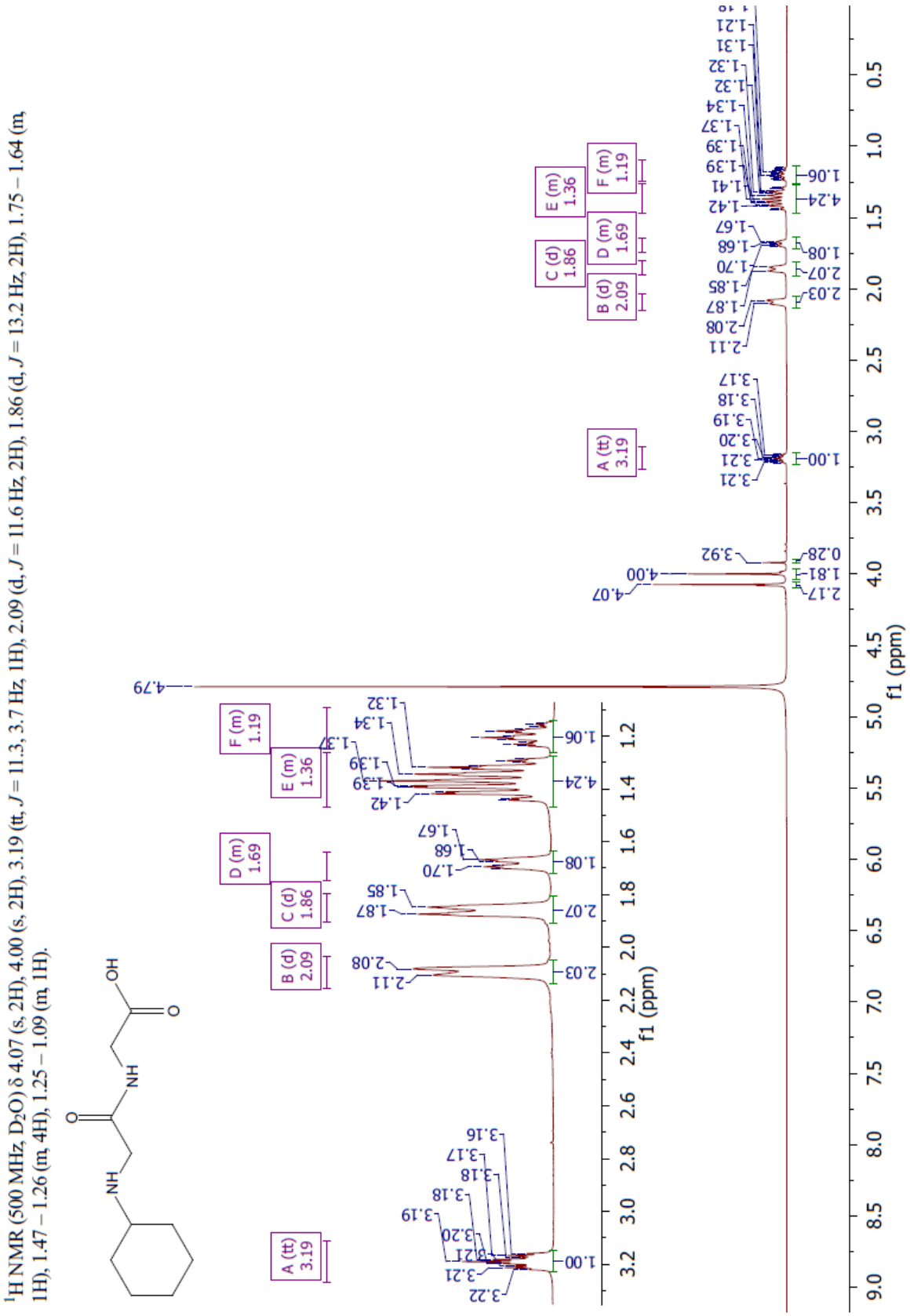

Figure 37. ^{1}H NMR spectra for compound **3s**

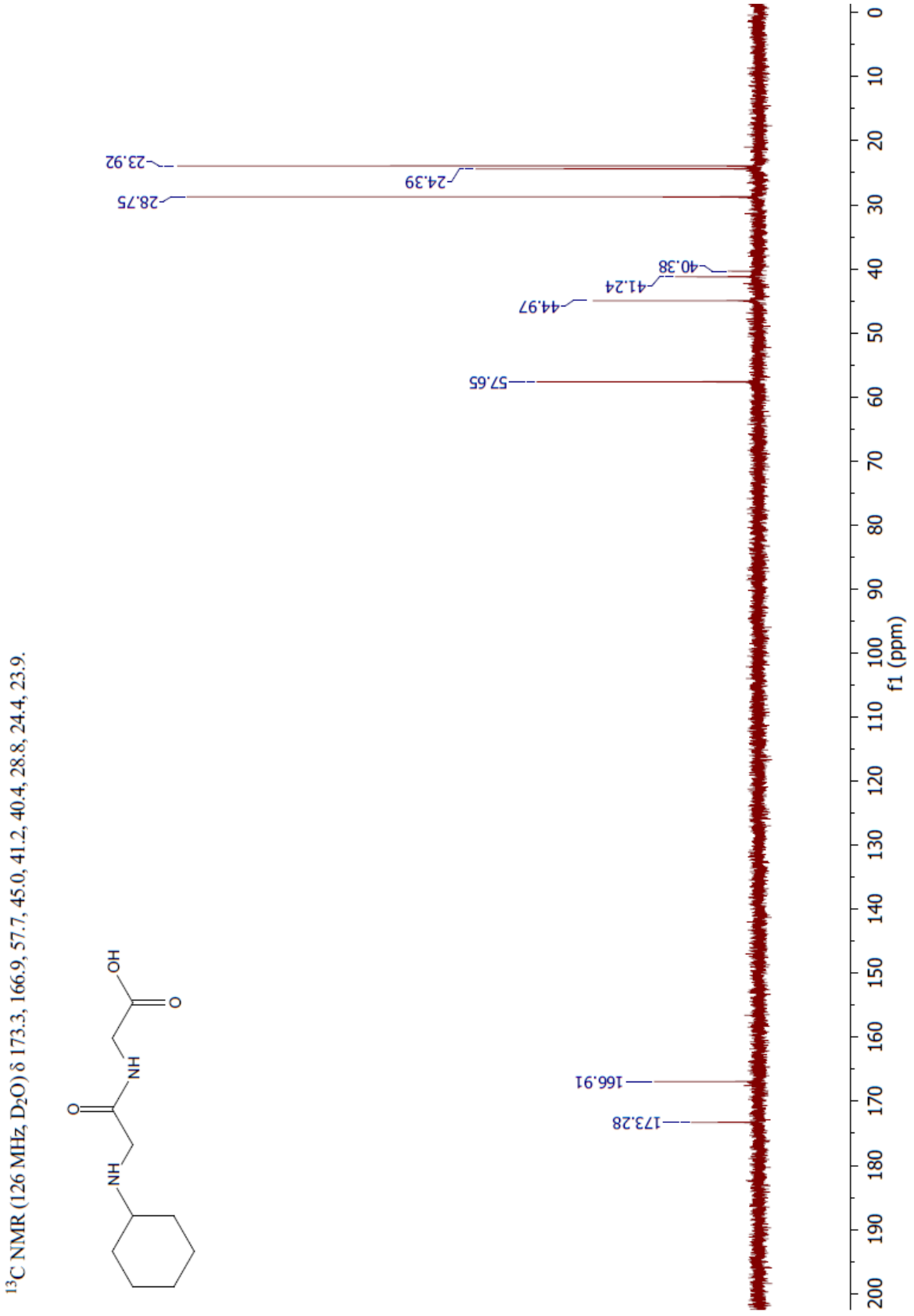

Figure 38. ^{13}C NMR spectra for compound **3s**

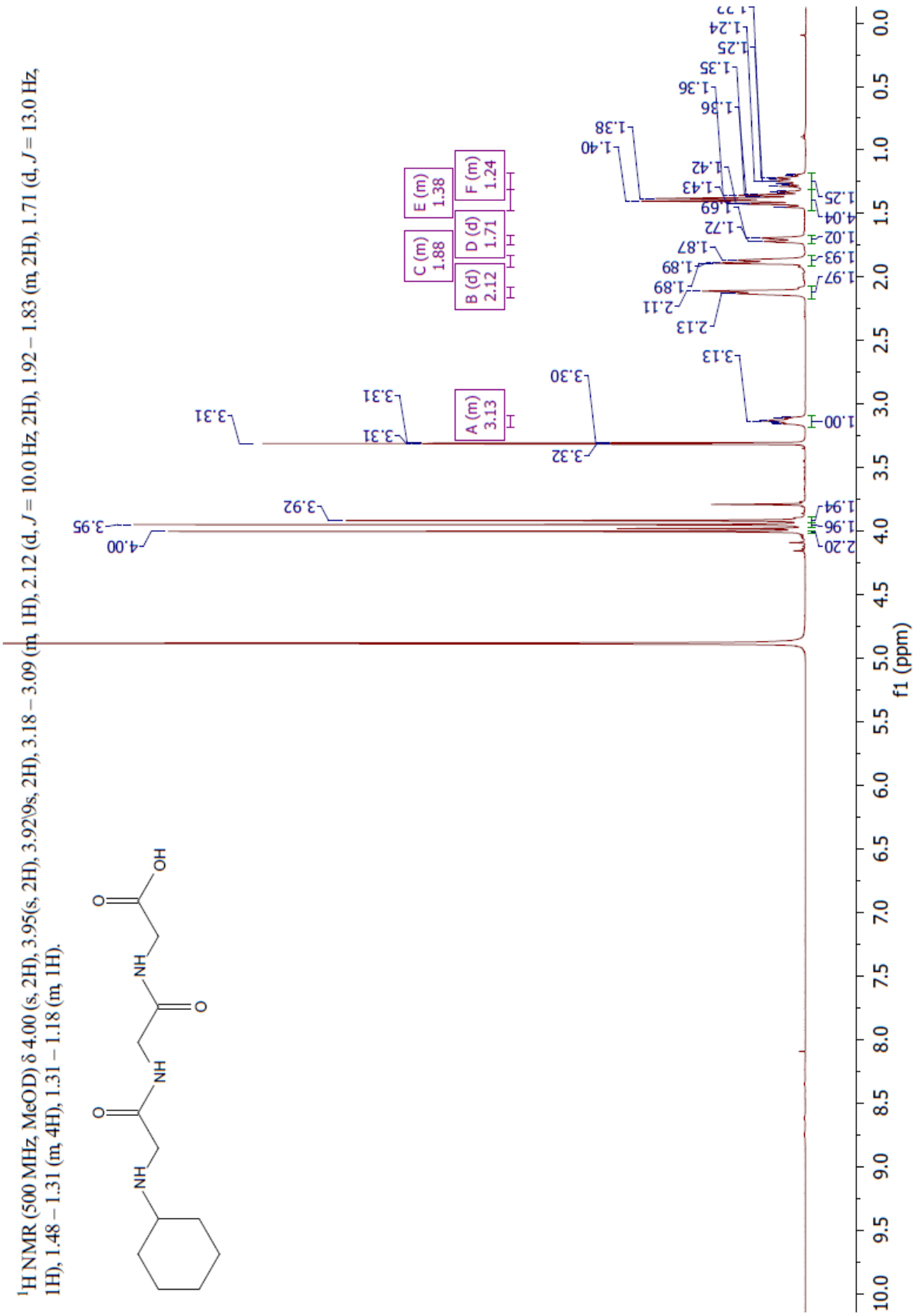

Figure 39. ^{1}H NMR spectra for compound **3t**

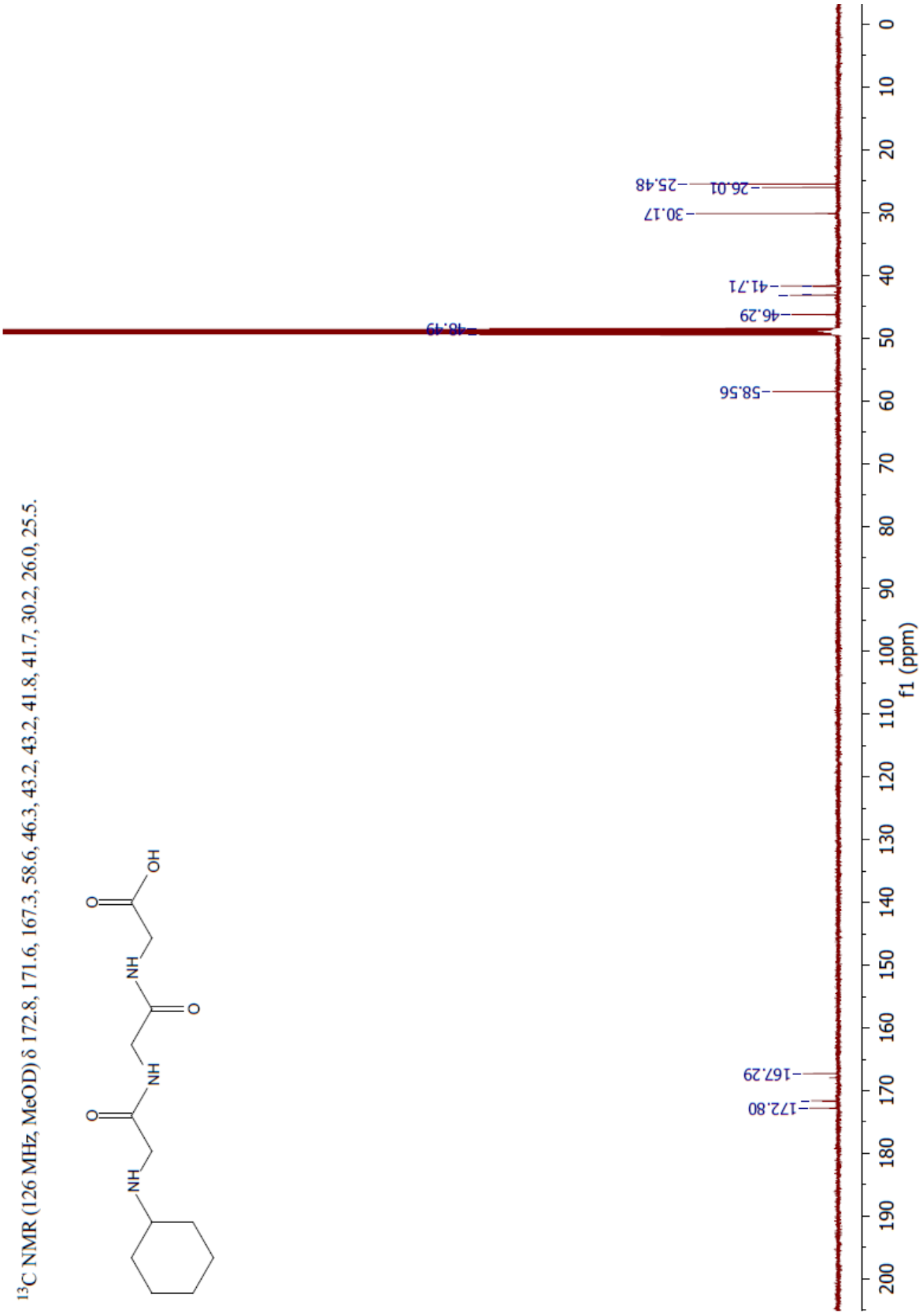

Figure 40. ^{13}C NMR spectra for compound **3t**

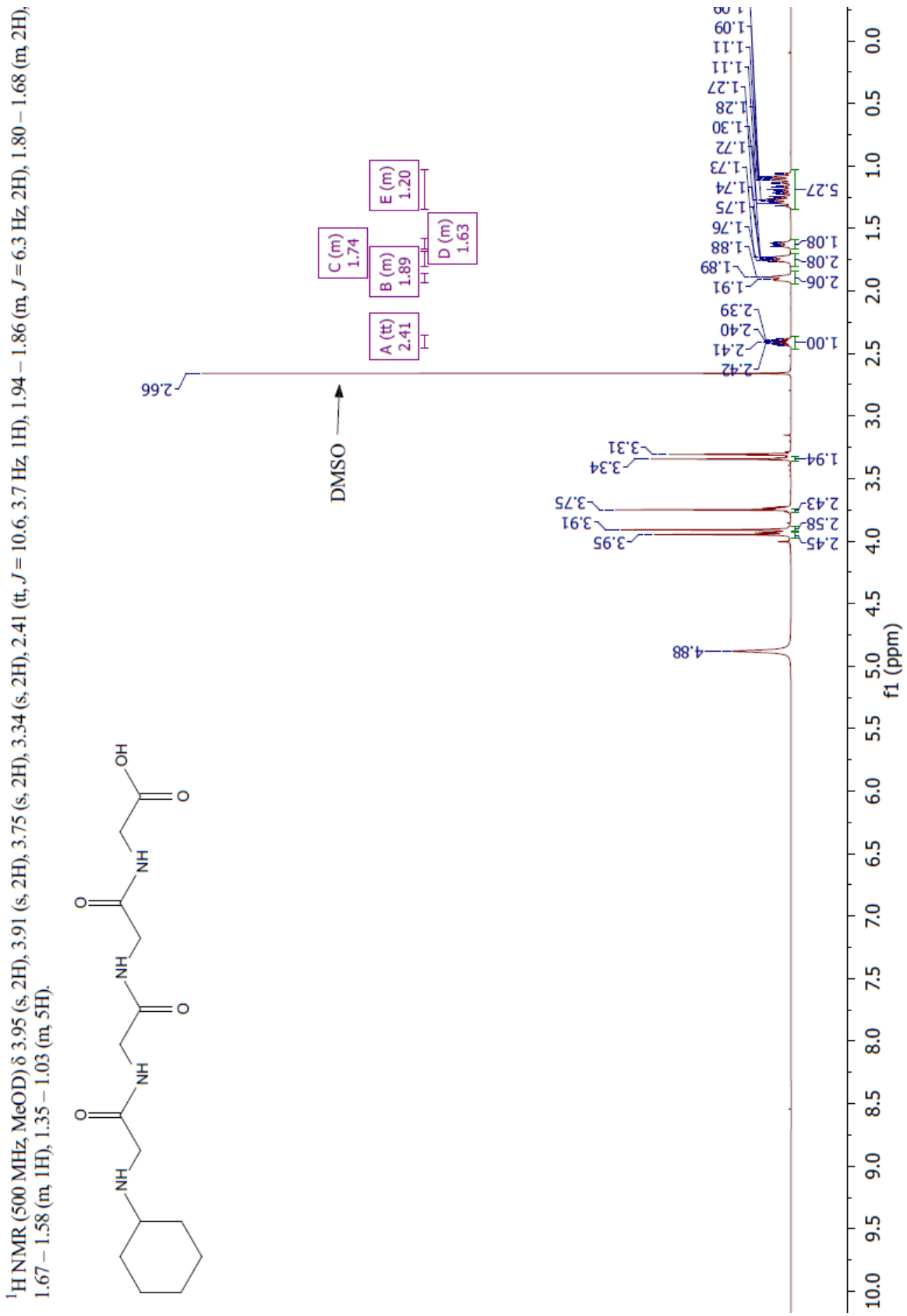

Figure 41. ^{1}H NMR spectra for compound **3u**

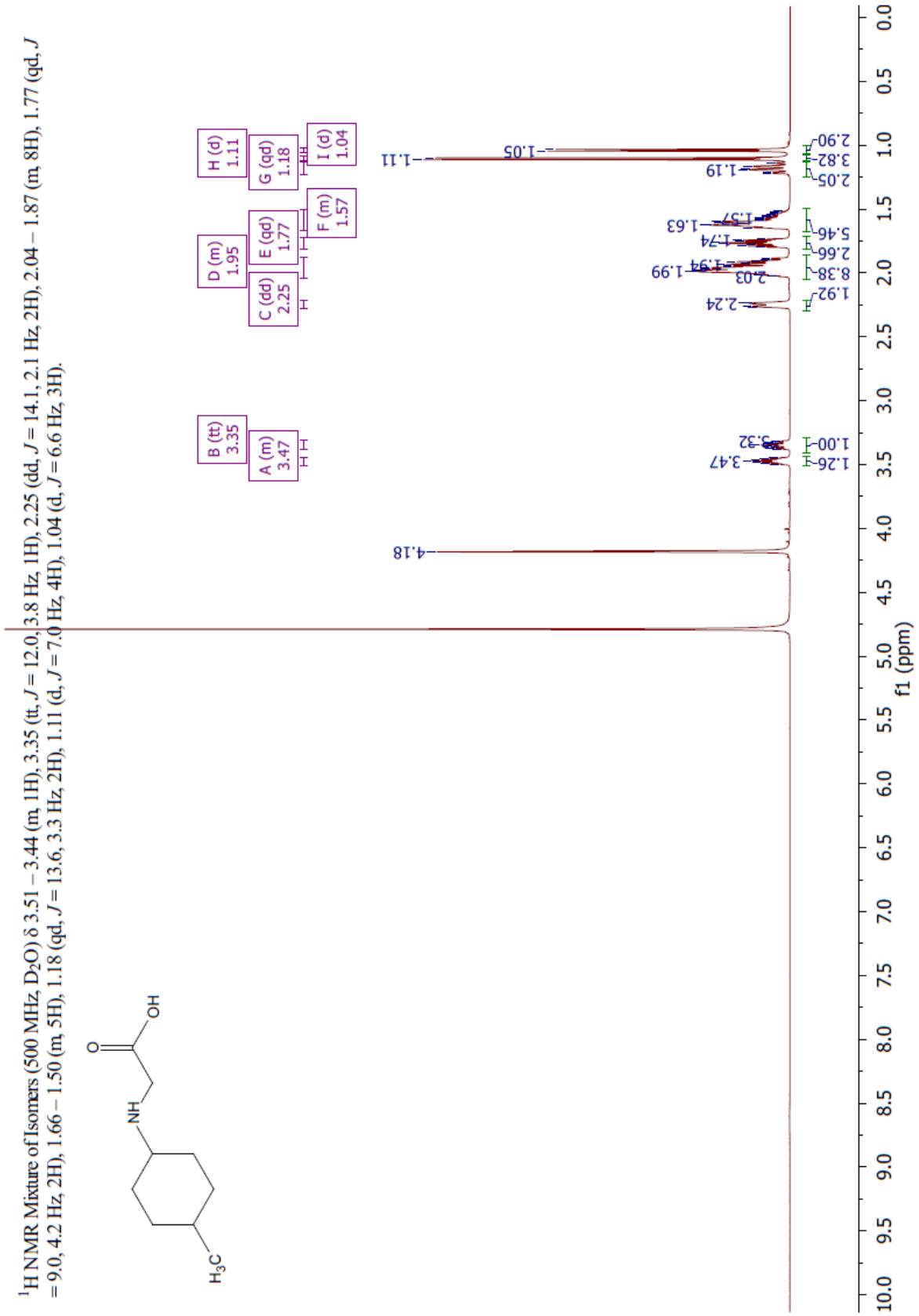

Figure 42. ^{1}H NMR spectra for compound **3v**

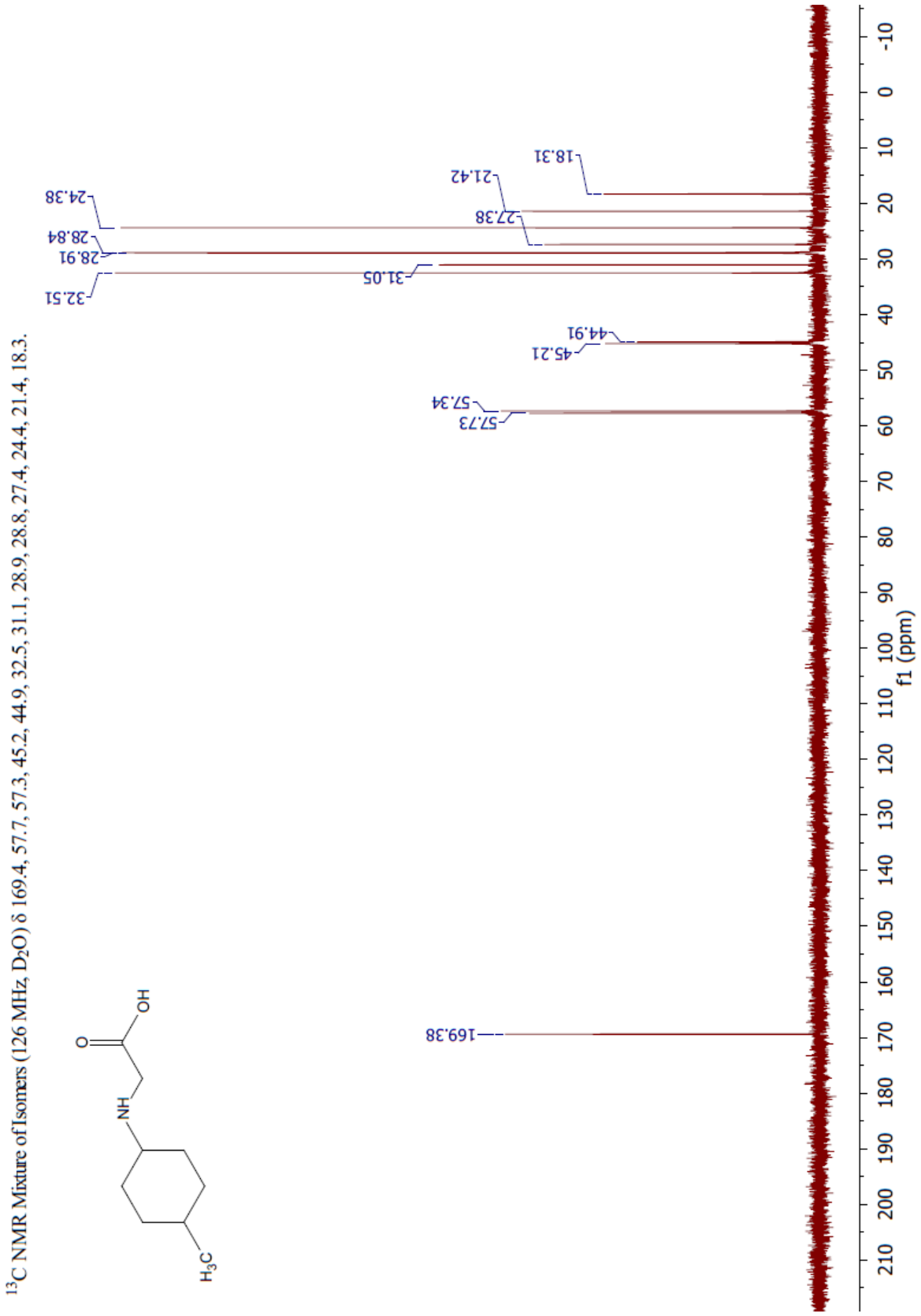

Figure 43. ^{13}C NMR spectra for compound **3v**

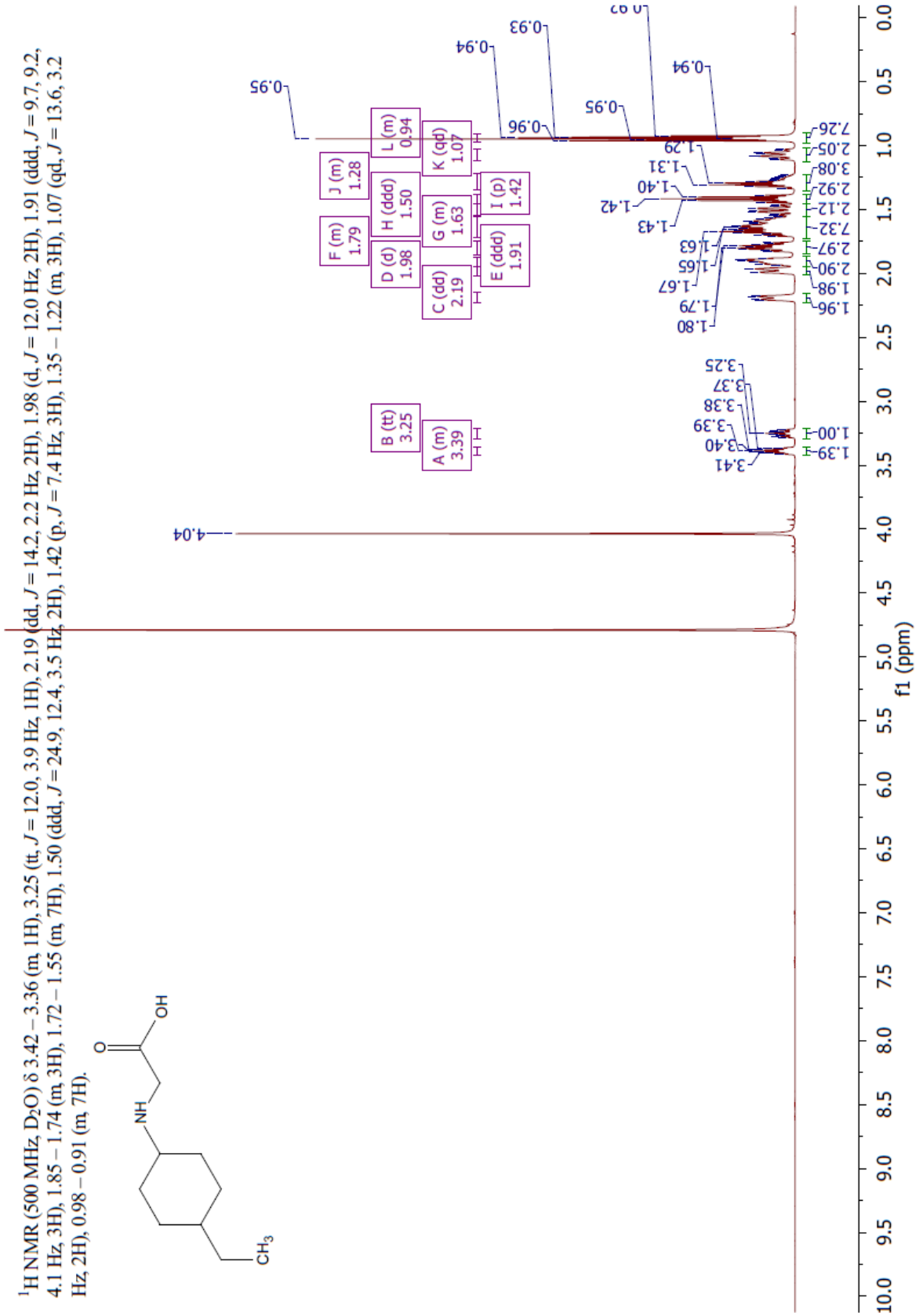

Figure 44. ^{1}H NMR spectra for compound **3w**

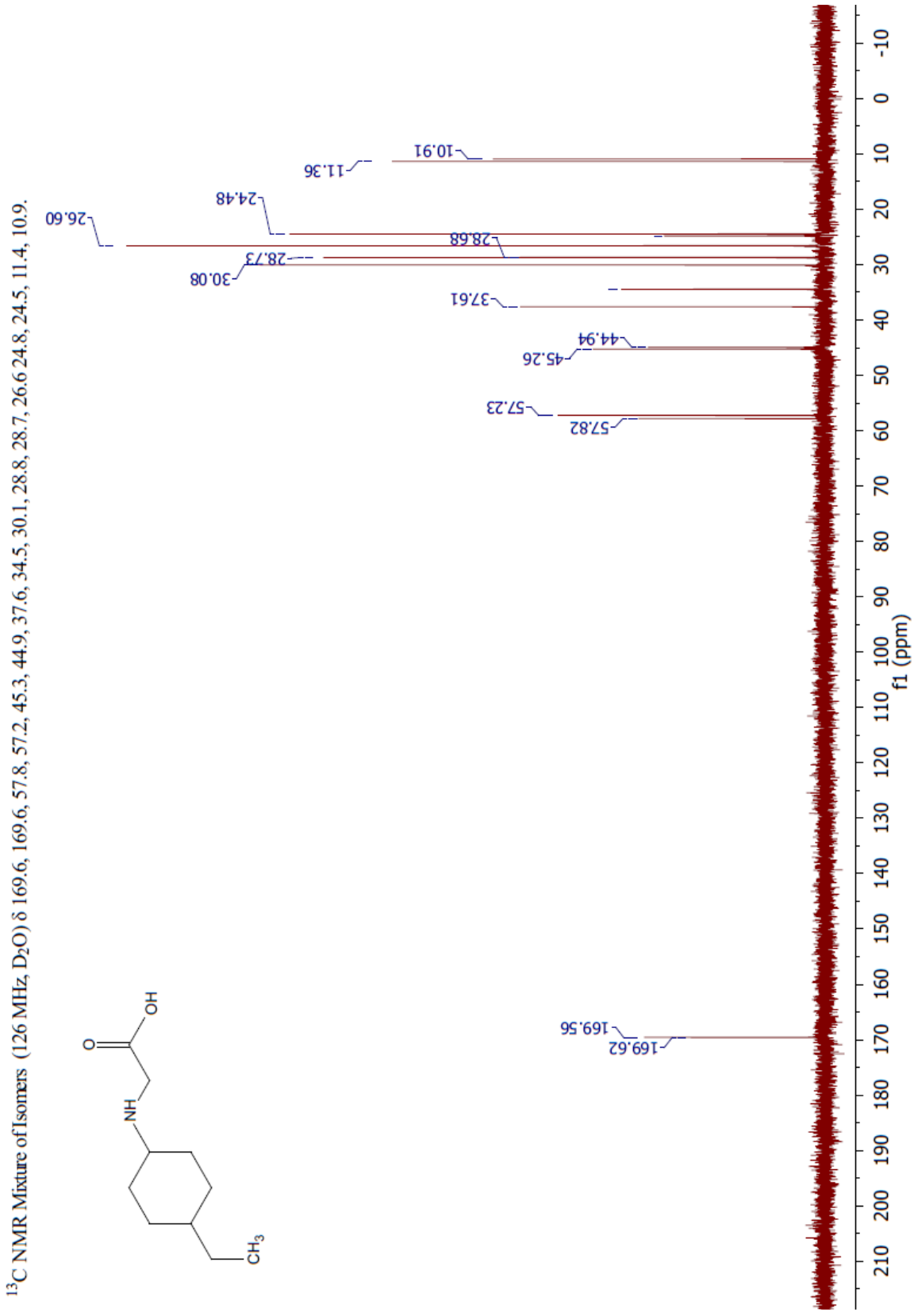

Figure 45. ^{13}C NMR spectra for compound **3w**

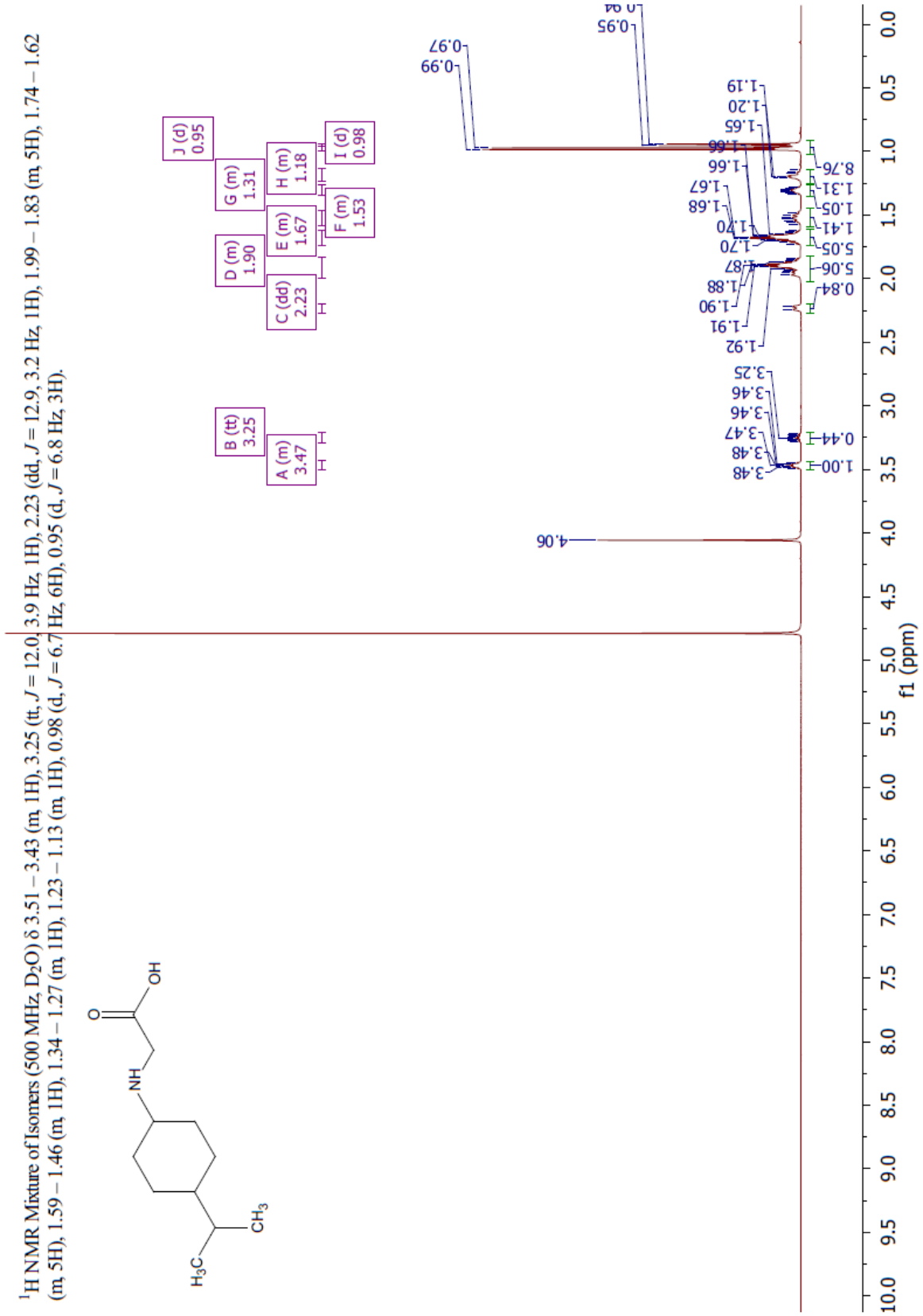

Figure 46. ^{1}H NMR spectra for compound **3x**

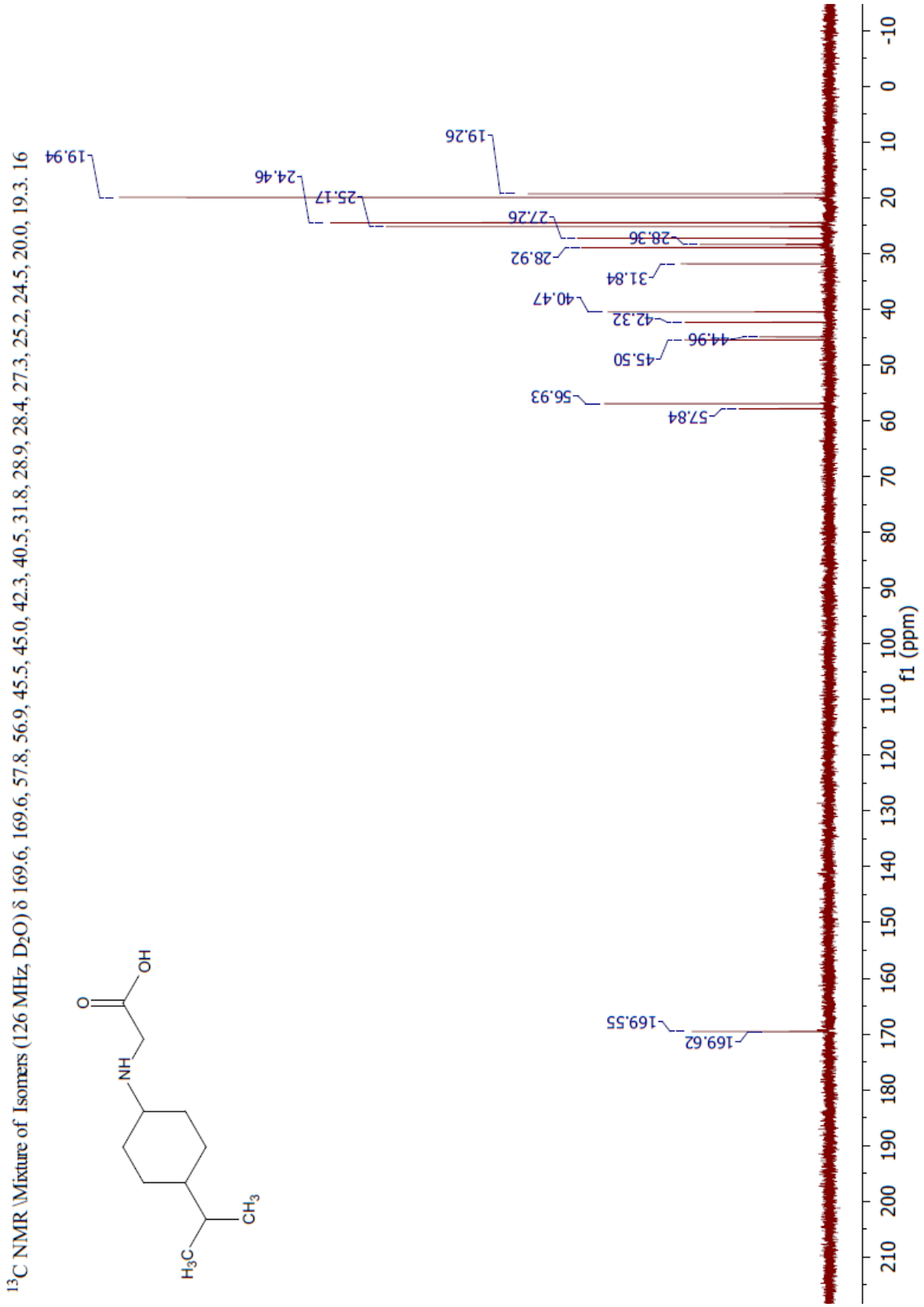

Figure 47. ^{13}C NMR spectra for compound **3x**

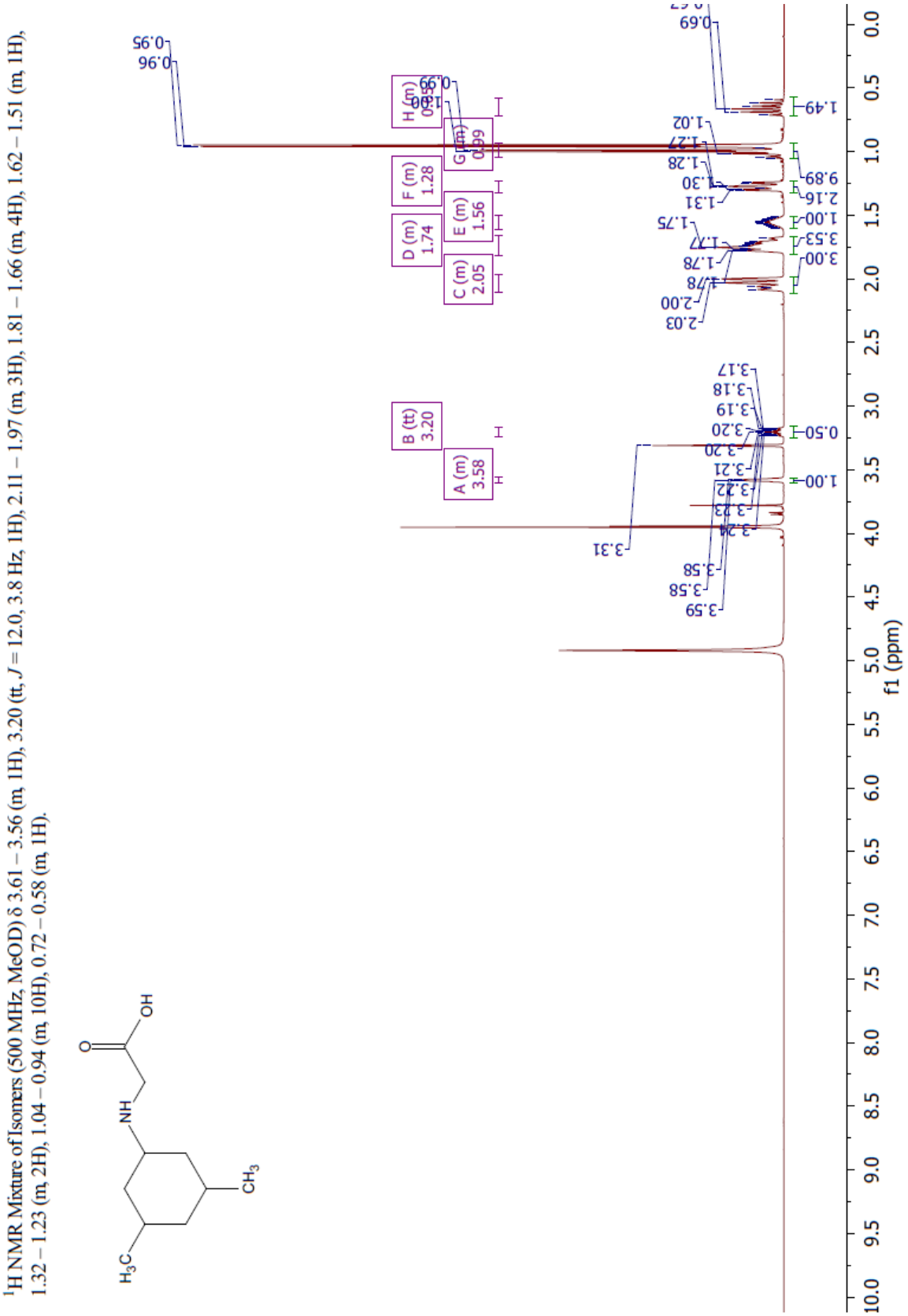

Figure 48. ^{1}H NMR spectra for compound **3y**

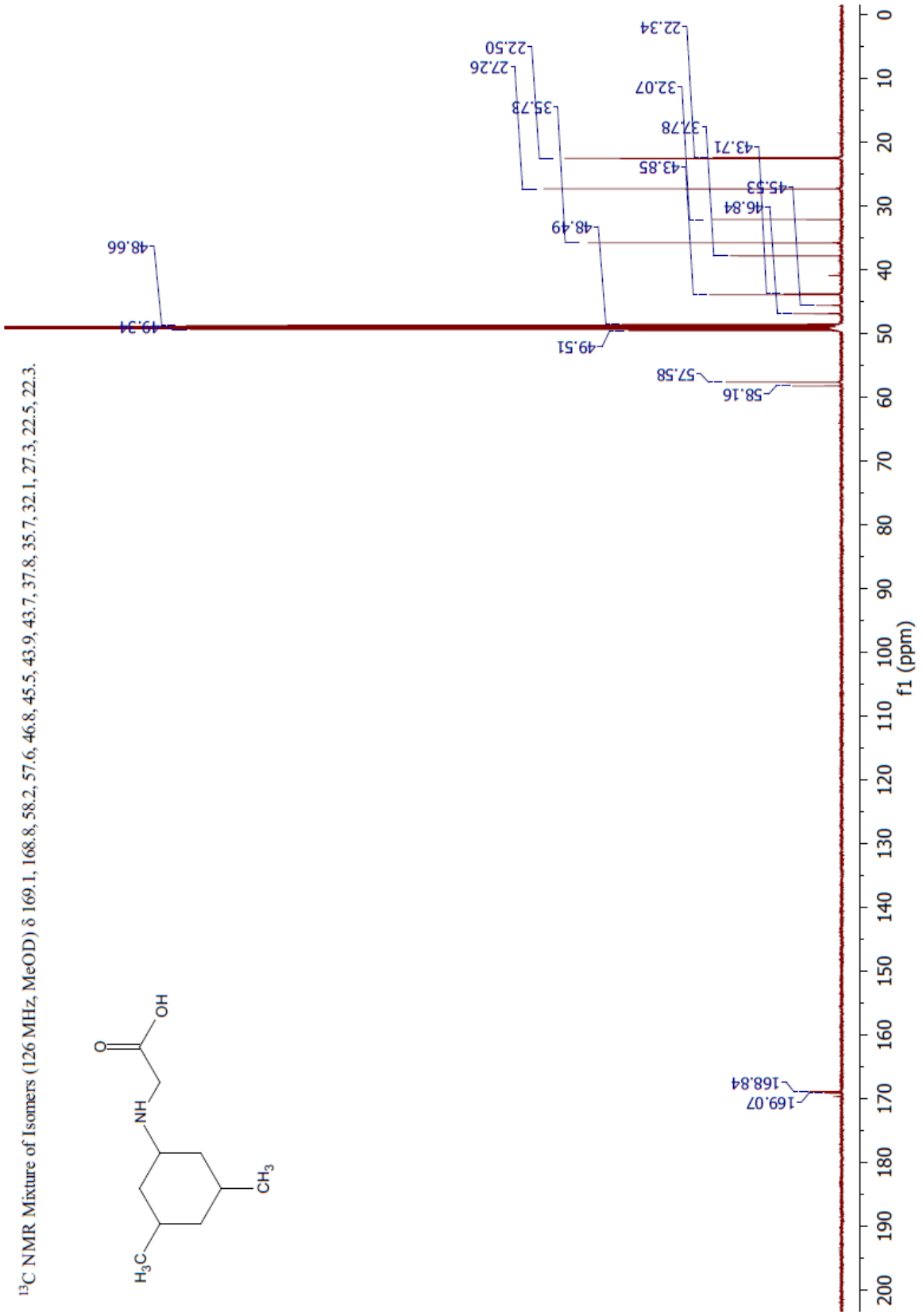

Figure 49. ^{13}C NMR spectra for compound **3y**

Appendix 3. NMR Spectral Data for Chapter 4

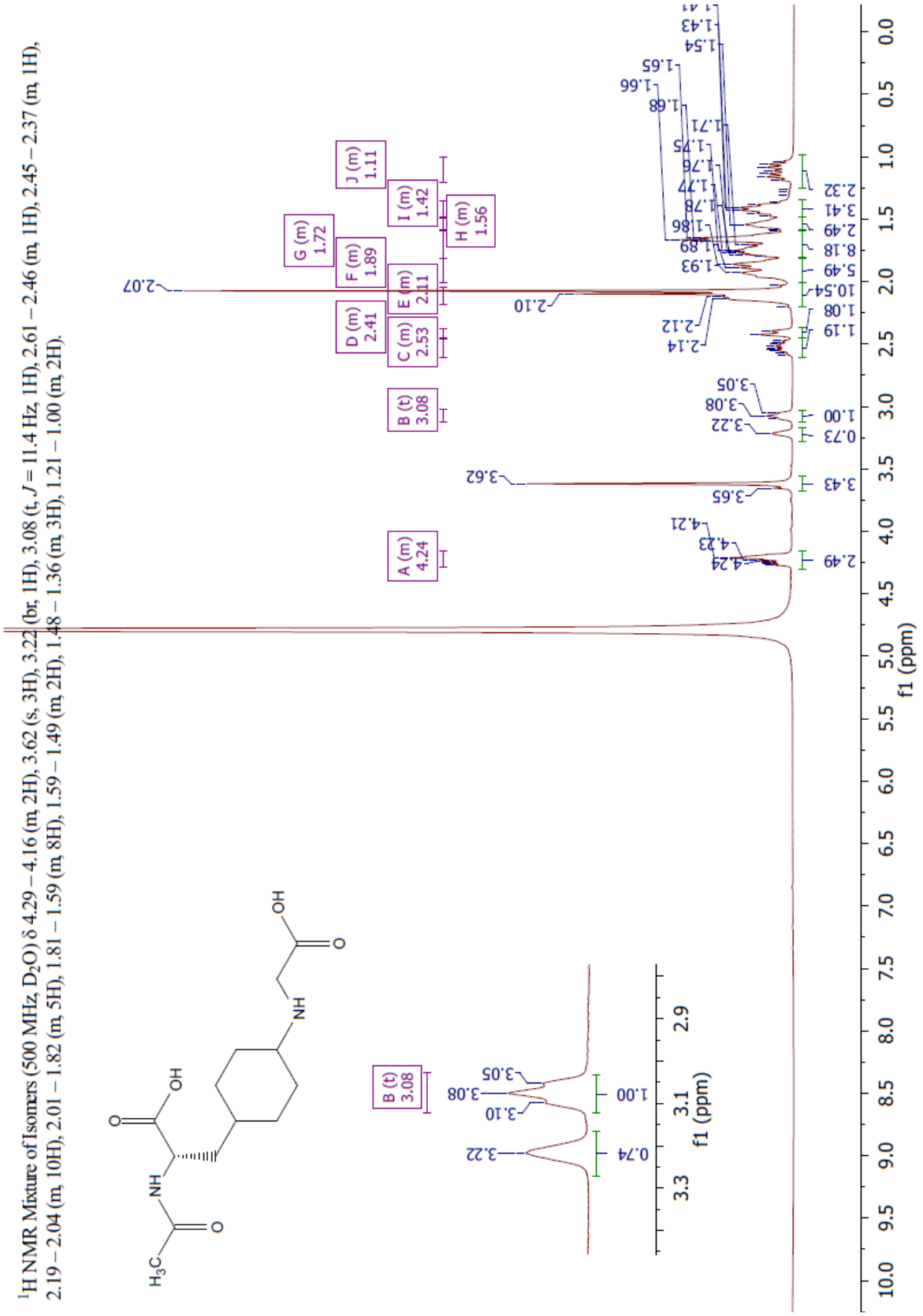

Figure 1. ^{1}H NMR spectra for compound **3**

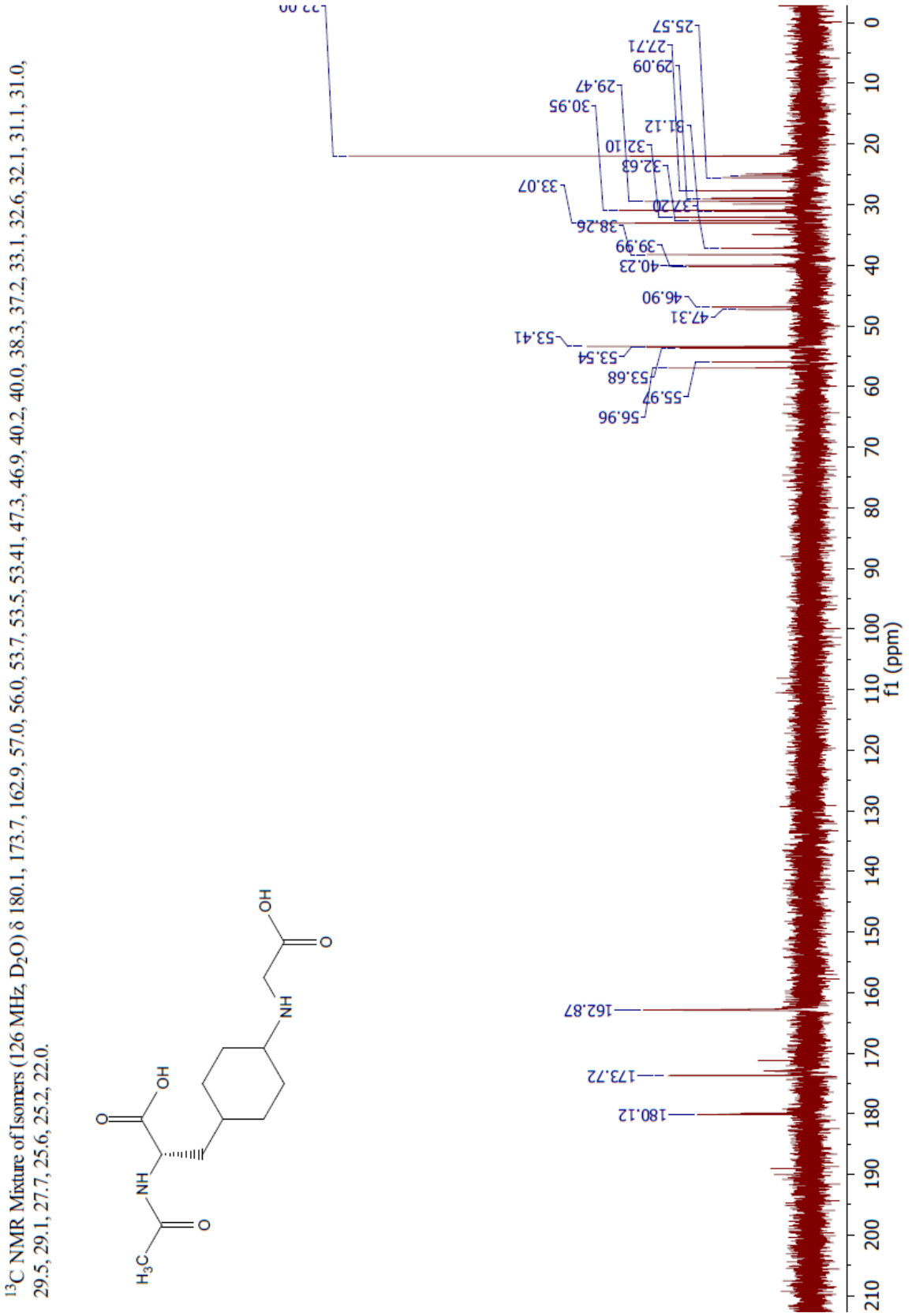

Figure 2. ^{13}C NMR spectra for compound **3**

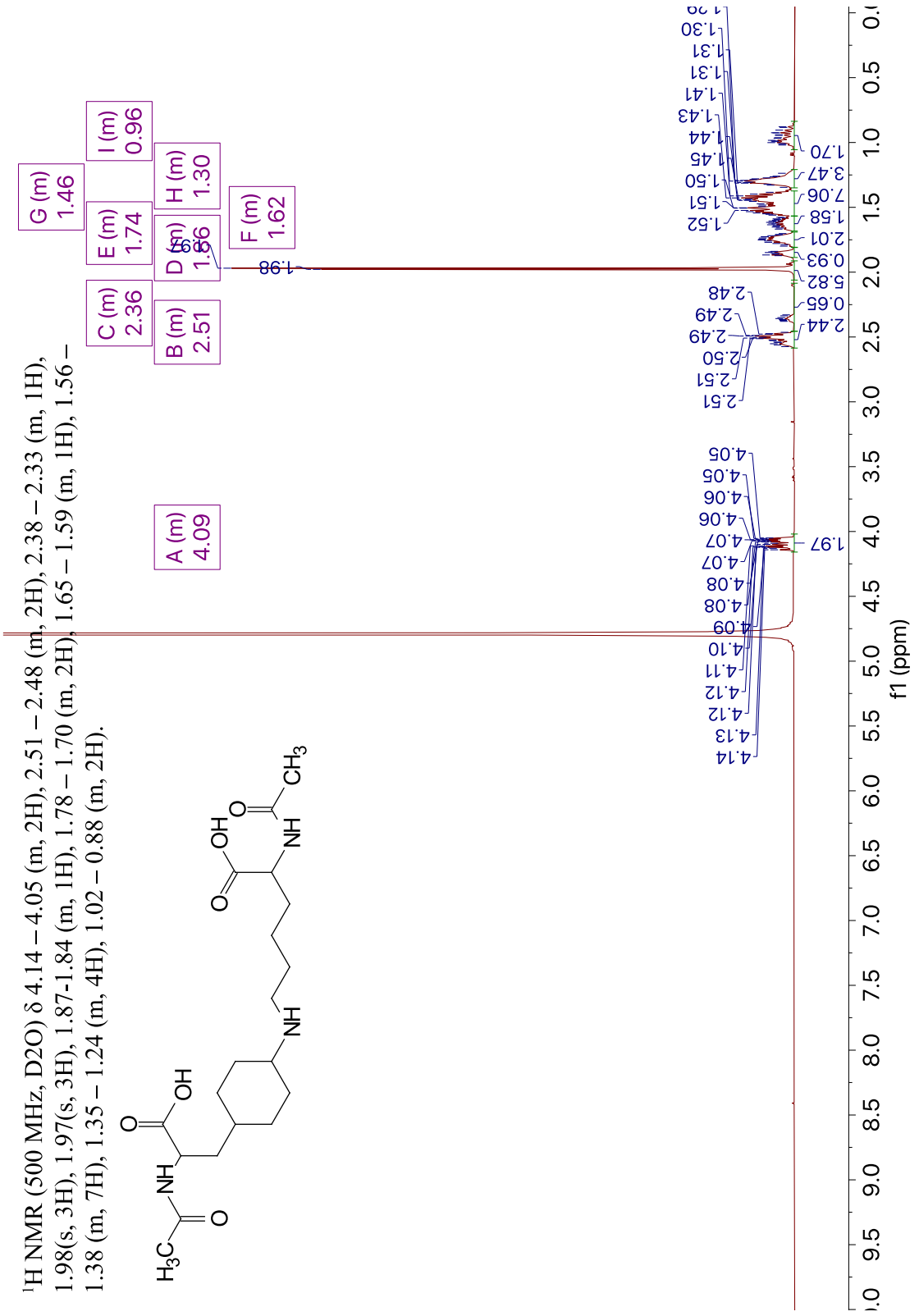

Figure 3. ^{1}H NMR spectra for compound **5**

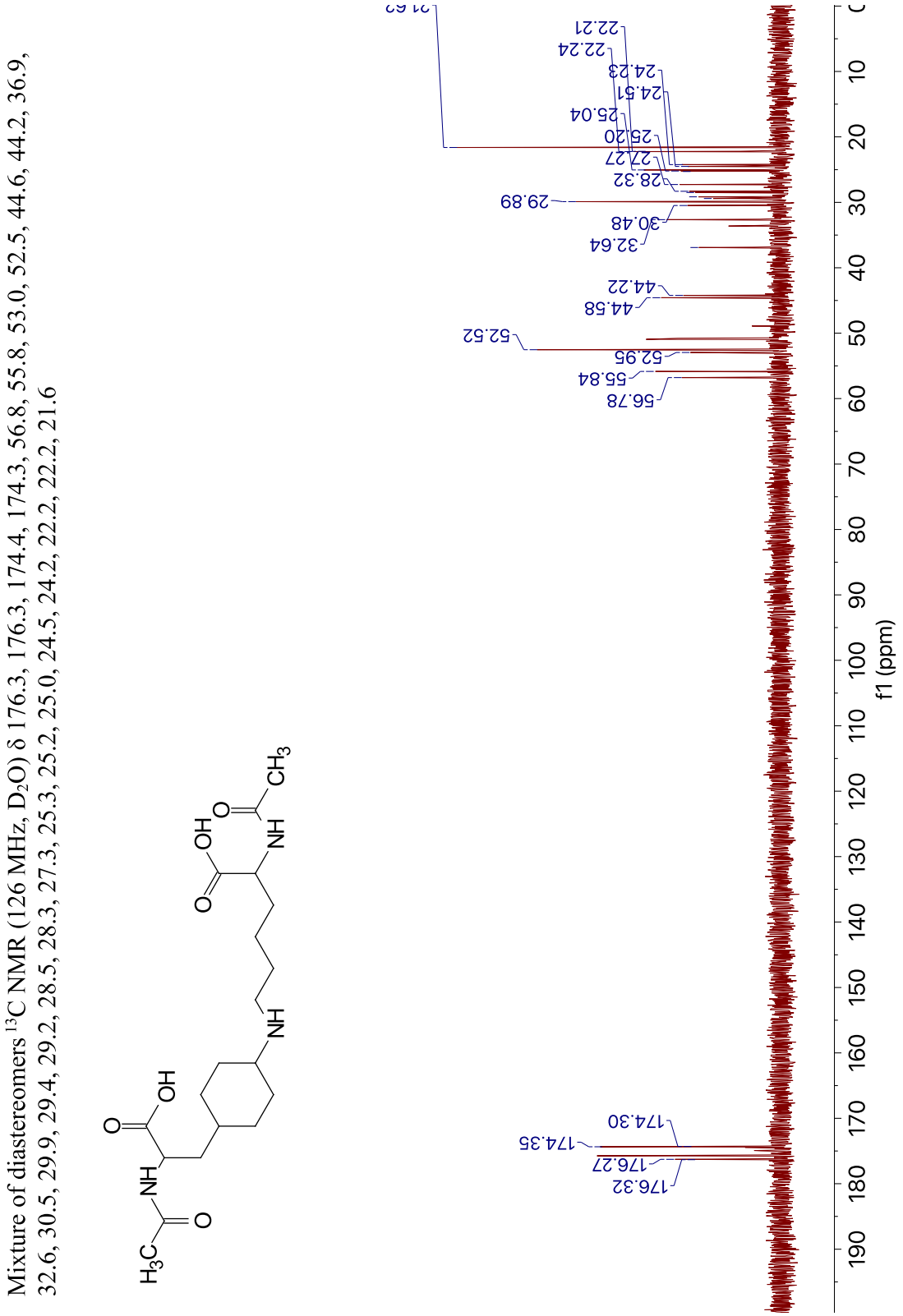

Figure 4. ^{13}C NMR spectra for compound **5**

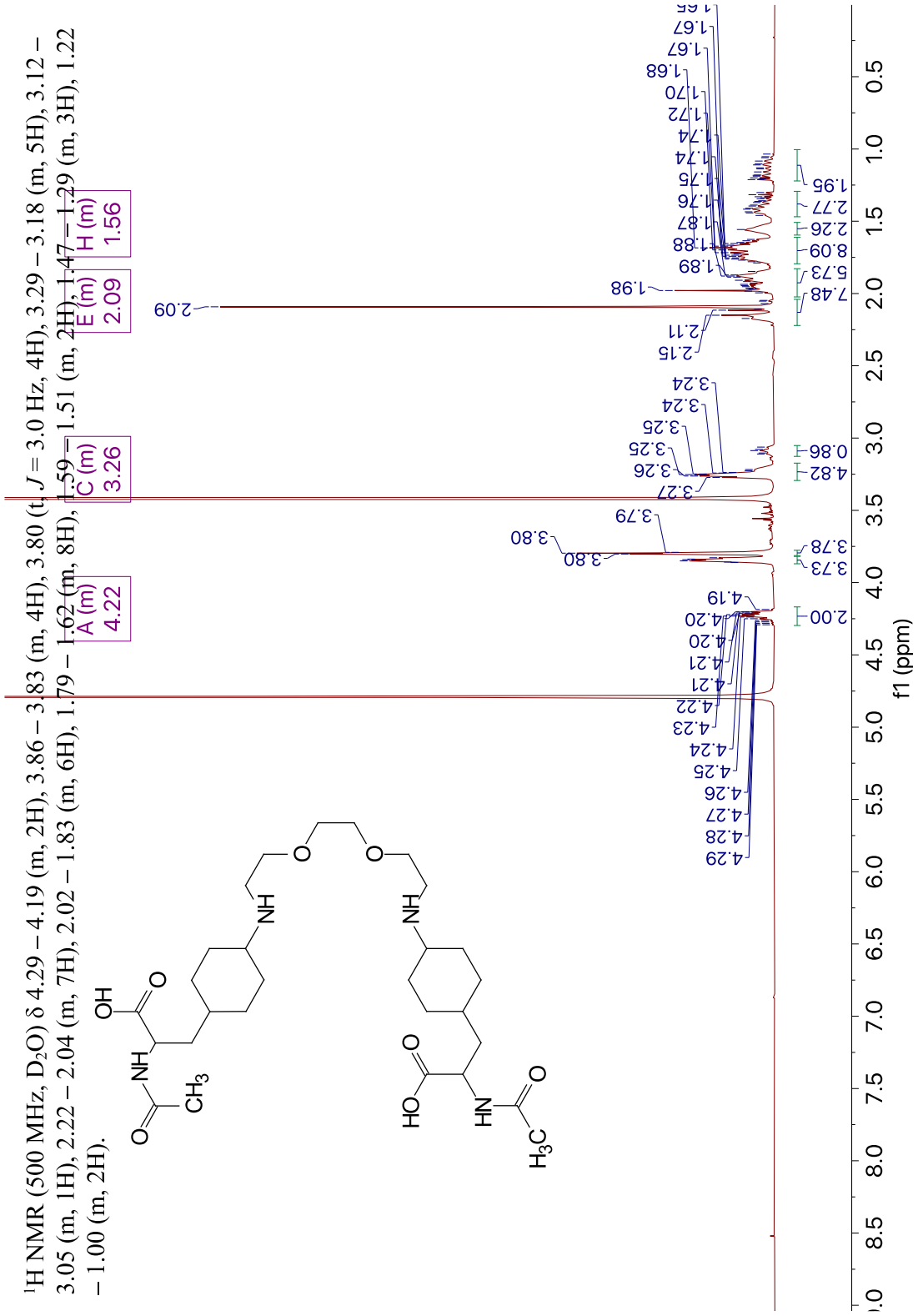

Figure 5. ^{1}H NMR spectra for compound **7**

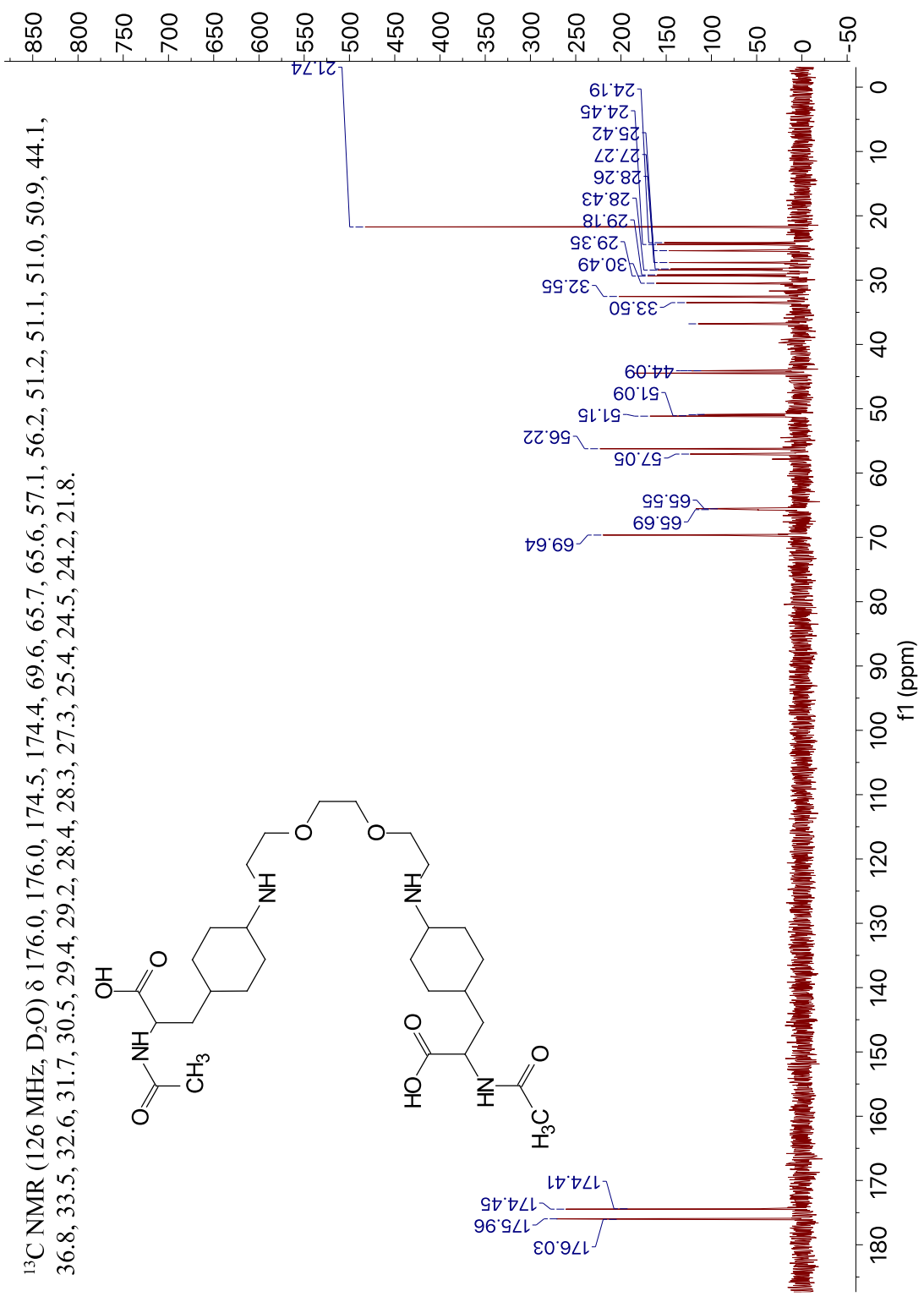

Figure 6. ^{13}C NMR spectra for compound **7**

Appendix 4. NMR Spectral Data for Chapter 5

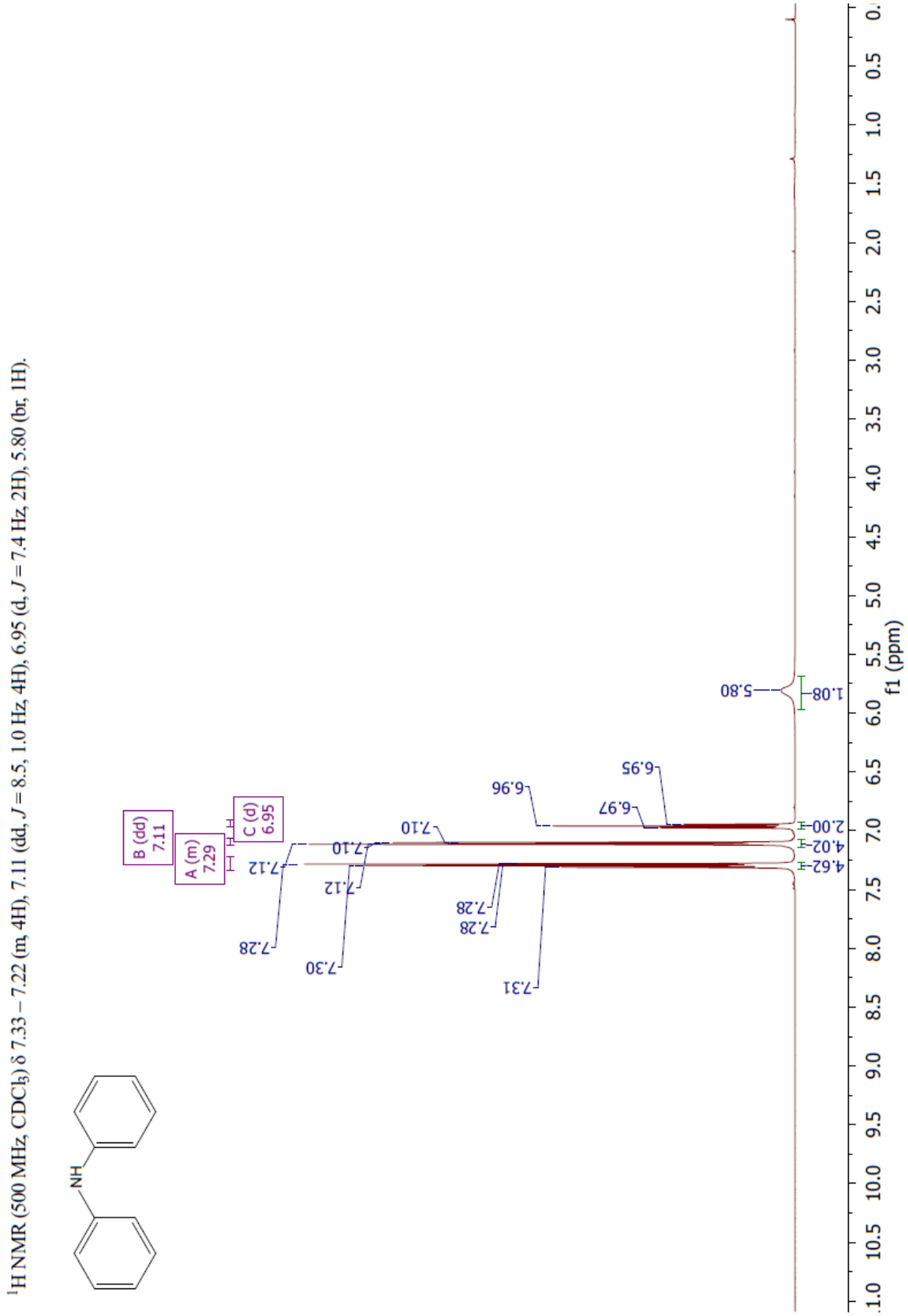

Figure 1. ^{1}H NMR spectra for compound **3a**

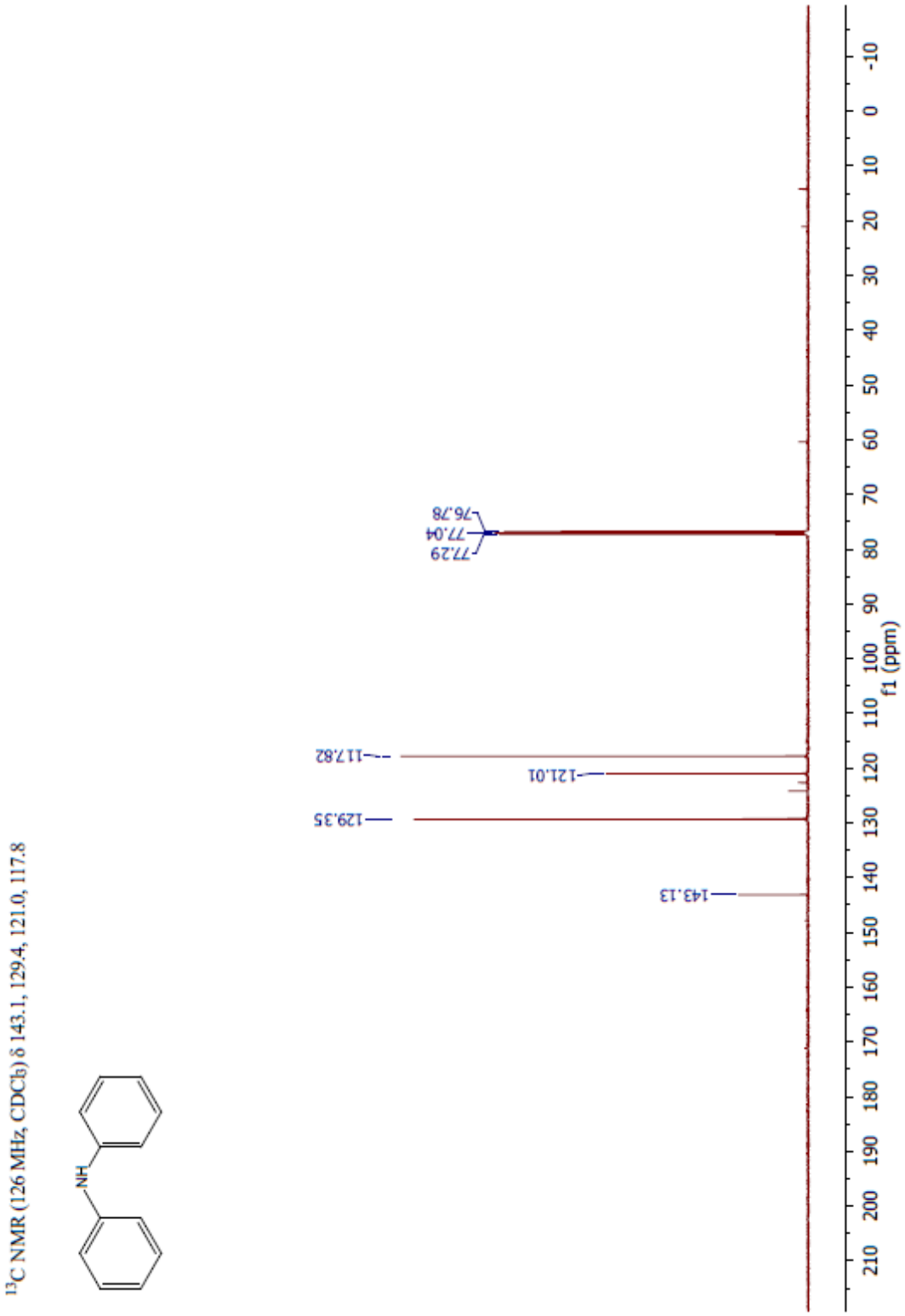

Figure 2. ^{13}C NMR spectra for compound **3a**

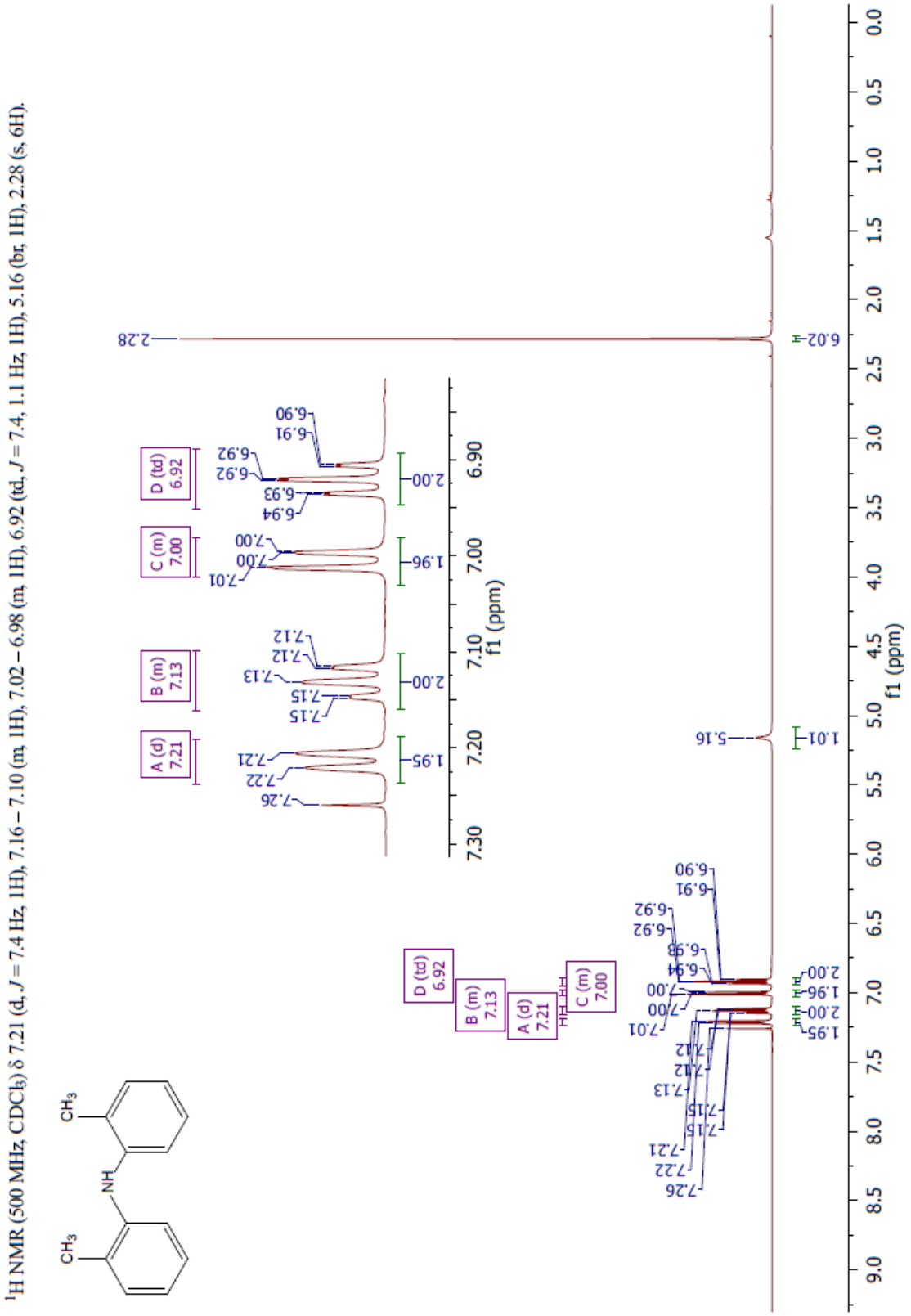

Figure 3. ^{1}H NMR spectra for compound **3b**

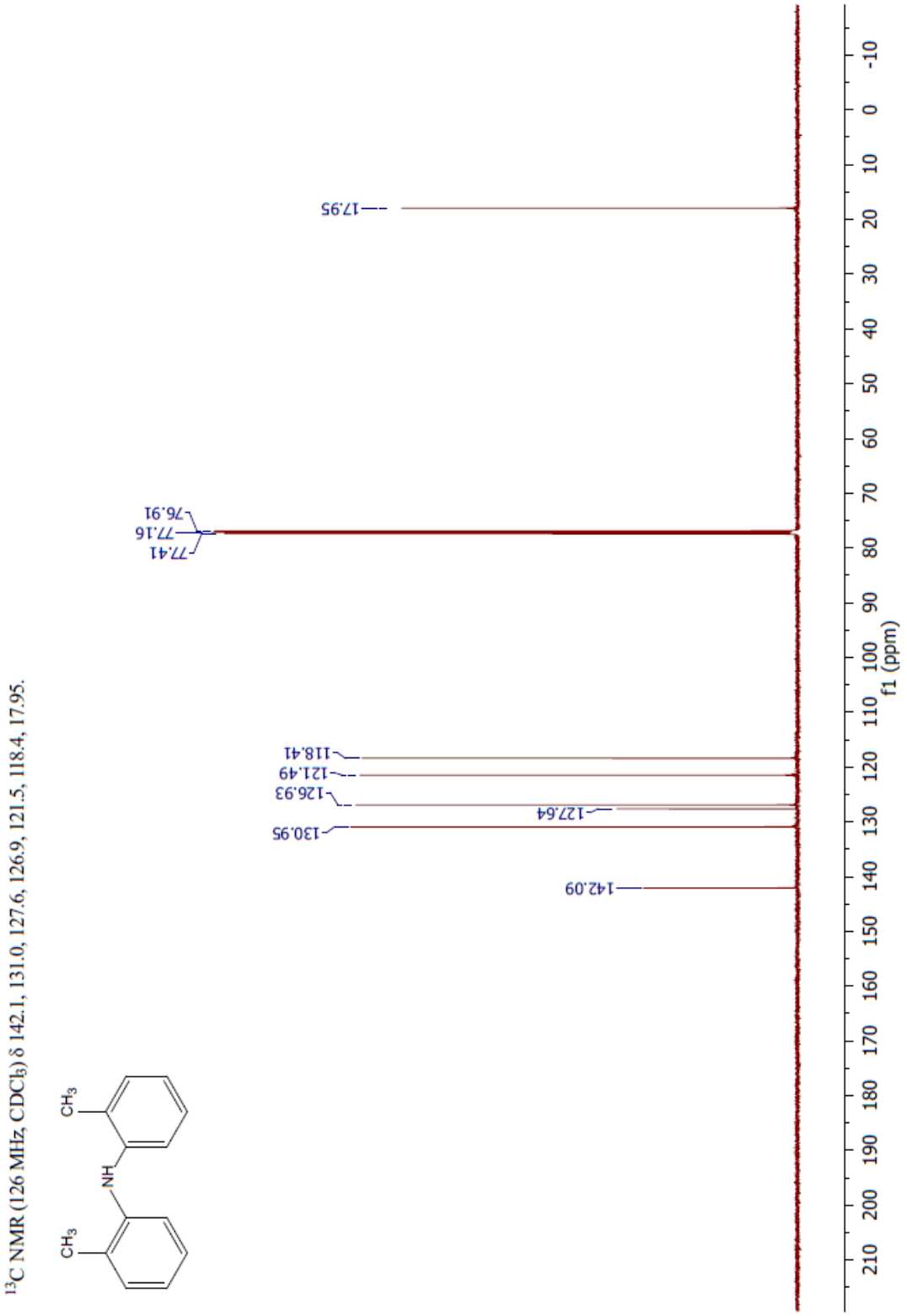

Figure 4. ^{13}C NMR spectra for compound **3b**

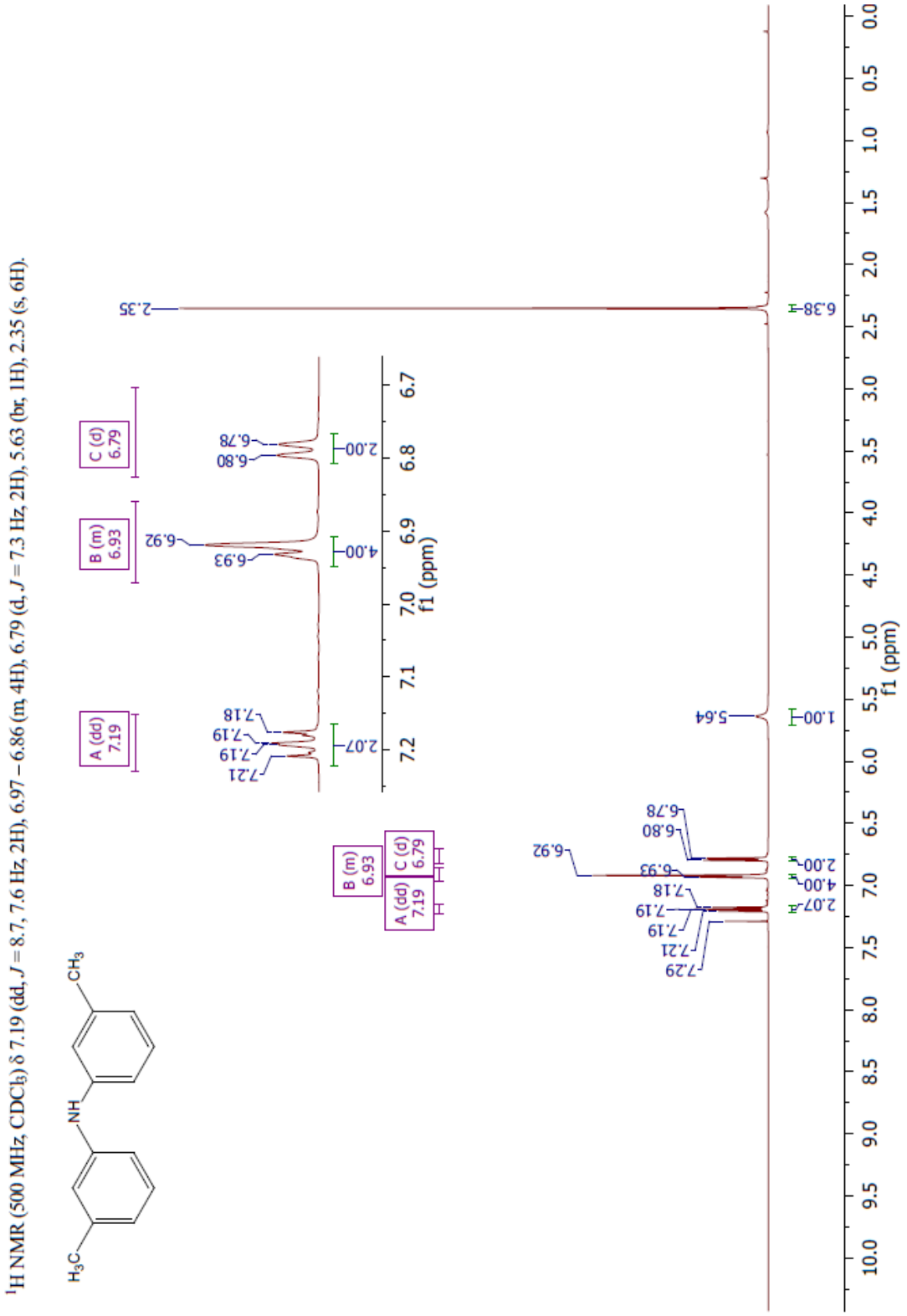

Figure 5. ^{1}H NMR spectra for compound **3c**

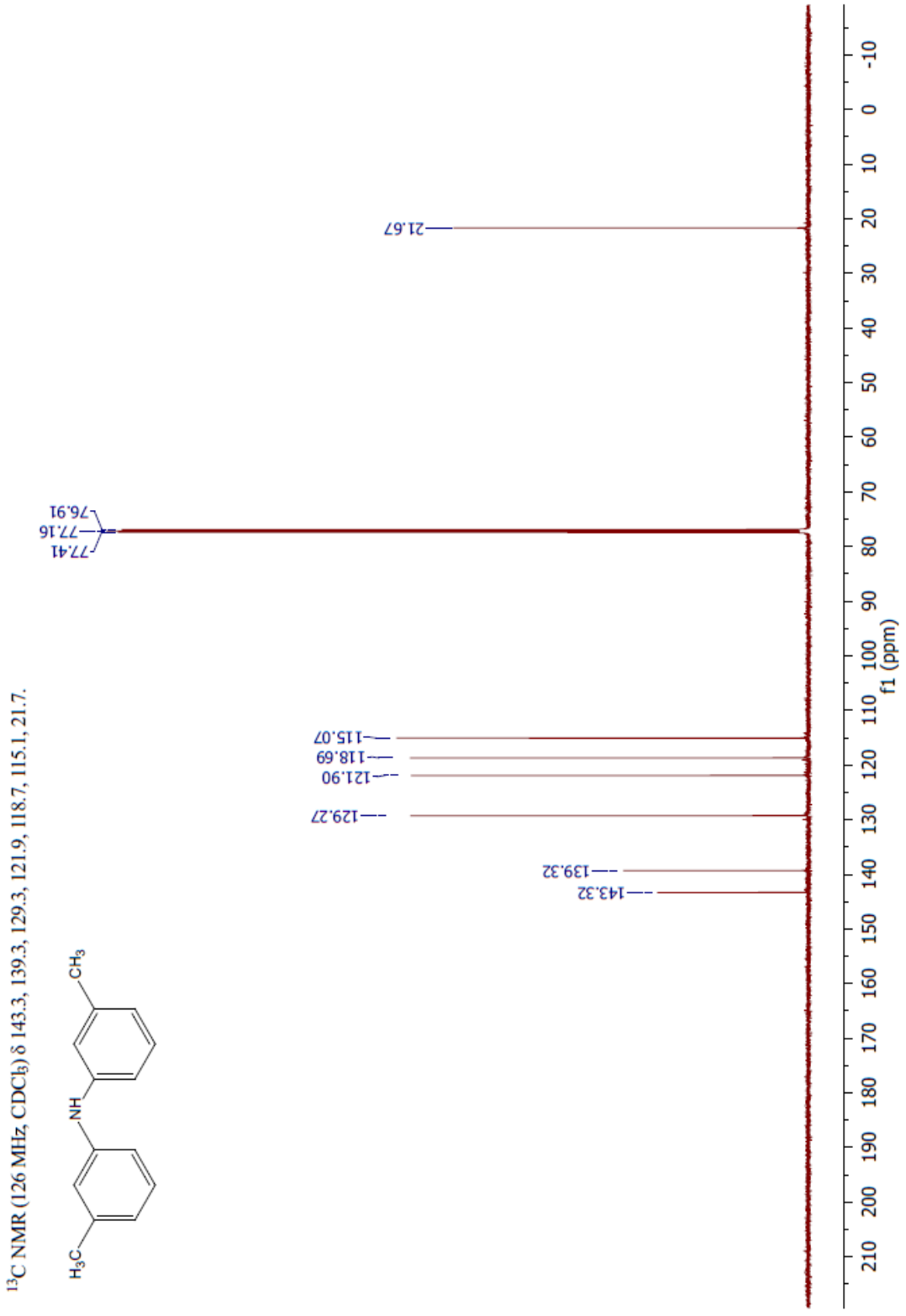

Figure 6. ^{13}C NMR spectra for compound **3c**

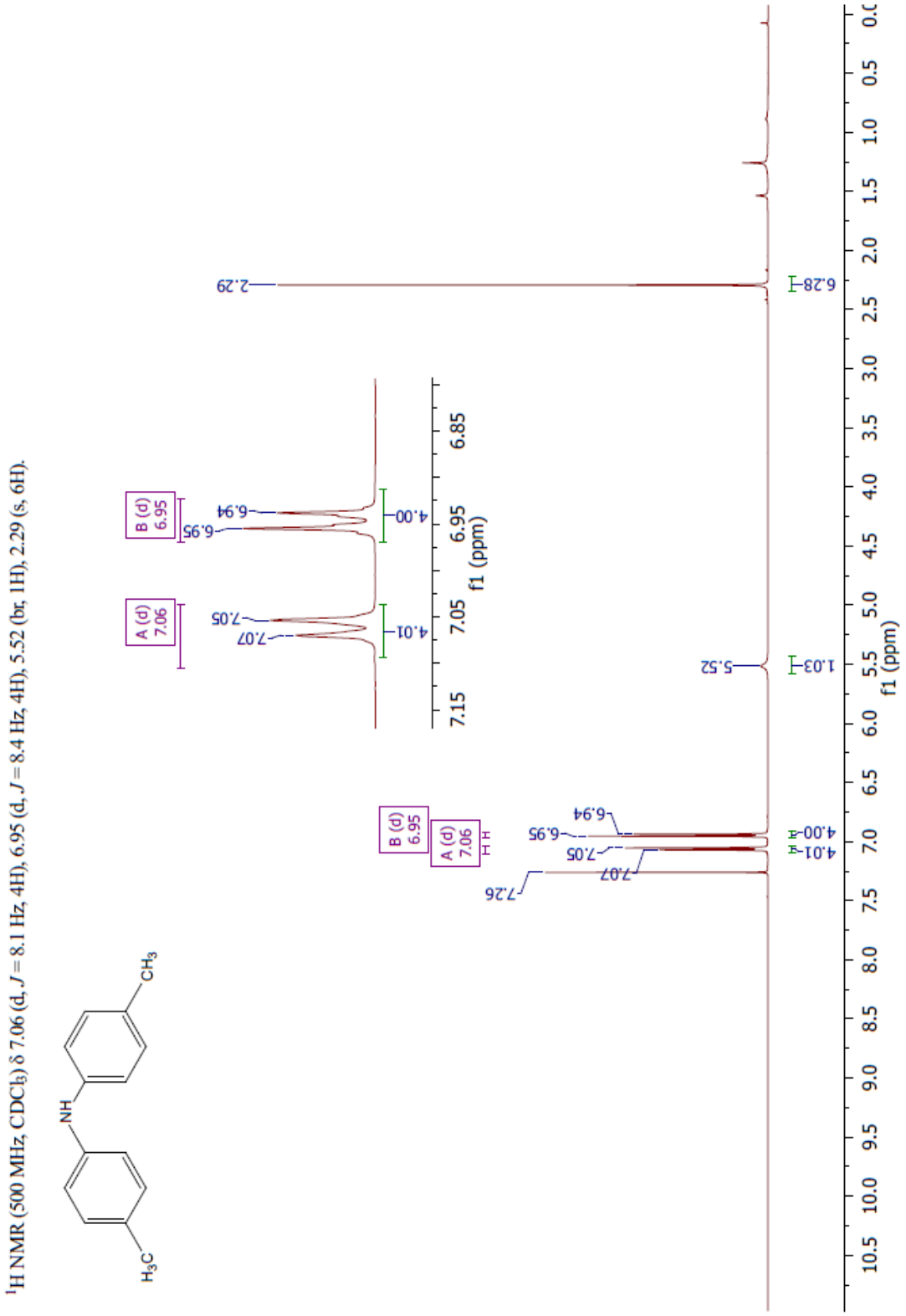

Figure 7. ^{1}H NMR spectra for compound **3d**

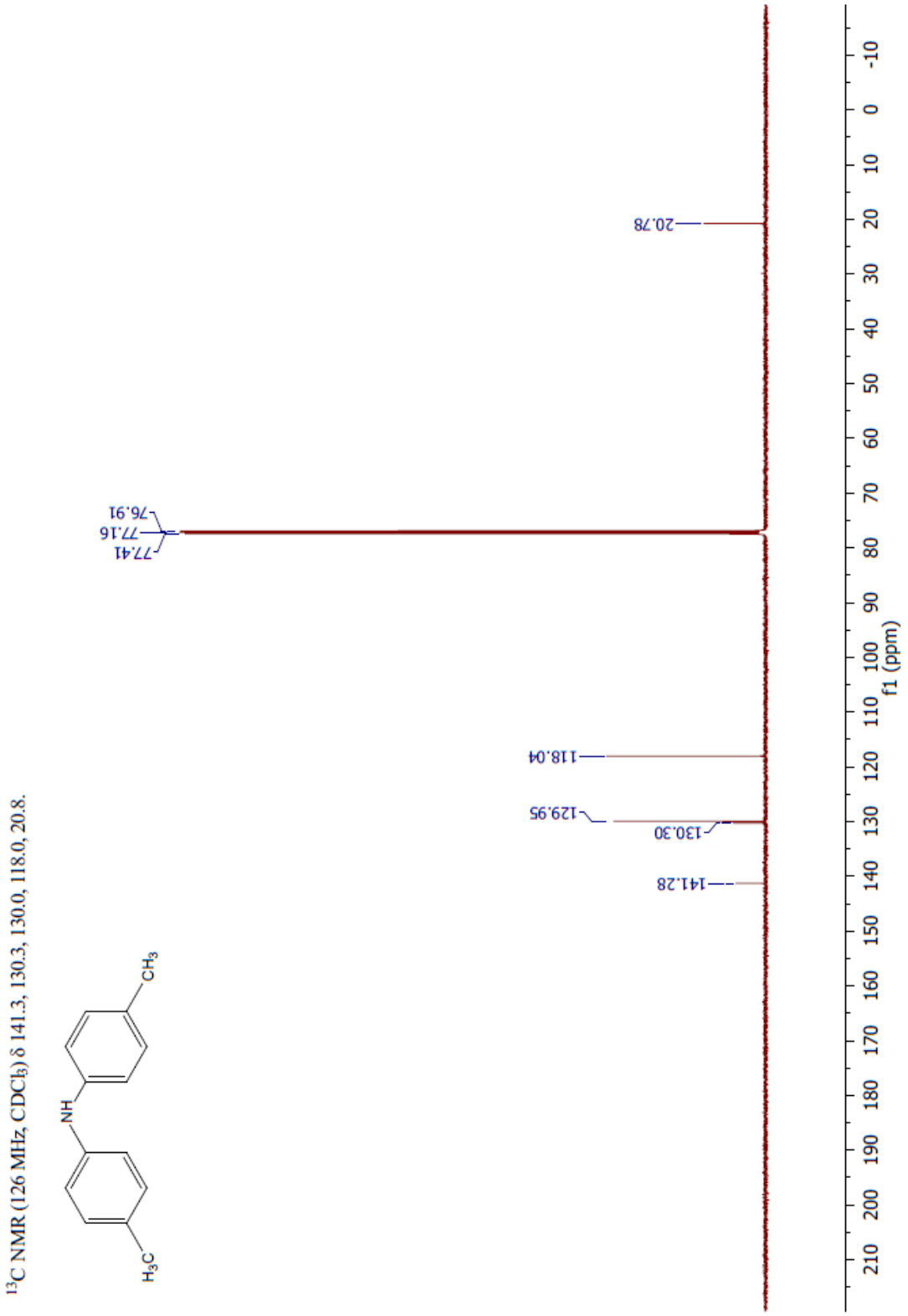

Figure 8. ^{13}C NMR spectra for compound **3d**

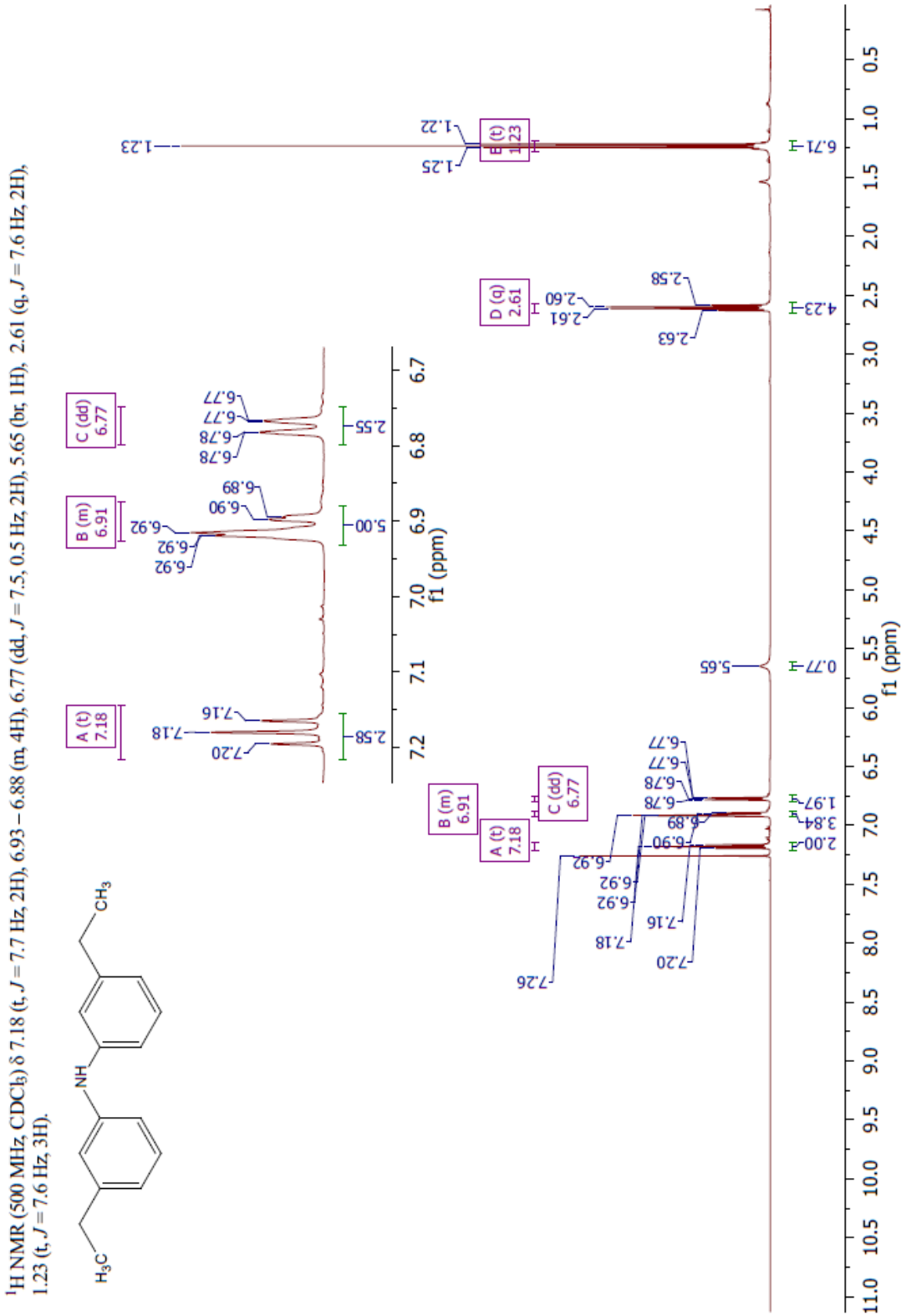

Figure 9. ^{1}H NMR spectra for compound **3e**

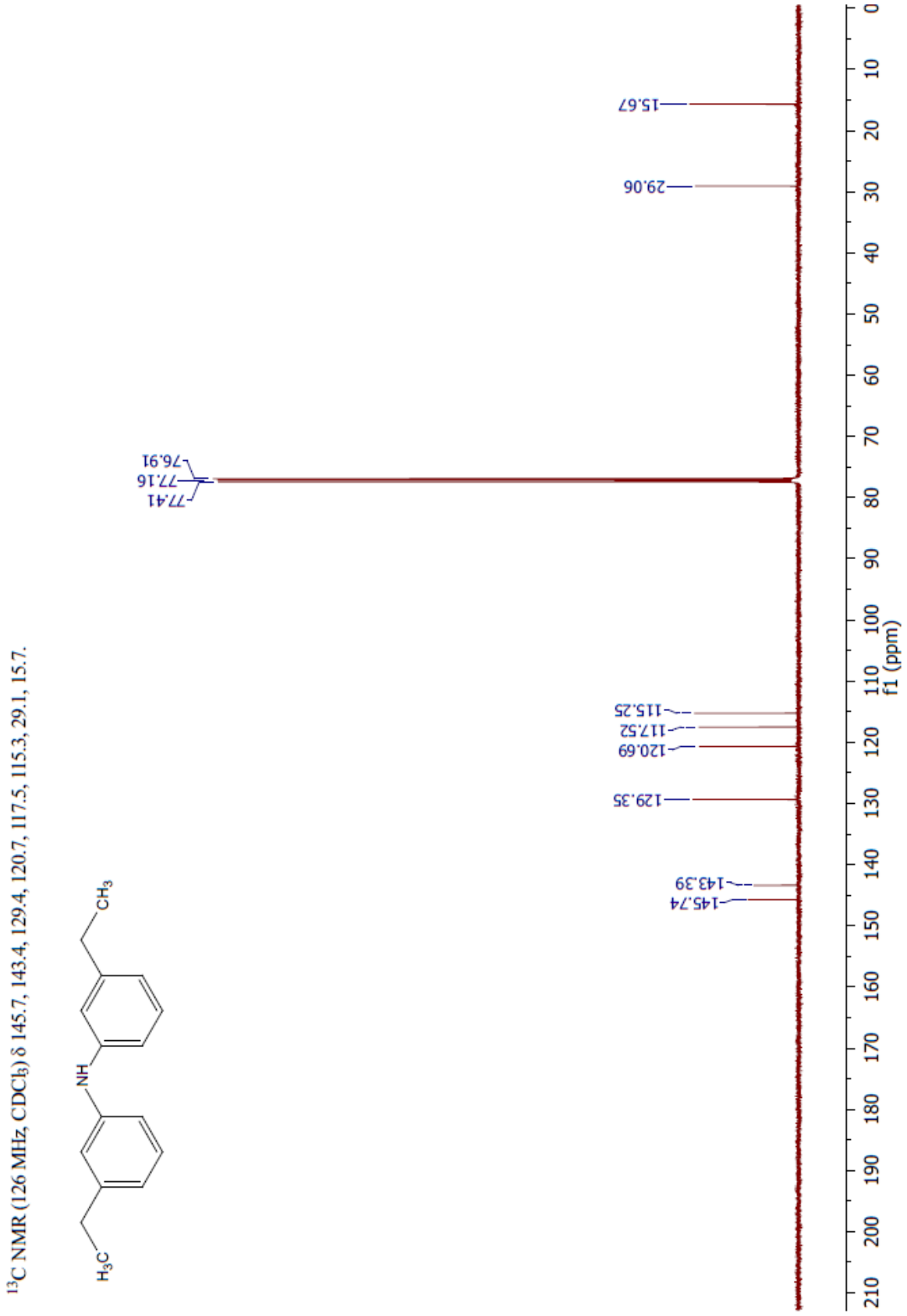

Figure 10. ^{13}C NMR spectra for compound **3e**

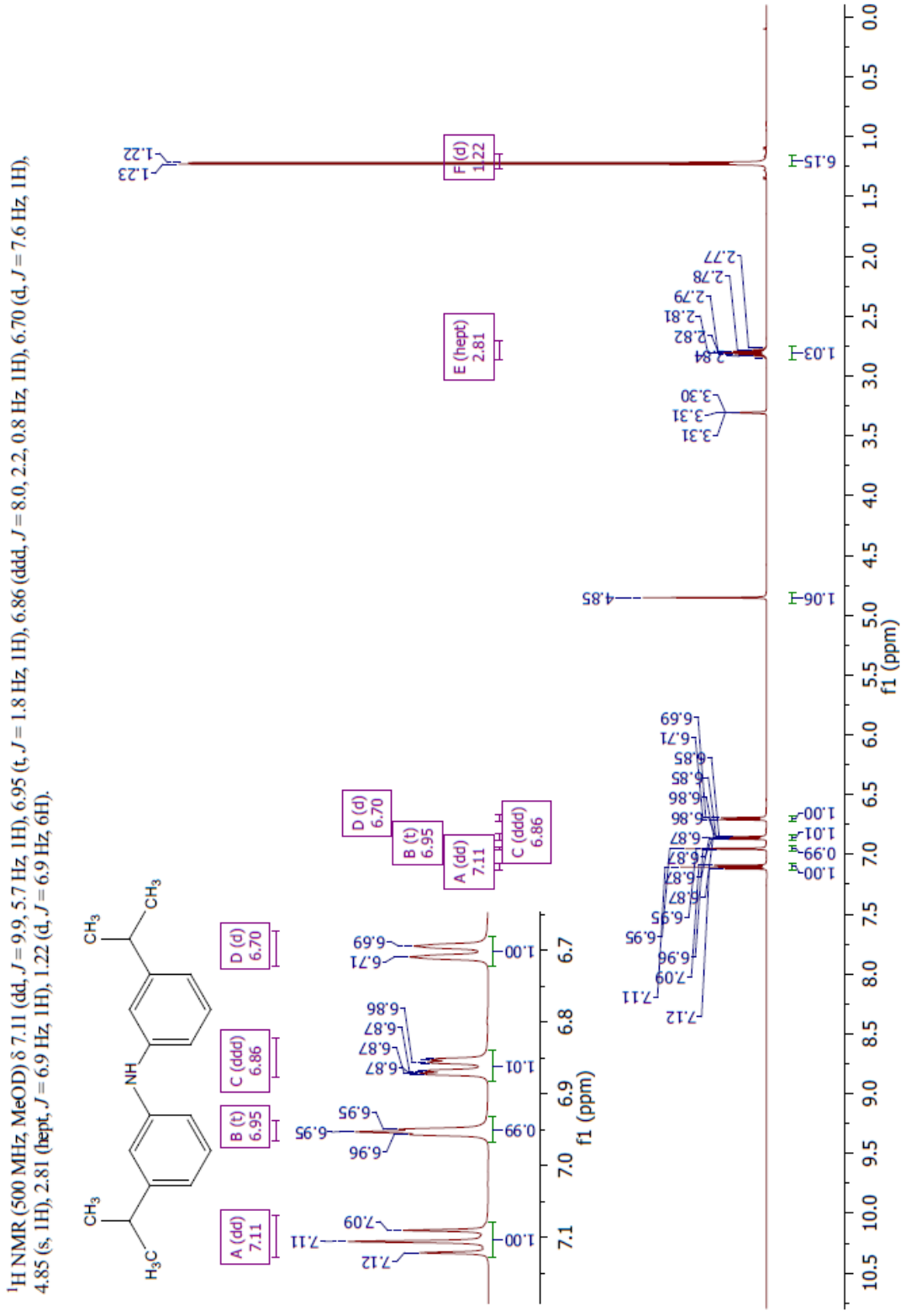

Figure 11. ^{1}H NMR spectra for compound **3f**

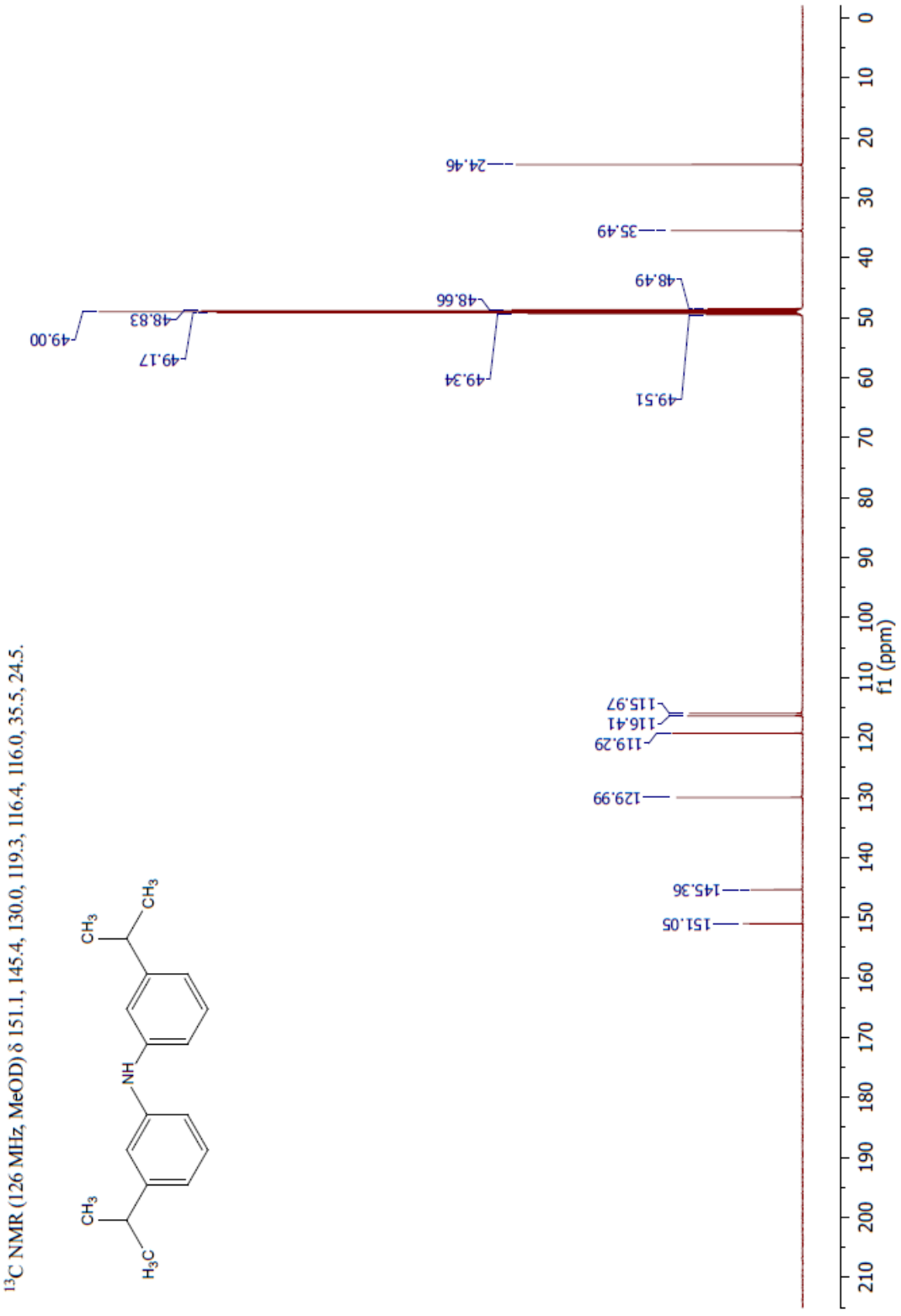

Figure 12. ^{13}C NMR spectra for compound **3f**

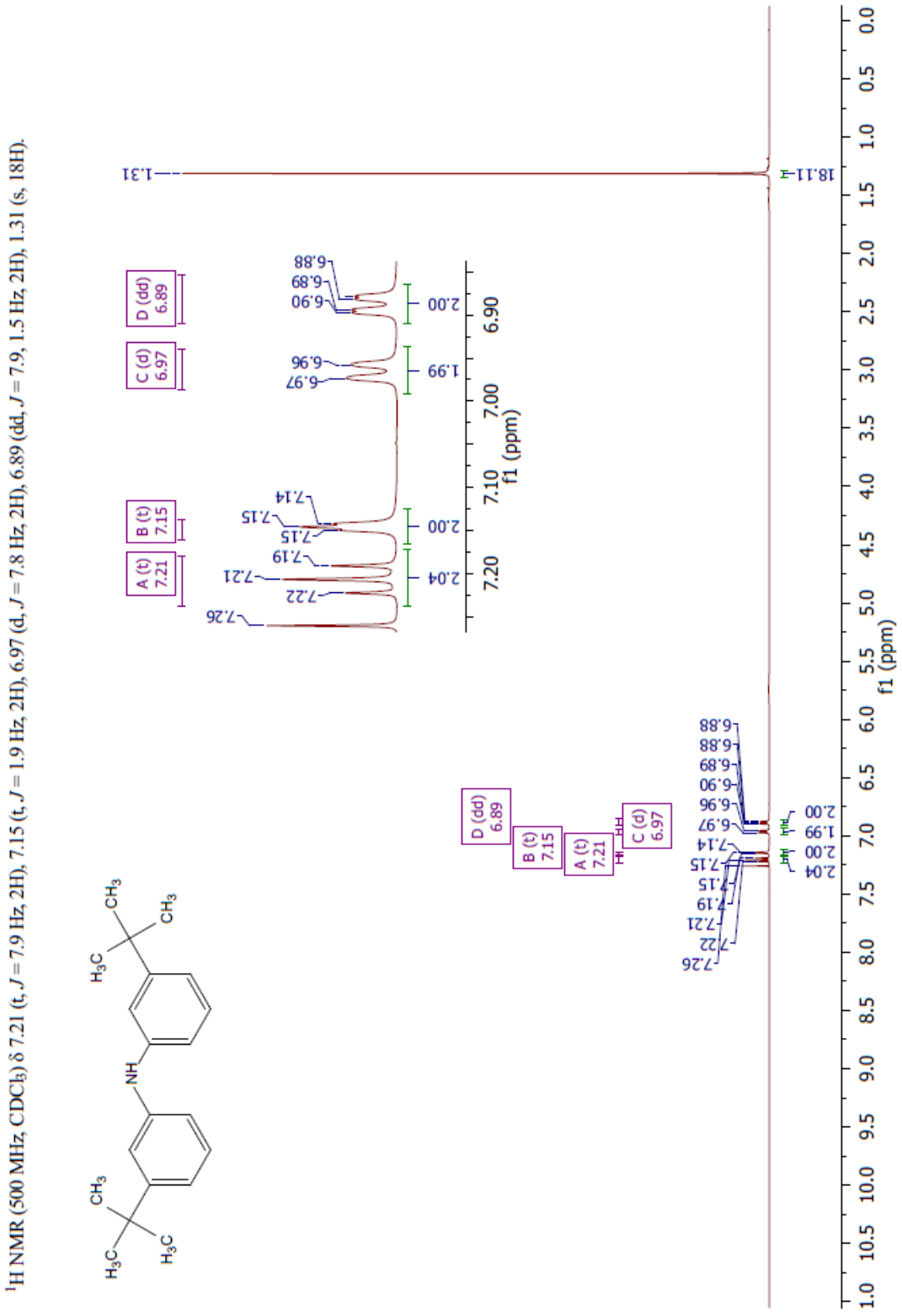

Figure 13. ^{1}H NMR spectra for compound **3g**

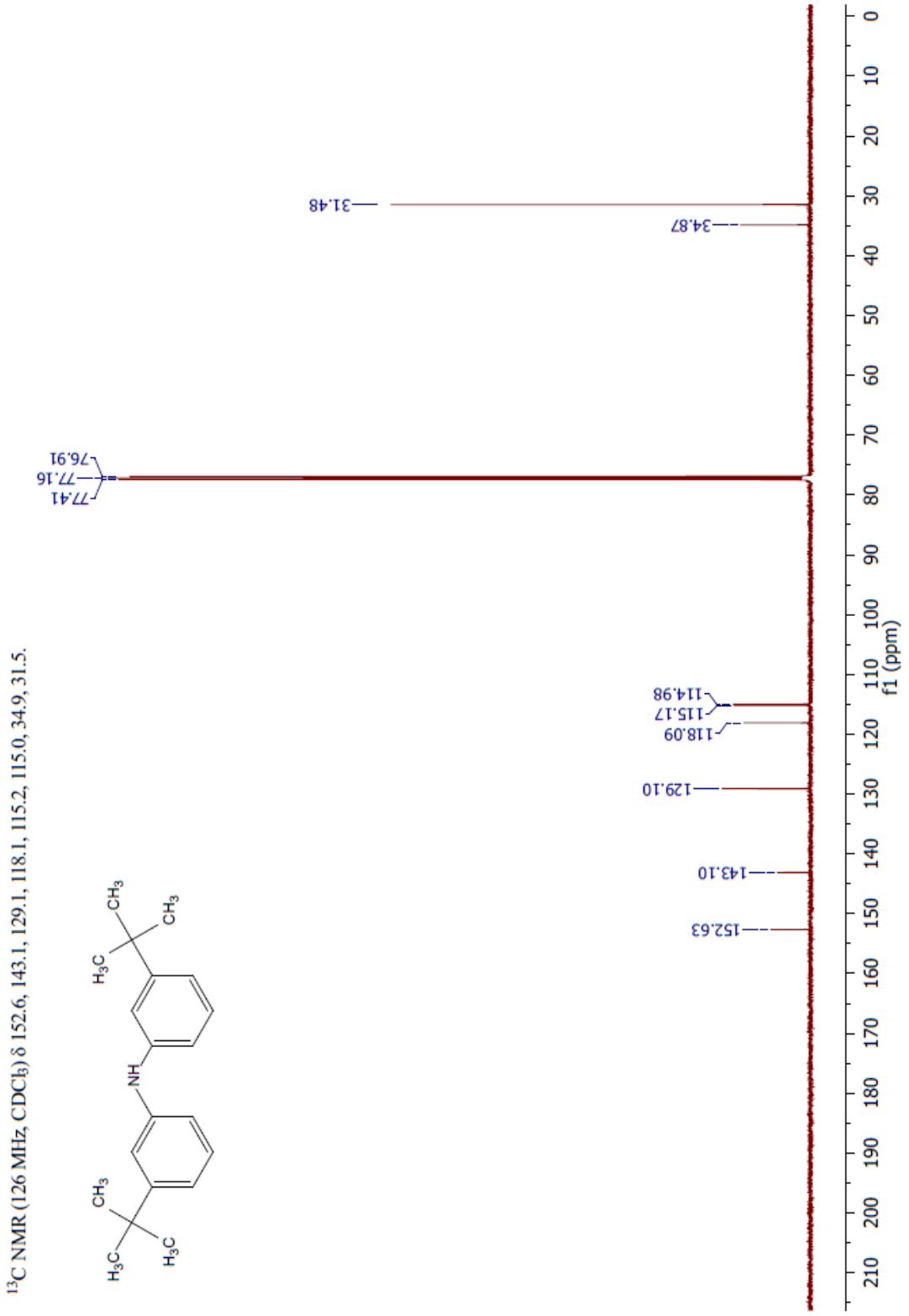

Figure 14. ^{13}C NMR spectra for compound **3g**

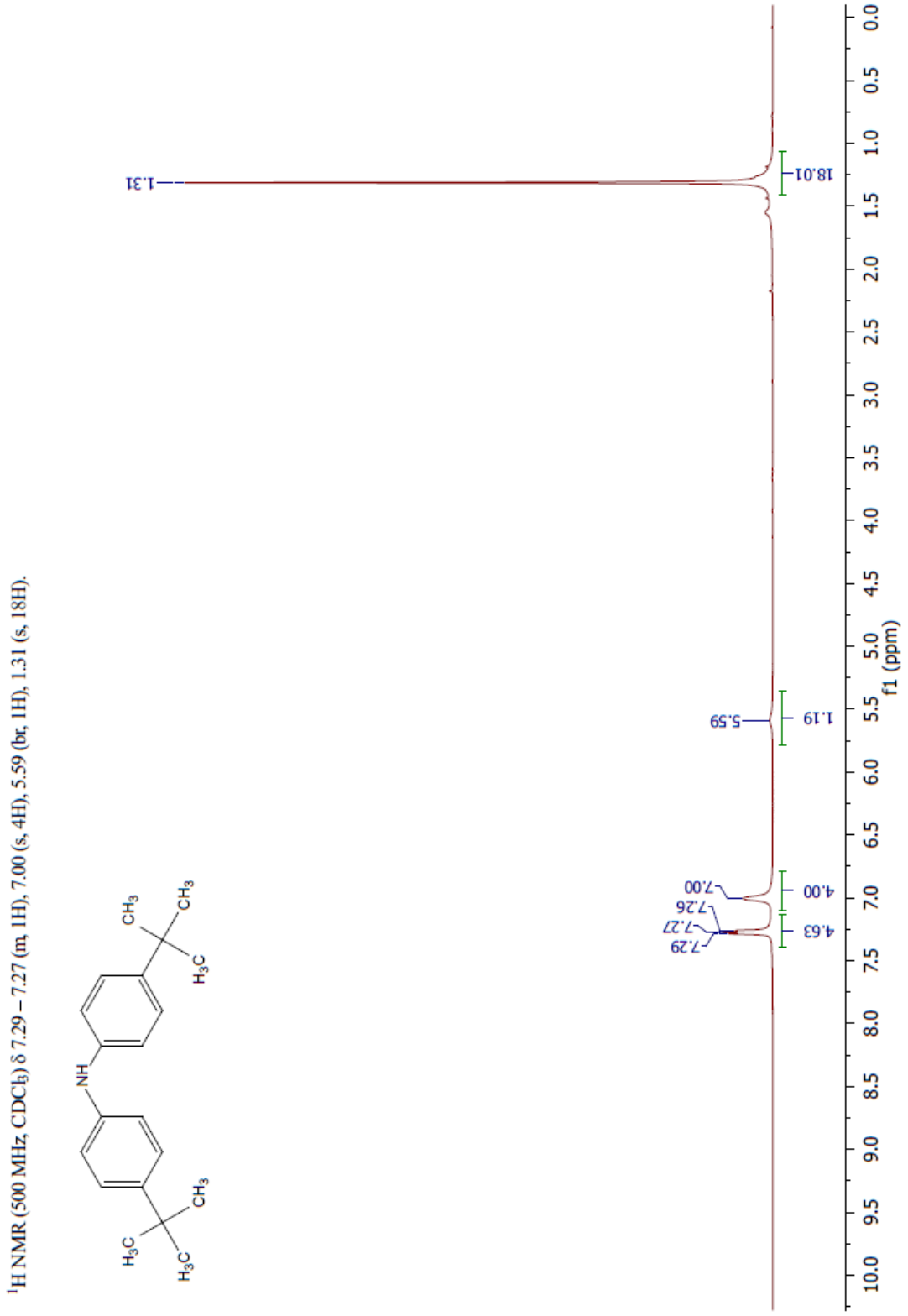

Figure 15. ^{1}H NMR spectra for compound **3h**

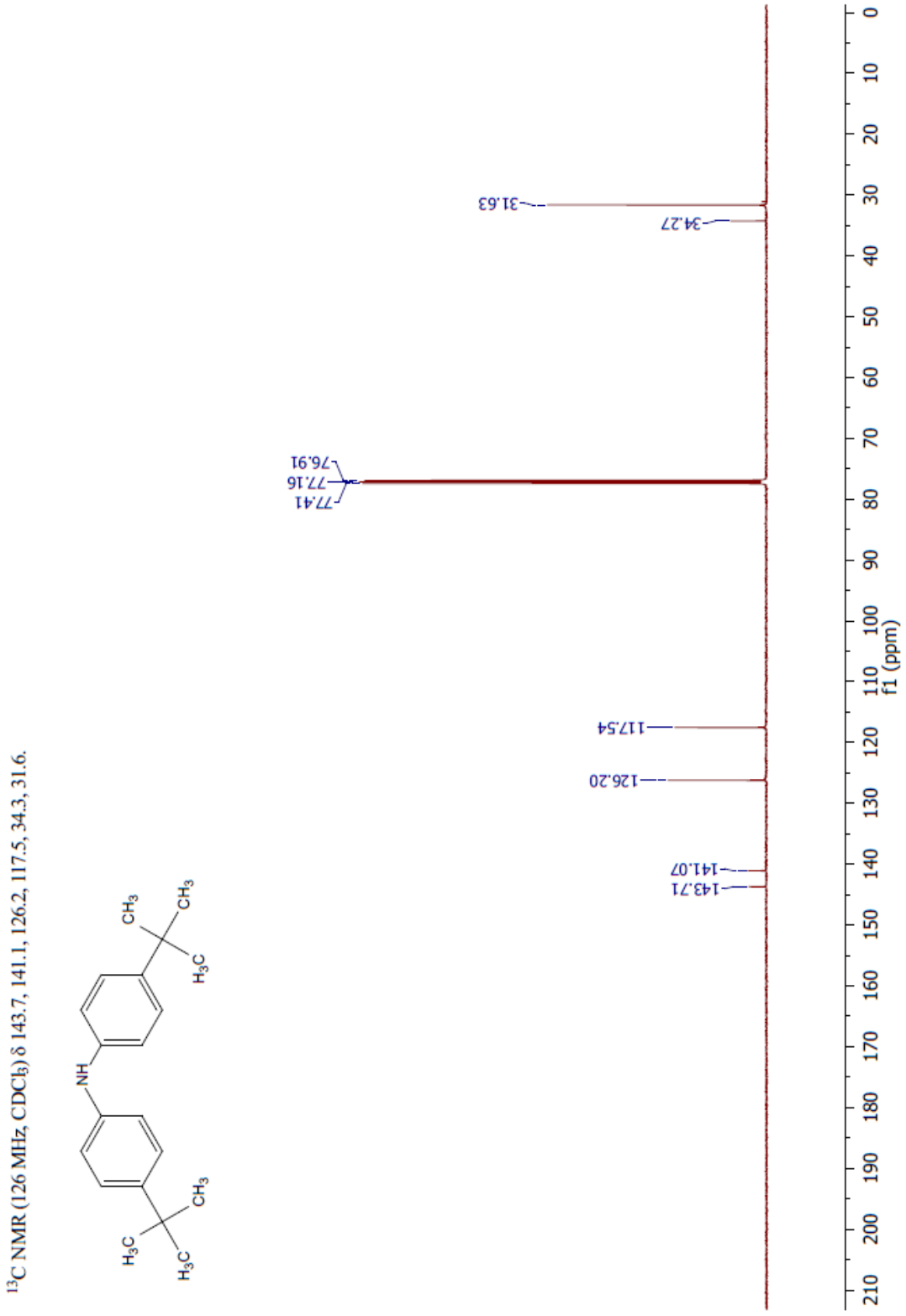

Figure 16. ^{13}C NMR spectra for compound **3h**

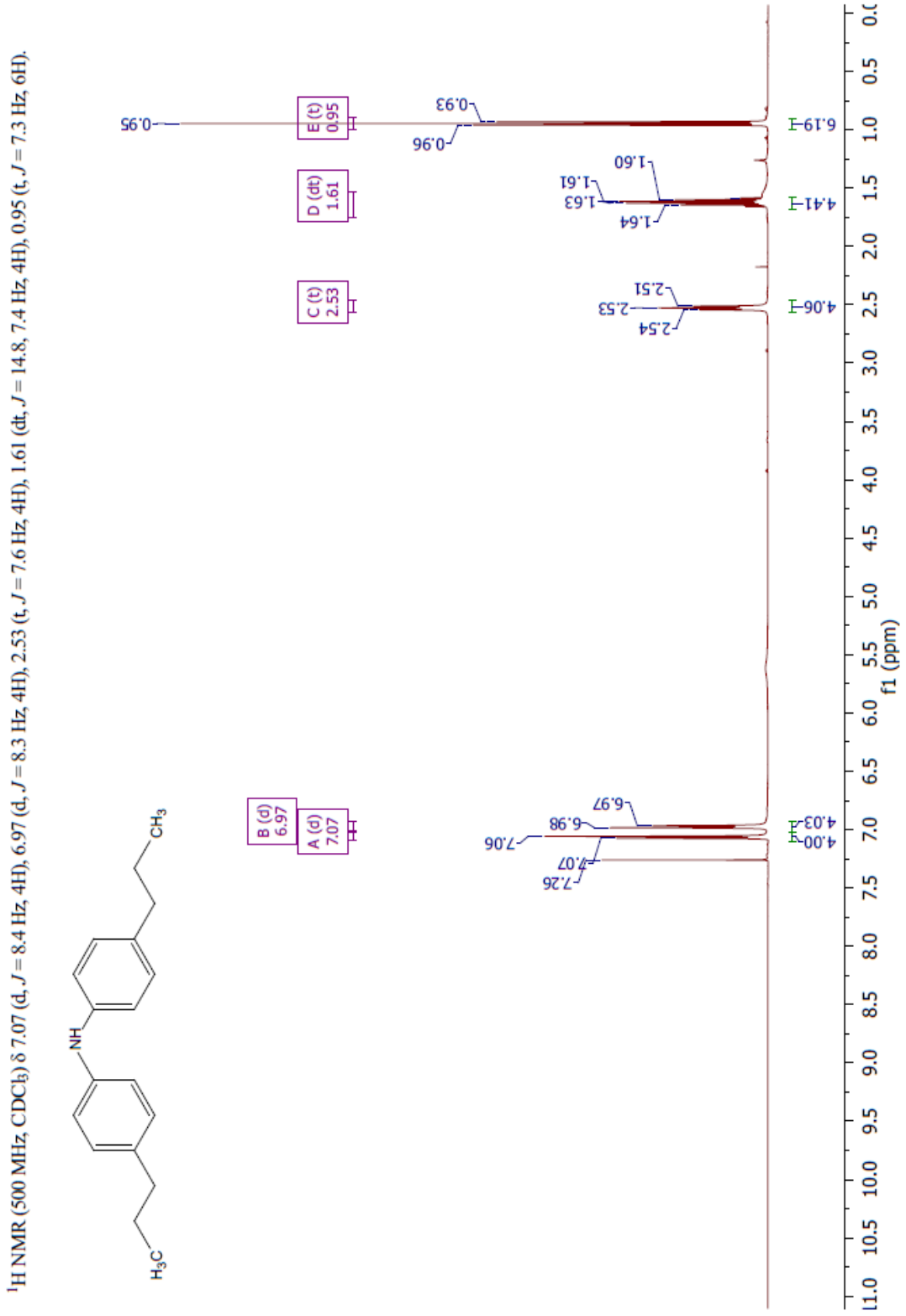

Figure 17. ^{1}H NMR spectra for compound **3i**

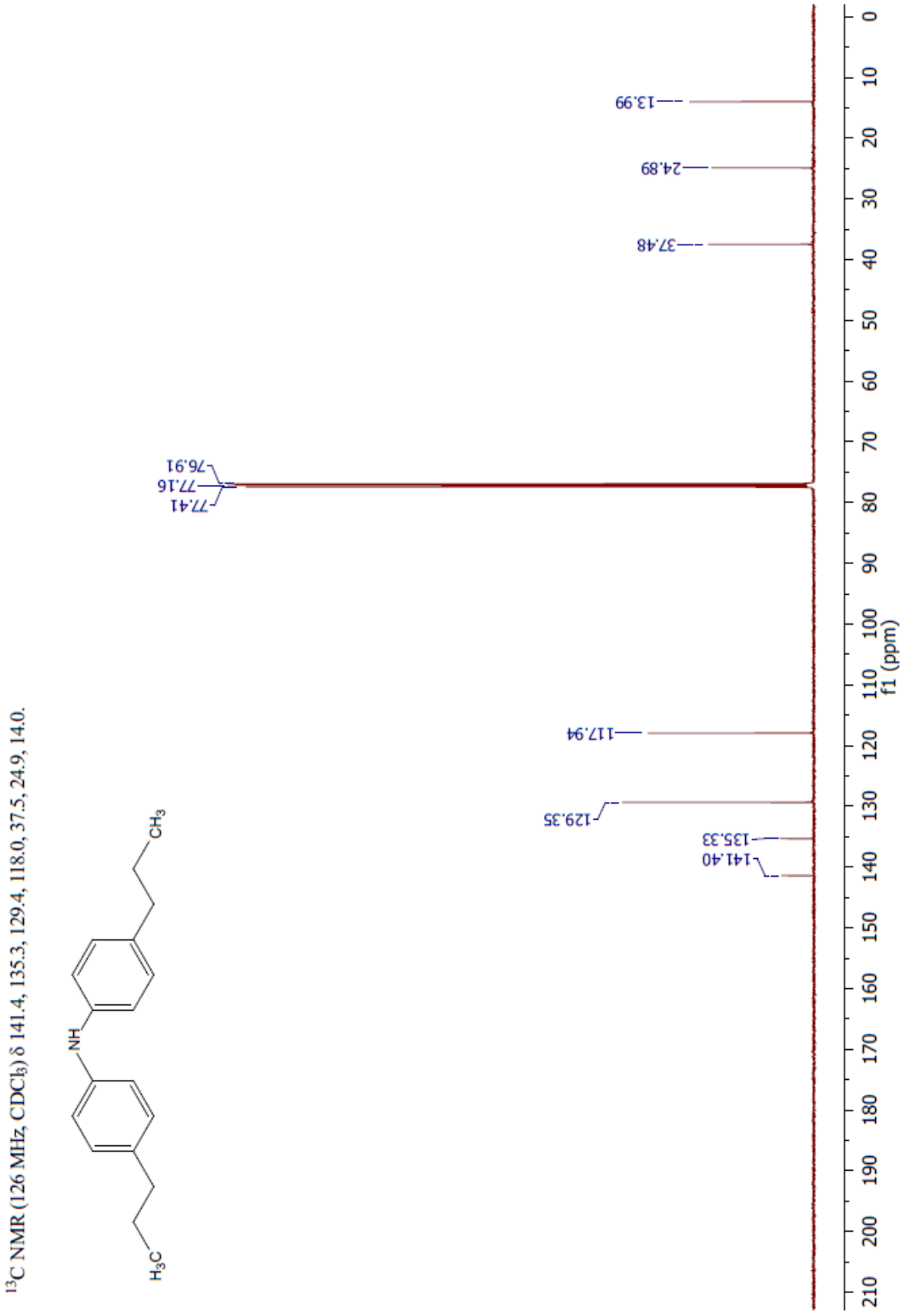

Figure 18. ^{13}C NMR spectra for compound **3i**

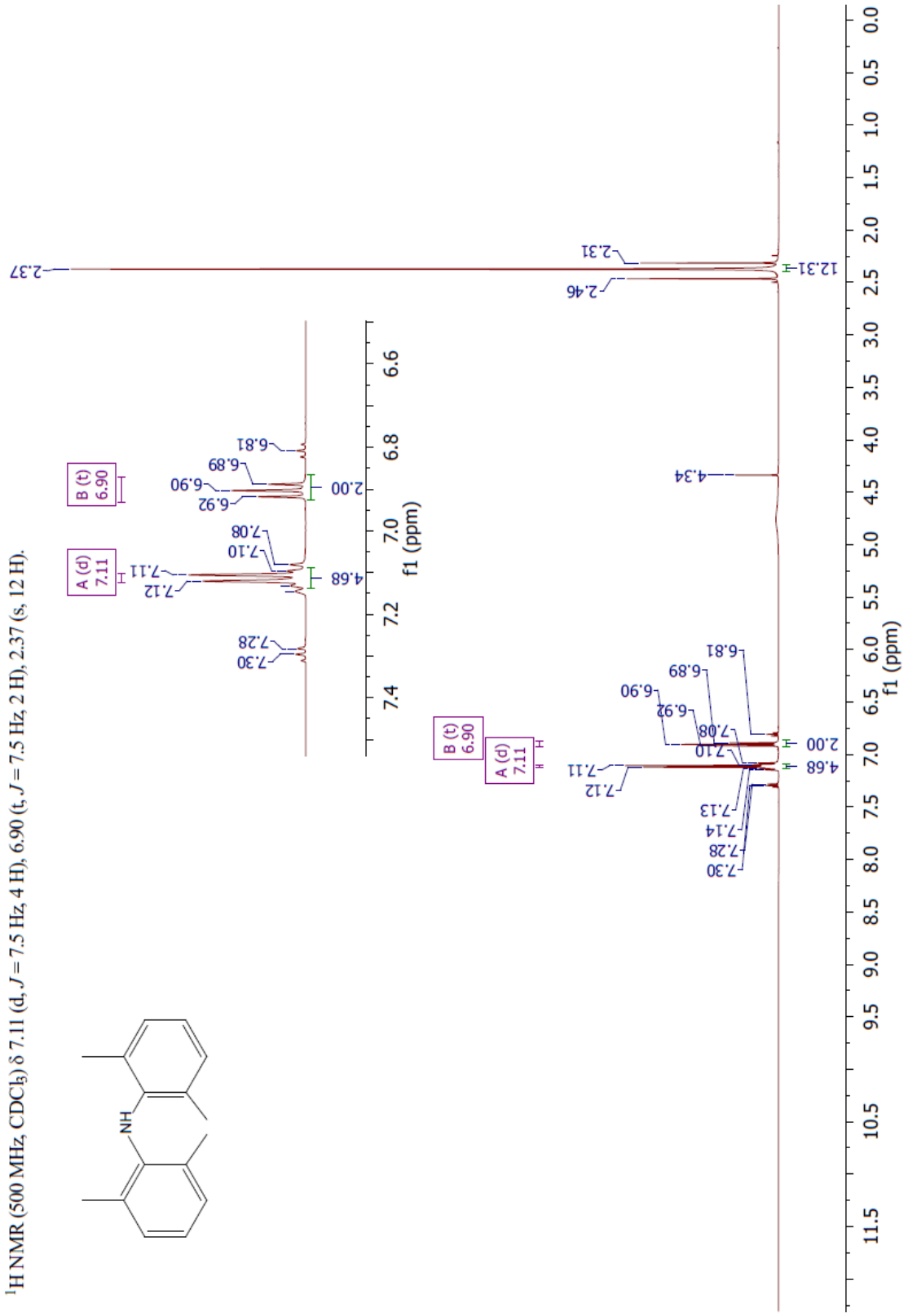

Figure 19. Crude ^{1}H NMR spectra for compound **3j**

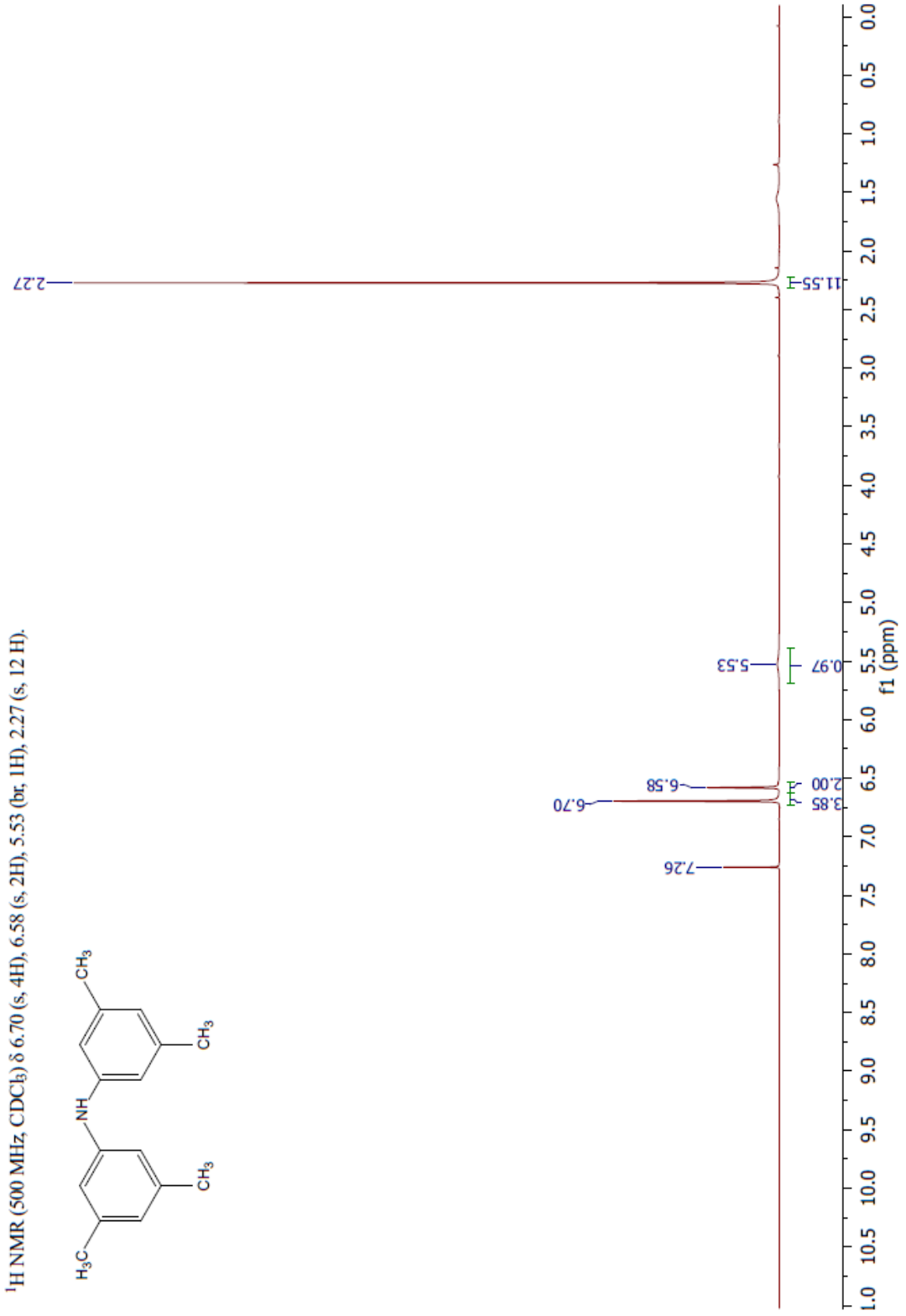

Figure 20. ^{1}H NMR spectra for compound **3k**

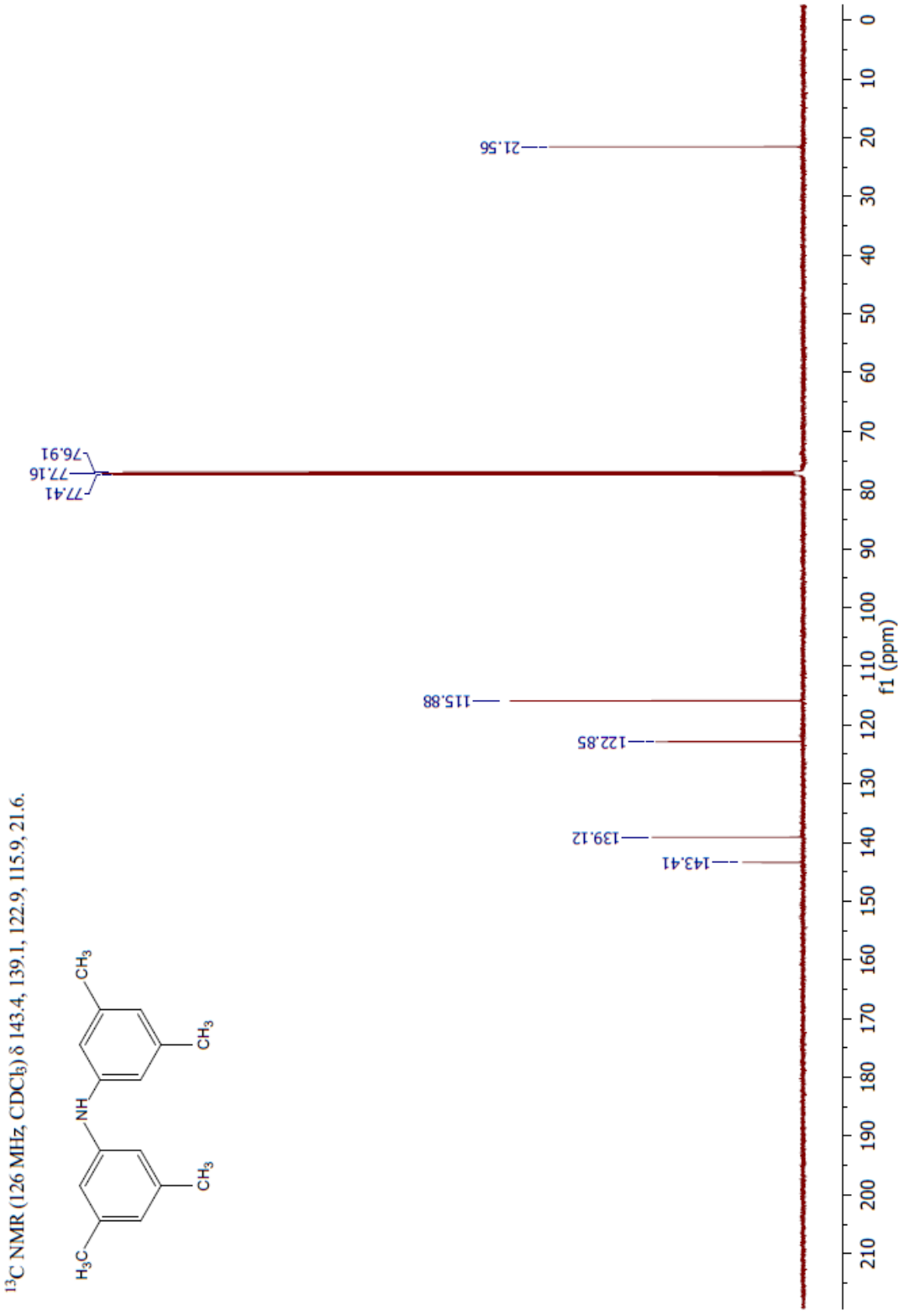

Figure 21. ^{13}C NMR spectra for compound **3k**

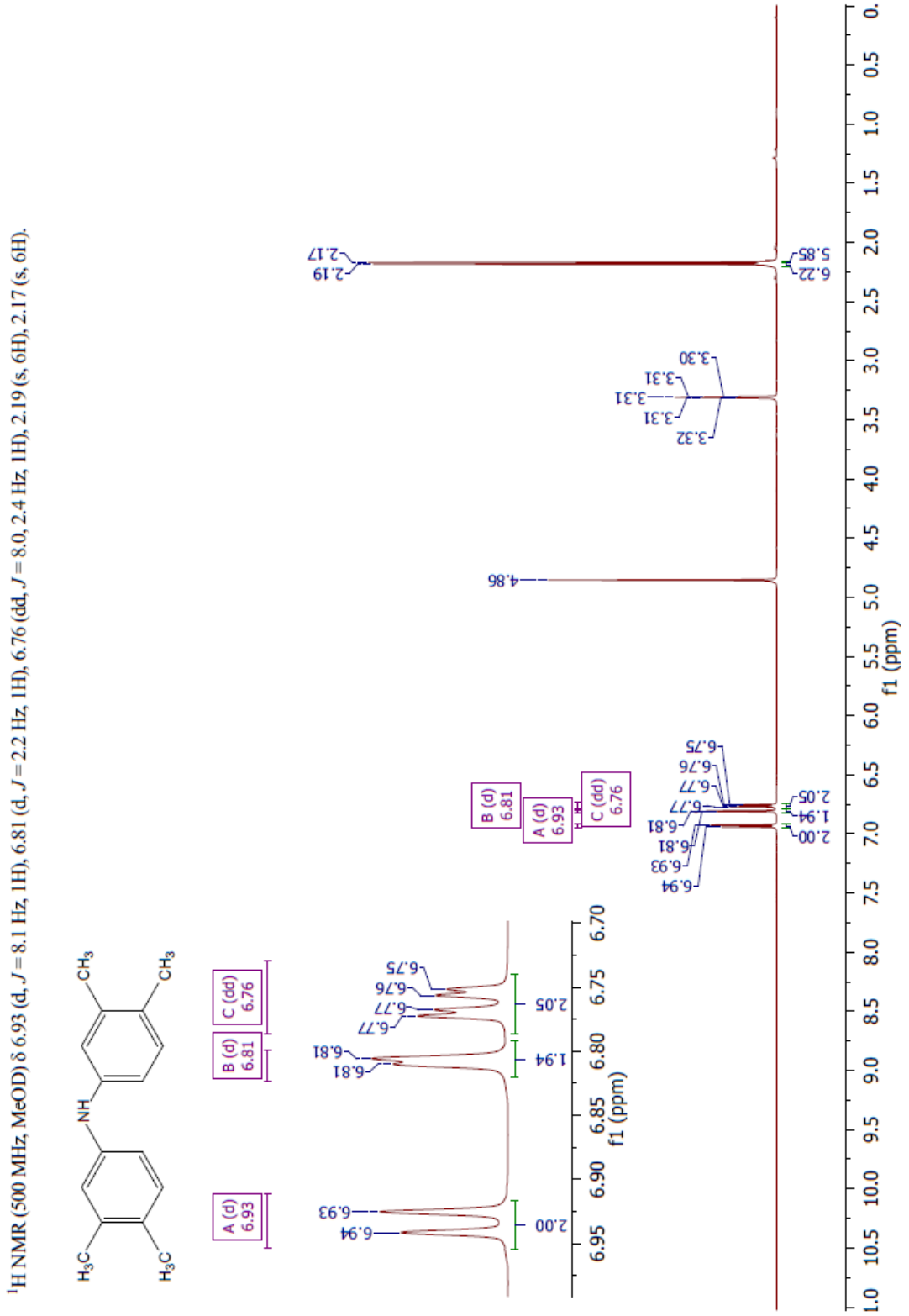

Figure 22. ^{1}H NMR spectra for compound **3l**

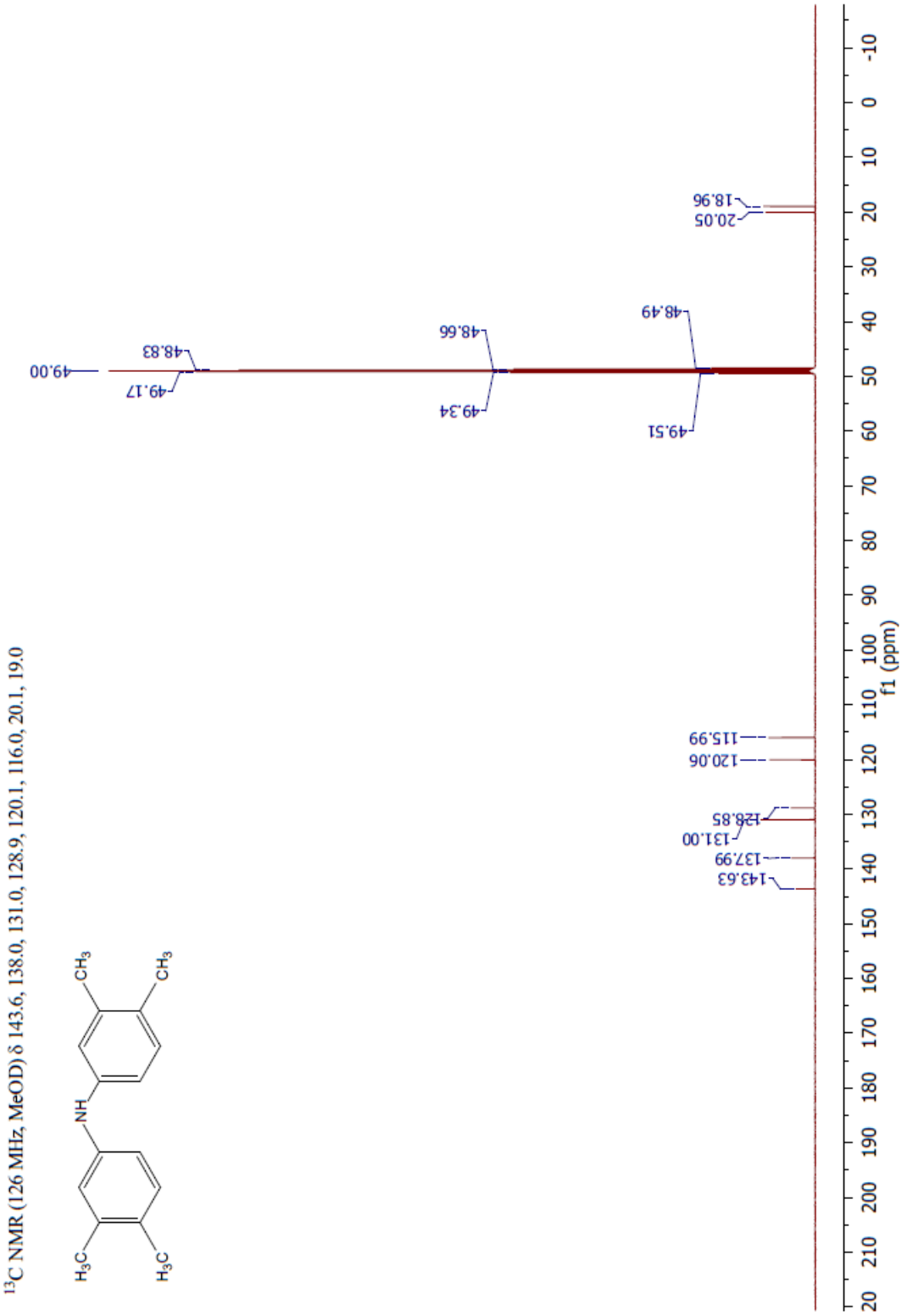

Figure 23. ^{13}C NMR spectra for compound **3l**

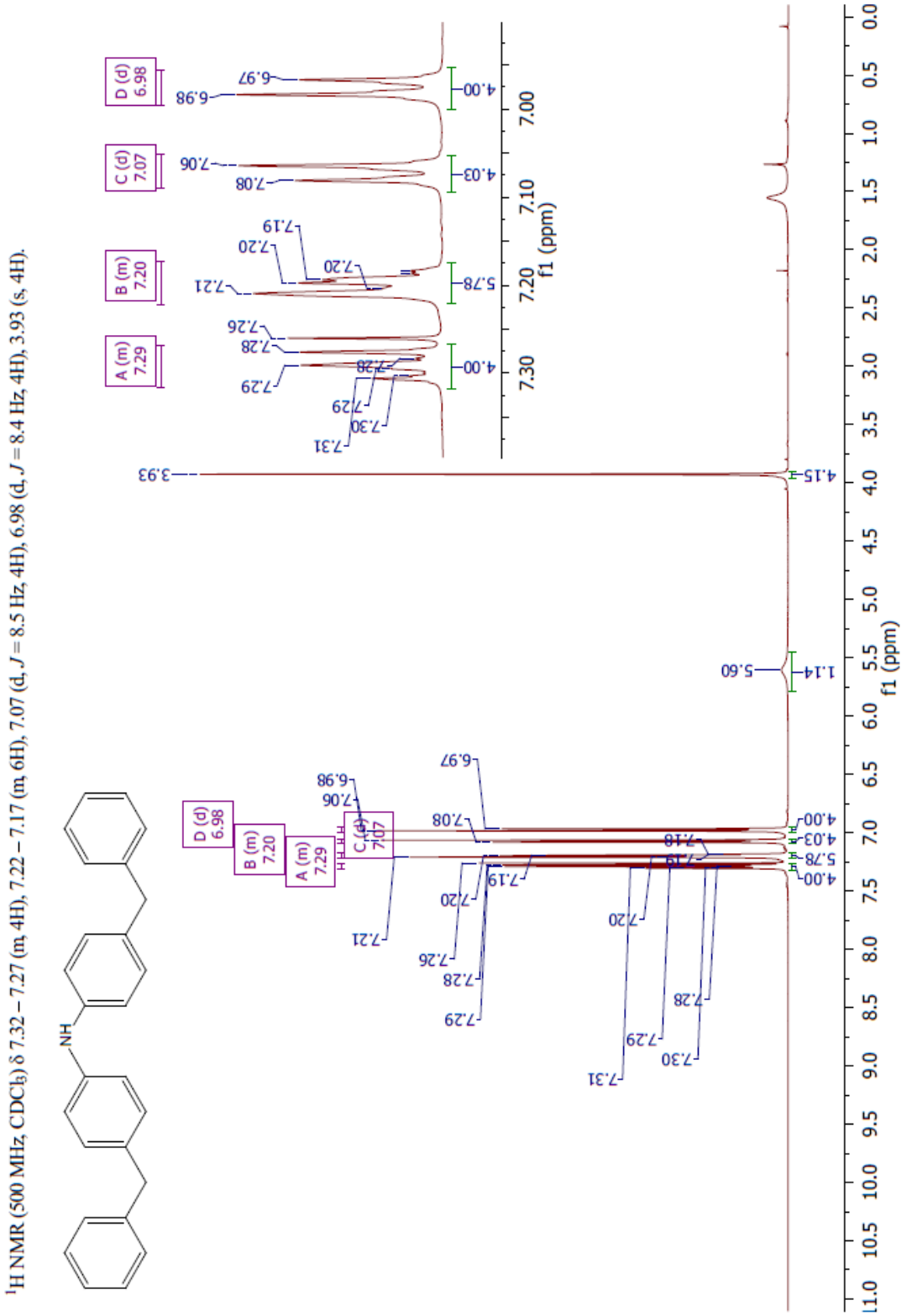

Figure 24. ^{1}H NMR spectra for compound **3m**

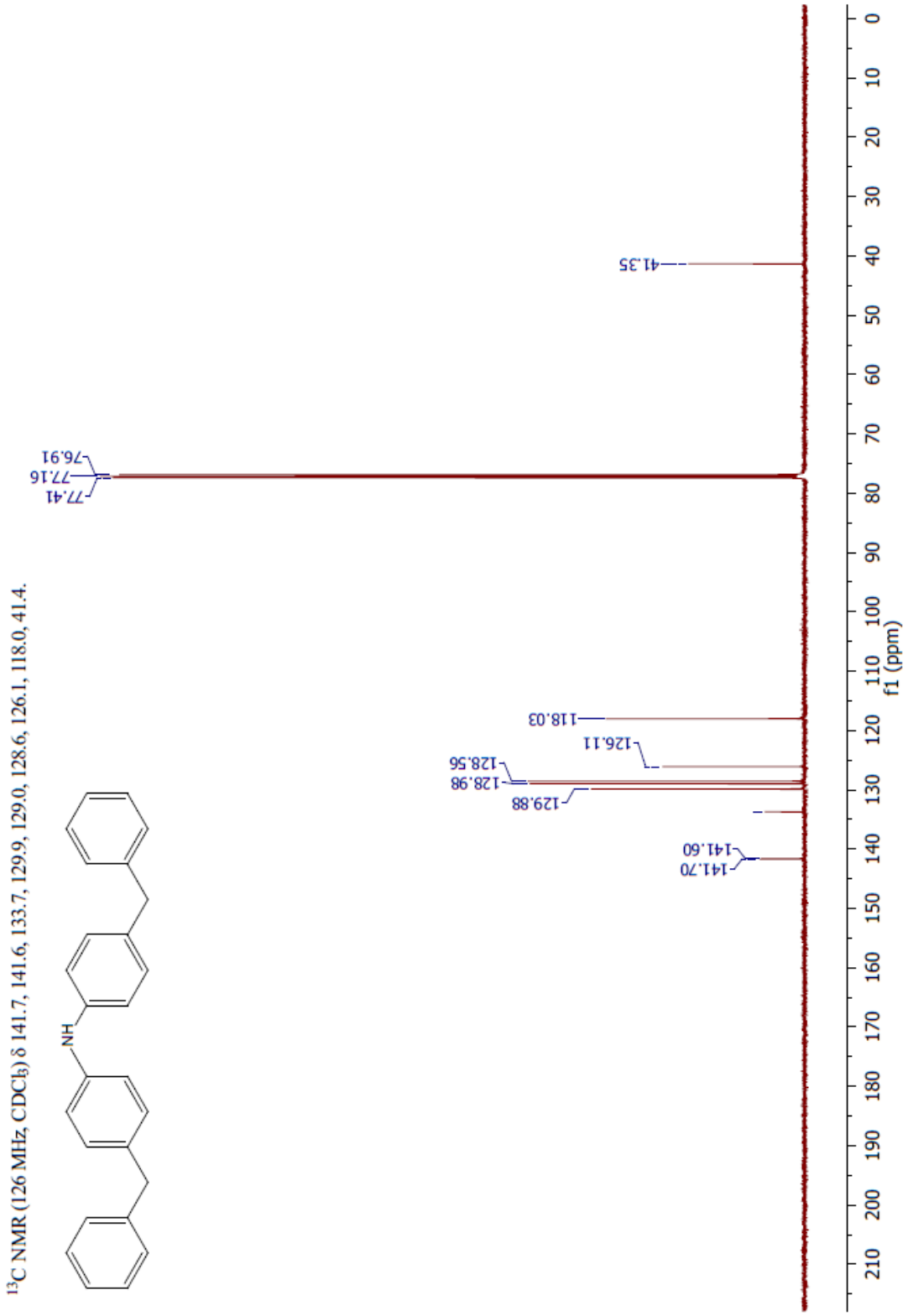

Figure 25. ^{13}C NMR spectra for compound **3m**

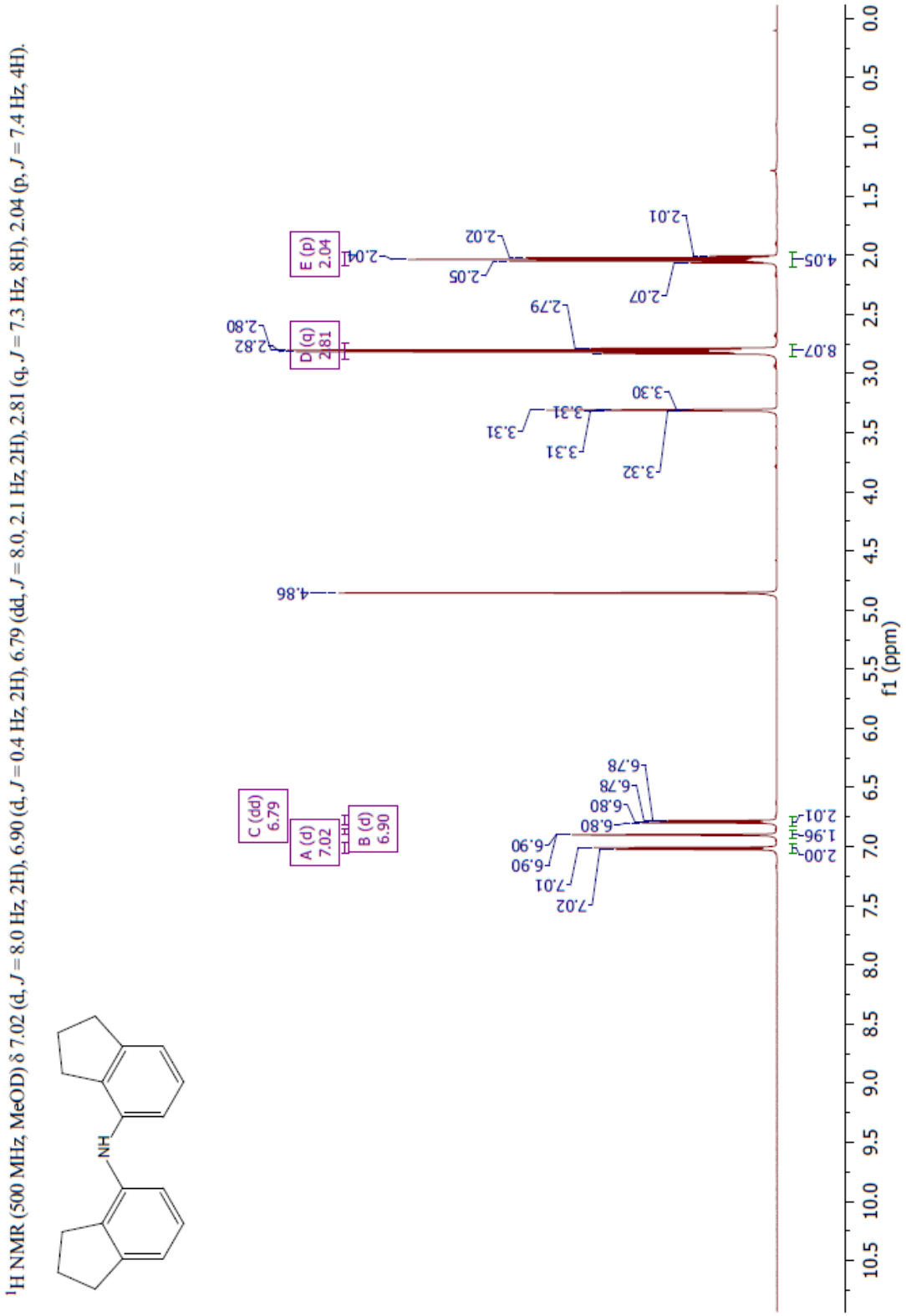

Figure 26. ^{1}H NMR spectra for compound **3n**

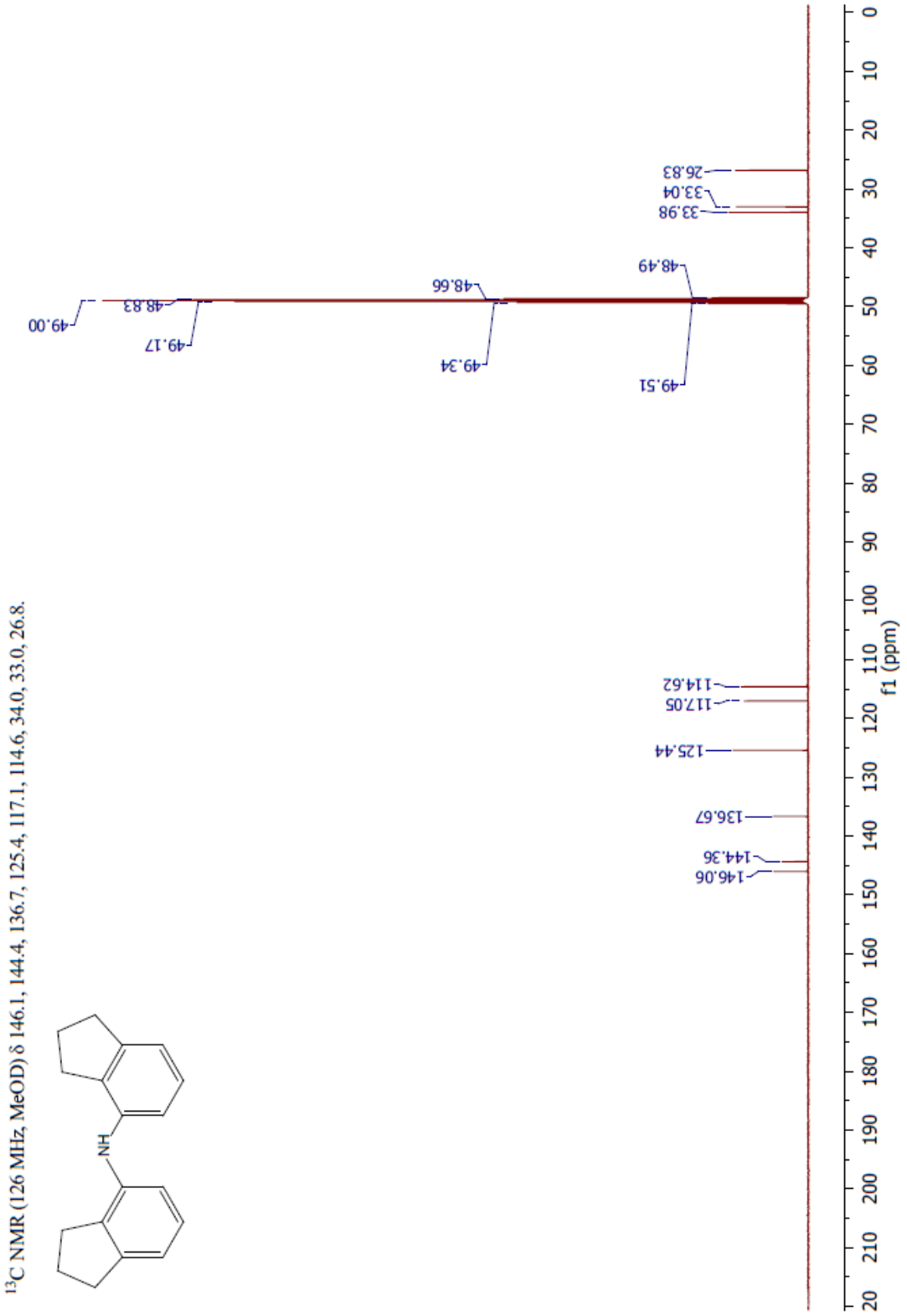

Figure 27. ^{13}C NMR spectra for compound **3n**

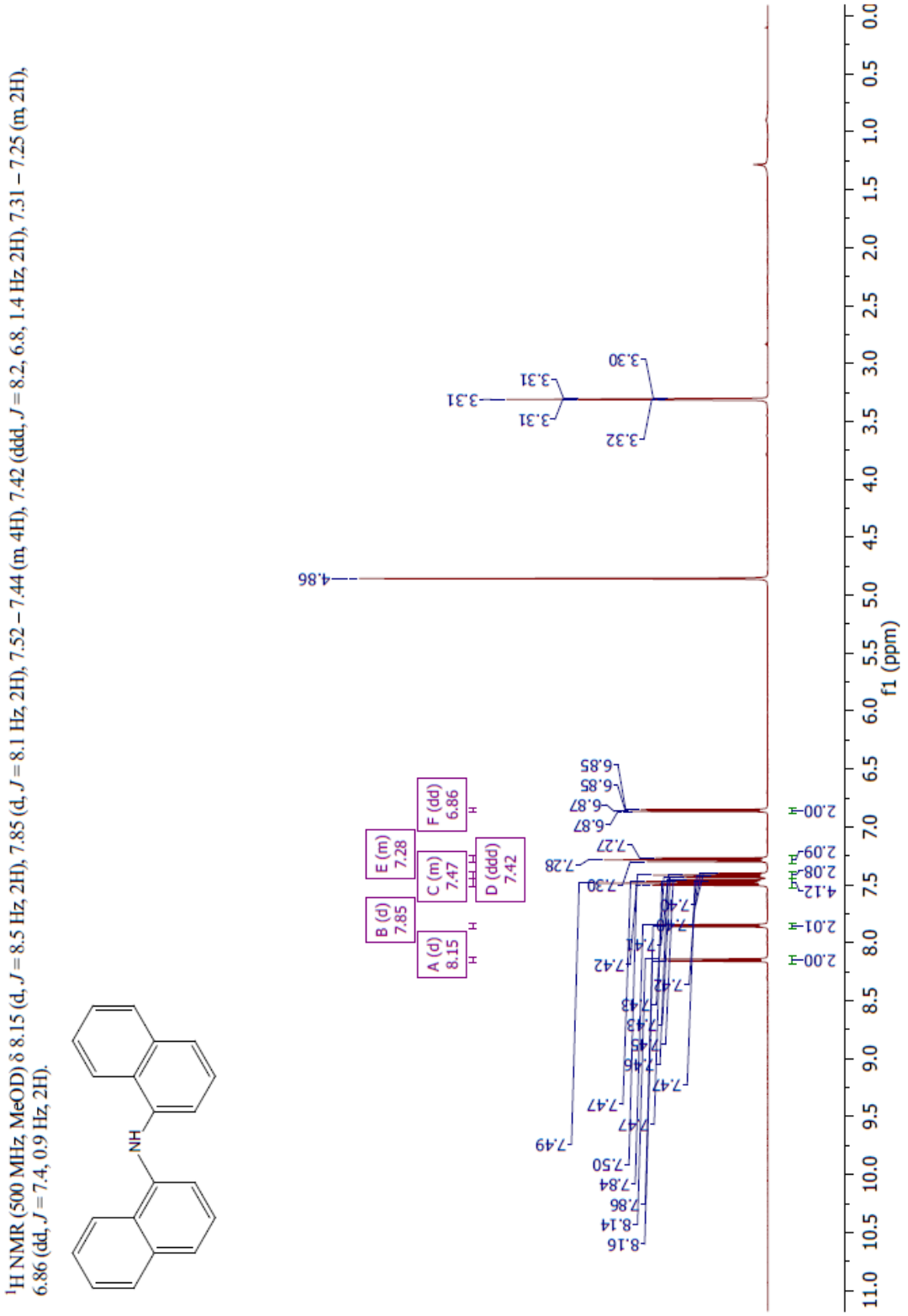

Figure 28. ^{1}H NMR spectra for compound **3o**

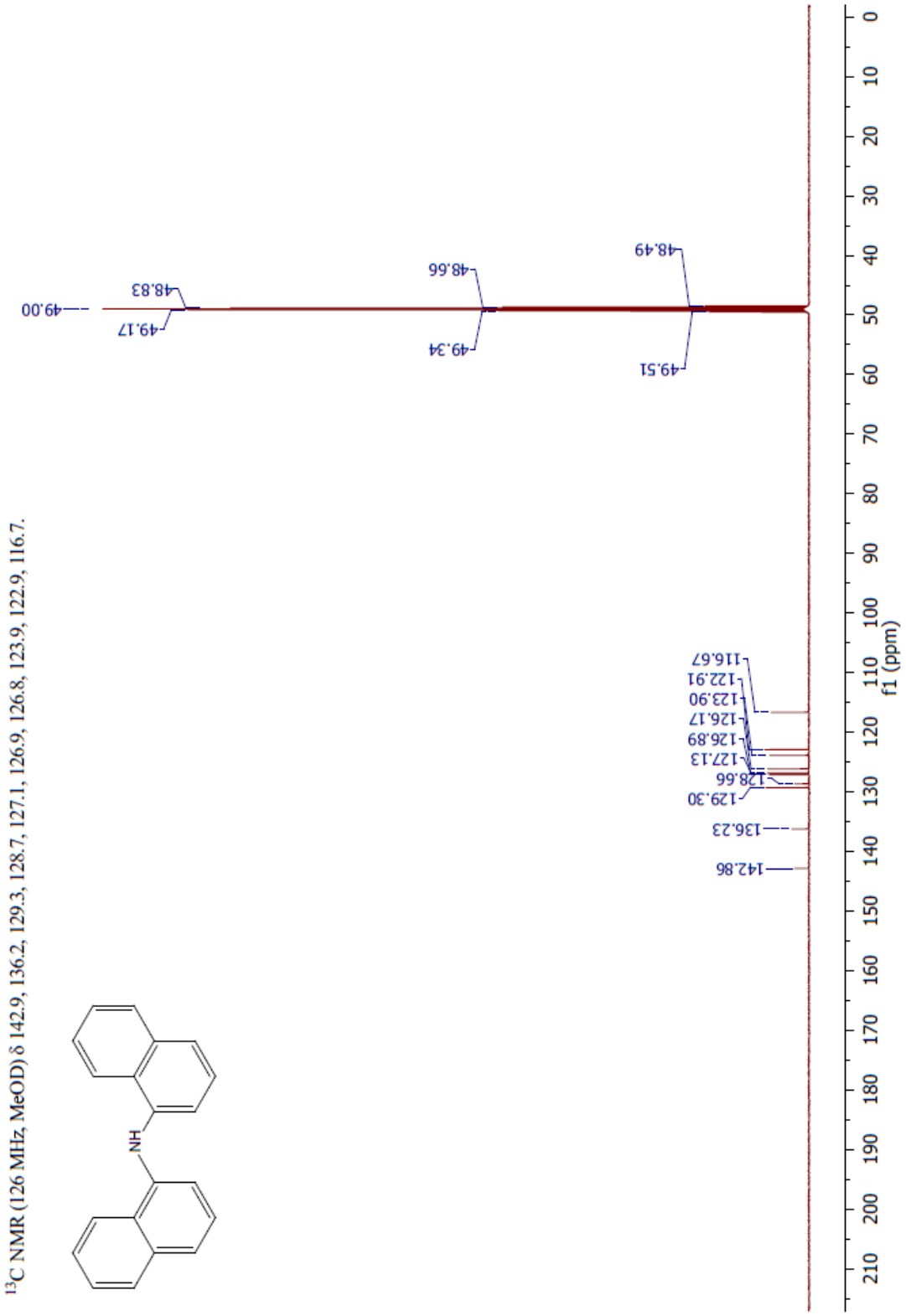

Figure 29. ^{13}C NMR spectra for compound **3o**

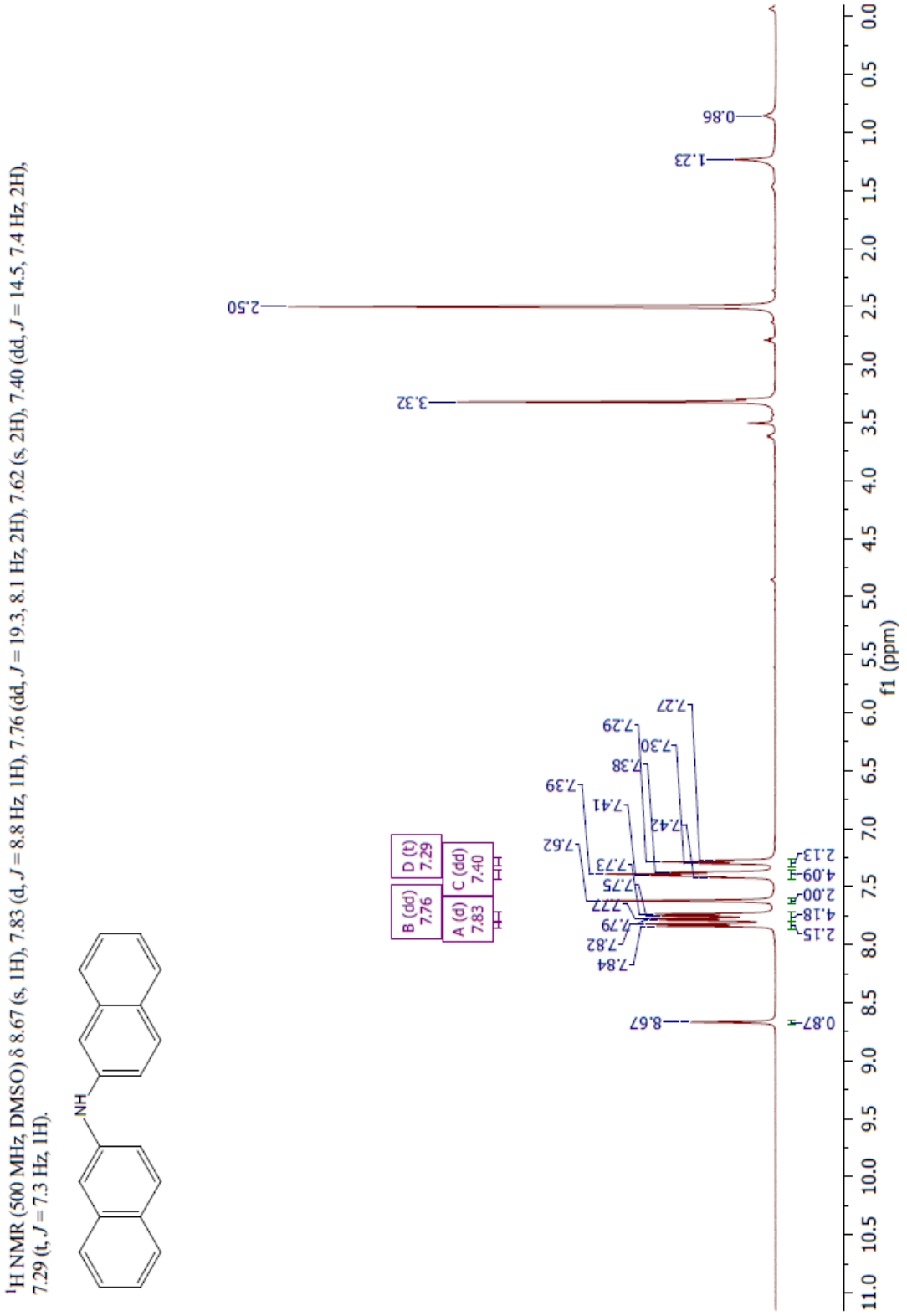

Figure 30. ^{1}H NMR spectra for compound **3p**

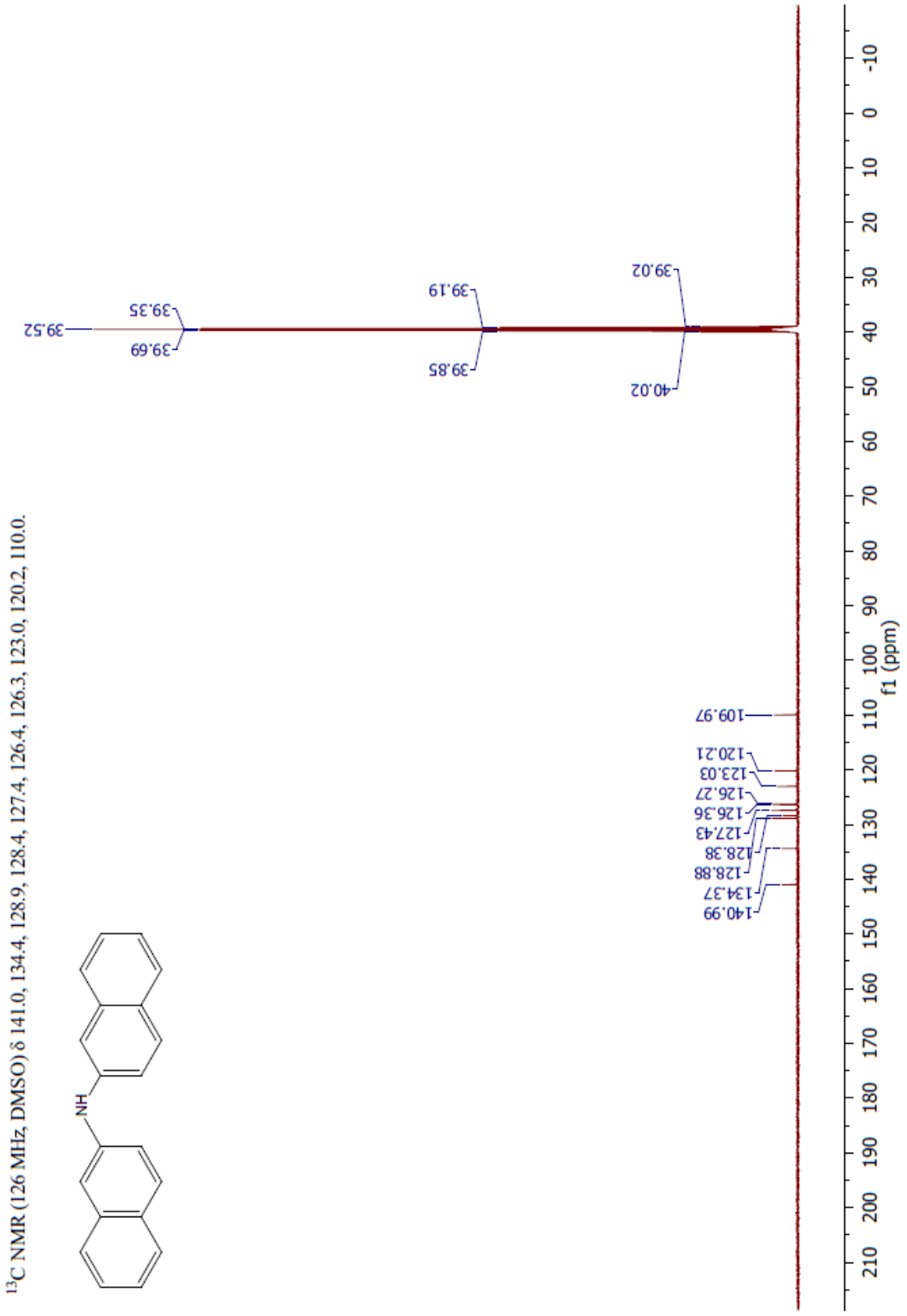

Figure 31. ^{13}C NMR spectra for compound **3p**

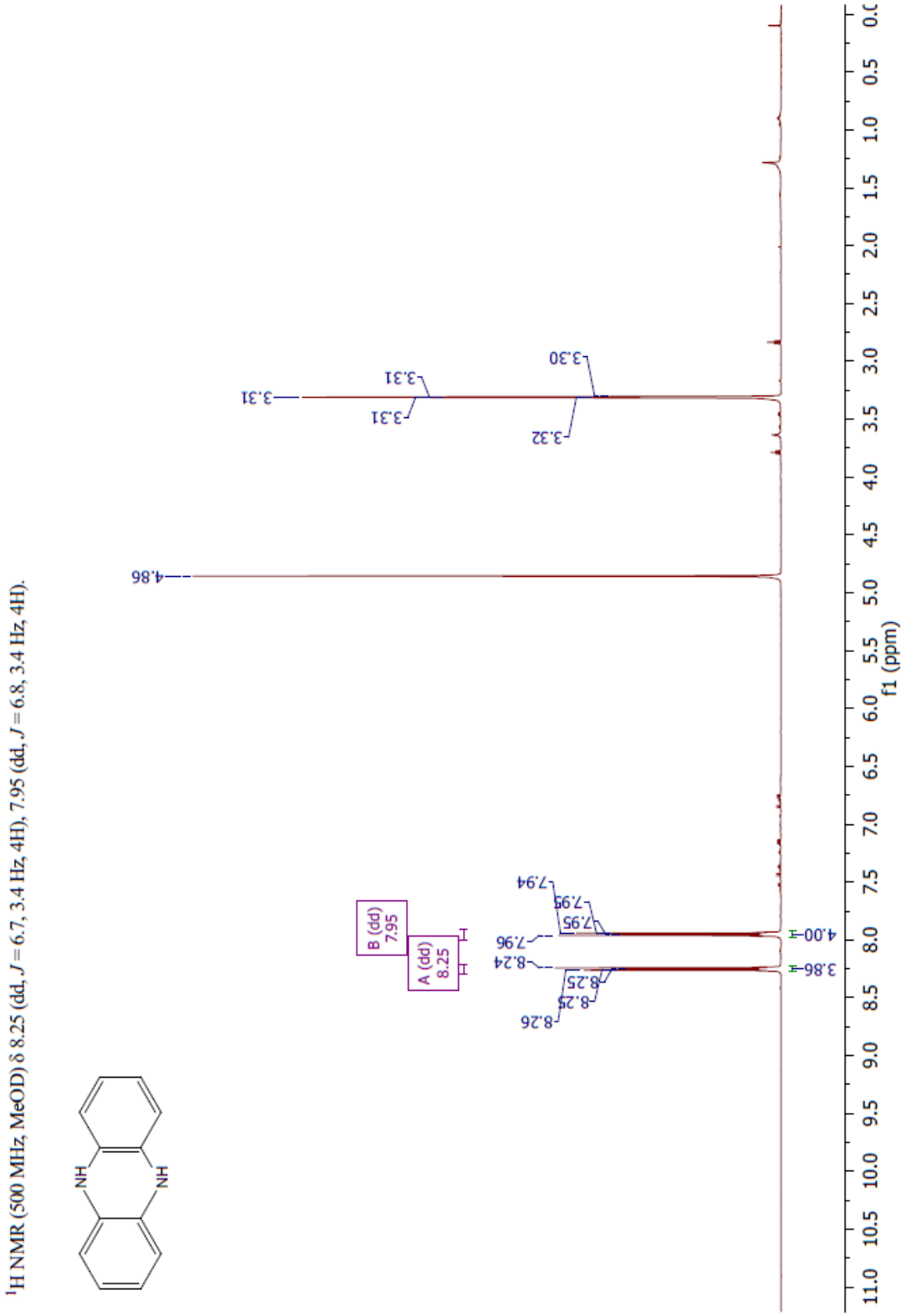

Figure 32. ^{1}H NMR spectra for compound **3q**

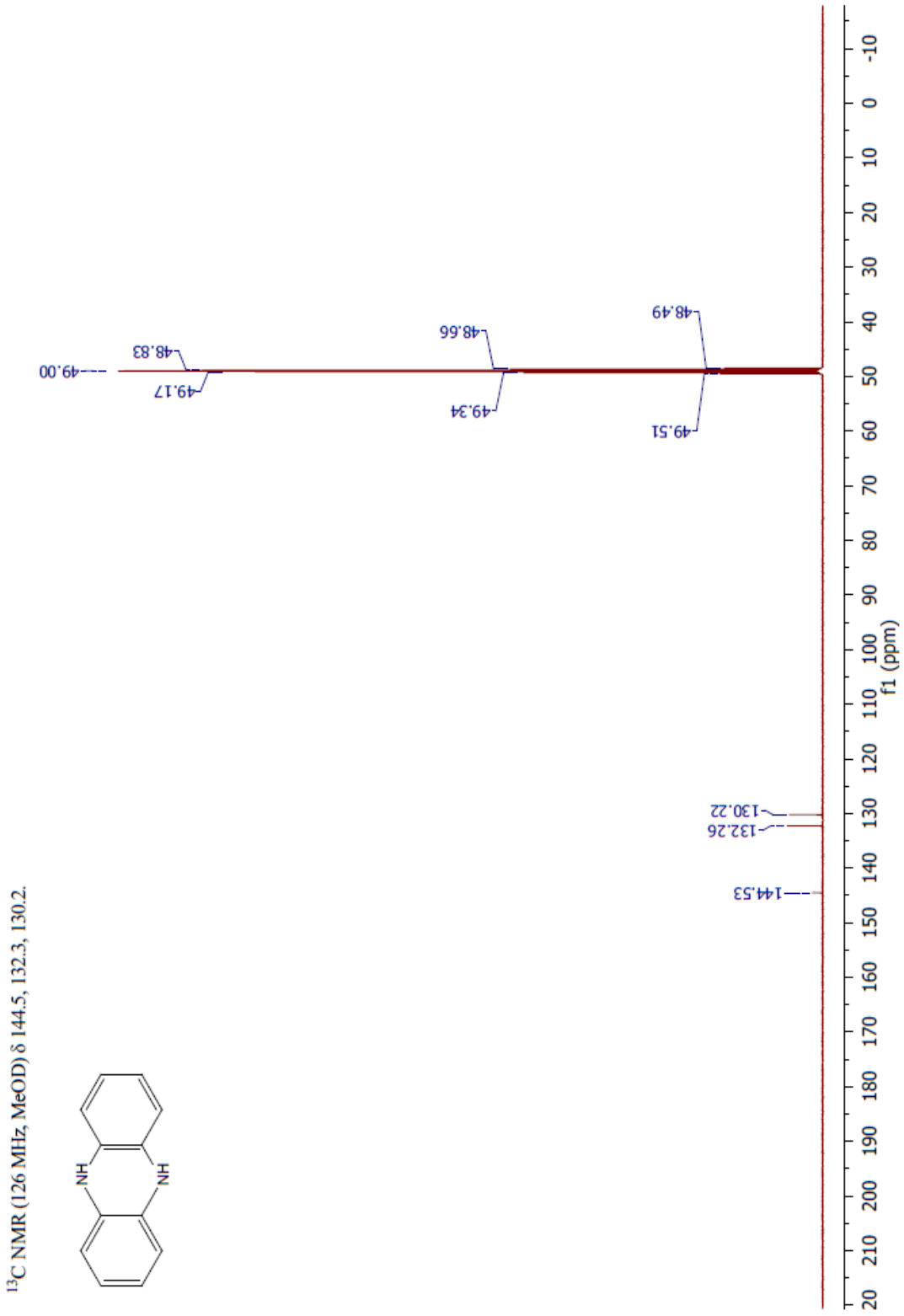

Figure 33. ^{13}C NMR spectra for compound **3q**

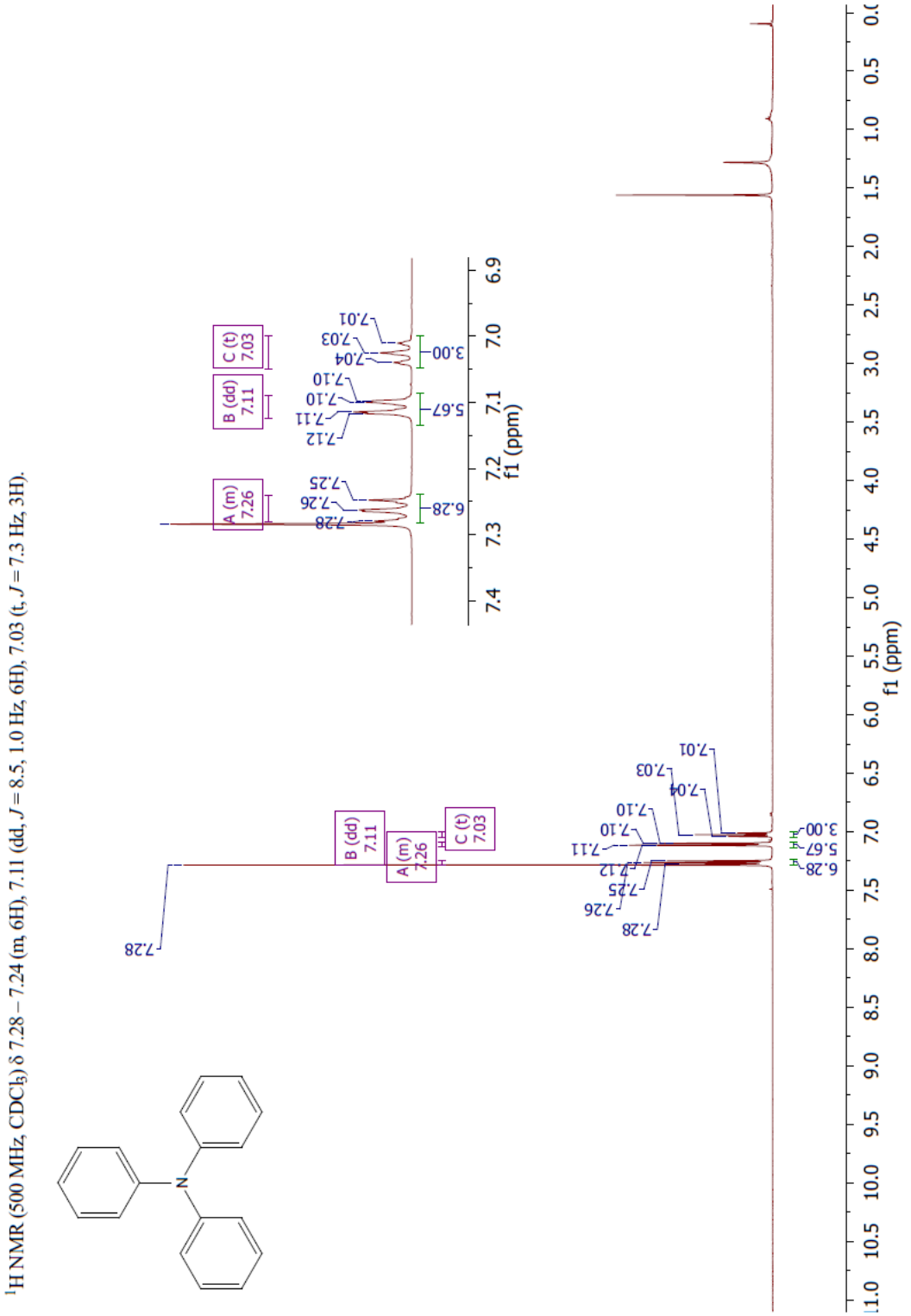

Figure 34. ^{1}H NMR spectra for compound **4a**

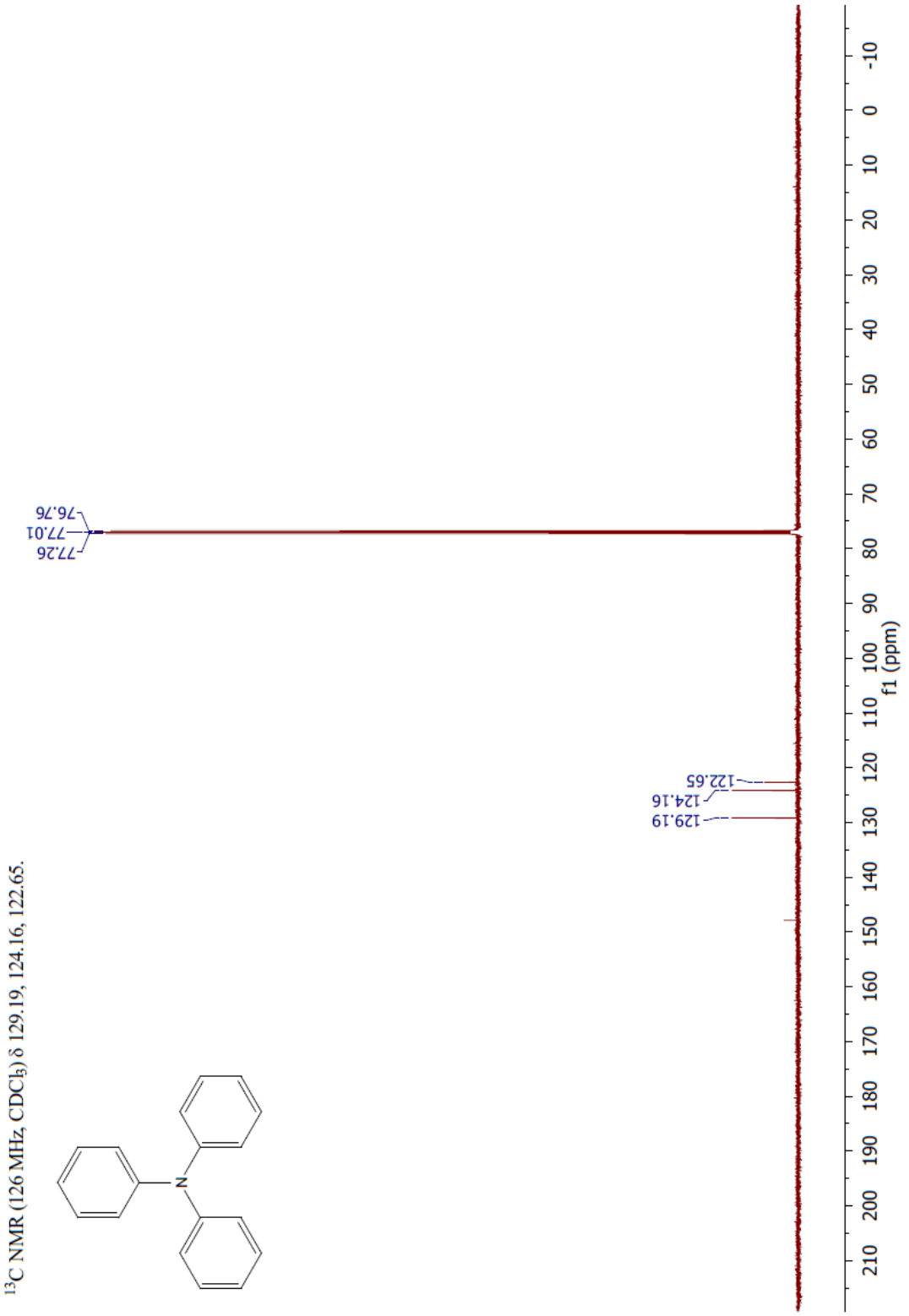

Figure 35. ^{13}C NMR spectra for compound **4a**